IMPROVING THE CULTIVATION EFFICIENCY OF MICROALGAE FOR BIOFUELS: SPANNING BIOFILM AND BIOPROCESSING SCALES

by

Julian Noah Rosenberg

A thesis submitted to the Johns Hopkins University in conformity with the requirements for the degree of Doctor of Philosophy

Baltimore, Maryland

October 2014

© MMXIV Julian N. Rosenberg

All rights reserved

Abstract

Microalgae are versatile photosynthetic production platforms for recombinant proteins, nutritional commodities, and biofuels. The demand for liquid transportation fuels has recently propelled these organisms to the forefront of the bioenergy stage. While algal biomass is poised to become a widely recognized feedstock, existing bioprocessing challenges continue to limit its full production potential at large scales. This dissertation offers an analysis of the engineering approaches that have previously guided algae farm development in order to inform future process design at the scales necessary for biofuel applications. Ultimately, the findings confront conventional microalgal cultivation by exploring novel methodologies to increase oil yield, integrate alternative sources of nutrients, and minimize water usage.

In order to quantify resource demands for algal biofuels using conventional raceway ponds, technoeconomic modeling identified carbon dioxide (CO_2) sourcing logistics, lipid content, and water handling as the major factors affecting cost of production. To address CO_2 feedstock availability, integrated algae production using biogenic CO_2 from an ethanol biorefinery was assessed. Together, these models predicted the cost of unrefined algal oil to be \$10–40 gal^{-1} at baseline biomass productivities of 15–20 g m^{-2} d^{-1} and 25% total extractable lipids. The technical and economic obstacles associated with both production scenarios motivated experimental work to increase cellular lipid content with strategic nutrient supplementation and explore the potential for adherent algal growth systems.

By investigating the differential impact of light and organic carbon on microalgal lipid composition, a species selection pipeline focused on strains with the potential to accumulate triacylglycerol (TAG) as a biofuel precursor. From a collection of over thirty phylogenetically distinct *Chlorella* strains, *C. sorokiniana* UTEX 1230 was chosen based on its robust autotrophic growth and enrichment with TAG during heterotrophy— as much as 90% of the total lipid fraction. However, its lipid productivity was suppressed under mixotrophic conditions with light and glucose. This constraint on carbon flux offered insights into the metabolic regulation of lipid biosynthesis in this organism and prompted further analysis of two-stage bioprocessing to maximize TAG yield.

Finally, to improve the volumetric efficiency of algal cultivation, photosynthetic biofilms were examined as an alternative to suspension culture. The formation of algal monolayers on membranes was improved 8-fold by employing protein-mediated cellular attachments. To encourage multi-layer outgrowth, natural microbial communities containing filamentous cyanobacteria were studied as potential scaffolds for biofilm architectures. The spatial and temporal dynamics of unicellular algal growth and migration within these biofilm microenvironments were characterized using molecular genetic tools and fluorescent microscopy to resolve cellular-level detail. Ultimately, immobilized biofilms inhabited by *C. sorokiniana* UTEX 1230 reached a maximal thickness of 150 µm and achieved areal productivities comparable to raceway pond production.

Collectively, the results in this thesis address bioprocessing bottlenecks associated with algal cultivation by increasing oil content and reducing water requirements. By investigating the influence of nutrient regimes on algal lipid composition and interrogating the fate of single algal cells within biofilms, this dissertation connects biochemical and physical factors to the economics and environmental impact of algal biofuels.

Advisor

Dr. Michael Betenbaugh
Professor, Department of Chemical & Biomolecular Engineering
Whiting School of Engineering, Johns Hopkins University

Committee Members

Dr. Marc Donohue
Professor, Department of Chemical & Biomolecular Engineering
Whiting School of Engineering, Johns Hopkins University

Dr. George Oyler
Associate Research Professor, Chemical & Biomolecular Engineering
Whiting School of Engineering, Johns Hopkins University

President, Synaptic Research, LLC
President, Clean Green Chesapeake, LLC

Dr. Edward Bouwer
Professor, Department of Geography & Environmental Engineering
Whiting School of Engineering, Johns Hopkins University

Dr. Royce Francis
Adjunct Assistant Professor, Geography & Environmental Engineering
Whiting School of Engineering, Johns Hopkins University

Assistant Professor, Engineering Management & Systems Engineering
The George Washington University

Acknowledgements

This work would not have been possible without the sincere dedication of Dr. Michael Betenbaugh as my advisor. As the first student to bring microalgae into his lab, I am grateful for Professor Betenbaugh's willingness embark on a new project with a new organism and a new doctoral student, which has led to a rewarding research program and many new collaborations. I cannot fully express my gratitude to Dr. George Oyler, who has been an invaluable mentor to me. I have learned a tremendous amount from him and gratefully acknowledge his intellectual contributions to the work in this thesis and his critical role in initiating our efforts in algae biotechnology. Furthermore, I am appreciative of Dr. Marc Donohue, Thomas Fekete, and Loy Wilkinson for guiding my professional development by sharing seasoned engineering insights and industry perspectives with an engineer-in-training.

I recognize that my PhD experience has been highly collaborative, so I must give thanks to the members of the Betenbaugh Lab for their continuous support with experiments and manuscript preparation. I have benefited greatly from working with Dr. Minxi Wan, Dr. Scott Williams, Dr. Geng Yu, Junaid Faruq, Coral Fung Shek, Jordan Baker, and the undergraduates in the lab. I am particularly appreciative of the tireless efforts of Jonathan Rogers, Bernardo Guzman, Victor Oh and contributions to the TEA model described in Chapter 2. I gratefully acknowledge Joshua Baker for his diligent work coding the CyteSeeker program described in Chapter 6. In the Department of Geography & Environmental Engineering, I would

like to thank Professors Edward Bouwer and Royce Francis for serving on my graduate board review committee. In Professor Bouwer's lab, I am particularly indebted to Pavlo Bohutskyi for our collaboration on the EPA People, Prosperity, and the Planet (P3) grant as well as other interdisciplinary projects and proposal writing we have shared throughout our graduate work together. I appreciate the time that Drs. Richard Potember and Julia Patrone spent with me at the JHU Applied Physics Laboratory to develop the initial concepts on membrane-based growth described in Chapter 7. Much of this doctoral research was supported by funding and cross-functional opportunities afforded to me by the Environment, Energy, Sustainability and Health Institute (E^2SHI), directed by Professors Cindy Parker and Ben Hobbs. Through my work with E^2SHI, I was able to forge deeper relationships with my co-advisors on the project: Professors Bouwer, Oyler, and Donohue on the Homewood Campus and Dr. David Love at the Johns Hopkins School of Public Health. I owe a special thanks to Courtney Akitake from Zeiss for her assistance operating the Lightsheet microscope. Furthermore, I am sincerely grateful for the financial support from the Johns Hopkins Libraries Open Access Promotion Fund, which enabled much of this work to be published in open access journals.

Outside of the Johns Hopkins community, I thoroughly enjoyed my laboratory training experiences in antibody generation and phage library panning at Tufts Cummings School of Veterinary Medicine and was humbled by the personal and professional generosity of Dr. Charles Shoemaker and Jacqueline Tremblay. I am also

glad to have been able to visit the Golden LEAF Biomanufacturing Training and Education Center (BTEC) at North Carolina State University and appreciate the time that Professor Michael Flickinger and Oscar Bernal Zuniga spent with me to share their experience with photosynthetic biofilms. I would like to extend immense thanks to the faculty at University of Nebraska–Lincoln (UNL), Professors Donald Weeks and Jim Van Etten, as well as Wen Zhi Jiang, Naoko Kobayashi, Austin Barnes, and Eric Noel, with whom I routinely collaborated. I also owe particular appreciation to Synaptic Research (SR) and Clean Green Chesapeake (CGC) in the Maryland Clean Energy Incubator at UMBC's South Campus. Not only were they kind enough to share lab space with me, but my molecular biology work would not have been possible without their assistance. The advice and protocols from Drs. Akelia Wauchope, Kyle Krady, Yung Nien-Chang, Barry Gertz were vital to my success. I am especially grateful for the tremendous efforts of Gunjan Andlay, who provided assistance with large-scale algal cultivation along with undergraduate interns Ashrith Mathias, Adithya Balasubramanian, Douglas Morton, Heather Jacobs, Scott Johnson, Greg Barnes, Josh Merwin, and Supraja Prasad. Furthermore, the organizational support of Kevin McIntosh (SR) and Wendell Leimbach (CGC) was remarkable.

I would like to thank the few remaining Hopkins alumni in the area, Jasmine Serlemitsos and Isaac Katz, for their support and friendship. This dissertation is dedicated to my parents, who have inspired me to seek knowledge from an early age

and always encouraged my interests in “chemical engineering” by allowing me to create concoctions in the kitchen. My sisters Jenna and Meris have been a constant source of inspiration throughout my life. They may look up to me (at least in the literal sense, if nothing else), but probably don’t realize how proud I am of all of their accomplishments. Shannon has provided constant emotional support and a pragmatic approach to help me complete this thesis. While I close this chapter of my life, I look forward to continuing the next with her. Finally, I would be remiss if I did not acknowledge my “scientific advisors” in the family, Eric and Lawrence Rosenberg, for instilling in me an intellectual curiosity and introducing me to my first biochemistry lab where I marveled at magnetic stir bars and the material properties of parafilm.

Statement of Originality

The results included in this dissertation represent the original work of JNR except when due acknowledgements are given. While the material presented in Chapters 5 and 8 are unique to this thesis, other results have been presented at conferences or appeared in journal publications. Excerpts from papers are reprinted in this dissertation with permission from the publishers (Appendix A). Specifically, the results in Chapter 2, Section 2.2 were attained through collaborative research led by Professor Donohue and co-authored by ROGERS, ROSENBERG *et al.* in *Algal Research* (2013) and the results in Chapter 2, Section 2.6 were published by ROSENBERG *et al.* in *Biomass & Bioenergy* (2011). Chapter 1 also contains introductory material from these two publications. Chapters 1 and 6 both contain excerpts from a book chapter that was submitted to Elsevier Academic Press by ROSENBERG *et al.* in 2014.

Preliminary data leading to Chapter 3 and the V_HH library characterization in Chapter 6 are the result of collective efforts involving the Oyler Lab at the University of Nebraska–Lincoln, which were presented by JNR at the 2012 Algae Biomass Summit in panel presentation[1] and poster[2] formats. Publications containing

[1] Rosenberg JN. A comparative analysis of *Chlorella* species' heterotrophic growth characteristics and lipid composition, Algae Biomass Organization (ABO) Algae Biomass Summit (Denver, CO), September 27, 2012.

[2] Rosenberg JN, Wauchope AD, Jiang WZ, Kang M, Kobayashi N, Tremblay JM, Shoemaker CB, Weeks DP, Hildebrand M, Betenbaugh MJ, Mayfield SP, Oyler GA. Development of a single-chain antibody toolkit to interrogate and manipulate the microalgal cell, ABO Algae Biomass Summit (Denver, CO), September 24-27, 2012.

results from Chapters 3 and 6 were published in *PLoS ONE* by ROSENBERG *et al.* (2014) and *The Plant Journal* by JIANG, ROSENBERG *et al.* (2013). A poster[3] describing the results of Chapter 4 and presentation on this topic[4] were delivered by JNR at the 2014 Algae Biomass Summit.

Chapter 6 describes fluorescent algal cell line development and chloroplast V_HH expression projects led by the Mayfield Lab at University of California–San Diego and co-authored with JNR by RASALA *et al.* in *The Plant Journal* (2013) and BARRERA, ROSENBERG *et al.* in *Plant Biotechnology Journal* (2014). Figures from these publications are reprinted with permission from the publishers (Appendix A). Data included in Chapter 7 are the result of an initial collaboration with Dr. Richard Potember at the Johns Hopkins Applied Physics Laboratory. Posters describing the work in Chapters 6 and 7 were presented at the 2013 Algae Biomass Summit.[5,6]

---

[3] Rosenberg JN, Kobayashi N, Andlay GA, Barnes A, Oyler GA, Betenbaugh MJ. Comparative analyses of microalgae in response to light and sugar reveal distinctive lipid induction patterns for two-stage biofuel production, ABO Algae Biomass Summit (San Diego, CA), September 29 - October 2, 2014.

[4] Rosenberg JN. Biochemical shifts in *Chlorella* lipid metabolism for two-stage bioprocessing, ABO Algae Biomass Summit (San Diego, CA), Biology Breakout Session: Metabolic Regulation, September 30, 2014.

[5] Rosenberg JN, Jacobs H, Balasubramanian A, Betenbaugh MJ, Potember RS, Oyler GA. Cultivation ecology of immobilized microalgae within photosynthetic biofilms, ABO Algae Biomass Summit (Orlando, FL), October 1-3, 2013.

[6] Rasala BA, Lee P, Ng J, Barrera D, Plucinak TM, Rosenberg J, Weeks D, Oyler G, Mayfield S. Development of molecular genetic tools for algae biotechnology, ABO Algae Biomass Summit (Denver, CO), September 24-27, 2012.

Table of Contents

List of Tables

List of Figures

Everything that lives, lives not alone, nor for itself.
William Blake (1757-1827) *The Book of Thel*

1

AN INTRODUCTION TO THE CHALLENGES FACING ALGAL BIOFUEL PRODUCTION[‡]

By following the contours that civilization has carved into the global energy landscape, current societal and economic growth indicate that we are approaching perhaps the steepest gradient in energy production to date. The rise of developing nations coupled with an accelerating expansion of the global population to at least 9 billion by 2050 correlate to an increase in energy use from 533 quadrillion (10^{15}) kJ in 2008 to 812 quadrillion kJ by 2035 in order to sustain human activity [1×10^{15} kJ $\approx$ 4 million transatlantic jet flights] (Chamie 2004). Moreover, the environmental concerns related to carbon emissions and other forms of pollution from fossil fuels

[‡] This chapter contains excerpts from papers by Rosenberg *et al.* 2011 and Rogers, Rosenberg *et al.* 2014 that appeared in *Biomass & Bioenergy* and *Algal Research*, respectively. Portions of these works are reprinted here with permission from the publishers (Appendix A). Since the *Algal Research* article is available by open access, its reproduction is attributed to a Creative Commons License.

add complexity to this energy challenge. From a 4 million year old process condensing prehistoric biomass into energy-rich deposits to the discoveries and innovations in crude oil recovery over the past 400 years, it is now predicted that we may have only 40 years to wean ourselves from this expendable resource and develop sustainable alternatives (HANSEN *et al.* 2005). Accordingly, fossil fuel production in the United States is predicted to decline while renewables will continue to grow from 8% to 14% by 2035 as a result of State and Federal renewable energy portfolio programs (*e.g.*, Federal Renewable Fuels Standard) ((ENERGY INFORMATION ADMINISTRATION 2012).

It is well known that photosynthetic biomass can contribute a significant amount of renewable fuel while also assimilating carbon dioxide (CO_2). In the United States, the current goal for industrial CO_2 emission reduction is 17% by 2020, which can be accomplished by replacing fossil fuels with "carbon neutral" biofuels. However, current projections show energy-related CO_2 emissions in 2020 to reach only 9% below their 2005 level (ENERGY INFORMATION ADMINISTRATION 2013). As such, there is a need for intensified development of biofuel feedstocks (*e.g.*, starch and oilseed crops; cellulosic biomass; and microalgae) in order to meet this milestone within the coming years. In 2010, liquid biofuels represented only 1% of the total U.S. fuel portfolio but are expected to reach 4% by 2035 with nearly all consumption attributed to the transportation sector (ENERGY INFORMATION ADMINISTRATION 2012). In addition to technical obstacles facing sustainable biofuel development

(Bazilian *et al.* 2013), these next-generation liquid fuels must compete with the sheer magnitude of energy required for travel and transit.

1.1 Anthropogenic energy networks and demand for transportation fuels

Like a living organism whose body and organs are nourished by a vascular system, the vital fluid that supports our global economy is petroleum. Liquid transportation fuels for air-, sea-, and land vehicles each require unique fractions of crude oil distillates, which has enabled a steady increase in international shipments to reach over 25 million tons of air cargo and 8 billions tons of exports by boat in 2007 (U.S. Department of Transportation 2010). Aside from the cost of the goods that are bought and sold, the amount of energy that is exchanged during these transactions is enormous— each ton of air freight can require as much as 15,000 kJ per mile [1,000 kJ $\approx$ 7 hours of illumination from a 40-watt light bulb] (Cushman-Roisin 2012). While the exact amount of energy required for moving freight depends heavily on the mode of transport, the worldwide energy expenditure for shipping is still perhaps the most underappreciated form of currency, but carries a long history of technological development that once captivated our nation.

In the 1600s, the discovery of coal deposits in the U.S. along the Illinois River led to the first major commercial mining operations, permitting cross-country freight transit by railroad steam engines and eventually widespread electricity generation (Nicolls 1904). Compared to wood with an energy density of roughly 15,000 kJ per kg, coal is a more effective solid fuel at 25,000 kJ per kg and incredibly abundant with nearly 850 billion tons of reserves— sufficient for over 100 years of electricity at current

global consumption rates. Coal now accounts for 56% of the U.S. electric supply and contributes 93%, 80%, and 43% of the U.S. SO_x, NO_x, and CO_2 emissions, respectively (SPATH *et al.* 1999). For land-based transportation, the transition from a solid to liquid fuels with energy densities between 45,000–47,000 kJ per kg greatly changed the pace of travel and its accessibility for individual use and personal leisure. This paradigm shift was largely pioneered by Rudolph Diesel's engine in the late 1890s, which has led to contemporary internal combustion and jet engines (DIESEL 1898). Within the past 20 years, this inertia has propelled us into the next era of energy commerce with electric and hybrid personal vehicles employing lithium ion batteries. Compared to the previous linear progression of fossil fuels, our energy web is becoming increasingly tangled, since much of the domestic U.S. electricity is generated by burning coal (at 30% efficiency). While electric engines will continue to mature as a means of travel, they may never be a practical fuel alternative for aviation or maritime shipping and are still faced with their own sustainability issues (*e.g.*, the carbon footprint of rare metal batteries).

It is evident from recent trends in the crude oil market that the price-point of petroleum is not expected to decrease (Figure 1) while the volume of transportation may even intensify (VAN ATTEN *et al.* 2012). In addition to obvious economic implications, the interdependent factors of oil supply and demand further accentuate the need for conscientious decisions about fossil fuel emissions that may affect the environment. Regardless of proposed carbon taxes, cap-and-trade, or any other credit programs that may be able to regulate the CO_2 market going forward, the

Intergovernmental Panel on Climate Change has declared that human activity is "extremely likely" to be the "dominant" cause of climate change. This statement may finally help to motivate a targeted 80% reduction in worldwide greenhouse gas emissions by 2050 (IPCC 2013).

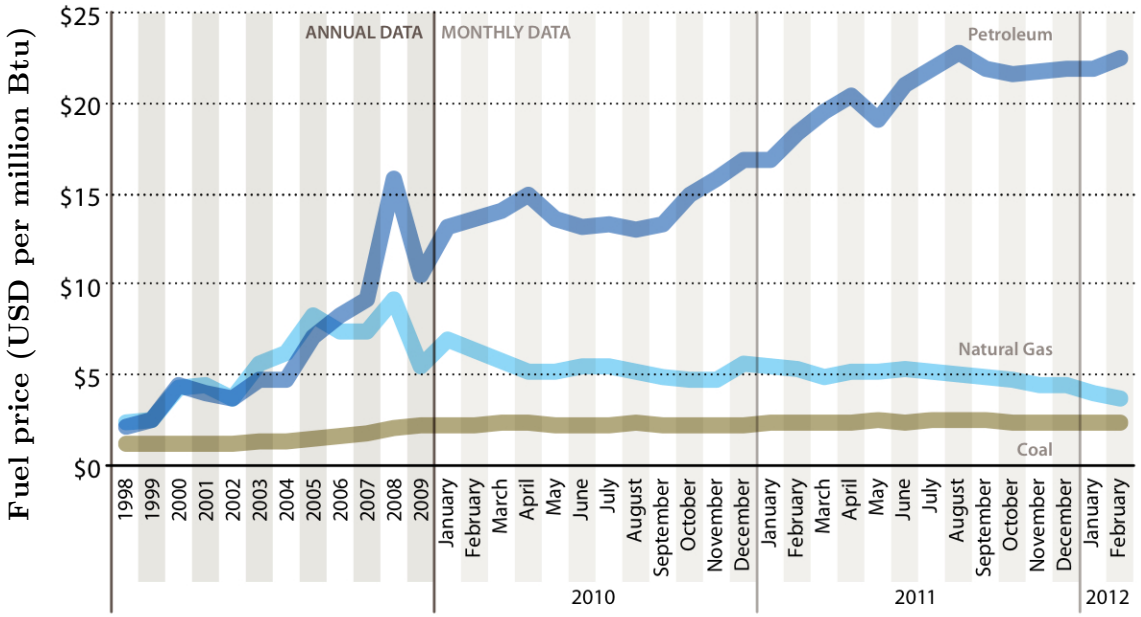

Figure 1. Comparative trends in fossil fuel cost normalized to electricity generation (1 Btu ≈ 1.06 kJ). Since 1999, the market value of coal has remained relatively constant while the prices of petroleum and natural gas have experienced significant volatility. In 2005, for example, the price of coal was $1.54 while petroleum and natural gas were sold at $7.59 and $8.21 per million Btu, respectively. Since 2010, petroleum and natural gas prices have experienced a dramatic divergence with petroleum reaching nearly $25 per million Btu while natural gas continues to approach the current cost of coal ($2.50 per million Btu). Plotted data originates from the U.S. Energy Information Administration, Electric Power Annual 2010 Data Table 3.5 and is reprinted with permission from M.J. Bradley & Associates (2012).

As an alternative to petroleum and coal, natural gas has recently gained attention as an exceedingly abundant domestic energy source for electricity generation that burns cleaner than coal, diesel, or gasoline in terms of SO_x, NO_x, and CO_2 and possesses additional benefits of fewer particulates and heavy metals (Energy Information Administration 2011). The availability of roughly 827 trillion cubic feet (TCF) of natural gas in the U.S. may reign in a new era of inexpensive and abundant fuel to different energy sectors; the current U.S. demand for natural gas is 22 TCF per year (Energy Information Administration 2011). While natural gas consumption is expected to steadily increase by 0.4% each year— ultimately reaching 26% of U.S. energy use in 2035 —the environmental impact of hydraulic fracturing (so-called "fracking") required to release shale gas is still a topic of political debate when balancing the advantages of energy independence with the risks of ecological damage. For transportation, renewable diesel and gasoline alternatives are still anticipated to bridge the gap between combustion and compressed/liquid natural gas vehicles.

1.1.1 Biorenewables as alternative liquid fuels

In the broadest sense, our entire energy landscape has been shaped by solar energy. Fossil fuels are derived from prehistoric plant material; biofuel feedstocks are comprised of modern bioenergy crops and cellulosic residuals. There are essentially no forms of energy that the sun has not touched at some point in history. In recent decades, domestic biofuel production has evolved far beyond Rudolph Diesel's original concept of using peanut oil in his engine (Diesel 1898). Many types of biofuel feedstocks have been developed and evaluated from a sustainability

perspective, beginning with the first generation of liquid biofuels produced from existing terrestrial crops, such as corn and soy for ethanol and biodiesel blends, respectively. In order to avoid the competition between food and fuel, second-generation biofuels rely on cellulose-based plant material rather than grains or oil seeds. By thermochemical or enzymatic means, cellulosic biomass, such as wood fibers and grasses, could be deconstructed to produce sugars from the cellulose (Lewandowski *et al.* 2003; Leboreiro & Hilaly 2013). The liberated sugars can ultimately be used as a substrate for microbial fermentation to produce alcohols or other hydrocarbons (Singh *et al.* 2013). Third-generation biofuels depend on non-terrestrial (typically microbial) platforms of producing liquid hydrocarbons directly, or indirectly, from concentrated sources of CO_2 (Li-Beisson & Peltier 2013; Ahmad *et al.* 2011).

One of the major contributions to climate instability comes from the increasing levels of CO_2 in the atmosphere. If left unresolved, this may pass a critical point, after which our efforts to solve this problem will be ineffective (McKibben 2008). Since it is well known that fossil fuels are significant contributors to greenhouse gas (GHG) emissions, advanced biofuels represent a positive step toward a more environmentally sound approach to transportation. While biofuels may ease this inevitable energy transition, they are certainly not a single solution for climate change. It is important to note that unless biomass grown on concentrated sources of industrial CO_2 is converted to a non-combustible state, biofuel production does not mitigate CO_2 emissions. Third-generation biofuel feedstocks can, however, leverage a second round

of combustion from CO_2 that would otherwise be released to the atmosphere.

As a third-generation biofuel feedstock, algae are perhaps the most prolific source of plant biomass on the planet and have upheld this reputation for millions of years. As a testament to their photosynthetic capacity, the crude oil and coal deposits that exist today are the result of prehistoric algae blooms that once flourished in ancient oceans. In particular, the once swamp-like environment of the Western Interior Seaway that supported rich aquatic vegetation over 100 million years ago is now mined for coal and petroleum in North America (Nicolls 1904). In the same way that algae and other aquatic organisms assimilated carbon from an ancient CO_2-rich atmosphere, the opportunity to recapitulate this process with the controlled cultivation of microalgae on large-scale farms offers a unique opportunity to enhance domestic energy production.

Microalgae have been promoted as one of the more promising third-generation biofuels and possess the hallmarks of a sustainable feedstock. Each algal cell functions as a microscopic biological factory to convert sunlight, CO_2, and nutrients (nitrogen and phosphorus) into plant-like biomass with many benefits over terrestrial crops. The unicellular structure of microalgae allows for rapid growth rates without the need for roots, shoots, or leaves, so much of the CO_2 fixed by photosynthesis can be stored as lipids, such as triacylglycerol (TAG). Unlike terrestrial bioenergy crops, microalgae do not require fertile land with extensive irrigation and can be harvested continuously. Several species of algae provide an alternative to freshwater cultivation because they are able to grow in seawater, low quality brackish water, and even

hypersaline environments.

As the foundation of aquatic food chains, microalgae are also primary producers of biomolecules with high nutritional value, such as antioxidant pigments, edible proteins, and nutraceutical oils that other crops lack (Spolaore *et al.* 2006). As such, these photosynthetic organisms have been commercially cultivated for protein, oils, and pigments for over five decades, particularly for use in aquaculture feeds. Microalgae are now poised to be a mainstay of sustainable bioprocessing for their ability to use agricultural residues and generate renewable oils that can be converted to petroleum-like "drop-in" biofuels (Rosenberg *et al.* 2008).

1.2 Toward a feasible proposition for sustainable algal biofuel production

Despite the general public awareness of the various biological sources of liquid fuels and their potential contribution to GHG reduction (Jensen & Anderson 2013), there remains little consensus on the lifecycle analyses (LCA) of many biofuels. Although there is some debate surrounding the "carbon neutrality" of biofuels in general, algae offer significant advantages as a source of aquatic biomass that can be cultivated where terrestrial bioenergy crops cannot (Wiley *et al.* 2013). As shown in Figure 2, some of the most recently compiled information on biofuel technoeconomics suggests that algae have a marginally positive energy return on investment (EROI $>$ 1), but not nearly as favorable as fossil fuels or cellulosic ethanol (National Research Council 2012). It is evident that algal feedstocks still require substantial research and development before they can compete in the bioenergy arena. For commodity-scale production of any biofuel, the choice between terrestrial, microbial,

and aquatic crops also depends strongly on the target compounds and balance between natural metabolic traits of the host and tools available for genetic improvement. To this end, another in-depth LCA and environmental performance assessment for a variety of algal biofuel production scenarios was able to quantify the GHG emissions that are contributed from each stage of the cultivation, harvesting, and extraction processes (Vasudevan *et al.* 2012) in order to demonstrate which production pathways can lead to greater reductions in GHG emissions. The most ideal cases, however, rely on biotechnological improvement of the algal organism, including genetic engineering of oil secretion capabilities (Devroe *et al.* 2010), which may not be possible with other crops. The inherent metabolic versatility of algae is certainly attractive; however, genetic improvement of strains will likely face environmental regulation upon commercial deployment (Snow & Smith 2012).

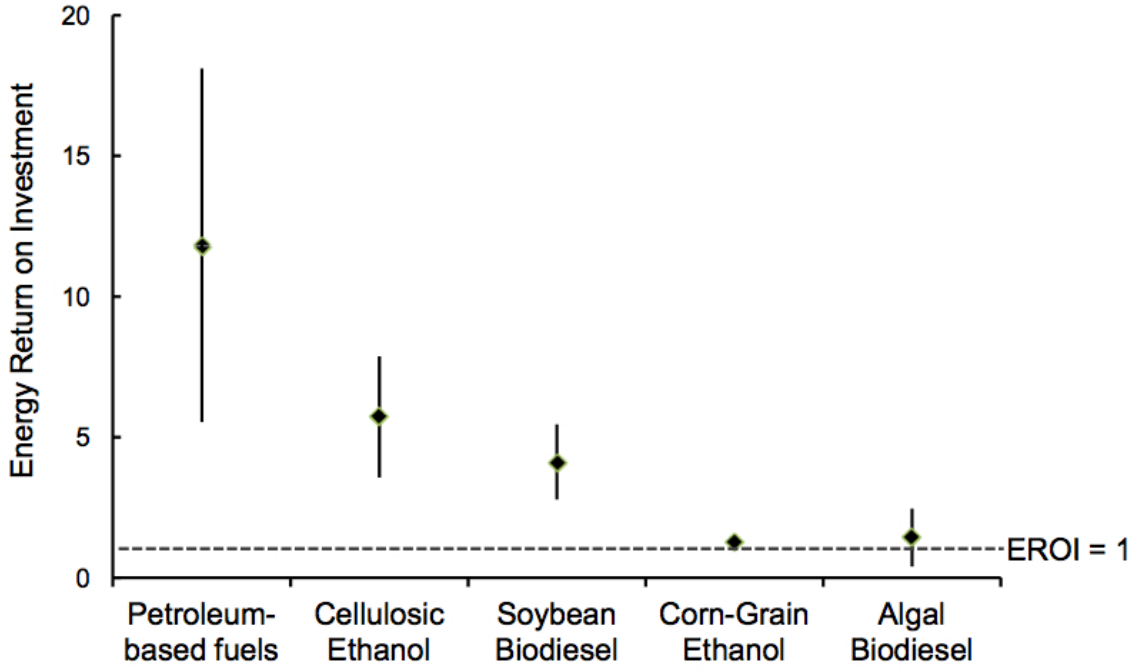

Figure 2. A comparison of energy return on investment (EROI) for a variety of biofuels as well as fossil fuel. A key determinant of the overall feasibility of fuel production pathways is the EROI. Despite relative uncertainties associated with each production process, this figure illustrates the superior energy value of petroleum-based fuel relative to the energy required to unearth this resource. Conversely, biofuels are listed in descending order of EROI with corn and algal-based fuels barely surpassing the critical threshold of EROI = 1. Error lines associated with each data point represent one standard deviation from the mean. (National Research Council 2012). Reprinted with permission from the National Academy of Sciences report entitled *Sustainable Development of Algal Biofuels in the United States* (2012). Courtesy of the National Academies Press, Washington DC.

Within the past five years, some of the first large-scale algal biofuel production facilities have broken ground in the U.S. (Table 1). While these operations act as beacons to guide the path of advanced algal biofuel development, the lack of uniformity in technology and crop still makes it difficult to evaluate their impact. Although there is well-documented literature on the domestication of algal species for natural products as well as applied biological and engineering research to improve PBR and pond design, these organisms have yet to gain full traction at large scales.

As in many bioprocessing and biotechnology fields, commercial ventures exploring algal biofuel production appear to be moving at an accelerated rate compared to academic research. However, it has been proposed that some of the most effective steps forward can be achieved through the synergies of public-private partnerships, as evidenced by the formation of a number of national consortia for algae biofuel development and academic testbeds— *e.g.*, the National Alliance for Advanced Biofuels and Bioproducts (NAABB), the Algae Testbed Public-Private Partnership (ATP^3), and the Consortium for Algal Biofuels Commercialization (CAB-Comm). These strategic partnerships underscore the need for government subsidies at this early stage in an emerging field. While the instigation of both public and private acceptance of microalgal feedstocks has also taken time, recent legislation finally considers algae a "qualified feedstock," making algae-derived biofuels eligible for $1.01 tax credit per gallon (Section 40 of United States Code). Previously, algae-based feedstocks were specifically excluded from the U.S. Farm Bill, despite lobbying efforts seeking to allow algae projects to be eligible for additional support.

Nonetheless, the reluctance to fully accept microalgae as a viable feedstock is warranted due to photosynthetic constraints and bioprocessing challenges related to large-scale cultivation of microbes in water. Furthermore, geographic site selection based on climate and resource availability critically impacts the feasibility of algae farms. Many commercial ventures have chosen New Mexico as a preferred location for microalgal biofuel production due to its flat geography, warm climate, and high levels of year-round solar irradiance. In September of 2012, Joule Unlimited Technologies piloted its *SunSprings*^{TM} technology for bioethanol production in Hobbs, NM using bioengineered cyanobacteria to secrete ethanol into the aqueous media. A similar technology developed by Algenol Biofuels is poised for commercial-scale deployment in Florida and Texas. Sapphire Energy is another algae biofuel company with focusing on the production of biofuel from algae as opposed to co-products in a more flexible biorefinery model (Sabarsky 2010; Liu *et al.* 2013). Sapphire is currently constructing its first large-scale plant in Columbus, NM with a target production rates of 100 bbl d^{-1} using 300 acres of raceway ponds.

Company	Location	Technology
Algae Systems	Daphne, AL	Offshore membrane enclosed algae growth
Algae to Omega	Oakland Park, FL	Closed bioreactors for oils and supplements
Algenol	Fort Myers, FL*	Photosynthetic ethanol secretion in PBR
Aurora Algae	Hayward, CA	Strain development for food, feed, & fuel
BioProcess Algae	Shenandoah, IA	Solid-phase growth, integrated biorefinery
Cellana	Kona, HI	Hybrid system for biofuel and fishfeed
Cyanotech	Kona, HI	Open ponds for high-value nutritionals
Earthrise Farms	Irvine, CA	Nutritional algae in 4-ha raceway ponds
Heliae	Gilbert, AZ	Modular ponds for mixotrophic growth
Hydromentia	Tampa, FL	Benthic algal turf scrubber, bioremediation
Joule Unlimited	Hobbs, NM*	Photosynthetic biofuel secretion in PBR
Martek/DSM	Columbia, MD	Heterotrophic algae for nutrition & biofuels
Phycal	Highland Heights, OH	Biofuels from auto/hetero algae, cassava
Sapphire Energy	Columbus, NM*	Open raceway ponds for green crude
Solazyme	Peoria, IL*	Heterotrophic algae for nutritional oils
Triton	San Diego, CA	Strain engineering, recombinant proteins
University		
Arizona State University	Mesa, AZ	Outdoor raceway ponds and PBRs
California Polytechnic	San Luis Obispo, CA	Algae biofuel from wastewater
New Mexico State University	Las Crusas, NM	Geothermal greenhouse testbed
UC-San Diego	La Jolla, CA*	Outdoor raceway ponds and PBRs

Table 1. Industrial and academic operations exploring research, development, and commercialization of algae biotechnologies. This list of companies and universities with large-scale facilities in the United States showcases sites that have received regulatory approval for outdoor field testing and commercial production (*). The demonstration-scale academic testbeds are also examining alternative pathways to algal biomass production in parallel. Adapted from Rosenberg *et al.* 2014.

1.2.1 Established methods of microalgal cultivation for biofuels

Cyanobacteria and microalgae include countless species and strains that are adept at surviving in diverse habitats (Tirichine & Bowler 2011). As a result, these microbes have evolved unique and versatile metabolic functions, which give rise to varying biomass compositions (Singh *et al.* 2013). Over the past five decades, various classes of metabolites produced by algae have been used as animal-free nutritional additives and high-value pigments for cosmetics and biotechnology (Pulz & Gross 2004). Unlike most microbial feedstocks that are produced exclusively in closed bioreactors with heterotrophic fermentation, algae prosper from open-air cultivation where sunlight is readily available. With these simple growth requirements of CO_2 and sunlight, photosynthetic microbes exhibit fast growth rates and produce biomass that is "generally regarded as safe" (GRAS) for human consumption. As such, natural products derived from algae have contributed to markets including fish feed, human nutritional supplements, and cosmetic pigments, as well as specialty chemicals for research purposes (Rosenberg *et al.* 2008). A number of different photosynthetic microalgal species have been cultivated commercially for both nutritional applications and the production of unique fine biochemicals. Some genera, including *Haematococcus*, *Dunaliella*, and *Chlorella* have the capacity to produce high-value carotenoids, such as β-carotene, lutein, and astaxanthin, which have been shown to provide various health benefits as powerful antioxidants (Fernandez-Sevilla *et al.* 2010; Barbosa *et al.* 2005; Lorenz & Cysewski 2000). Beta-carotene and astaxanthin have been demonstrated to limit the ability of free radicals to damage cells (Rao *et al.* 2007; Guerin *et al.* 2003). Most

people would recognize astaxanthin as the pigment that adds red color to crustaceans; the pink flesh of salmon is another example (Dufossé 2007). *Spirulina* specie have also been cultivated historically as a protein-rich food supplement and aquaculture feed additive (Radmer & Parker 1993). The success of these species is largely attributed to their low-cost culturing systems as well as their ability to grown in extreme conditions. *Spirulina* can grow in highly alkaline conditions with a pH as high as 10, while *D. salina* can withstand highly saline conditions ten-fold greater than seawater (Weldy & Huesemann 2007).

In the United States, algae have been typically grown in the southwest to produce edible biomass and nutraceuticals (Olaizola 2003). Depending on the species and growth conditions, algae can be selected to produce large quantities of lipids, protein or carbohydrates. Over the course of three decades, the National Renewable Energy Laboratory conducted extensive research into the capacity of algae to produce usable lipids under the Aquatic Species Program (Sheehan *et al.* 1998). Now, over 15 years after the program's close-out, the ability to generate large quantities of lipids, specifically energy-dense extractable TAGs, on non-arable land has led to a renewed interest in using microalgae to produce biofuels (Hu *et al* 2008). While producing biomass photosynthetically, algae assimilate CO_2 as their primary carbon source and have demonstrated the capacity to sequester flue gas from power plants (Kadam 1997; Nishikawa *et al.* 1992). Microalgae can be continuously harvested for their lipids, which can be further processed into a variety of biofuels (Schlaggerman *et al.* 2012). As an example, photosynthetically grown *Chlorella* can achieve total oil

contents between roughly 20-35% of its dry biomass (Benemann & Oswald 1996; Chisti 2007). *Chlorella* and *Scenedesmus* species both have significant potential for fuel production due to their high biomass productivities and compositions (Hu *et al.* 2008).

Two of the most common microalgal culturing systems are outdoor raceway ponds and closed photobioreactors (PBR). These technologies have been proven and successfully operated by different sectors of the algaculture industry, in which arrays of PBRs are typically used to grow axenic seed cultures to inoculate large acreage farms of raceway ponds (Huntley & Redalje 2007). However, some of the major hurdles in commercially cultivating algae outdoors are low areal productivity and low culture density. Algae grow to average densities between 0.5-2.0 g L^{-1} in outdoor raceway ponds at areal productivities of 5-20 g m^{-2} d^{-1} (Weissman *et al.* 1989). This wide range of areal productivities is oftentimes due to the variability in temperature and sunlight. High rates of productivity can be maintained by harvesting the culture on a daily basis, which promotes high growth rates by preventing nutrient depletion and mutual shading, caused by high-density cultures.

Mass cultivation of microalgae was pioneered in the early 1950s with *Chlorella* (Burlew 1953) and quickly transitioned into a modular production process using Oswald's raceway design termed "high rate ponds" (HRPs) for large-scale recirculating algae cultivation (Oswald 1962), which is now regarded as the most cost-effective vessel for growing algae at large-scales. The predominant design for these ponds is a rectangular raceway made from two trenches dug in the ground with

a separating barrier; this allows for water to flow in a circular motion around the pond, similar to a racetrack (Figure 3A). Raceway ponds have been used since the 1970s and are currently being operated in Japan, Taiwan, Mexico, Israel, Thailand and the United States (Archer & Barber 2004). The bottom of the pond is compacted and typically lined with a heavy duty plastic, such as polyvinyl chloride (PVC) or high-density polyethylene (HDPE), to prevent the loss of media and nutrients. A pond depth between 10-30 cm allows for maximum sunlight penetration and a paddlewheel mixer is used to prevent the algae from settling (Chisti 2007; Neenan *et al.* 1986). The paddlewheel has a low clearance with the sides and the bottom of the pond, which prevents backflow and allows all of the power of the paddlewheel to mix the pond, ensuring that algal cells are equally exposed to sunlight. The paddlewheel, along with the smooth plastic lining also prevents regions of nutrient deprivation. An added benefit of raceway ponds is their low construction costs relative to PBRs and more simple operation, requiring only a few parameters to be controlled, such as CO_2, mixing velocity, and nutrient concentration. Commercial scale raceway ponds as large as four hectares have been operated by Earthrise Farms in California (Benemann 2003).

Evaporation and convection can account for substantial losses in culture volume from algae farm operations. To prevent the escape water from open raceway ponds, a greenhouse structure can be erected directly over each raceway pond (Figure 3B). This physical barrier also serves to protect the pond from contamination. Key criteria for selecting a glazing material are cost, lifespan, strength, weight, light

transmission, and thermal conductance. While greenhouse enclosures represent an additional capital cost, they may be necessary to reduce evaporative losses and maintain monocultures through biocontainment. This issue remains an ongoing topic of investigation and the proceeding chapter incorporates this variable into the technoeconomics of algal biomass production. For example, Sapphire Energy's farm in New Mexico consists entirely of open ponds, while Heliae is pioneering a modular raceway production system (Volaris^{TM}) contained in a greenhouse with process control feedback for mixotrophic growth with both light and sugar sources.

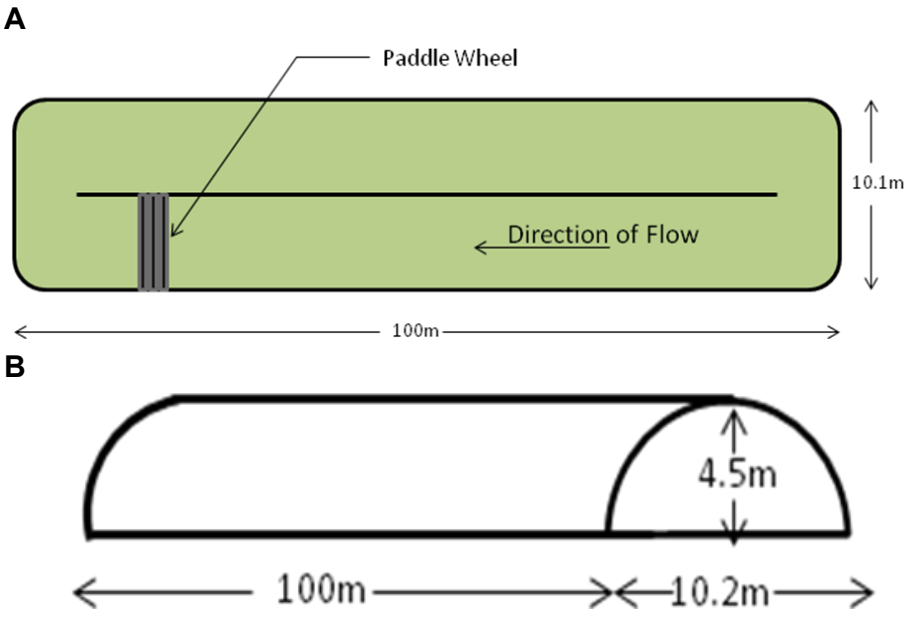

Figure 3. Schematic diagram of single high-rate pond (HRP) commonly used in raceway pond arrays. The dimensions of a quarter-acre raceway pond are shown as an **(A)** aerial view with **(B)** a possible greenhouse covering.

Species selection and strain development for large-scale production

Despite recent fluctuations in U.S. Renewable Fuel Standards, the Energy Independence and Security Act of 2007 mandated a 36 billion gallon per year production goal for renewable liquid fuels. In order for algae to meaningfully contribute to even a fraction of this benchmark, the scale of algal cultivation will require farms that are many orders of magnitude larger than most current operations. These immense projects are coupled with entirely different technical hurdles, ranging from the logistics of watering handling to regulatory control, and potential for varying degrees of public acceptance. Although outdoor evaluation of algal cultivation in raceway ponds and other photobioreactor systems is becoming more prevalent (Table 1), microalgae and cyanobacteria have yet to reach production maturity at commercial scales (tens of thousands of acres). Aside from capital and operating costs of algae biofuel production in the field, which is evaluated in the next chapter, there is a considerable amount of research and development (R&D) necessary to generate production organisms that will both meet (or exceed) biological objectives and adhere to environmental regulation.

Initial regulatory oversight for outdoor algal cultivation in the United States was considered by the U.S. Department of Agriculture's Animal and Plant Health Inspection Service (USDA APHIS), the Environmental Protection Agency (EPA), and the U.S. Food and Drug Administration (FDA). Ultimately, transgenic algae for renewable fuel production fell under the EPA's existing mechanisms of assessing biotechnological use of microorganisms. While this is appropriate for biofels, future

applications of algal cultivation for agricultural use may be regulated by the USDA. In 1998, the EPA established two routes for regulatory review of transgenic microbes, focusing on associated environmental safety and human pathogen control. The EPA's "Microbial Commercial Activity Notice" (MCAN) is typically filed before pre-commercial field-testing in either closed bioreactors or well-controlled open systems. For commercial-scale operations, photosynthetic microbes and their byproducts will be regulated under the EPA's Toxic Substances Control Act (TSCA), for which a "TSCA Environmental Release Application" (TERA) must be filed to rule out the possibility that any recombinant products or non-essential transgenes may carry toxic or allergenic effects. Historically, MCANs and TERAs have sought approval for the production of biochemicals, such as industrial enzymes (*e.g.*, amylase, phytase), cellulosic ethanol, and soil additives using recombinant heterotrophs. These host organisms were predominantly bacteria and fungi including *E. coli*, *Trichoderma*, *Pseudomonas*, *Bacillus*, *Zymomonas*, *Saccharomyces*, and *Pichia* species cultivated in closed bioreactors with contained effluent.

Before new embodiments of GM microalgae can even be considered for EPA approval, a lengthy pipeline of trait selection and design of a suitable expression system must be developed for each region of deployment and specific biofuel application. This timeline can span many months to multiple years prior to filing TERA or MCAN requests (Figure 4). For example, native strains of algae and cyanobacteria are often bioprospected as platforms for biofuel production with certain selection criteria, such as robust growth, hardiness during conditions of

environmental stress, resilient population dynamics in response to intruding microbes, and resistance to predation. After these algal strains are identified, transgene expression systems can be developed by adapting known genetic elements and selectable markers to the strains' unique genome. Various classical methods of genetic transformation including agrobacterium vectors, plant promoters, and other basic methods of gene incorporation such as microparticle bombardment or electroporation can then be used to accomplish transgene integration (ROSENBERG *et al.* 2008). Concurrently, gene targets that may confer industrial fitness, expanded metabolic capabilities, or increased rates of biomass production can be determined in a somewhat independent manner. Trait discovery campaigns may follow a few different approaches to achieve lead transgene candidates including (1) panning large cDNA libraries generated from different organisms grown under different conditions; (2) pursuing directed evolution of proteins for variants with enhanced enzymatic or regulatory characteristics; and (3) executing hypothesis based selection of previously characterized genes with desired function. Once gene targets are identified, they can be cloned into expression vectors and transformed in an algal platform ready to enter the GM strain pipeline for assessment and validation. For example, competition-driven selection of industrial fitness can be accomplished using turbidostat experiments in which a mixed culture of wild-type algal cells are grown with a minority population of engineered organisms. While keeping the culture's cell density constant, GM cells with particular survival advantages will dominate the population over the growth period and can be recovered for further analysis and characterization.

Figure 4. (*next page*) Schematic timelines for commercial strain development. This figure depicts milestones for three production scenarios: **(A)** commodity-scale products derived from algae biomass (*e.g.*, biofuel) including an initial bioprospecting stage for a novel strain platform; **(B)** similar commodity-scale algae production using an existing transgenic strain platform; and **(C)** recombinant expression of high-value proteins in *C. reinhardtii*. All of these laboratory research and field development activities can require millions of dollars in upfront investment (*e.g.*, intellectual property). While the TEA analysis in the next chapter does not take these considerations into account, they should not be underestimated.

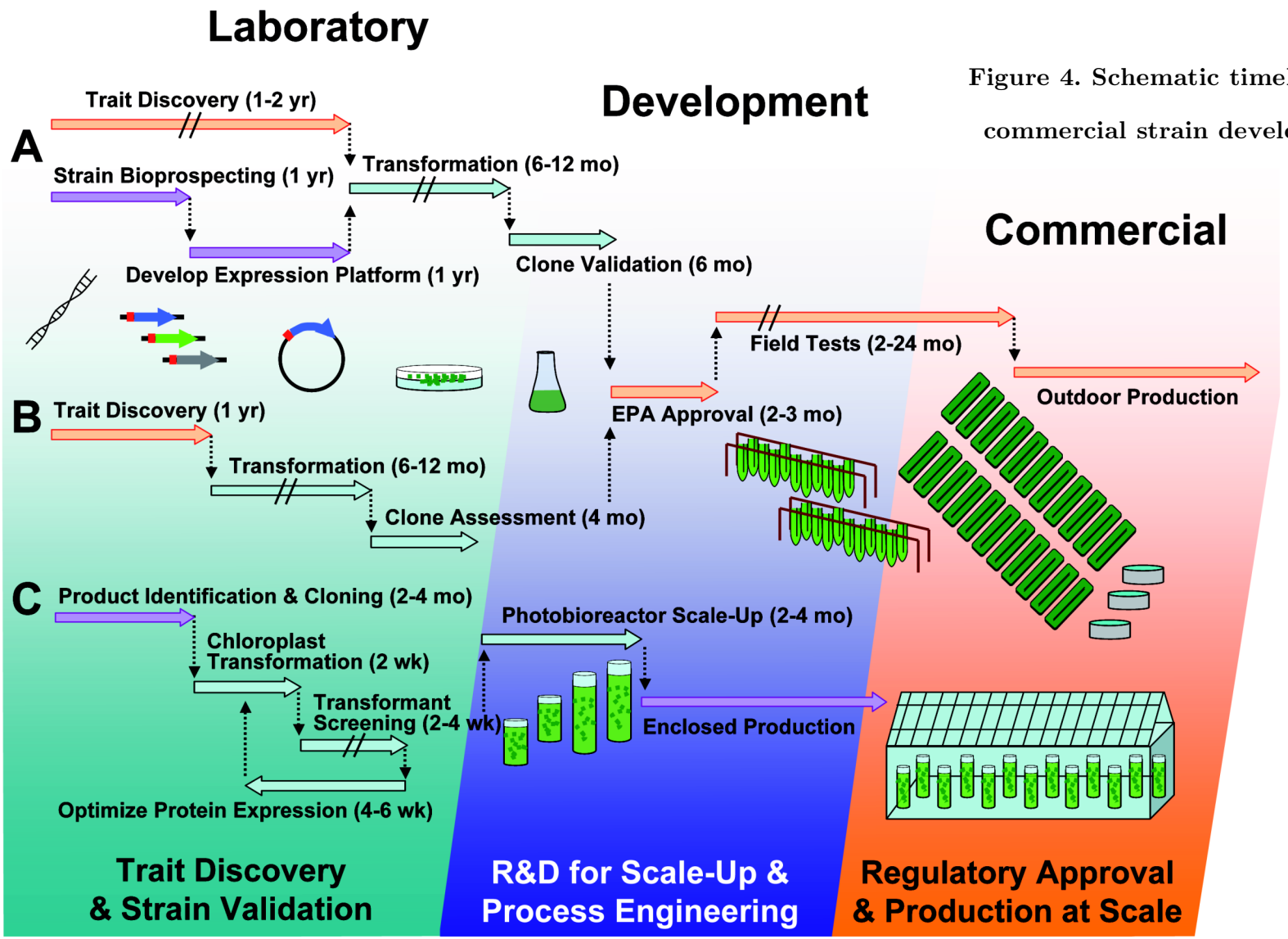

Figure 4. Schematic timelines for commercial strain development.

With a wide range of efforts focused on enabling the transition of these organisms from bench-top laboratory experiments to field trials, two algal biofuel companies have already received regulatory approval for the controlled outdoor cultivation of proprietary transgenic algae and cyanobacteria, which is truly an industry first (Joule Unlimited Technologies 2012; Sapphire Energy 2013). Two additional companies currently have EPA TSCA applications under review (Table 1). Aside from Sapphire Energy, all of these applications involve contained growth systems, but still represents a significant step toward commercialization of GM algae in outdoor environments. One of roughly five national testbeds for open-air algae cultivation is the University of California–San Diego (UCSD) Biology Field Station, which is the designated experimental site for Sapphire's TERA. Scale-up of open cultures at this facility using polyethylene hanging bags and air-lift driven raceway ponds has been described recently with anticipated transition to the 300-acre commercial site in Columbus, NM (Schoepp *et al.* 2014). With a nearly exponential increase in MCAN filings between 2010 and 2013, it is anticipated that GM microbes will become even more prevalent in industrial biochemical production. While strain selection and engineering is an integral part of algal biofuel development that can significantly impact biofuel processing, this dissertation will focus on mechanisms to improve algal biomass cultivation in the field. Once production strains actually reach pond or PBR production, the next major upstream considerations for algal cultivation involve energy input and associated costs required for growth as well as nutrient sourcing logistics. These topics are discussed in the following sections.

1.2.2 Limitations of conventional algae growth systems

Despite their prevalence in the algae industry, high volume recirculating ponds (*i.e.*, raceway ponds) and high performance PBRs are associated with significant water and energy demands for both the cultivation and harvesting of biomass from relatively dilute solutions (< 2 g L^{-1}). This bottleneck may certainly pose a concern for the sustainability of algal biofuels. Nonetheless, raceways dominate the algae farm landscape and continued R&D efforts seem to remain on course with their deployment despite potential challenges in scaling of these ponds originally designed by Oswald (1962). Individual 2-acre high rate ponds (HRPs) were originally designed for nitrogen and phosphate remediation in the final "polishing" stages of wastewater treatment (WWT), not for highly productive biomass growth. While algae are very effective at removing low concentrations of nutrients from water, the productivity of algae in HRPs is many orders of magnitude below the yields necessary to make biofuels a national commodity. In order to minimize liquid volume during growth, a paradigm shift in the structure of cultivation systems will be necessary.

In addition to pond design, the algae industry also has the unique opportunity to learn from prior agricultural missteps while developing the infrastructure for this new energy crop. The avoidance of synthetic fertilizers and other unsustainable feedstocks for growth will be another challenge for the algae industry. Algae, like terrestrial plants, require nitrogen- and phosphorus-based fertilizers, which are readily available at existing wastewater treatment sites and agricultural point sources. By co-localizing large-scale microalgal cultivation with existing sources of carbon, N, and P

emissions, CO_2 sequestration and nutrient absorption can be coupled with the growth of algae, which can then be used as feedstock for biofuel production.

As an alternative to photosynthetic growth of algae, heterotrophic cultivation (with organic substrates, without light) has been used commercially to enhance lipid biosynthesis in algae. As an example, omega-3 fatty acids produced by heterotrophic algae are useful dietary supplements for humans. Omega-3s are a family of long chain polyunsaturated lipids that have been shown to improve early brain developmental in children and sustain healthy cardiac function in adults (Mozaffarian & Wu 2011). Paramount candidates in this group are eicosapentaenoic acid and docosahexaenoic acid (Lippmeier *et al.* 2009). In addition to these high-value fatty acids, algae naturally store energy as lipids in the form of TAGs during heterotrophy. Unless autotrophic cultures are nitrogen-deprived, actively growing photosynthetic microalgae contain between 10-35% of their total dry weight as oils, which exist as mostly polar lipids in the cell membrane and small qualities of neutral lipids (TAGs). Conversely, heterotrophic algae grown with sugar can routinely reach 30-60% total lipids with high percentages of TAGs (Miao & Wu 2006). While these favorable neutral lipid contents are appealing for bioenergy applications, constraints imposed by both the cost of sugar substrates and the potential for bacterial and fungal contamination have limited the potential for heterotrophic microalgae to be scaled to biofuel proportions. Overcoming the bioprocessing challenges associated with both photoautotrophic (N, P) and heterotrophic (sugars) nutrient sourcing are active areas of research, which are described in detail in the following sections.

1.3 Integrated algal cultivation as a mechanism of nutrient reclamation

In order to ensure global food security, the agricultural revolution has successfully provided sustenance for our rapidly expanding population. However, by 2008, farmers were applying 37.4 billion pounds of phosphorus to their fields annually (Elser & White 2010). In Maryland alone, roughly 300 million pounds of nitrogen are discharged into the Chesapeake Bay each year (Burke 2008). Nutrient runoff presents a worldwide concern as manifested by the coastal "dead zones" caused by algae overgrowth— skewing the balance of aquatic ecosystems. Despite this unfavorable reputation, microalgal biomass is well suited for water restoration and alternative energy production to attenuate climate change. Compared to phytoremediation with terrestrial crops such as switchgrass and poplar, or even macroalgae turf scrubbers located in waterways to absorb fertilizer runoff from non-point sources (Mulbry *et al.* 2010), microalgae are well suited for nutrient mitigation from point-sources, such as concentrated livestock operations and wastewater treatment facilities.

The accomplishments of agricultural plant science have set a precedent for algal biotechnology and serve as a blueprint for continued development of this emerging industry. Progressive trends in effective fertilizer utilization and nutrient recycle, offer particular advantages to algal biofuel production with a foundation of sustainable and environmentally-conscious practices. While large-scale microalgal operations can benefit from the knowledge and experience of thousands of years of seasonal crop rotation, the industry may also learn from aspects of the agribusiness

model that may be untenable in aquatic systems. For example, preservation of terrestrial monocultures in the field is often accomplished by genetic resistance to herbicides and pesticides. For algal biofuels, the scale (and volume) of cultivation may prohibit the use of these chemical countermeasures. Thus, expanding upon the current methods of algae cultivation for nutrient bioremediation, potentially in a distributed fashion, will further support algae as a viable microbial crop.

1.3.1 Biogeochemical nitrogen, phosphorus, and organic carbon cycles

All living organisms participate in the physical state of our planet, which has recently adapted to the rapidly changing role of humans in natural ecosystems. This concept remains a central tenet in both biology and geochemistry. The Earth can even be compared to a living being itself, with the atmosphere and ozone layer exhibiting the fluidity of a cell membrane. For example, the atmosphere has changed significantly from a state of high CO_2 and low O_2— the current composition of roughly 21% oxygen was created by photosynthesis. Plants have not only played a dedicated role in this metamorphosis, but have also evolved to cope with the dynamic environmental conditions. In turn, nutrient cycles have been regulated and modulated by these *bio*-geochemical events. Marine microalgae and cyanobacteria have historically accounted for a significant portion of the nitrogen fixation, oxygen evolution, and photosynthetic activity on Earth (Martiny *et al.* 2013). Furthermore, modern human interaction with the geochemistry of our planet is evidenced by the fact that 120 million tons of the global bioavailable nitrogen (N) comes from the hundred-year-old Haber-Bosch process to chemically synthesize ammonia, which

accounts for approximately half of the N in your body right now (Erisman *et al.* 2008). However, as we adopt biological production pathways in place of conventional chemical processing, biogeochemical engineering approaches may fulfill our escalating demands for natural resources. As an example, phosphorus (P) is a finite resource that is mined from limited rock salt reserves. The idea of "peak phosphorus" has even been proposed recently, which underscores an incentive to recycle these vital elements (Cordell 2010). Thus, rather than burning fossil fuels to accomplish Haber-Bosch nitrogen fixation, we may envision the reciprocal objective of producing renewable energy and nutritional feedstocks from residual fertilizers, CO_2 emissions, and organic wastes with algae. Many of the aforementioned biogeochemical factors leading to this unique position of integrated algae cultivation are depicted in Figure 5.

Figure 5. ***(next page)*** **A schematic diagram of integrated algae cultivation.** The major nodes and pathways within the nutrient recycle network toward end products of biofuels and animal feed are illustrated. With N and P originating from chemical synthesis and mined reserves at the top of this info-graphic, their use can be followed down to agriculture and livestock. These nutrients can ultimately be recovered from open waterways via macroalgae on an "algal turf scrubber" or by microalgae in raceway ponds after the N and P are converted to bioavailable forms using anaerobic digestion (AD). The natural synergies between bioremediation and bioenergy production can also permit the integration of industrial CO_2 emissions (*e.g.*, ethanol biorefinery).

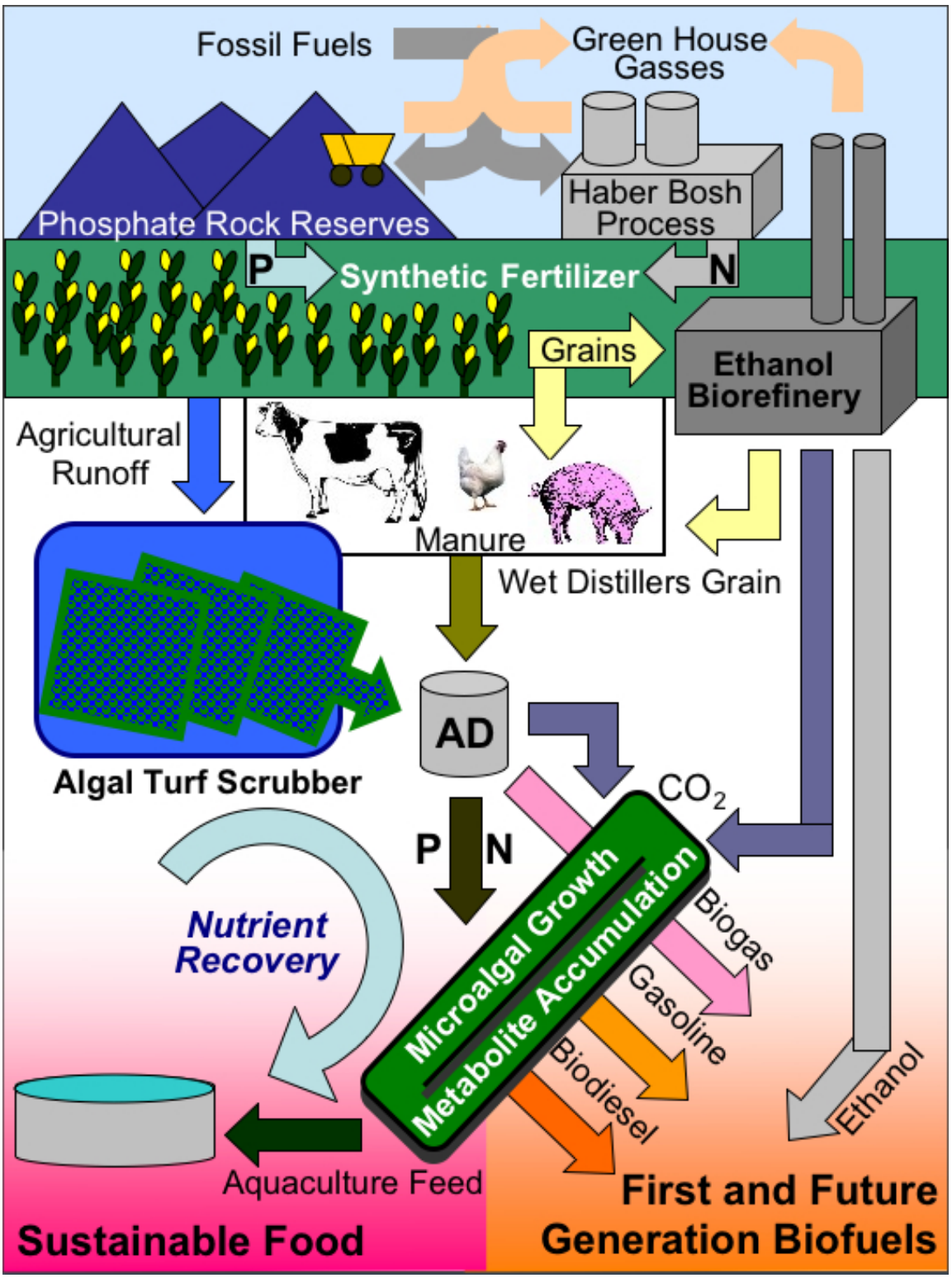

Figure 5. A schematic diagram of integrated algae cultivation.

1.3.2 Bioenergy from industrial emissions and agricultural residues

In order to both produce algal biomass and mitigate point sources of GHGs, coupling microalgal production facilities and industrial CO_2 emissions has been promoted and investigated for decades (Sheehan *et al.* 1998; Benemann & Oswald 1996; Neenan *et al.* 1986). Despite many years of interest in this approach, the technology has only reached pilot-scale development within recent years and is still not entirely successful. For instance, an early venture carried out by the start-up, GreenFuel Technologies, aimed to adapt microalgal species to grow in closed PBRs aerated with unfiltered flue gas. Due to inconsistencies and unexpected consequences of large-scale growth in closed systems during demonstration-scale production, the company quickly discontinued the technology (Dimitrov 2007). However, this has not stopped the ongoing pursuit of CO_2 capture with integrated algae cultivation. For example, based on the long history of algae biotechnology and favorable climate of Israel, a partnership between the algal cultivation leader Seambiotic Inc. and the Israeli Electric Company plans to produce algal biofuel using flue gas from coal-fired power plants (Dr. Ami Ben-Amotz, personal communication). While other domestic and international sites with flue gas are being evaluated for algae co-utilization, only small-scale demonstrations have been successful (Razzak *et al.* 2013). Despite the prospects of these technologies, extrapolating CO_2 feedstock demand to the scales required for commercial algae production suggestes that the magnitude of concentrated industrial CO_2 emissions alone is inadequate to sustain the amount of biofuels required to meet projected energy consumption rates (Chisti 2013). Based on this fundamental feedstock limitation to photosynthetic cultivation of microalgae,

heterotrophic or mixotrophic production strategies may still have a role in the future commercialization of algal biofuels with the opportunity for *strategic* nutrient supplementation. For example, most model algal organisms used to study photosynthesis, physiology, and molecular biology in the laboratory exhibit high growth rates because they are cultivated mixotrophically (*e.g.*, *Chlamydomonas reinhardtii* with acetate), which makes the timescales for growth experiments more practical. This approach is suitable at small to moderate scales, but does not always translate to production scales with algae crops on the global bioenergy stage. Nonetheless, there exist a variety of industrial-scale sources of organic wastes that could support mixo– or heterotrophic growth of algae at large scales, including aquaculture wastewater, leachate from food composting and processing industry (*e.g.*, potato starches, residual sugars), and glycerol byproducts of biodiesel production.

Regardless of the type of carbon feedstock, all algae require N and P for the biosynthesis of basic amino acids, DNA, and other components of their biomass. These common components of plant fertilizers are readily available at existing WWT sites and agricultural point sources as concentrated nutrient resources. Anaerobic digestion (AD) is a well-established process to degrade solids (*e.g.*, manure) into bioavailable N and P as liquid effluent, which has been known to promote prolific photosynthetic growth of microalgae (Olguín *et al.* 1994) and has been reviewed extensively (Razzak *et al.* 2013). Therefore, integrating algae growth systems with N and P nutrients from aqua– and agricultural sources may assure a more competitive

role for algae by both improving the composition of biomass for end-products and overcoming feedstock limitations cost and availability.

1.3.3 Algae as the biological integrator of locally abundant "wastes"

Based on the longstanding role of microalgae in WWT technologies, it is not surprising that the successful growth of many species of green algae has been accomplished using waste effluents from industrial, municipal, and agricultural sources (Cho *et al.* 2011; Li *et al.* 2011; Kothari *et al.* 2012; Hu *et al.* 2012; Chinnasamy *et al.* 2010; Razzak *et al.* 2013). However, many of these studies have used sterilized wastewaters in order to assess the nutrient status alone and avoid contamination issues with algal cultivation. While this is a standard and pragmatic approach for laboratory evaluation, it would be unrealistic and economically prohibitive to sterilize these effluents for commercial-scale algae production. Furthermore, a critical objective of future algal biofuel production will be to integrate waste nutrients while sustaining maximal accumulation of high energy-density oils in algal biomass by pairing proper cultivation systems with proper waste nutrients sources. Collectively, the cited studies demonstrate that a wide range of waste streams can support algae growth, but variation in lipid content can be attributed to biochemical factors involved in triggering lipid storage in green algae: nitrogen limitation and/or the presence of fixed organic substrates to support heterotrophic metabolism. Therefore, some remaining research questions pertain to the actual configuration of integrated algae cultivation directed at algal oil production. Can integrated cultivation be deployed in a distributed fashion that is

tailored to each application and still meet the same production goals? Alternatively, could waste be transported to centralized algae farms and, if so, at what scale would this be feasible? Does the incorporation of biological wastes at large-scales carry any environmental or public health implications?

For any of these scenarios, a minimal footprint for cultivation is desirable. As such, optimization of the physical attributes of photobioreactors and their placement in an integrated process aims to maximize solar collection and high-density algal biomass production on minimal acreage. For non-point sources, such as waterways and tributaries that suffer from abundant nutrient run-off, an "algal turfs scrubber" (ATS) relies on the natural adhesion of benthic macroalgae and potentially microalgal organisms on floating plastic screens to grow biomass from excess N and P in open waters (Mulbry *et al.* 2010; Sandefur *et al.* 2014). These systems have the advantage of growing algae totally independent of land and groundwater usage, but do not allow any control over the biomass that is grown. In most cases the total lipid content of ATS-derived biomass is low and the harvested material can contain high amounts of debris and silk. Nonetheless, this is essentially the only feasible option for nutrient reduction in open waters. For the assimilation of N and P from point sources, however, algae production in raceway ponds is commonplace (0.05% solids), but yields are generally constrained by light penetration and require harvesting methods that can be costly to scale-up (flocculation, settling, and centrifugation). Photobioreactors can increase biomass productivity with higher cell densities (1% solids) due to more sufficient exposure to light and are appealing for

small-scale applications or offshore production (Wiley *et al.* 2013). For on-site WWT, rotating biofilm surface contactors or "rotating algae biofilm reactors" (RABRs) have been used for many decades and have been successfully adapted to current algal biomass production objectives (Christenson & Sims 2012). More recently, redesigned RABR systems employ naturally adherent biofilms as a substratum that can be implanted with an addition of a dense inoculum of a desired microalgae species (Blanken *et al.* 2014). However, RABRs operated in open systems with natural biofilms still lack full biological control over the cultivated biomass and have similar energy requirements as the paddlewheels in raceway ponds. To overcome these issues, alternative configurations of immobilized microalgae—either as biofilms or polymer bead entrapments—have been developed for wastewater remediation and have structural advantages over prior growth systems (Mallick 2002; de-Bashan & Bashan 2010; Eroglu *et al.* 2012; Muñoz *et al.* 2009). Immobilized biofilms represent an ideal architecture to absorb nutrients from wastewater and can generally achieve higher biomass densities of 5-15% solids (Schnurr *et al.* 2013). This may certainly reduce typical harvesting costs required to bring algae culture to at least 10% solids before oil processing or other conversion to biofuel. Due to variation in both microalgal populations and culture environment, algae biofilm productivities have been reported anywhere between 2–30 g m^{-2} d^{-1} (Sandefur *et al.* 2014; Blanken *et al.* 2014). However, the oil content of this biomass may be a more critical determinant in assessing these technologies for biofuel applications (Schnurr *et al.* 2013).

1.4 Research objectives and structure of this dissertation

As detailed in the prior sections of this chapter, microalgae are versatile organisms with many advantages over other microbes and terrestrial crops. They have a long history of large-scale cultivation in various settings for wide-ranging applications. For biofuel applications, however, a number of bioprocessing issues must be addressed before microalgal biomass can compete with fossil fuels. This body of work examines strategies to improve biofuel production efficiency from three important perspectives. First, by identifying cost sensitivities using technoeconomics and, then, using that framework to address two biological aspects of algal production: (1) maximizing oil yield under different nutrient regimes and (2) developing methods to immobilize algal biofilms as a novel growth system, capable of minimizing water requirements.

In order to quantify the potential impact of these intuitively appealing improvements to conventional algae culture, Chapter 2 describes a feasibility study for algal biofuel production in an ideal location (New Mexico, Section 2.2) that acts as a baseline and best-case scenario using current practices in microalgal bioprocessing (*i.e.*, pond production with synthetic fertilizer). To then examine integrated nutrient sourcing and co-localization with industrial emissions, Section 2.6 assesses the role of waste CO_2 and excess heat in a non-ideal climate (Iowa), focusing on smaller-scale integrated algae production in traditional raceways for more distributed applications of bioremediation and bioenergy production— in this case, to improve the sustainability profile of an existing corn ethanol biorefinery. Both case studies employ cost-benefit analysis of raceway pond cultivation to strike a balance between

economics and sustainability. The end product of both processes is separated algal biomass to be used as a source of oils (TAG) for biofuel as well as residual proteins and carbohydrates as a renewable source of animal feed.

Based on the results of these technoeconomic models, further experimental work to validate novel approaches to algal biofuel production (*e.g.*, nutrient amendments, biofilm substrates) and their potential impact on cost of biofuel production is pursued. Chapters 3 and 4 focus on the impact of exogenous organic compounds on the growth, physiology, and lipid profiles of microalgal strains. Ultimately, using a two-stage process to not only increase total lipid content, but also beneficially shift the lipid profiles toward neutral storage lipids as triacylglycerol (TAG), which can be easily extracted and converted to biofuel. The remainder of the thesis (Chapters 5-8) provides a review of biofilm systems that have been previously employed, which underscores the need for dedicated immobilization techniques to improve the robustness of photosynthetic biofilms. Chapters 6 and 7 describe molecular and computational tools that were developed to interrogate the critical time and length scales involved in biofilm formation. Chapter 8 provides a detailed assessment of naturally isolated filamentous biofilms as a scaffold to improve the retention of unicellular algae of interest. The dynamics of biofilm growth using this biomimetic approach are analyzed using 3-dimensional fluorescent microscopy to probe the behavior of single algal cells in real time. Finally, the collective improvements in oil yield and algal biomass growth in low-water environments are connected to the technoeconomics of algal biofuel production.

1.5 References

Ahmad AL, Mat Yasin NH, Derek CJC, Lim JK (2011) Microalgae as a sustainable energy source for biodiesel production: A review. Renew Sust Energ Rev 15: 584-593.

Archer MD, Barber J, Ed. (2004) Molecular to Global Photosynthesis. London: Imperial College Press.

Barbosa MJ, Zijffers JW, Nisworo A, Vaes W, van Schoonhoven J, Wijffels RH (2005) Optimization of biomass, vitamins, and carotenoid yield on light energy in a flat-panel reactor using the A-stat technique. Biotechnology and Bioengineering 8: 233-242.

Bazilian M, Davis R, Pienkos PT, Douglas A (2013) The energy-water-food nexus through the lens of algal systems**.** Industrial Biotechnology 9: 158-162.

Benemann JR (2003) Biofixation of CO_2 and greenhouse gas abatement with microalgae-technology roadmap. U.S. Department of Energy, Final Report 7010000926.

Benemann JR, Oswald WJ (1996) Systems and Economic Analysis of Microalgae Ponds for Conversion of CO_2 to Biomass. Pittsburg, PA: DOE/PC/93204--T5, U.S. Department of Energy

Blanken W, Janssen M, Cuaresma M, Libor Z, Bhaiji T, Wijffels RH (2014) Biofilm growth of *Chlorella sorokiniana* in a rotating biological contactor based photobioreactor. Biotechnology & Bioengineering. *In Press*

Burke A (2008) Agriculture in Chesapeake Bay Watershed Contributes to Bay's Decline. Abt Associates. Available: http://www.abtassociates.com. Accessed 20 September 2008.

Burlew JS (1953) Algal Culture from Laboratory to Pilot Plant. Washington DC: Carnegie Institution of Washington.

Chamie J (2004) World Population to 2030. Department of Economic and Social Affairs, Population Division, Report Number: ST/ESA/SER.A/236. United Nations: New York, NY.

Chinnasamy S, Bhatnagar A, Hunt RW, Das KC (2010) Microalgae cultivation in a wastewater dominated by carpet mill effluents for biofuel applications. Bioresource Technology 101: 3097-3105.

Chisti Y (2007) Biodiesel from microalgae. Biotechnology Advances 25: 294-306.

Chisti Y (2013) Constraints to commercialization of algal fuels. J Biotechnol 167: 201-214.

Cho S, Luong TT, Lee D, Oh Y-K, Lee T (2011) Reuse of effluent water from a municipal wastewater treatment plant in microalgae cultivation for biofuel production. Bioresource Technology 102: 8639-8645.

Christenson LB, Sims RC (2012) Rotating algal biofilm reactor and spool harvester for wastewater treatment with biofuels by-products Biotechnology and Bioengineering. 109: 1674-1684.

Cordell D (2010) The story of phosphorus: sustainability implications of global phosphorus scarcity for food security. ISSN 0282-9800.

Croft MT, Lawrence AD, Raux-Deery E, Warren MJ, Smith AG (2005) Algae acquire vitamin B_{12} through a symbiotic relationship with bacteria. Nature Letters. 438: 90-93.

Cushman-Roisin B (2012) Some useful numbers. ENGS-171 Industrial Ecology Course Materials. Dartmouth College. Accessed 12 August 2014. Available: engineering.dartmouth.edu/~d30345d/courses/engs171/UsefulNumbers.pdf

de-Bashan LE, Bashan Y (2010) Immobilized microalgae for removing pollutants: Review of practical aspects. Bioresource Technology 101: 1611-1627.

Devroe EJ, Kosuri S, Berry DA, Afeyan NB, Skraly FA, Robertson DE, et al. (2010) Hyperphotosynthetic Organisms. U.S. Patent No. 7,785,861

Diesel R (1898) Internal-combustion engine. U.S. Patent Pub. No. US608845.

Dimitrov K (2007) GreenFuel Technologies: A Case Study for Industrial Photosynthetic Energy Capture. Accessed 21 August 2014. Available: ecolo.org/documents/documents_in_english/biofuels-Algae-CaseStudy-09.pdf

Dufossé L (2007) Pigments from microalgae and microorganisms: sources of food colorants. In: Colorants F, Ed. Chemical and Functional Properties, CRC Press; p. 399-426.

Elser J, White S (2010) Peak Phosphorus, and Why It Matters. Available: http://www.foreignpolicy.com Accessed 25 April 2010.

Energy Information Administration. (2011) Annual Energy Outlook. DOE/EIA-0383(2011) April 2011. www.eia.gov/forecasts/aeo. Accessed 12 August 2014.

Energy Information Administration. (2012) Annual Energy Outlook. DOE/EIA-0383(2012) June 2012. www.eia.gov/forecasts/aeo. Accessed 25 September 2013.

Energy Information Administration. (2013) Annual Energy Outlook. DOE/EIA-0383(2013) April 2013. www.eia.gov/forecasts/aeo. Accessed 27 September 2013.

Erisman JW, Sutton MA, Galloway J, Klimont Z, Winiwarter W (2008) How a century of ammonia synthesis changed the world. Nature Geoscience 1: 636-639.

Eroglu E, Agarwal V, Bradshaw M, Chen X, Smith SM, Raston CL, Iyer KS (2012) Nitrate removal from liquid effluents using microalgae immobilized on chitosan nanofiber mats. Green Chem. 14: 2682-2685.

Fernandez-Sevilla JM, Acien Fernandez FG, Molina Grima E (2010) Biotechnological production of lutein and its applications. Applied Microbiology and Biotechnology 86: 27-40.

Guerin M, Huntley ME, Olaizola M (2003) *Haematococcus* astaxanthin: applications for human health and nutrition. Trends Biotechnol 21: 210-216.

Hansen J, Nazarenko L, Ruedy R, Sato M, Willis J, Del Genio A, Koch D, et al. (2005) Earth's energy imbalance: confirmation and implications. Science 308: 1431-1435.

Hu B, Min M, Zhou W, Du Z, Mohr M, Chen P, Zhu J, et al. (2012) Enhanced mixotrophic growth of microalga *Chlorella* sp. on pretreated swine manure for simultaneous biofuel feedstock production and nutrient removal. Bioresource Technology 126: 71-79.

Hu Q, Sommerfeld M, Jarvis E, Ghirardi M, Posewitz M, Seibert M, Darzins A (2008) Microalgal triacylglycerols as feedstocks for biofuel production: perspectives and advances. J Plant. 54: 621-639.

Huntley ME, Redalje DG (2007) CO_2 mitigation and renewable oil from photosynthetic microbes: a new appraisal. Mitigation and Adaptation Strategies for Global Change 12: 573-608.

IPCC (2013) Fifth Assessment Report (AR5). Intergovernmental Panel on Climate Change: Working Group Reports. Available: http://www.ipcc.ch/report/ar5/ Accessed 25 December 2013.

Jensen M, Andersen AH (2013) Biofuels: a contested response to climate change. Sustainability: Science, Practice, & Policy 9: 42-56.

Joule Unlimited Technologies (2012) Contained use of modified *Synechococcus* strain JPS1 for the production of ethanol. Joule Unlimited Technologies, Inc.

EPA MCAN Case Number: TS-JUT001. Accessed 8 April 2014. Available: http://www.epa.gov/biotech_rule/pubs/submiss.htm

Kadam KL (1997) Power Plant Flue Gas as a Source of CO_2 for Microalgae Cultivation: Economic Impact of Different Process Options. Energy Conversion and Management. 38: S505-S510.

Kendall A, Yuan J (2013) Comparing life cycle assessments of different biofuel options. Current Opinion in Chemical Biology. 17: 439-443.

Kothari R, Pathak VV, Kumar V, Singh DP (2012) Experimental study for growth potential of unicellular alga *Chlorella pyrenoidosa* on dairy waste water: An integrated approach for treatment and biofuel production. Bioresource Technology 116:466-470.

Leboreiro J, Hilaly AK (2013) Analysis of supply chain, scale factor, and optimum plant capacity for the production of ethanol from corn stover. Biomass Bioenerg 54: 158-169.

Lewandowski I, Scurlock JMO, Lindvall E, Christou M (2003) The development and current status of perennial rhizomatous grasses as energy crops in the US and Europe. Biomass Bioenerg 25: 335-361.

Li Y, Chen Y-F, Chen P, Min M, Zhou W, Martinez B, Zhu J, Ruan R (2011) Characterization of a microalga *Chlorella* sp. well adapted to highly concentrated municipal wastewater for nutrient removal and biodiesel production. Bioresource Technology 102: 5138-5144.

Li-Beisson, Peltier G (2013) Third-generation biofuels: current and future research on microalgal lipid biotechnology. OCL Journal. 20(6): Article No: D606

Lippmeier JC, Crawford KS, Owen CB, Rivas AA, Metz JG, Apt KE (2009) Characterization of both polyunsaturated fatty acid biosynthetic pathways in *Schizochytrium* sp. Lipids 44: 621-630.

Liu ZY, Liu CF, Hou YY, Chen SL, Xiao DG, Zhang JK et al. (2013) Isolation and characterization of a marine microalga for biofuel production with astaxanthin as a co-product. Energies 2013; 6: 2759-2772.

Lorenz TR, Cysewski GR. (2000) Commercial potential for *Haematococcus* microalgae as a natural source of astaxanthin TIBTECH 18: 160-167.

Mallick N (2002) Biotechnological potential of immobilized algae for wastewater N, P and metal removal: A review. BioMetals. 15: 377-390.

Martiny AC, Pham CTA, Primeau FW, Vrugt JA, Moore JK, et al. (2013) Strong latitudinal patterns in the elemental ratios of marine plankton and organic matter. Nature Geoscience. 6: 279-283.

McKibben, B (2008) The Tipping Point. Accessed 26 August 2014. Available: http://e360.yale.edu/content/feature.msp?id=2012

Miao X, Wu Q (2006) Biodiesel production from heterotrophic microalgal oil. Bioresource Technology 97: 841-846.

Mozaffarian D, Wu JH (2011) Omega-3 fatty acids and cardiovascular disease effects on risk factors, molecular pathways and clinical events. J Am Coll Cardiol. 58: 2047-2067.

Mulbry W, Kangas P, Kondrad S (2010) Toward scrubbing the bay: Nutrient removal using small algal turf scrubbers on Chesapeake Bay tributaries Ecological Engineering. 36: 536-541.

Muñoz R, Köllner C, Guieysse B (2009) Biofilm photobioreactors for the treatment of industrial wastewaters. Journal of Hazardous Materials 161: 29-34.

National Research Council (2012) Sustainable Development of Algal Biofuels, National Academies Press, ISBN: 978-0-309-26032-9. Available at: http://www.nap.edu/catalog.php?record_id=13437

Neenan B, Feinberg D, Mcintosh A, Terry K (1986) Fuels from Microalgae: Technology Status, Potential, and Research Requirements. Golden, CO: SERI/SP-231-2550, Solar Energy Research Institute.

Nicolls WJ (1904) The Story of American Coals. 2nd Ed: JB Lippincott Company.

Nishikawa N, Hon-Nami K, Hirano A, Ikuta Y, Hukuda Y, Negoro M, et al. (1992) Reduction of carbon dioxide emission from flue gas with microalgae cultivation. Energy Conversion and Management 33: 530-560.

Olaizola M (2003) Commercial development of of microalgal biotechnology: from the test tube to the marketplace. Biomolecular Engineering 20: 459-466.

Olguín EJ, Hernández B, Araus A, Camacho R, González R, et al. (1994) Simultaneous high-biomass protein production and nutrient removal using *Spirulina maxima* in seawater supplemented with anaerobic effluents. World J Microbiol Biotech. 10: 576-578.

Oswald WJ (1962) The coming industry of controlled photosynthesis. Am J Public Health. 52: 235-242.

Pulz O, Gross W. (2004) Valuable products from biotechnology of microalgae. Appl Microbiol Biotechnol. 65: 635-648.

Radmer RJ, Parker BC (1993) Commercial applications of algae: opportunities and constraints. Journal of Applied Phycology 6: 93-98.

Rao AR, Sarada R, Ravishankar A (2007) Stabilization of astaxanthin in edible oils and its use as an antioxidant. J Sci Food Agric. 87: 957-965.

Razzak SA, Hossain MM, Lucky RA, Bassi AS, de Lasa H (2013) Integrated CO_2 capture, wastewater treatment and biofuel production by microalgae culturing—A review. Renewable and Sustainable Energy Reviews 27: 622-653.

Rosenberg JN, Oh VH, Yu G, Guzman BJ, Oyler GA, Betenbaugh MJ (2014) Chapter 25: Exploiting the molecular genetics of microalgae: from strain development pipelines to the uncharted waters of mass production. S-K Kim (Ed.), In: Handbook of Microalgae: Biotechnology Advances, Elsevier. *In Press*

Rosenberg JN, Oyler GA, Wilkinson L, Betenbaugh MJ (2008) A green light for engineered algae: redirecting metabolism to fuel a biotechnology revolution. Curr Opin Biotechnol, 19: 430-436.

Sabarsky M (2010) Accelerating Next-Generation Biofuels Available: rady.ucsd.edu/rbj/2010/biofuels/ Accessed 20 August 2014

Sandefur HN, Johnston RZ, Matlock MD, Costello TA, Adey WH, Laughinghouse HD (2014) Hydrodynamic regime considerations for the cultivation of periphytic biofilms in two tertiary wastewater treatment systems. Ecological Engineering 71: 527-532.

Sapphire Energy (2013) Evaluation of genetically-modified *Scenedesmus dimorphus* in open ponds for the production of green crude. Sapphire Energy, Inc. EPA TERA Case Numbers: R13-0003 through R13-0007. Accessed 8 April 2014. Available: http://www.epa.gov/biotech_rule/pubs/submiss.htm

Schlagermann P, Göttlicher G, Dillschneider R, Rosello-Sastre R, Posten C (2012) Composition of algal oil and its potential as biofuel. Journal of Combustion, Article ID: 285185.

Schnurr PJ, Espie GS, Allen DG (2013) Algae biofilm growth and the potential to stimulate lipid accumulation through nutrient starvation. Bioresour Technol 136: 337-344.

Schoepp NG, Stewart RL, Sun V, Quigley AJ, Mendola D, et al. (2014) System and method for research-scale outdoor production of microalgae and cyanobacteria. Bioresource Technology 166: 273-281.

Sheehan J, Dunahay T, Benemann J, Roessler P (1998) A Look Back at the U.S. Department of Energy's Aquatic Species Program: Biodiesel from Algae. Golden, CO: TP-580-24190, National Renewable Energy Laboratory.

Singh A, Sharma P, Saran AK, Singh N, Bishnoi NR (2013) Comparative study on ethanol production from pretreated sugarcane bagasse using immobilized *S. cerevisiae* on various matrices. Renew Energ 50: 488-493.

Singh S, Kate BN, Banerjee UC (2005) Bioactive compounds from *cyanobacteria* and microalgae: an overview. Crit Rev Biotechnol 25: 73-95.

Snow AA, Smith VH (2012) Genetically engineered algae for biofuels: a key role for ecologists. BioScience. 62: 765-768.

Spath P, Mann MK, Kerr DR (1999) Life cycle assessment of coal-fired power production. NREL Report No. TP-570-25119

Spolaore P, Joannis-Cassan C, Duran E, Isambert A (2006) Commercial applications of microalgae. J Biosci Bioeng 101: 87-96.

Tirichine L, Bowler C (2011) Decoding algal genomes: tracing back the history of photosynthetic life on Earth. The Plant Journal 66: 45-57.

U.S. Department of Transportation (2010) Freight Transportation: Global Highlights, 2010. Research & Innovative Technology Administration (RITA), Bureau of Transportation Statistics Report: Washington, DC. Available: http://www.bts.gov Accessed 12 August 2014.

Van Atten C, Saha A, Reynolds L (2012) Benchmarking Air Emissions of the 100 Largest Electric Power Producers in the United States. M.J. Bradley & Associates. Available: www.mjbradley.com/sites/default/files/Benchmarking-Air-Emissions-2012.pdf Accessed 18 August 2014.

Vasudevan V, Stratton RW, Pearlson MN, Jersey GR, Beyene AG, Weissman JC, Rubino M, Hileman JI (2012) Environmental performance of algal biofuel technology options. Environ Sci Technol. 46: 2451-2459.

Weissman JC, Tillet DM, Goebel RP (1989) Design & operation of an outdoor microalgae test facility. Solar Energy Research Institute: SERI/STR-232-3569.

Weldy CS, Huesemann M. (2007) Lipid roduction by *Dunaliella salina* in batch culture: effects of nitrogen limitation and light intensity. U.S. Department of Energy Journal of Undergraduate Research 7: 115-122.

Wiley P, Harris L, Reinsch S, Tozzi S, Embaye T, Clark K, McKuin B, et al. (2013) Microalgae cultivation using offshore membrane enclosures for growing algae (OMEGA). J Sustainable Bioenergy Systems 3: 18-32.

2

TECHNOECONOMIC ANALYSES OF ALGAL BIOFUELS[⊥]

It is remarkable that crude oil deposits can be accurately located, drilled with precision, refined into usable fuel fractions, and ultimately piped to the consumer at a reasonable price. The same may become true for algae-derived oils, but in order to deliver next-generation renewable fuels at a competitive cost, there is value in dissecting each competent of the algal biofuel production process. In order to better understand the technical, economic, and sustainability challenges associated with current best practices in algal biofuel production, technoeconomic modeling and lifecycle analyses remain important tools for the industry. Extensive "harmonization" of existing algal biofuel models has been recently published and serves as a blueprint

[⊥] This chapter contains excerpts from papers by Rosenberg *et al.* 2011 and Rogers, Rosenberg *et al.* 2014 that appeared in *Biomass & Bioenergy* and *Algal Research*, respectively. Portions of these works are reprinted here with permission from the publishers (Appendix A). Since the *Algal Research* article is available by open access, its reproduction is attributed to a Creative Commons License.

for future analytical efforts (DAVIS *et al.* 2012). In the interest of creating a more versatile model that is capable of predicting cost breakdowns and resource requirements for a variety of operating conditions, this chapter describes independent efforts to define a "conventional" production pathway in a putatively ideal location (New Mexico) as a best-case scenario for algal biofuel commercial viability. By using many similar assumptions, our results were found to be in close accord with prior models of algal biomass production for this region. Using these production figures as a baseline, upstream biological parameters were also adjusted to examine the potential for integrated nutrient sourcing in non-ideal climates (Iowa) and, ultimately, incorporating alternative technologies (*e.g.,* novel growth systems).

The first section of this chapter demonstrates the robustness of a technoeconomic model based on a range of operating parameters for a fully functional algae farm in New Mexico with the engineering design objective of 1,000 barrels of crude algae oil per day. Using a conservative microalgal growth rate (15 g m^{-2} d^{-1}) and lipid content (25% by dry weight) for the green microalga *Chlorella vulgaris*, a proportionally sized algae cultivation farm was estimated to require 12,000 acres for solar collection to meet the demand for daily biomass harvest. By modeling the entire biofuel production process from "pond-to-pump," this technoeconomic analysis (TEA) of raceway ponds driven by paddlewheels also revealed that the electrical energy input remains an immense annual operating expense. Furthermore, algal oil production at 1,000 barrels per day (bpd) would require over 50 tons of nutrients and over 350 million gallons of water to be circulated and recovered daily, which is nearly twice

the average volumetric capacity of Baltimore City's main wastewater treatment plant (Back River). To address some of these major cost barriers associated with raceway pond production (*e.g.* high capital costs, low areal productivity, paddlewheels electricity, and evaporation), various levels of energy input were examined along with the possibility to cover the ponds with greenhouse material. Ultimately, the baseline cost of production (COP) for biocrude algae oil fell between \$10-16 gal^{-1} and the possibility for individual production factors to further perturb this estimate were quantified by COP sensitivity analysis. In terms of sustainability, the baseline energy return on investment (EROI) was found to be 2.73; however, increasing the power input for paddlewheel mixing rendered the EROI unsustainable (*i.e.*, less than 1).

The second section of this chapter examines algal biofuel production in a less favorable location with significant seasonal variation in temperature and suboptimal solar irradiance. Nonetheless, Iowa was chosen for the opportunity to take advantage of locally abundant resources such as waste heat and CO_2 from a 50 million gallon per year (mgy) ethanol biorefinery, which was hypothesized to offset the technical hurdles associated with some of the location's inherent challenges. In this model, the design criterion of producing 1,000 bbl d^{-1} was not feasible and, instead, the TEA focused on upstream benefits associated with co-localization with the ethanol biorefinery. In this case, covered raceway ponds were required to contain CO_2 and heat and just over 2,000 acres of cultivation area was found to be necessary to utilize all of the CO_2 emission from the ethanol plant. With greater control over an enclosed

pond system with regulated temperature and CO_2 conditions, a slightly higher average areal productivity of 20 g m^{-2} d^{-1} was assumed for *C. vulgaris*. However, this process was indeed limited by the amount of waste heat available to maintain winter production, which was only capable of keeping 40 acres of ponds in year-round production. Cost of production ranged from \$10-40 gal^{-1}. As opposed to a positive EROI, it was concluded that CO_2 abatement was the main benefit of co-localization due to anticipated regulations on carbon capture and recycle. Thus, rather than emitting or sequestering this waste CO_2, it can be feasibly converted to a locally usable fuel. While this is still not cost competitive with fossil fuels, it may provide an alternative to potentially costly sequestration technologies.

In both geographic locations, water usage and energy costs associated with pond production were some of the major upstream engineering parameters involved in driving the COP. In terms of downstream processing of algal biomass, extraction efficiency and harvesting costs also had significant impacts on COP and sustainability. Due to the magnitude of biofuel production sought in the New Mexico case study, both the cost and availability of CO_2 were found to be technical obstacles. In Iowa, however, inexpensive CO_2 was actually available in overabundance compared to the heated process water from the ethanol biorefinery necessary to sustain algal growth in the winter. Since both models relied on high rate ponds (HRPs), the potential for novel growth systems to address issues of mass transfer and gas exchange as well as harvesting and water utilization exist. Moreover, sensitivity analyses in both TEA cases identified lipid content as the

single most influential factor with direct impact on COP. Given the importance of this biological variable and its interdependence on algal growth (*i.e.* areal productivity), experimental work in the following chapters of this dissertation investigate the effect of nutrient regimes on the lipid content and composition of *Chlorella* species in detail.

2.1 Variation in economic projections for algal biofuels: cost of production

While both case studies modeled in this chapter focus on COP as the critical metric to determine economic feasibility, performance indicators throughout upstream and downstream processing of algal biomass also help to identify major resource issues and sustainability. However, due to the existence of multiple pathways to algal biofuel production (Williams & Laurens 2010; Sun *et al.* 2010), modeled predictions for the price of crude algal oil has ranged from less than $3.00 to over $1,000 per gallon (Pate 2009). These projected values are the result of an extensive review of the literature, in which cultivation methods included raceway ponds and tubular PBRs with potentially integrated feedstocks, such as waste heat and wastewater. The average cost of production was found to be roughly $100 gal^{-1} and the most common route to microalgal biocrude is depicted in Figure 6. For the purpose of TEA, the model in this chapter was built to describe the simplified unit processes shown in this process flow diagram.

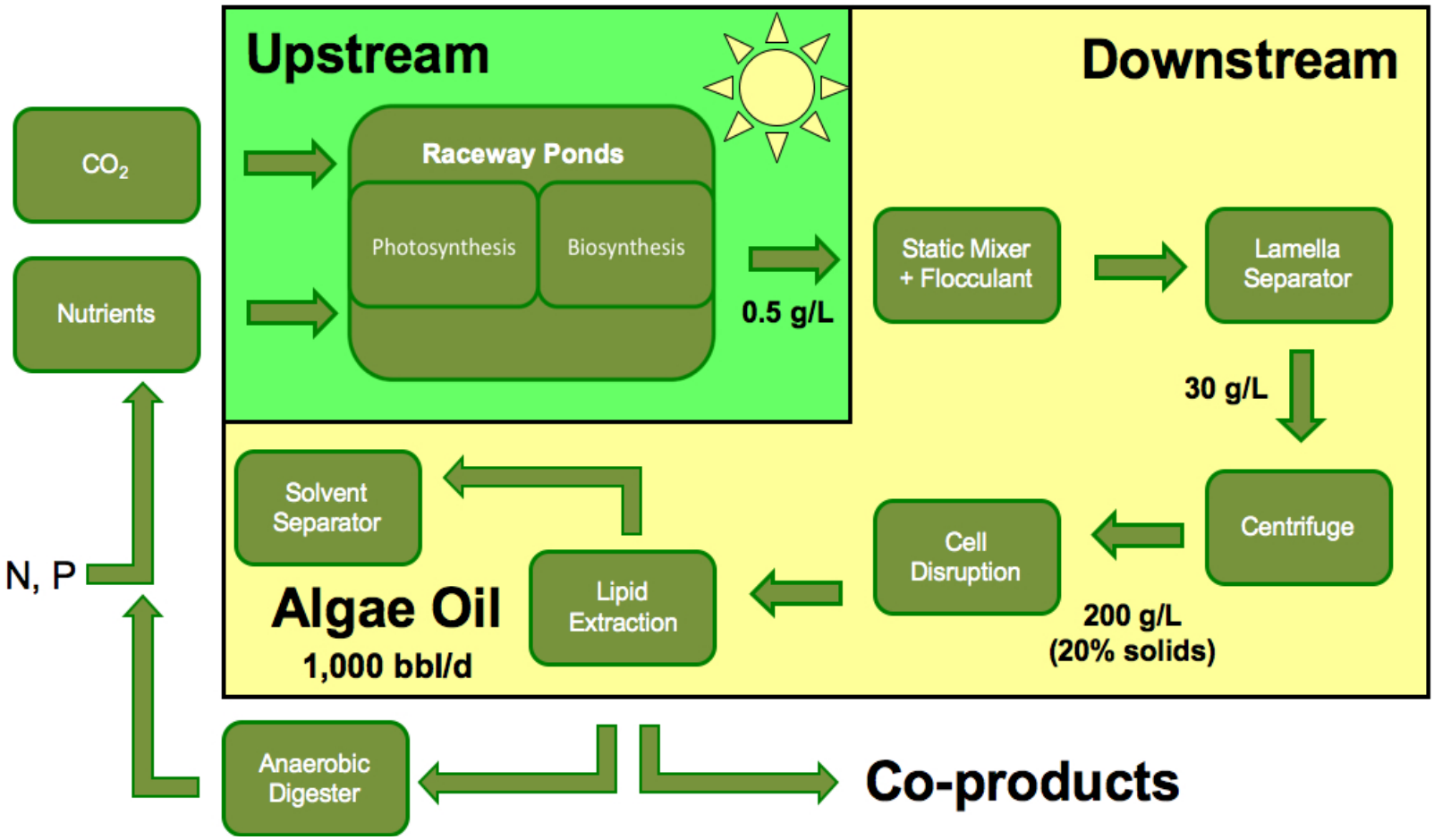

Figure 6. Schematic diagram of microalgae cultivation for biofuels. This simplified network of unit processes depicts the major steps of upstream algae growth and downstream biomass harvesting toward end products of biofuels and co-products with nutrient recycle.

2.2 An analysis of paddlewheel-driven raceway ponds in New Mexico

In this analysis, the baseline production costs and energy return on investment (EROI) of crude algal oil were evaluated for a variety of operating scenarios. The technoeconomic feasibility of a hypothetical algae farm and biocrude oil refinery in New Mexico was evaluated in order to meet a predicted production target of 1,000 barrels of crude algae oil per day, which represents a moderate output rate for a third-generation biofuel plant. Specifically, this algae oil process model focuses on upstream cultivation using conventional technologies (*i.e.*, raceway ponds) and locally sourced water and energy inputs. The impact of well-established harvesting, dewatering, and separation methodologies on the sustainability of downstream processing were also assessed. The results of this technoeconomic study identify the major energy demands, water requirements, and capital investments associated with traditional algal biofuel production. The ultimate conclusions regarding COP and sustainability are held in comparison with empirical data from the New Mexico State University (NMSU) microalgae cultivation testbed.[7]

---

[7] The following sections contain a synopsis of the work published by ROGERS, ROSENBERG *et al.* 2014 in the *ALGAL RESEARCH* journal. For a more detailed description of this TEA model, readers are referred to the open access article online, where all supporting spreadsheets can be found as freely available material: dx.doi.org/10.1016/j.algal.2013.11.007

2.3 Materials and Methods

2.3.1 Symbols and Abbreviations

BGY	billion gallons per year
Btu	British Thermal Unit
COP	cost of production
DAP	diammonium phosphate
DW	dry weight
EIA	Energy Information Administration
EROI	energy return on investment
g L^{-1}	grams per liter
GHG	green house gas
gpm	gallons per minute
ha	hectare
HDPE	high-density polyethylene
HRP	high rate pond
kW	kilowatts
kWh	kilowatt hours
LCA	life-cycle analysis
LEA	lipid extracted algae
LLE	liquid-liquid extraction
mgy	million gallons per year
PBR	photobioreactor
ppm	parts per million
TEA	technoeconomic analysis
WWT	wastewater treatment
WWTP	wastewater treatment plant

2.3.2 Fundamental assumptions for pond production of algal biofuel

Basic biological productivity and raceway pond sizing

This TEA model was constructed using a hybrid approach employing both Excel (Microsoft, Inc.) spreadsheets and the Aspen Plus v7.3 (Aspen Technology, Inc.) chemical process modeling software suite to compute mass and energy balances. These methods were primarily used to estimate the size (*i.e.*, acreage) of an algae production facility to meet the engineering design goal of 1,000 barrels of crude algae oil per day (bbl d^{-1} or bpd). A number of simplifying assumptions were made for the production process. For example, the feeding rate of nutrients to the raceway pond media was determined using the Redfield ratio of 106:16:1 for carbon, nitrogen, and phosphorus (C:N:P) based on a year-round average areal productivity of 15 g m^{-2} d^{-1} (Redfield 1934). A brief assessment of microalgal species that could fulfill the biological assumptions of at least 15 g m^{-2} d^{-1} and consistent oil content of 25% was undertaken. The lead candidate species are listed in Table 2 and it was concluded that *Chlorella vulgaris* would serve as a suitable production organism for photoautotrophic biofuel production in New Mexico. In addition to species selection, genetic manipulation may also produce strains with superior growth and lipid characteristics, but further research needs to be conducted to determine the stability of these organisms (Rosenberg *et al.* 2008). Therefore, only productivity ranges for naturally occurring strains were considered in this study.

Species	Habitat	Oil Content	Source
Chlorella sp.	Freshwater	26-32%	Benemann & Oswald 1996; Chisti 2007
Scenedesmus sp.	Freshwater	16-40%	Kadam 1997
Neochloris oleabundans	Freshwater	29-54%	Sheehan *et al.* 1998; Chisti 2007
Botryococcus braunii	Freshwater & Marine	25-75%	Sheehan *et al.* 1998; Chisti 2007
Arthrospira sp.	Freshwater	22%	Neenan *et al.* 1986
Nannochloropsis sp.	Marine	29-68%	Chaumont 1993

Table 2. Candidate algal strains for the production of biofuels. Of the thousands of algal species that have been characterized, only a handful of organisms have been exploited in production scenarios. The microalgae in this table represent some of the more commonly used species, although they are actually quite distantly related— each with their own advantages and disadvantages. For example, species of *Arthrospira* (also known as *Spirulina*) grow quickly and are used in nutritional supplements for their high protein content. Their corkscrew shaped cells allow for more straightforward approaches to harvesting. For biofuels, however, these cyanobacteria have low lipid contents, most of which are membrane lipids that can be difficult to extract. Alternatively, *Botryococcus braunii* cells secrete an interesting class of hydrocarbons applicable to biofuels, but grow extremely slowly. *Nannochloropsis* are marine species with very small cells (1-2 µm) that can be difficult to harvest, but have very high lipid contents with favorable TAG composition. Both *Chlorella* and *Scenedesmus* are robust green algae often found growing in wastewater. Both can accumulate significant amounts of TAG under certain conditions. *Neochloris oleoabundans* is a less common organism, but has demonstrated potential for biofuel production due to its high lipid content.

Due to limitations of light penetration and hydrodynamic factors in raceway ponds, a maximal culture density of 0.5 g L^{-1} was assumed along with conservative values for harvesting rate (10%) and lipid content (25%). Based on these assumptions, the area required for pond surface was calculated to be 4,875 hectares (roughly 12,000 acres or 18.75 square miles). By harvesting 10% of the entire farm volume each day, 730,000 ± 2,000 kg algal biomass by dry weight (DW) is collected daily, yielding the target of 1,000 bbl d^{-1} crude algae oil. Biomass is concentrated from dilute culture to 30 g L^{-1} using flocculation and ultimately a 200 g L^{-1} wet paste by centrifugation before lipid extraction efficiency (80%). Growth variability resulting on over-production of biomass during high growth periods was not considered in this model, but is known to be a concern when sizing actual algal biofuel plants for peak loads (Behnke 2013).

The entire algae farm consists of repeating units of high rate pond (HRPs) based on the classic design proposed by Oswald. Each raceway pond unit covers two acres of land and is constructed with a 30 cm depth. Accordingly, 6,000 continuously operating ponds are required for full production resulting in a total farm volume of 3.85 billion gallons. Based on a 30 cm s^{-1} velocity of water flow imparted by a pair of paddlewheels, the circulation time for each pond is 16 minutes. With the 10% harvest/dilution rate this corresponds to an average residence time of 4-10 days.

2.3.3 Economic and energy projections

Material flow for raceway pond inoculation and operation

The baseline TEA model was devised for an ideal production location in the U.S., namely New Mexico, due to its favorable climate with low seasonal temperature variation and high solar irradiance, relatively flat topography, and usable aquifers. The basic process flow for the upstream and downstream processing of algal biofuels were devised and sized as follows. Major operating parameters are listed in Table 3 and the complete cost breakdown can be found in supplementary material to Rogers *et al.* 2014. In brief, for inoculation and dilution of the raceway ponds, water and nutrients are introduced using three static mixers (Westfall Manufacturing), each with two ports for the addition of CO_2 (Linde, \$40 ton^{-1}). Carbonation of the water with CO_2 is accomplished before entering the ponds using an absorption tower modeled in Aspen Plus. Solid fertilizer-grade nutrients are provided as diammonium phosphate (DAP, 18% P; 46% P; \$499 ton^{-1}) and urea (46% N ton^{-1}; \$379 ton^{-1}) with uptake rates of 50% and 76%, respectively (Index Mundi 2012). Two propeller pumps are used for this high-volume, low head-pressure water transfer, which feed a network of distribution pipes to raceway ponds.

All raceway ponds are lined with 40-mil, high-density polyethylene (HDPE) at \$0.77 m^{-2}. In the conventional design of high rate ponds (HRPs), there is typically a direct correlation between the power required to drive the paddlewheels and the pond's mixing velocity; however, this energy input can significantly impact the economic feasibility and overall sustainability of algal biomass production. This model

examined three different scenarios of paddlewheel driving motors: 0.22 W m^{-2} (baseline), 0.73 W m^{-2}, and empirical data from pilot scale ponds at New Mexico State University (NMSU), which required 8.16 W m^{-2}. In total, 24,000 paddlewheel units (Waterwheel Factory, Inc.) are required to keep 12,000 acres of pond surface area in motion. A greenhouse-like covering for the ponds made from polyethylene ($0.98 m^{-2}) was also investigated (ROSENBERG *et al.* 2011).

Algal biomass harvesting for downstream processing

In order to reduce energy costs associated with pumping, raceway ponds are continually drained by gravity into a centralized wet-well, which is sized for a time window of safety in the event of potential overflow. The culture liquid is continuously pumped out of the well through two static mixers where a polymer flocculant (SNF Polydyne, $100 ton^{-1}) is added and the treated algae culture is transferred to two lamella clarifiers where solids settle to reach a biomass density 30 g L^{-1} DW. Water and nutrient recycle from the clarifiers is accomplished by gravity and drained to a well, which is then recirculated back to the actively growing ponds after treatment. The major energy input at this stage is attributed to the rakes at the bottom of each clarifier that continuously scrape biomass buildup. The flocculated mixture is pumped out of the clarifiers using two main turbine pumps and then split into twelve pipes, one for each centrifuge (GEA Westfalia). Collectively, this array of centrifuges is able to process the required biomass to a 200 g L^{-1} paste for solvent extraction.

Solvent extraction of algal lipids

Conventional organic solvent extraction using hexane ($3,000 ton^{-1}) in excess to biomass (10:1) is employed to separate lipids from residual algal biomass after cell lysis using thirteen industrial sonicators (Hielsher Ultrasonics). The solvent-algae mixture moves through a single static mixer (Westfall Manufacturing) while accounting for unavoidable solvent loss by evaporation. Another extraction scenario examines a dry extraction process in which the biomass is dried to 10% moisture content before solvent addition. Biomass separation from the aqueous solution is accomplished with an oil-water separator (Hydro-Flo Technologies) and is collected as "lipid extracted algae" (LEA) biomass. The solvent system is recovered and recycled with a distillation column as modeled by Aspen Plus with the heavy distillate stored as the final biocrude product. A simplified process flow diagram for the current model is shown in Figure 6 and more detailed stages of the process as modeled in Aspen Plus are shown in Appendix B.

Operating Parameter	Assumption
Microalgal species	*Chlorella vulgaris*
Elemental composition of algal biomass	$C_{106}H_{181}O_{45}N_{16}P$
Microalgal growth rate	15 g m^{-2} d^{-1}
Biomass lipid content	25%
Daily biocrude production	1,000 bbl d^{-1}
Oil density	920 kg m^{-3}
Extraction efficiency	80%
Required daily biomass (dry weight)	730,000 ± 2,000 kg d^{-1}
Dilution rate	10%
Total biomass in raceways	7.31 million kg
Required growth surface area for daily production	4,875 ha (12,000 acres)
Growth surface area per pond	0.81 ha (2 acres)
Number of ponds in plant	6,000
Maximum culture density	0.5 g L^{-1}
Raceway depth	30 cm
Raceway volume	14.6 billion L (3.86B gal)
CO_2 recovery to culture	50%
Nitrogen recovery to culture	76%
Phosphorus recovery to culture	50%
Net nitrogen demand	91.9 mg g^{-1} algae
Net phosphorus demand	12.7 mg g^{-1} algae
Pond mixing (base case)	0.22 W m^{-2}
Pond mixing (case 2)	0.73 W m^{-2}
Pond mixing (case 3)	8.16 W m^{-2}
Lamella separator power	3.91 10^{-4} kWh kg^{-1} algae
Centrifuge power	2.17 10^{-2} kWh kg^{-1} algae
Cell disruption	6.83 10^{-3} kWh kg^{-1} algae
Biomass separator	1.97 10^{-4} kWh kg^{-1} algae
Solvent recovery	4.68 10^{-1} kWh kg^{-1} oil
Groundwater depth	375 ft (114.3 m)
Pumping water from off-site	2.12 10^{-3} kWh L^{-1}
Evaporation (base case)	0.05 cm d^{-1}
Evaporation (case 2)	0.50 cm d^{-1}
On-site pumping circulation (base case) (20 ft head)	9.84 10^{-5} kWh L^{-1}
On-site pumping circulation (case 2) (40 ft head)	1.97 10^{-4} kWh L^{-1}

Table 3. Key assumptions for raceway pond cultivation of algae and downstream production of biocrude in New Mexico.

Land siting and groundwater availability

In search of an ideal location for algal biofuel production, New Mexico was identified as lead candidate with approximately 39,000 ha of flat land and between 750-1,630 billion gallons of groundwater suitable for microalgal cultivation (Lansford *et al.* 1990). For the present model, the price of this type of property is assumed to be \$1,500 acre^{-1} (CoStar 2013). Average of groundwater level measurements were used to calculate pumping requirements for two scenarios: 20 ft (baseline) and 40 ft head. For water handling, appropriate sizing of pipes was calculated using volumetric flow rates of approximately 2.5 m s^{-1}. Evaporation scenarios were assessed for both open ponds (0.5 cm d^{-1}) and covered raceways (0.05 cm d^{-1}, baseline). Suitable wastewater treatment (WWT) of approximately 386 MGD recycled media was assumed necessary to remove potential growth inhibitors (Oakland URS 2007). On-site infrastructure included rail and road connecting the central processing facilities to satellite process buildings and a chemical storage warehouse (Good 2008; Mile Models 2012).

2.4 Results of TEA model for algal biofuels in New Mexico

2.4.1 Capital investment for raceway ponds & biocrude processing

The baseline assumptions for microalgal cultivation, harvesting, and oil extraction listed in Table 3 enabled all mass and energy balances in this model of algal biofuel production to be fully defined. These calculations translated to a base-case capital investment of approximately $1.04 billion. An itemized distribution of capital costs is shown along with corresponding operating expenses in Figure 7.

As shown in Figure 7, there is an overwhelming disparity between the capital cost of pond-related infrastructure compared to all other capital investments. Pond materials (liner/cover) and the required land coupled with the equipment necessary for 386 MGD water handling (paddlewheels/WWT) contribute over 95% of the plant's total capital investment. In terms of water handling, the capital cost of pumps through the facility is actually relatively low ($1.27 million) compared to paddlewheels at $120 million. Wastewater treatment equipment required to remove residual flocculant and potential growth inhibitors that may accumulate in the recycle stream constitute $245 million (25%) of the plant's capital costs. Regarding pond construction, the cost of liners alone also represents about one-quarter of the total capital. The greenhouse covering used to enclose the raceways can significantly improve the sustainability of cultivation by limiting evaporative water loss; however, the $315 million investment in transparent polyethylene accounts for nearly one-third of the plant's capital.

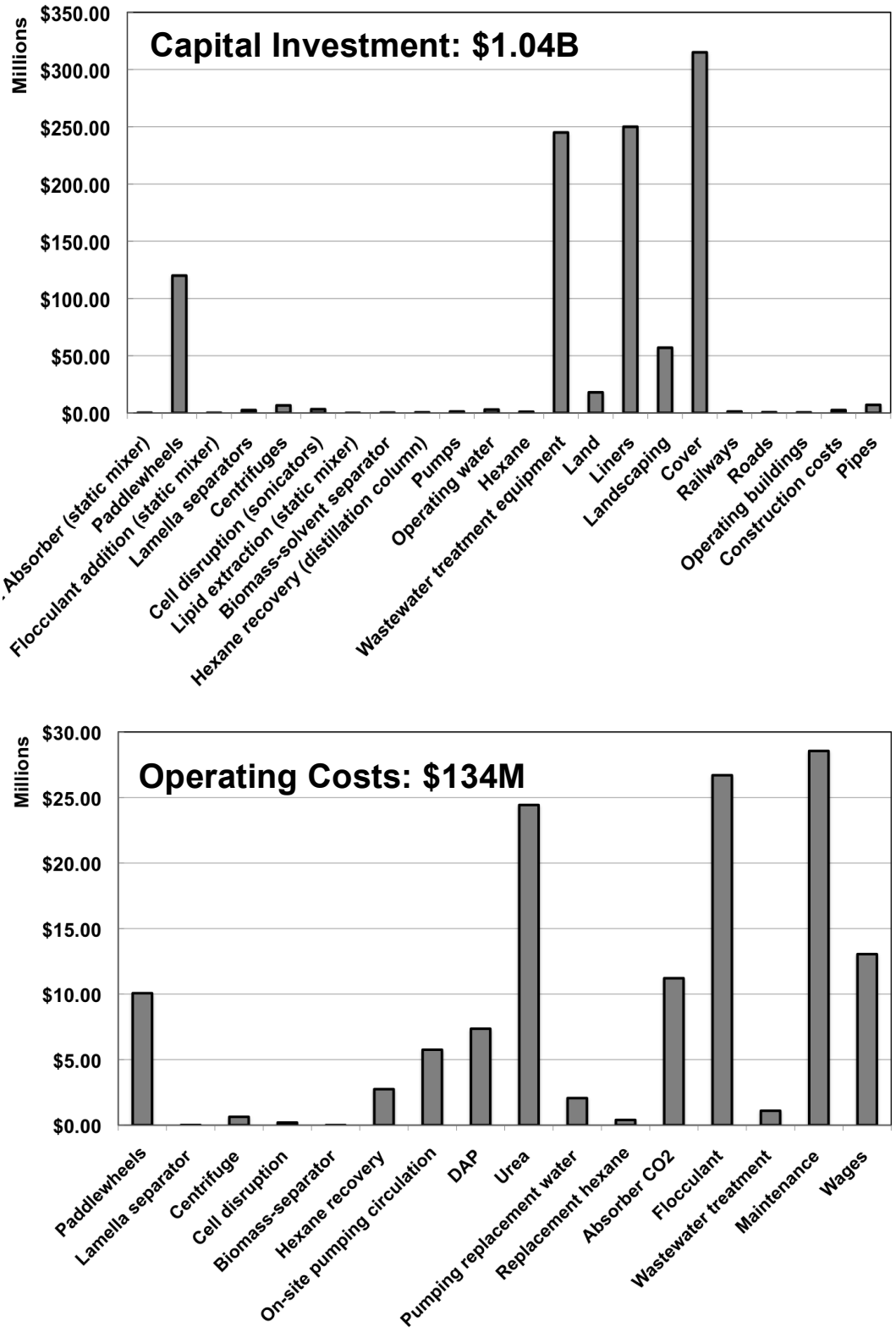

Figure 7. Itemized breakdown of capital and operating expenses for the 1,000 bpd biocrude plant in New Mexico.

2.4.2 Annual operating expenses for full production capacity

In order to meet the engineering design goal of 1,000 bbl d^{-1} of algae biocrude, 6,000 modular paddlewheel-driven ponds built over 4,875 ha (12,000 acres) in New Mexico resulted in baseline COP of $15.52 and $12.14 gal^{-1} for 10- and 20-year capital return scenarios, respectively. The base case for operating conditions also results in a maximal energy return on investment (EROI) of 2.73.

In particular, the production parameters that support these figures dictate the growth of 730,000 kg ± 2,000 kg d^{-1} of algal biomass (depending on inconsistencies in bioproduction) to fulfill of 1,000 bbl d^{-1}. The algae farm requires an impressive 386 million gallons per day of water handling capacity and an annual CO_2 demand of 280,000 tons. After separation of oil as the biocrude fraction, 585 tons of lipid extracted algae daily is generated, which can either be sold as a feedstock for other bioproducts or act as a recycled nutrient stream through anaerobic digestion (Bohutskyi & Bouwer 2013; Aslan & Kapdan 2006). In total, the baseline operating cost of production was estimated to be $134 million annually. In addition to ongoing maintenance costs, the following operating factors were found to most significantly influence either COP or sustainability: paddlewheel energy inputs, nutrient supplementation, and water handling. All of these operational burdens are directly related to pond production and are described as follows.

Major energy considerations

Since paddlewheels represent one of the largest consistent costs in this model, from both capital and operating perspectives, three different energy input scenarios were evaluated. In the base case, the operating costs associated with a theoretical 0.22 W m^{-2} power usage totaled $10.1M annually (7.5% of baseline operating budget). In the second case, paddlewheels were assumed to operate continuously at 0.73 W m^{-2} based on specifications from an industrial supplier (Waterwheel Factory Inc.). Under this condition, the total operating costs from paddlewheels totaled $34.5M annually. In the third scenario, the paddlewheel energy requirements from two pilot-scale ponds at the NMSU testbed facility were calculated and scaled to the operating capacity of this model using 8.16 W m^{-2}. In this case, the paddlewheel energy input became prohibitively expensive at a predicted annual cost of $383M.

Nutrient supplementation

As with all agricultural operations, nutrients in the form of crop fertilizers must account for a significant fraction of the operating costs. While carbon is perhaps the most fundamental component of biomass, this nutrient often goes unrecognized in terrestrial crops because CO_2 is sourced directly from the air. For photoautotrophic algae production, however, a concentrated CO_2 supply is required to maintain high productivities at commercial scale. The current model was estimated to require roughly 280,000 tons of CO_2 annually. At the market price of $40 per ton, this contributes $11.2M (8.3%) of the annual operating costs. In terms of nitrogen and phosphorus, diammonium phosphate (DAP) and urea are applied to all ponds in a

semi-continuous manner. Annually, nearly 15,000 tons of DAP and 65,500 tons of urea contribute $7.4M and $24.4M to the plant's operating costs, respectively. Collectively, these N and P nutrients account for 23.7% of the annual operating budget.

Water handling and biomass harvesting

Based on the continuous movement of water throughout the facility, the model estimates a marginal 0.03% loss of process water. Based on the total 386 MGD water handling, this represents about 1 MGD. However, inevitable water loss from the growth ponds due to evaporation is a much larger concern for maintaining a viable algal biofuel operation. As such, the model accounts for two evaporation scenarios. An aggressive and untenable case with uncovered ponds assumes a loss of 0.5 cm of water per day (64.4 MGD or 45,000 GPM as shown in Figure 8). By covering all raceways ponds with greenhouse-like transparent plastic, water loss is reduced to 10% of the uncovered case (0.05 cm d^{-1} evaporation, 6.4 MGD) and serves as the baseline for this TEA model. Corresponding energy input associated with groundwater pumping to replenish 65.4 MGD (0.5 cm d^{-1} evaporation and process loss) or 7.4 MGD (0.05 cm d^{-1} evaporation and process loss) were considered. The costs of these make-up water scenarios were found to be $18.3M and $2.1M per year, respectively. Two on-site pumping conditions were also evaluated with annual operating costs ranging from $5.7M (20 ft head, baseline) to $11.5M (40 ft head).

Beyond maintaining water levels in the ponds, the downstream process of harvesting biomass (dewatering) is another substantial cost attributed to water management.

The current model employs a common cationic polymer used in wastewater treatment to pre-treat the algal slurry before centrifugation (SNF Polydene). Interestingly, the operating costs required for centrifugation are actually quite small in comparison to polymer flocculant dosing at $100 per ton of algae processed, which contributes $26.7M to the annual operating costs (20%). As a result of all processes involving water (including recycle), the final ratios balancing amount of water used to algae oil produced greatly exceed 100:1 even for the baseline scenario, which has certain implications for sustainability.

Plant operating overhead

As a direct result of the physical area needed for solar collection, the large footprint and high cost of infrastructure on this algae farm have a direct influence on employee wages and ongoing costs of maintenance. Maintenance was estimated as 3% of the capital costs and wages were assumed to be 12% of the total operating costs based on similar industries (PETERS *et al.* 2002). Together, these overhead expenses account for over one-third of the total operating budget.

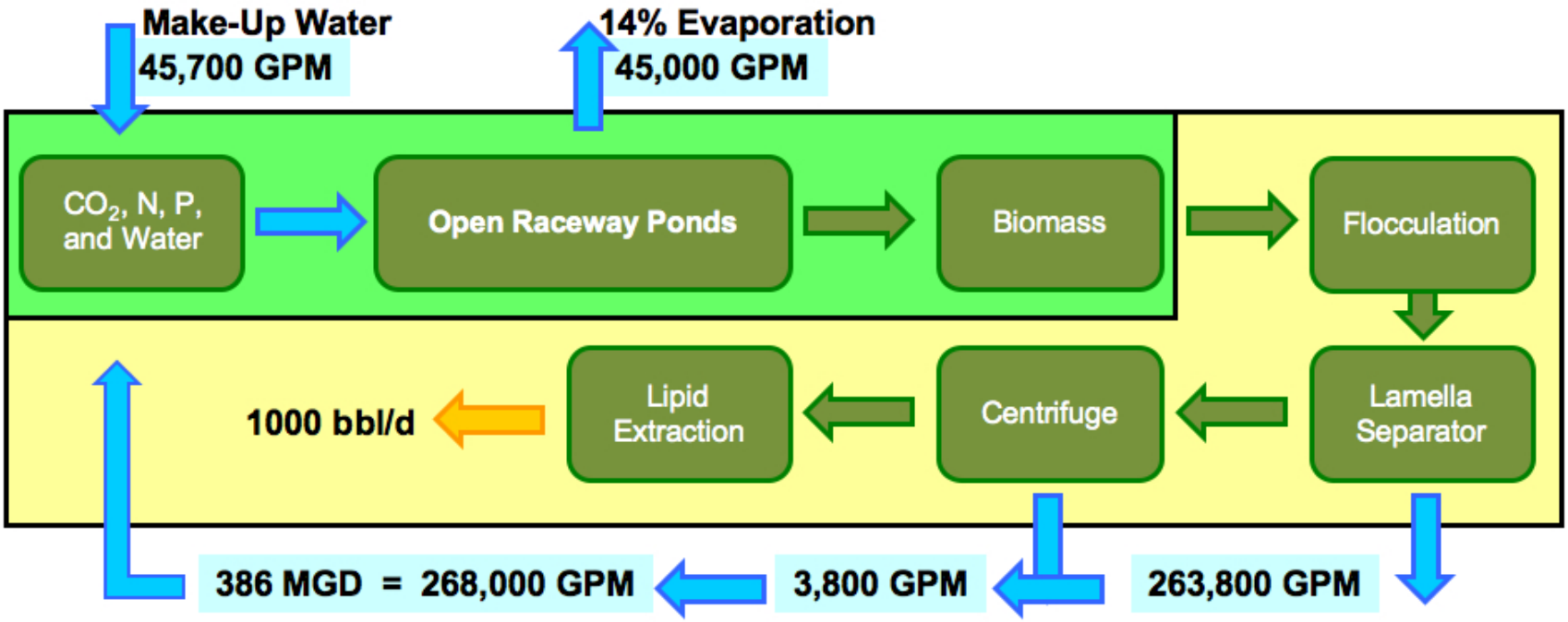

Figure 8. Overview of water flows in the TEA model for open pond production of algal biofuel in New Mexico. This diagram illustrates the large percentage of make-up water required to offset evaporative losses in the unsustainable open raceway pond scenario. Flow rates throughout the recycle process are reported as thousands of gallons per minute (GPM), which highlights the pond-related water handling issues symptomatic of the challenges of scaling open HRPs for biofuel production.

2.4.3 Principal cost sensitivities in the New Mexico TEA model

The TEA model was purposefully constructed with discrete variables rather than lumped parameters (when possible) in an attempt to most accurately assess the technical and economic feasibility of algal biofuel production. As such, by perturbing some of the more critical operating parameters, the model is able to predict ranges of COP. The results of this sensitivity analysis can be seen in Figure 9 as a "tornado plot," which sorts these tunable operating ranges in descending order, with those affecting COP the most at the top based on a 10-year return of capital investment. A similar analysis was performed using a 20-year ROI and follows similar trends, but is not shown here for the sake of brevity. For this production pathway using current best practices in algal bioprocessing, both sensitivity analyses reveal that COP is heavily influenced by biological factors.

The most obvious parameter to affect algal biofuel production is the inherent areal productivity of the algal organism since this assumption sets the throughput of biomass in the system and influences many other operating parameters by actually increasing or decreasing the final biocrude yield. While this variable sits high on the tornado plot (+\$7.59; –\$3.77 gal^{-1}), our model found that the extractable lipid content of the algae remains the single most important biological factor in determining the COP. Increasing algal lipid content from the baseline value of 25% to 35% has the potential to reduce COP by \$4.33 gal^{-1} with respect to a 10-year ROI. Conversely, reducing lipid content to 15% can nearly double COP by adding an additional \$10.10 gal^{-1} to the baseline cost of \$15.52 gal^{-1}. While the downstream oil

extraction efficiency also has the potential to seriously impact COP, downstream factors are not necessarily a focus of this dissertation. In terms of oil extraction, significant gains can be made with biological approaches to increasing the content of "extractable" lipids. Unlike polar lipids, present in cell membranes, neutral lipids are more easily separated from wet biomass by conventional solvent systems. Therefore, COP may be positively impacted not only by increasing the total lipid content in algal cells, but also shifting the composition of these lipids toward more favorable oils that are amenable to scalable extraction technologies.

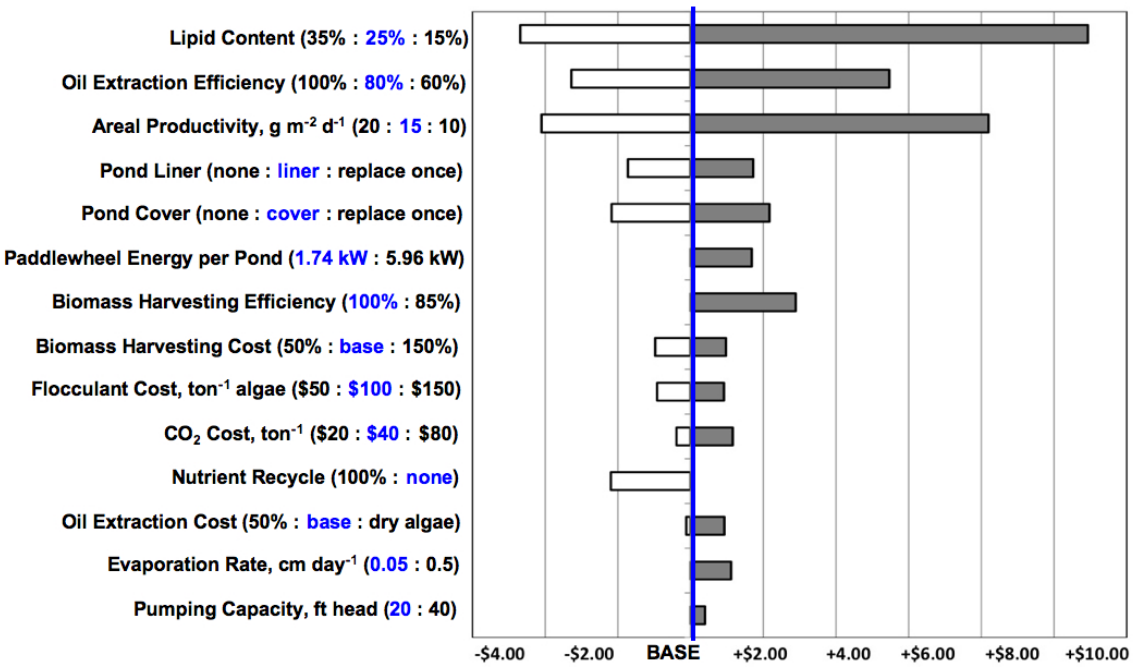

Figure 9. Sensitivity analysis of various production variables on algae biocrude COP for a 10-year return on capital investment. In this case, the base COP is \$15.52 gal^{-1} as a result of \$134M operating costs and annual payments of \$104M to cover the \$1.04B capital investment.

After lipid content, oil extractability, and areal productivity, the next major variables affecting the viability of algal biofuel production are all associated with pond production and, more specifically, water handling in these ponds. The decision to line each raceway pond with high-density polyethylene can reduce water and nutrient loss while easing pond maintenance throughout the lifetime of the plant; however, this capital investment impacts the COP by ± \$1.63 gal^{-1}. Furthermore, by enclosing all raceway ponds, the COP is increased \$2.05 gal^{-1} in the 10-yr return case. These costs are intimately linked to evaporation rate, which can add \$1.06 gal^{-1} to COP if the ponds are left uncovered. While this tradeoff is not economically favorable, the reduction in water loss afforded by covered ponds is necessary to maintain a positive sustainability profile for biofuel production in regions with water scarcity. However, the overheating of algal cultures in closed growth systems is a concern that must be balanced by the natural discharge of heat by evaporation while still reducing excessive water loss (Waller *et al.* 2012). Lastly, by augmenting the energy requirements for paddlewheel operation from 0.22 to 0.73 W m^{-2}, COP is increased by \$1.59 gal^{-1}. The energy scenario based on empirical data from the NMSU pilot pond paddlewheel operation at 8.16 W m^{-2} does not justify biofuel production at commercial-scale due to an EROI < 1.

In terms of additives to the plant's process water, such as nutrients and flocculant, these factors do not contribute as much variation to COP, but are certainly not insignificant. It is evident that the cost of flocculant constitutes the majority of harvesting costs and can vary the COP by \$0.87 gal^{-1} if this cost parameter is shifted

± $50 per ton of algae harvested. If fertilizer nutrients are sourced at no cost from wastewater or other N- and P-rich effluents, COP can be decreased by $2.08 gal^{-1}. Furthermore, the integration of CO_2 emission from power plants or other industrial sources may only result in a marginal reduction of COP ($< \$0.50\ gal^{-1}$), but this scenario may allow distributed (but smaller-scale) approaches to algal biofuel production to overcome feedstock limitations (*i.e.*, lack of centralized CO_2 supply). Together, these highlight the significance of finite nutrient resources that have both sustainability and financial impacts.

2.5 Discussion and Conclusions

Based on this technoeconomic model of algal biofuel production in New Mexico, the results of cost sensitivity analysis are consistent with the most comprehensive "harmonized" model of TEA and lifecycle analysis reported by Davis *et al.* (2012) for renewable algal biodiesel. Furthermore, the range in COP determined to be $10-16 gal^{-1} by the present model falls in line with the figures supported by Davis *et al.* (2012). As such, the results of this model support the DOE Bioenergy Technologies Office (BETO) target of reducing the "modeled mature plant cost of algal open pond oil" by $2.35 gal^{-1} (gasoline equivalent) by 2014 (EERE 2013). Most importantly, the cost sensitivity analysis based on the current model concludes that total lipid content represents a single biological variable with the ability to surpass this goal. Therefore, a priority of future research will be to evaluate different approaches to increase microalgal oil content on a cellular basis, whether by means of genetic intervention or controlled nutrient regimens, such as nitrogen deprivation. Alternatively, organic

supplementation may also be a viable route to not only increase total oil content, but also to drive lipid composition toward preferential fatty acid profiles that are enriched in energy-dense lipids (saturated) with considerable ease of extraction (neutral lipids).

The major capital and operating expenses identified by the New Mexico case study are largely due to water handling/dewatering (*e.g.*, paddlewheels, flocculant). The facility operating costs for pond construction and maintenance dominate the economics of production. As an example, wages and maintenance overhead costs can be minimized by systemically reducing capital costs associated with raceway ponds. For bioenergy production with algae, scalability is key. While ponds are suitable for small- to moderate-scale algal biomass production, the present model reinforces the notion that ponds are not necessarily scalable at the magnitude required for biofuel production. Promising alternative bioreactor designs to eliminate mechanical mixing include raceway ponds with slanted or corrugated channels to reduce energy input while still achieving adequate mixing (DARPA 2013; Craggs *et al.* 1997) and inexpensive air-lift ponds driven by pumps rather than paddlewheels (Ketheesan & Nirmalakhandan 2012, Schoepp *et al.* 2014)

Nutrient sourcing is another potential barrier to large-scale algal cultivation due to the massive quantities required for biofuel production goals. For photoautotrophic growth, carbon is the most substantial nutrient requirement for biomass production and requires roughly 0.28 million tons of CO_2 annually, corresponding to just over 700 tons of CO_2 daily. At the market price of $40 per ton, CO_2 contributes $11.2M

of the annual operating costs. Coupling algal production with industrial CO_2 emissions rather than purchasing CO_2 as a feedstock represents a more sustainable and potentially less expensive option. In fact, carbon credits associated with its capture and re-use may even help to offset some the initial investment required for algae farms. While CO_2 from industrial point sources can provide an abundant supply of carbon for algae, the actual amounts flue gas required for commodity-scale algal biofuel production could be quite massive. Based on an estimated 1.6 billion tons of CO_2 emitted from U.S. coal-fired power plants each year, if microalgae production were to be scaled to a national production rate of 10 billion gallons per year, this would require 11.4% of the coal-fired emissions in the United States (EPA 2013). The U.S. Energy Independence and Security Act projects renewable fuel production targets on the order of 30-60 billion gallons per year (EPA 2007). Combined with inadequate land available for algae cultivation directly surrounding many coal-fired power plants, limitations in CO_2 sourcing could be possible. While increasing oil content and reducing water usage may require more long-term research trajectories to have significant impact, alternative approaches to CO_2 sourcing from flue gas can be investigated relatively easily with TEA (Section 2.6). By first identifying these technoeconomic hurdles, the results of this section focus attention on opportunities and quantify attainable targets for improved algal biofuel production.

In terms of nitrogen and phosphorus requirements, the present model calls for nearly 65,000 tons of urea and 15,000 tons of DAP annually. Together, these chemical

fertilizers contribute in excess of $30 million of the annual operating costs. Ammonia can serve as an alternative nitrogen source and may have comparable market prices as urea (Davis *et al.* 2012), but can be present in greater abundance in wastewater effluents (see Chapter 8). Based on both the cost and sustainability factors associated with N- and P-based fertilizers, it is critical that algal biofuel operations continue to explore options for nutrient recycle in both upstream and downstream processing.

2.5.1 Interface of upstream and downstream processing

Harvesting by flocculation and settling

As a result of dilute biomass concentrations in raceway pond culture media, harvesting single cells from liquid suspension is energy intensive and difficult when applied to continuous operation of large-scale bioprocessing facilities (Hellwig *et al.* 2004). Membrane filtration by size exclusion is a simple and cost effective separation technique; however, even advanced filtration methods are subject to caking and erosion based on the throughput of biomass needed for biofuel production, which can lead to significant reductions in efficiency over the lifetime of the membrane (Mann *et al.* 2004). Low-speed centrifugation may be a more feasible alternative for algae if a flocculant agent is used to increase the average particle size of microalgae slurries from 10 µm to 10 mm by forming large masses of many small particles to facilitate solids separation from a liquid media (Schlesinger *et al.* 2012). The use of cationic polymers is a well-established method of flocculating particulate matter from large volumes of liquid as in WWT plants (Ghernaouta *et al.* 2010; Wyatt *et al.* 2012).

Dissolved air flotation and settling clarifiers have also been successfully implemented to harvest flocculated algal biomass at scale. The algal biomass harvesting process modeled in the present study relies on a flocculation step followed by lamella clarifiers to bring the ~2 g L^{-1} algae suspension to a 30 g L^{-1} slurry, followed by centrifugation of this slurry to a 200 g L^{-1} paste.

Polyacrylamide flocculants are widely used and can be effective with microalgal cells; however, if the biomass residues are to be used as co-products, polyacrylamide can foul the biomass from a health perspective. The process modeled in the present study employs a polymer dose costing roughly $100 per ton of dry algae biomass harvested. While flocculant costs in excess of $100 per ton of algae are prohibitive for biofuel production, a target of less than $40 per ton may be an achievable production target with alternative flocculants. Carbohydrate polymers have been used in the paper pulp industry for their advantages of being edible and amenable to biological degradation (personal communication, Norman Brent Wham, NALCO). The addition of such starches may even provide an added nutritional benefit to algal biomass residues if they are used for anaerobic digestion or animal feed. Metal ion based flocculants have been deemed incompatible with end biofuel standards and pH-induced changes are unfeasible for algal biofuel production at commercial scales; thus, biological approaches to flocculation have also gained significant attention in recent years. These processes can occur either as a natural "auto-flocculation" mechanism in mature or nutrient deprived algae cultures or instigated by a biological agent, such as the introduction of another microorganism (algae, bacteria,

cyanobacteria, or predatory grazers) (Gutzeit *et al.* 2005; Salim *et al.* 2010; Salim *et al.* 2012; Schlesinger *et al.* 2011) or a biomolecule with the bridging characteristics similar to a polymer or adhesive qualities of a coagulant (Oyler *et al.* 2012). By employing these methods, some estimates project that operating costs can be reduced by $200-400 per million gallons of process water treated by transitioning from chemical flocculants to bioflocculation (Lundquist *et al.* 2004). Furthermore, the production of biological flocculants on-site can be highly scalable and incorporated into the algae biofuel production process. Some studies have demonstrated that concentrating algae biomass from 0.05% in liquid media to 3% after flocculation and settling can be accomplished using biofilm growth systems (see Chapter 5). Collectively, the cost sensitivities associated with all aspects of water handling required for algae biofuel production are equally as significant as those tied to oil extraction or areal productivity alone.

Influence of biomass composition on biofuel and co-products

The actual composition of the algal biomass not only dictates overall mass balances for the plant, but determines if a single species can be used as both food and fuel. Maintaining high lipid content in the harvested biomass is critical for biofuel production, but depending on the species of algae, the composition of this lipid fraction can also contain high-value fatty acids for feed applications (Kagan *et al.* 2013). Of course, the residual biomass or "lipid extracted algae" (LEA) is predominantly comprised of proteins and carbohydrates that are the base of nutritional feedstocks. While there are some emerging applications in bioplastics, this

still remains a small market. The ability to extract and separate these different products with some degree of specificity and efficiency is a factor of the production process, but is decidedly not a focus of the present body of work. However, the potential uses of the residual biomass for nutrient recycling or a value-added product (*e.g.*, animal feed) is an important consideration for the lifecycle assessment. Algae biomass has been shown to be a suitable feed supplement or substitute for conventional animal feed sources (DHARGALKAR *et al.* 2009; RENAUD *et al.* 2002). Although lipid extraction processing for biofuels may also remove nutritionally important polyunsaturated fatty acids from the biomass, the LEA can still be high in protein and carbohydrates. The theoretical commercial scale algae facility in this study is estimated to produce 585 tons d^{-1} of LEA biomass with an estimated selling price between \$250-\$1,000 ton^{-1} (OLIVARES *et al.* 2011). Therefore, a 1,000 bbl d^{-1} facility could generate roughly \$50-200 million annually from the sale of LEA as a protein supplement. As such, coproducts are currently thought to be a necessary part of algal biorefineries until technological bottlenecks can be widened to allow for more economical biomass production.

Collectively, the modeled data pertaining to energy, nutrient, and water requirements for deployment of microalgal biofuel production in New Mexico pose certain challenges but are likely to be addressable with advances in algae cultivation methods. The continued development of mitigation strategies for each of these concerns will build a foundation to withstand the inevitable and necessary scrutiny for emerging energy technologies, such as algal biofuels. Ongoing research in this

active area of renewables will need to refine algae production systems in order to secure the economic viability of biofuels.

2.6 TEA of an integrated algae oil and corn ethanol biorefinery in Iowa[8]

While corn-based ethanol has led the way in providing a source of first-generation biofuel, it has also received criticism for its reliance on fossil fuels for production and the biogenesis of CO_2 as a result of fermentation. Lifecycle assessments indicate that corn-based ethanol would not qualify as an advanced biofuel, but one viable route to decrease the amount of CO_2 emitted from an ethanol biorefinery is through the co-cultivation of microalgae. Therefore, the possibility of decreasing the carbon footprint of corn-based ethanol while producing a third-generation biofuel is an appealing venture with an entirely different design goal than described in the previous chapter.

Iowa is one of the nation's largest ethanol-producing states, accounting for nearly 30% of the total U.S. ethanol production. While first generation corn ethanol has accounted for much of the production over the past five years, Iowa's biofuel industry reached a landmark accomplishment in 2014 with the first commercial scale cellulosic ethanol plant (URBANCHUK 2014). Based on a straightforward mass balance, the process for converting sugars to ethanol produces 2.85 kg of CO_2 for every gallon of ethanol, on average. The large supply of CO_2 in Iowa is attractive for

[8] The following sections contain a synopsis of a paper published by ROSENBERG *et al.* 2011 in *BIOMASS & BIOENERGY*. For a more detailed description of this case study, readers are referred to the online version of this article, where additional information can be found: dx.doi.org/10.1016/j.biombioe.2011.05.014

algae cultivation, but does come with a trade-off: the annual temperature variance is significant and can adversely affect the growth of algae.

The CO_2 concentration in the atmosphere is only ~400 ppm (KEELING 2008). For industrial purposes, relying only on diffusion of CO_2 from this low concentration of ambient air limits algal growth. As such, a constant supply of CO_2 during daylight hours is necessary to sustain the production of maximal biomass. This additional CO_2 can be supplied to allow for maximum algal biomass production; however, sourcing and distribution can be a significant cost barrier. Locating algal culture facilities in close proximity to an ethanol biorefinery allows for a constant source of carbon and can reduce the operating costs by as much as 20% (BROWN 2009). Since microalgae have the potential for higher biomass productivities than terrestrial plants, they are able to sequester more CO_2 per acre. On average, algae consume 1.83 g CO_2 to produce 1 g of biomass (WANG *et al.* 2008; SKJANES *et al.* 2007; CHISTI 2007). This capacity to sequester CO_2 makes them an ideal candidate for CO_2 mitigation. Studies conducted on the ability of algae to fix CO_2 emissions from industrial power plants show an overall 90% reduction in CO_2 from the flue gas (BROWN 1996). However, unlike the impure CO_2 emissions from coal-fired power plants, biogenic CO_2 produced by fermentation is a clean feedstock for algal growth.

The purpose of this case study was to determine the feasibility of integrated algal cultivation in non-ideal Midwest climates using locally abundant resources, focusing on CO_2 assimilation rather than meeting a target quantity of biofuel produced. A theoretical analysis of algal biomass production utilizing the excess heat and CO_2 of

an Iowa ethanol biorefinery is proposed. Although some inherent biological limitations do exist for microalgal productivity, the aim of this study was to determine the challenges that an integrated biorefinery may encounter and provide engineering recommendations.

By integrating large-scale microalgal cultivation with ethanol biorefineries, CO_2 sequestration can be coupled with the growth of algae, which can then be used as feedstock for biofuel production. In this case study, a 50-mgy ethanol biorefinery in Sioux City, Iowa was evaluated as a case study in order to reduce its carbon footprint. Theoretical projections for the amount of land needed to grow algae in raceway ponds and the oil yields of this operation were based on the amount of CO_2 from the ethanol plant. A practical algal productivity of 20 g m^{-2} d^{-1} would require over 2,000 acres of ponds for complete CO_2 abatement, but with an aggressive productivity of 40-60 g m^{-2} d^{-1}, a significant portion of the CO_2 could be consumed using less than 1,000 acres. Due to the cold temperatures in Iowa, a greenhouse covering and a method to recover waste heat from the biorefinery were devised. While an algal strain, such as *Chlorella vulgaris*, would be able to withstand some temperature fluctuations, it was concluded that this process is limited by the amount of available heat, which could maintain only 41 acres at 73° F. Additional heating requirements result in a cost of $10-40 per gallon of algal oil, which is prohibitively expensive for biodiesel production, but could be profitable with the incorporation of high-value algal coproducts.

2.7 Material and Methods

2.7.1 Climate and geography in Iowa for algae cultivation

In order to model algae growth in a Midwest climate, Figure 10 shows the average temperatures for Sioux City, Iowa, which were used to calculate the amount of addition heat required for the winter months.

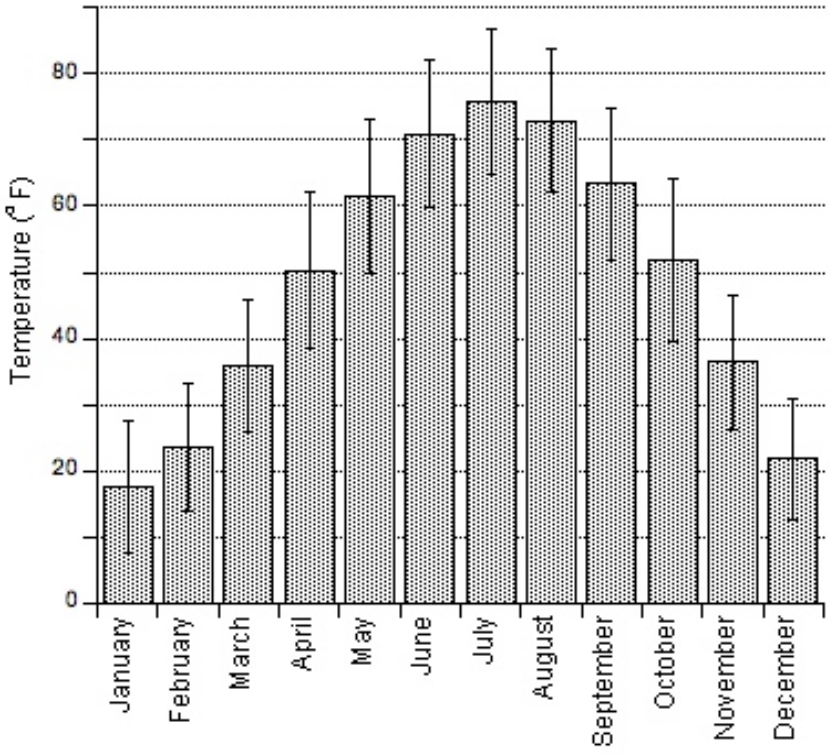

Figure 10. Monthly temperature data collected in Sioux City, Iowa from 2003 (Climate Zone 2010). Each shaded bar represents the average temperature for each month with the associated lines denoting maximum and minimum temperatures.

2.7.2 Theoretical design of microalgal raceway ponds in the Midwest

The proposed cultivation system is designed to maximize the use of available CO_2 and waste heat from a nearby ethanol biorefinery (Figure 11). The CO_2 produced from fermentation is mixed with air to create a 30-50% v/v mixture before it is filtered, injected into the culture system, and converted into biomass. The waste heat from the ethanol biorefinery will also be used to heat the liquid medium in the culture system during the winter months.

The proposed raceway pond is 100 m × 10.1 m × 0.2 m with a volumetric capacity of 200,000 L. The covering system will be constructed from greenhouse bays spaced 1.5 m apart and covered with a greenhouse glazing material. After analyzing several different glazing materials, the most suitable choice for the covered ponds was a double layer polyethylene film. This film consists of two layers of polyethylene inflated with a pocket of air between them. The presence of air between the two layers decreases condensation and provides further insulation to the greenhouse (Blom & Ingratta 1984). Polyethylene film has a light transmittance of 76% for a double layer (Thomas 2010). This provides more than adequate sunlight for maximal photosynthetic efficiency. Polyethylene is also a lightweight material that does not require a strong structural support. Polyethylene has a low thermal conductance of 0.7 Btu hr^{-1} ft^{-2} $°F^{-1}$ for a double layer film, which reduces the amount of heat lost from the structure (Both 2014; Sanford 2005). Capital and operating costs of this raceway pond design are listed in Supplementary Tables S1 and S2 (Appendix B).

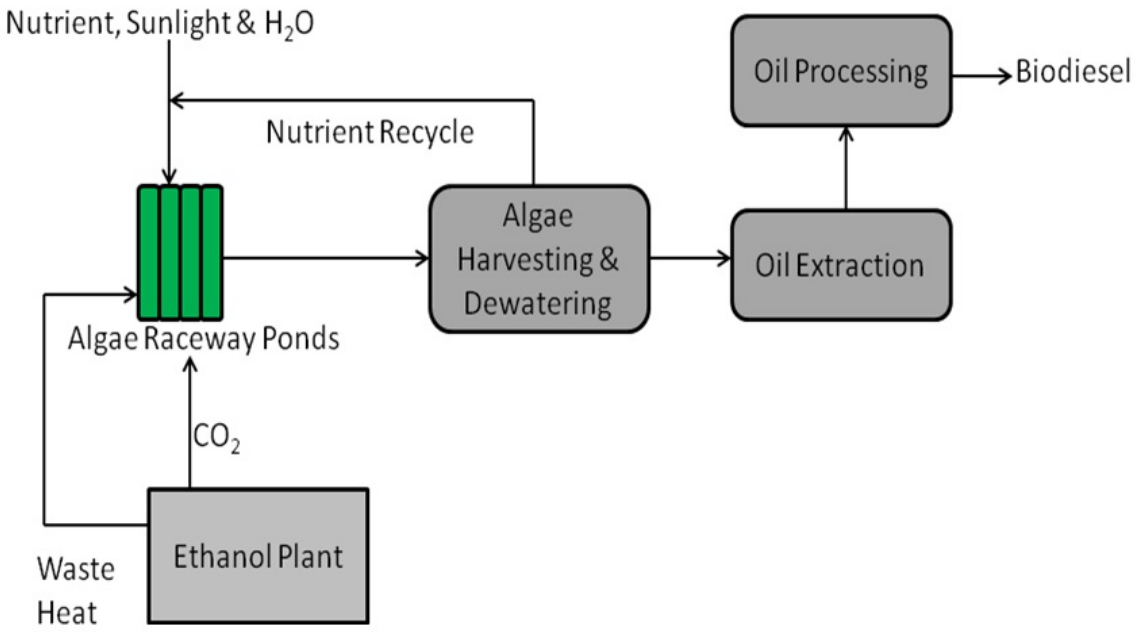

Figure 11. Simplified process flow diagram of integrated algae production with an ethanol biorefinery. Through co-localization with a 50-mgy ethanol plant, the same basic steps of pond cultivation, biomass harvesting, and downstream processing used to describe algal oil production in New Mexico were assessed in Iowa.

A two-stage cultivation system will maintain a monoculture of microalgae within the ponds and ensure dominance of the desired species (Huntley & Redalje 2007). The first culturing system employs photobioreactors (PBRs), which have been effective at growing algae at small scales (Lee 2001). These PBRs are fabricated with transparent materials and allow for accelerated growth rates in relatively dense cultures due to high surface area to volume ratios (Tsygankov *et al.* 1994). PBRs can produce up to 20 g biomass L^{-1} compared to the 0.5-1.5 g L^{-1} observed in raceway ponds (Lee & Palsson 1994). A high-density inoculum (grown in PBR) fed into the raceways coupled with daily harvesting is the most effective way to operate outdoor systems and encourages maximum utilization of available CO_2 and waste heat.

2.7.3 Engineering principles and mathematical projections

The land requirements to sequester the CO_2 are based on a range of areal productivities— a currently attainable 20 g m^{-2} d^{-1} through an aggressive estimate of 60 g m^{-2} d^{-1}. A value of 1.83 g CO_2 g^{-1} biomass was used to determine the amount of CO_2 sequestered. To estimate the theoretical maximum amount of biodiesel produced, complete mass conversion of CO_2 to algal biomass and 100% algal oil extraction and transesterification efficiency were used as simplifying assumptions. A value of 0.864 kg L^{-1} was used for the density of biodiesel (Miao & Wu 2006).

The peak heating requirements for the quarter-acre raceway pond were obtained using the convective, radiative and evaporative losses from the pond. Evaporative

losses accounted for the largest percent of heat loss from the pond (Rafferty & Culver 1998; Stoever 1941). Heat loss from the greenhouse to the outside air was also accounted for in the model. It was assumed that the greenhouse covering was well sealed with negligible air infiltration. An overall heat transfer coefficient for double-layer polyethylene insulation was used to determine the heat lost from the greenhouse to the atmosphere (Both 2014; Sanford 2005).

The available heat for the microalgal culture was designed to come from the ethanol biorefinery cooling tower stream. During the coldest part of the winter, wastewater streams exit the ethanol biorefinery at an average temperature of 29° C and are sent to a cooling tower where heat is removed. The cooling tower operating in Merill, Iowa is rated at 108 million Btu hr^{-1} and flows process water at 15,000 GPM. During the winter months the load on the cooling tower is lower due to a lower ambient temperature. The cooling water enters the cooling tower at 84.2° F and is reduced to 73.4° F. A potential 81 million Btu hr^{-1} of energy is available in this stream and could be used to heat the raceway ponds. This data was obtained in 2009 from a 50-mgy ethanol biorefinery operating in Merrill, Iowa (personal communication, CP Stremick, Plant Manager).

2.8 Results of integrated algae-ethanol biorefinery model

Based on the information available on the climate and geography of Iowa as well as the sources of CO_2 and heated water from a 50-mgy ethanol biorefinery, a detailed analysis was carried out to determine the feasibility of producing algal biofuels in the Midwest. The growth of a lead candidate alga under a variety of theoretical biomass and lipid productivity scenarios were used to determine the potential land areas and amount of CO_2 and additional heat required for biofuel production. The corresponding capital and operational costs of the culturing system were used to determine a cost of production for crude algal oil.

2.8.1 Algal species selection for Midwest climate

Compared to the climate of New Mexico, more scrutiny was applied when selecting a microalgal species for biomass production in Iowa. Careful consideration was given to the following: (1) ability to grow in extreme environments; (2) rapid growth rate/doubling time; (3) cell characteristics which might reduce harvesting costs; (4) tolerance of temperature variations as well as changes in light intensity; (5) optimized growth for varying light/dark cycles and (6) high lipid content within cells. All of these factors are important in producing a large quantity of biomass year-round and a high lipid content that can be converted to biofuel (Table 4).

Species	Advantages	Disadvantages	Source
Chlorella vulgaris	• Temperature tolerance 5-30°C • Capable of growing in 40% CO_2 • Rapid doubling time • Substantial literature available	• Optimum pH between 7.5-8	Wang *et al.* 2008; Chinnasamy *et al.* 2009; Maxwell *et al.* 1994
Botryococcus braunii	• High lipid content • Tolerates range of light intensities	• Slow doubling time • CO_2 & temperature tolerance unknown	Metzger *et al.* 1985
Scenedesmus sp.	• Cells form colonies; settle rapidly • Ease of availability	• Optimal temperature 30-35° C • Low CO_2 tolerance	Wang *et al.* 2008
Neochloris oleoabundans	• Grows well in high CO_2 levels • High lipid content	• Slow doubling time	Gouveia & Oliveira 2009

Table 4. Potential algal strains for the production of biodiesel in the Midwest. Although there can be significant variation in the physiology of different strains and cultivars of a single algal species, some generalized characteristics of four lead candidate microalgae are summarized here. The inherent positive and negative traits of these natural organisms serve as a suitable starting point for assumptions in algal productivity; however, the exact growth kinetics and lipid contents under production conditions remain necessary in order to explicitly model algal biofuel production. This line of research is further investigated in Chapters 3 and 4 by describing how strain selection can influence bioprocess design.

Adding high amounts of CO_2 into the algal ponds will also make the culture medium acidic. Therefore, it is important that the species selected can grow in acidic conditions and tolerate pH shifts. This quality will also aid in preventing foreign species of algae from competing with the desired species. Based on these criteria, and taking into account the local climate and available resources, *Chlorella vulgaris* was selected as an optimal species for outdoor ponds in Iowa. This organism is capable of growing within a wide range of temperatures and irradiance and has a rapid doubling rate. These desirable traits help to ensure a relative monoculture within the raceway ponds. Furthermore, a significant amount of research has already been conducted on its ability to produce large quantities of lipids for biofuel production and this choice in organism is consistent with our model of New Mexico (Khasanova *et al.* 1978; Nichols *et al.* 1967; Tipinis & Pratt 1960; Jeong *et al.* 2003; Wijanarko *et al.* 2004; Guarnieri *et al.* 2011; Guarnieri *et al.* 2013; Rosenberg *et al.* 2014). Additionally, *Chlorella* species have been successfully cultivated to produce up to 25 g m^{-2} d^{-1} in outdoor raceway ponds (Doucha & Livansky 1995; Hase *et al.* 2000).

2.8.2 Land requirements and CO_2 sequestration

For a biorefinery that produces 50 mgy of ethanol, 143,000 tons of biogenic CO_2 are generated annually from fermentation. This allows for an abundance of carbon feedstock to support algal production. In determining the land requirements, two criteria were analyzed: the average algal areal productivity and the percent of CO_2 to be sequestered. The areal productivity of microalgae is an important factor when determining the land requirement. Microalgae have been grown commercially with

areal productivities of at least 10 g m^{-2} d^{-1}, but studies have shown that biomass productivities of up to 60 g m^2 d^{-1} are attainable (GROBBELAAR 1999).

The second factor critical to determining the land requirements is the percent of CO_2 that can be assimilated by algal biomass. Sequestering all the CO_2 at 20 g m^{-2} d^{-1} will require 2,639 acres of continuous land, a large area that is not readily available. A more reasonable amount of land is 1,000 acres or about 1.56 square miles of land, where a potential 60% of CO_2 can be sequestered with an areal productivity of 30 g m^{-2} d^{-1}. (Figure 12). As the amount of land increases, the cost of pumping nutrients and harvesting the algae increases. Due to the shallow depth of raceway ponds, one of their innate flaws is their dependence on large areas of land. Therefore, careful consideration should be given to the balance between biomass productivity and cost of transporting CO_2, nutrients and water. Proposals to provide nutrients for algae growths such as nitrogen source, phosphates, and potassium through on site production from anaerobic digestions of biomass are appealing (MULBRY *et al.* 2008; IYOVO *et al.* 2010; WANG *et al.* 2010; NOUE & BASSERES 1989).

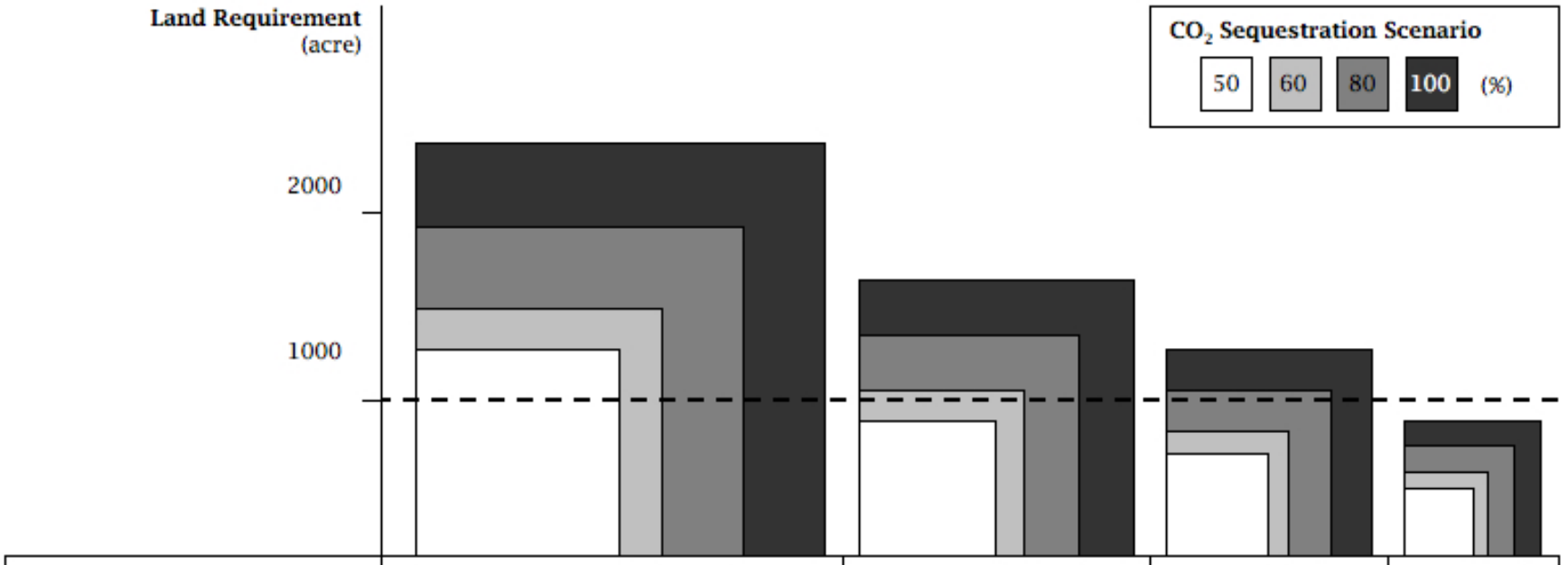

Areal Productivity ($g\ m^{-2}\ d^{-1}$)	20	30	40	60
Max CO_2 Consumption ($ton\ acre^{-1}\ yr^{-1}$)	54	81	108	162

Figure 12. Estimated land requirements for various scenarios of areal microalgal productivity and carbon dioxide consumption (shaded regions). The dashed line at 1,000 acres represents a realistic amount of usable land in close proximity to the ethanol plant. Shaded rectangles that fall within this region are deemed plausible cases; however, productivities greater than 30 g m^{-2} d^{-1} are considered extremely aggressive for raceway pond production.

The theoretical maximum amount of biodiesel that can be produced was calculated for various percentages of potential oil accumulation, assuming 1.83 g of CO_2 yields 1 g of biomass and a 1:1 mass conversion of algal oil to biodiesel. These projections also assume that the oil present in the algae is usable triacylglycerol (TAG) as an ideal feedstock for biodiesel production that can easily undergo transesterification in the presence of an alcohol, such as methanol or ethanol, and a catalyst, such a sodium hydroxide or potassium hydroxide (KADAM 1997). Based on the areal productivity of 20 g m^{-2} d^{-1}, a target goal of sequestering 50% of the available CO_2 is a possible option, requiring just over 1,000 acres and producing 2.4 million gallons of biodiesel (~57,000 barrels) annually. If higher contents of cellular lipids (*e.g.* 60%) are achievable in improved algal strains, a maximum of 7.2 million gallons (~171,000 barrels) of biodiesel could be expected per year (Table 5).

Percent of Total CO_2 Captured Annually	CO_2 Captured (metric tons $year^{-1}$)	Algal Biomass Produced (metric tons $year^{-1}$)	Oil Produced (million gallons $year^{-1}$) at Different Algal Lipid Contents (%)		
			20%	40%	60%
100%	143,000	78,000	4.8	9.5	14.3
80%	114,000	62,000	3.8	7.6	11.5
60%	86,000	47,000	2.9	5.7	8.6
50%	71,000	39,000	2.4	4.8	7.2

Table 5. Correlations between CO_2 utilization, biomass production, and oil yield. Based on different milestones of waste CO_2 conversion (% of total ethanol plant output), projections for the amount of algal oil that can be produced annually over a range of lipid contents are depicted. All values assume an areal productivity of 20 g m^{-2} d^{-1}; however, lipid accumulation scenarios between 20-60% of the algal biomass are modeled.

2.8.3 Heating requirements

Maintaining a constant water temperature during the winter months, especially during periods of irradiance is critical to ensure algal viability and high productivity. To maintain a constant temperature within the raceway ponds, the waste heat streams from the ethanol biorefinery were analyzed for available heat. The available sources of usable heat from the ethanol biorefinery are from the distillation tower and evaporator effluent as well as the fermentors. These heat source streams are sent to a cooling tower, which removes the heat and then recycles the water back into the ethanol production process.

The peak heating requirements for the quarter-acre raceway pond were obtained using the convective, radiative and evaporative losses from the pond. The amount of heat required on a monthly basis was calculated using the assumption that the peak heating requirements were needed for a 12-hour period during the night for the entire month (Figure 13). To estimate the maximum peak heating requirement for a quarter-acre raceway pond, January's minimum temperature of 7.7° F was used to determine a heating requirement of 490,000 Btu hr^{-1}. During the months of December and January, when the temperatures are the coldest, only a theoretical maximum of 41 acres can be heated to a temperature of 73.4° F.

Since 41 acres only accounts for a small fraction of 1,000 acres required to sequester 60% the CO_2, the temperature change in the raceway ponds was examined if only one quarter of the required heat was delivered to each raceway pond. The large quantity of water in the ponds contains thermal energy, which can be used in the

event of the lack of additional heat. Therefore, if 122,500 Btu hr^{-1} were supplied to each pond, over an 8-hour period the total heat loss from the raceways would be roughle 3 million Btu. This correlates to a 6.6° F change in the culture temperature overnight for 165 acres, which is still only one-sixth of the desired acreage. The sun's irradiance during the day is capable of heating the pond back to 73.4° F. In certain cases, a lower nighttime temperature can be beneficial by slowing down the aerobic respiration rate of the algae and can prevent the loss of up to 30% of the daily biomass production (VONSHANK 1997).

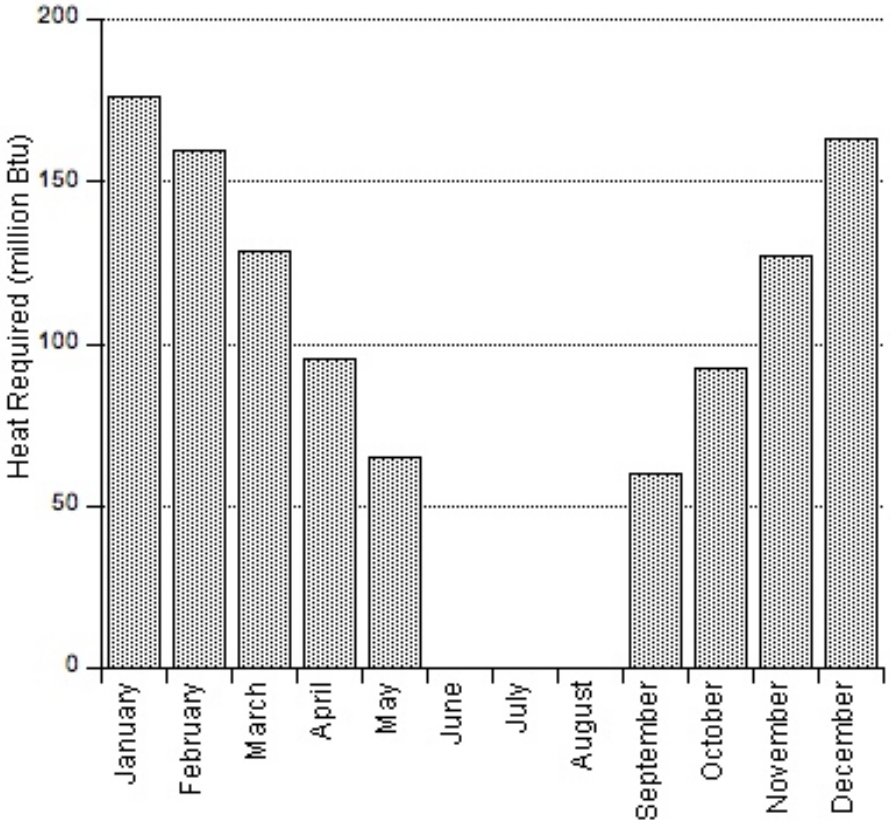

Figure 13. Monthly heating requirements for algal biomass production in raceway ponds in Iowa. Compared to Figure 10, the additional heat necessary is complementary to the temperature profiles for Sioux City, IA and no supplementary heat is required during the summer months.

2.8.4 Economic evaluation

In order to determine the financial viability of this integrated biorefinery, the capital and operational costs were analyzed for 1,000 acres. The capital costs include raceway construction, greenhouse structures and glazing material, and the CO_2 transfer system (Supplementary Table S1: Appendix B).

Next, the operating costs of sequestering CO_2 to produce biomass and harvest it were analyzed. The operational costs of the raceways include the maintenance of the ponds, harvesting and de-watering, algal nutrient costs as well as electricity and supplementary heating costs. Electricity costs include the pumps, paddle wheel motors, CO_2 blowers to deliver CO_2 into the ponds as well as blowers to keep the double layer polyethylene film inflated. The annual heating costs were estimated based on the assumption that the peak heating for each month was required for a daily period of 12 hours. It was also assumed that electricity would be used to heat the raceway ponds, at a cost of 4.95 cents kWh^{-1} (Energy Information Administration 2010). Finally, the heating costs were also adjusted to account for the 41 acres that could be supported through the heat from the ethanol biorefinery. The operational costs were calculated on a per acre basis. Expected annual operating costs for a quarter-acre covered raceway pond unit operating in Iowa are listed in Supplementary Table S2 (Appendix B). A large fraction of the operational cost, between 70-90%, is due to the heat required for the raceway ponds.

Based on the capital investment and operational costs at these various levels of areal productivity, the cost to produce wet algal biomass is estimated to be between $0.95

and $2.30 per kg, with values less than $1.25 kg^{-1} considered as highly optimistic cases. These calculations include de-watering and harvesting costs, but not the energy-intensive step of drying. The corresponding price of algal oil within these cells would be anywhere between $5.10 and $36.25 per gallon, again, with prices below $20.00 gal^{-1} for aggressive cases of high areal productivity and oil content – not including the costs to extract and reclaim the lipids for transesterification to biodiesel. Figure 14 shows the dependence of algal oil cost on both areal productivity and lipid content. Even for the lowest estimate of just over $5.00 gal^{-1} for an extremely aggressive case, algal biodiesel could not be produced economically.

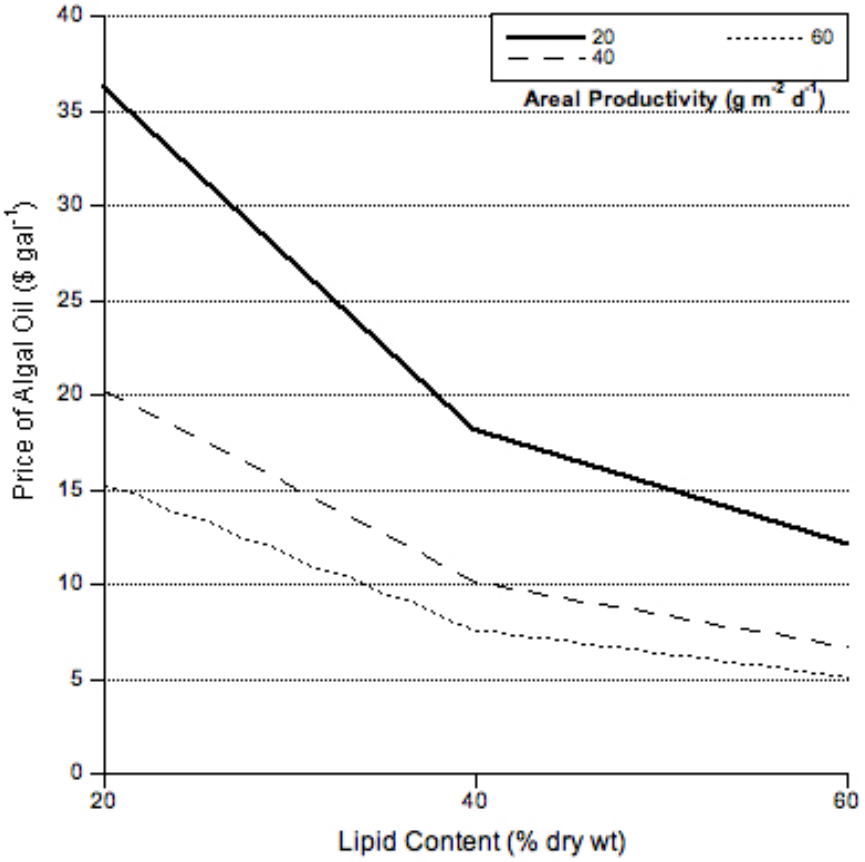

Figure 14. Price of microalgal oil over a range of areal productivities and lipid contents. These prices are relatively intangible because they account for only the cost to produce lipids within the algal cells, discounting any extraction or downstream processing costs; however, they provide a good benchmark when moving forward with the evaluation of biodiesel production.

2.9 Discussion and Conclusions

The ultimate feasibility of algal production systems with ethanol biorefineries depends on several factors that were taken into account in this analysis: (1) algal growth rate; (2) lipid content of the algae; (3) algal concentration in growth system; (4) cost of the growth system and, most importantly for Iowa, and (5) available heat. Based on current algal productivities alone, a large fraction of the CO_2 from the ethanol biorefinery could potentially be sequestered. Albeit technically feasible, the project is not currently economically viable for the purpose of producing biofuels. This conclusion is based principally on the large heating requirements well in excess of heat energy available from the ethanol biorefinery as a byproduct. It should be noted that this analysis does not provide a "fully burdened" cost of algal biofuel since it does not explicitly include post-processing. Instead, the assessment of algal biocrude production focuses heavily on upstream factors that influence biological production.

With current baseline technologies of growth systems, reasonably attainable algal productivities and lipid contents, the cost of producing biodiesel from algae in conjunction with an ethanol biorefinery would be in the range of $10.00 to $40.00 per gallon. For calculating the price of actual biodiesel we have assumed a price of approximately $5.00 gal^{-1} for extraction and downstream processing based on prior modeling and publicly available data for smaller-scale extraction equipment. While $10.00 would be the price for a somewhat impractical case of 60 g m^{-2} d^{-1}, a more probable estimate would be at least above $30.00 per gallon. Although this figure is

currently too high for the biodiesel market, these costs are likely to decrease with technological advancements that are currently underway.

The high heating costs incurred by maintaining a constant temperature within the ponds are prohibitive for producing biofuels at large scales in Iowa. Since evaporative losses appear to be the most significant source of heat dissipation, one possible solution would be to maintain the interior of the greenhouse at a high humidity by using the saturated water vapor from evaporative processes (distillation, cooling) of the refinery. This preemptive mechanism of using water vapor to reduce evaporation would minimize the amount of heat provided to the culture medium.

The small fraction of land sustainable by the available heat shows that raceway ponds may not be the best method to cultivate algae in the Midwest. Alternative culturing systems including enclosed PBRs, such as low-cost flat panel reactors, need to be investigated for this installation. While such enclosed growth systems represent higher initial capital costs, this can be compensated by improved efficiencies and lower ongoing heating costs. High-performance PBRs will also enhance the transfer of CO_2 to the culture medium. Furthermore, for practical implementation in close proximity to a biorefinery, a land requirement of even 1,000 acres may be unrealistic.

Two viable options to mitigate the CO_2 emissions of bioethanol production in the Midwest are (1) to operate the algal production ponds for a 6-month period during the warmer months or (2) produce algal biomass for high-value products, such as nutraceuticals or premium aquaculture feed to offset operating costs. The significant variation in average temperatures in Iowa suggests the necessity to develop at least

two strains of algae— one for summer and one for winter, akin to seasonal crop rotation. It is noteworthy that perhaps the most productive body of water on Earth for algal biomass is the South Ocean during the southern hemispheric summer. Even in summer months, such bodies of water are still relatively cool and capable of supporting very high algal productivities. The inherent flaws in growing algae in open raceway ponds are the low and inconsistent cell densities and large areal footprint. Photobioreactors can begin to address some of these problems, but improvements in manufacturing costs and design must be achieved for these PBRs to be a viable alternative. Higher culture densities achieved in PBRs can also reduce the harvesting costs. An alternative approach to addressing heating costs, areal productivity, and harvesting may include the development of immobilized algal growth systems, such as biofilm-based bioreactors examined in this dissertation.

Downstream of the growth process, some of the excess CO_2 can be used to extract the products produced by the algae with various CO_2-based extraction methods (Donohue *et al.* 2012; Donohue & Williams 2013). This environmentally conscious solution circumvents the use of toxic solvents, such as hexane, to isolate the lipids. By taking advantage of other naturally available clean biogenic resources in Iowa, additional mechanisms of reducing the overhead of this process may include solar and wind power generation to help reduce the carbon footprint of this process (Subhadra & Edwards 2010). Additionally, the cultivation of algal species tolerant of wastewater may also reduce the operating costs of this process; however, these

amendments would likely improve the economic viability only marginally, as the major bottleneck is still the high cost of supplementary heat during the winter.

It is important to note that the heating requirements for the algal growth systems described in this analysis are based on covered raceway ponds. The assumptions, including the use of raceways, in this analysis are based on *current* techniques, productivities, and processes for mass algal cultivation. We believe that this analysis is best applied as a guide for areas of research and improvement required to allow algal biofuels production in conjunction with bioethanol biorefineries to become fully viable. These areas include heat efficient, low-cost high-productivity PBRs, and high-productivity (potentially genetically engineered) algal organisms with perhaps different strains for different seasons. For downstream processing, the use of a range of biofuel metabolites in addition to lipids and lower cost mechanisms of harvesting, including secretion of the biofuels metabolites, will undoubtedly improve the process.

The findings presented in this section are corroborated by the fact that, presently, nearly all algal biomass production facilities are operated in temperate to tropical locations. Although algal biofuels may not yet be economically achievable in Iowa, algae show great promise for the remediation of CO_2 point sources. Integrated-ethanol biorefineries will, nonetheless, be an important step toward positive publicity of both ethanol and microalgal biomass production. Although affordable biofuel production from microalgae in Iowa is currently unattainable, this remains a very realistic goal provided research on the key barriers to production can be accomplished. This important mechanism enabling Midwest ethanol biorefineries to

sequester carbon dioxide biologically can begin immediately with small-scale system that take advantage of the profitable returns of high-value algal coproducts before algal biofuel production can be fully implemented.

2.10 Applicability of Southwest & Midwest TEA in future process design

Both of these TEA models describing algal biofuel production were created with the intention to objectively assess the current best practices in photoautotrophic algal bioprocessing for crude oil production. By identifying critical processing variables capable of influencing the cost of biocrude production, these models can act as engines to drive new conceptual developments in algal cultivation and are able to compare the challenges associated with different farm locations (Venteris *et al.* 2013). While the results of these modeling efforts are certainly nuanced and strongly influenced by the baseline assumptions, in the most general terms, two major opportunities to improve algal biofuel production are to **reduce water** requirements during cultivation and **increase oil** content recovered in the biomass. Improvements in either of these sensitivity variables will have positive effects on the sustainability and economics of biofuel production. In order to address these two fundamental issues, future process development must be targeted at engineering the **physical structure** of growth systems for cultivation and affecting the **biochemical composition** of cells enriched with desired metabolites for biofuels (*i.e.*, extractable lipids).

As a result of the cost sensitivity analysis summarized in Figure 9, lipid content was found to be the major *biological* factor that can most significantly affect the cost of algal oil production. This finding is reflected in both Southwest and Midwest geographies (Figure 14) and remains in close agreement with other recent TEA models (Sun *et al.* 2011; Davis *et al.* 2012). Collectively, the TEA and LCA work in this area suggest that large-scale cultivation will require more integrated methods of regulating biomass composition, maintaining high cultivation efficiencies, and carefully assessing feedstock availability (*e.g.*, carbon dioxide and water) to maintain high lipid yields. Although metabolic engineering of algae may offer improvements at the molecular level as well as diverse biosynthetic pathways to explore, there are a number of uncertainties associated with genetic manipulation at industrial scales (Flynn *et al.* 2013; Flynn *et al.* 2010; Gressel *et al.* 2013; Henley *et al.* 2013). Alternatively, biological optimization of culture conditions is indeed capable of inducing metabolite accumulation relevant to biofuel production using indigenous microalgae (Ho *et al.* 2013). Whether by genetic intervention or regulation of nutrient conditions, higher neutral lipid contents and augmented total lipid productivity directly affect the energy content of algal biomass (Illman *et al.* 2000). In addition to the recent advances in genetic improvement of production organisms, such as *Chlorella* and *Scenedesmus* (Vigeolas *et al.* 2012), a recent evaluation of over 2,000 algal strains from culture collections further exemplifies the vast biodiversity in lipid distribution that exists between different organisms under uniform autotrophic growth conditions (Lang *et al.* 2011). Since differential growth conditions add significant complexity to these oil profiles, strain selection must

ultimately be paired with culture conditions that are applicable to bioproduction objectives. In line with this goal, Chapters 3 and 4 of this thesis aim to exploit the metabolic flexibility of microalgae under photosynthetic and heterotrophic conditions to first identify robust organisms for oil production and then develop enrichment strategies using organic substrates.

Aside from biological parameters involved in algal biofuel production, the *engineering* aspects of facility design requiring intensive water and energy inputs over extensive land areas are related to paddlewheel-driven raceway ponds (Lee 2001; Ben-Amotz 2008). Lifecycle analyses of algal biofuels are favorable by only narrow margins depending on technologies employed for cultivation, harvesting, and extraction of oils (Williams & Laurens 2010). The significant variation in recent cost projections for unrefined algae oil not only illuminates an opportunity for technological improvement, but also underscores disparities among production processes within this nascent field. As we compare the conventional architecture of algal cultivation to land plants, which have evolved specialized structures (leaves & oil seeds) for distinct cellular functions, it follows that novel algae cultivation strategies may be biomimetic by employing a leaf-like structure to assemble algae cells as photocatalysts. Thus, another technical objective of this dissertation is to create a membrane support system to reduce energy and water inputs. In terms of the interrelated issues of nutrient sourcing and the potential for co-localization with industrial sources of CO_2, some have even posited that a potential bottleneck to such production goals arise from limitations in sufficient sources of concentrated CO_2 in

flue gas (CHISTI 2013). One potentially underutilized source of CO_2 comes from fermentation often associated with ethanol biorefineries at large scale. As an example of this type of integration, the ultimate value proposition and feasibility approach of BioProcess Algae, LLC exploits algal growth on solid substrates (biofilms) within closed greenhouses that are co-localized with the biogenic CO_2 sources of ethanol plants in the Midwest. With the first commercial-scale cellulosic ethanol plant in Iowa starting production in September 2014, future expansion of cellulosic ethanol will require methods for CO_2 capture and present opportunities for its reuse. Operated by POET-DSM in Emmetsburg, Iowa, the Project Liberty plant will produce 25-mgy of cellulosic ethanol at full capacity (~600,000 bbl yr^{-1}). Future development of integrated algal biorefineries should look toward co-localization with this type of waste CO_2, while also seeking supplemental organic feedstocks to enhance and diversify carbon nutrition to algae (*i.e.*, promote mixo– or heterotrophic growth).

In conclusion, progressive approaches to integrated algae production can permit next-generation biofuel in non-ideal climates that have previously been dominated by corn-based ethanol. By co-localizing with an ethanol biorefinery, the use of waste heat and CO_2 is technically feasible with conventional technologies at small- to moderate scales ($<$ 100 acres), but limited by the balance of carbon dioxide to heat (ROSENBERG *et al.* 2011). In New Mexico, a more robust technoeconomic analysis and critical evaluation of the scalability of raceway ponds driven by paddlewheels revealed that water requirements are massive and the energy required to circulate

water by paddlewheels is a prohibitive operating expense (Rogers *et al.* 2014). Having now quantified the potential improvement goals and tradeoffs between lipid, water, and nutrients from both economic and environmental perspectives, these underpinnings will enable the design of more cost effective, sustainable algae production systems with a focus on EROI (Beal *et al.* 2012). The proceeding body of work aims to develop the knowledge base to implement bio-*film*-reactors in concert with strategic nutrient regimes to augment lipid productivity and minimize water use.

2.11 References

Aslan S, Kapdan IK (2006) Batch kinetics of nitrogen and phosphorus removal from synthetic wastewater by algae. Ecological Engineering 28: 64-70.

Beal CM, Hebner RE, Webber ME, Ruoff RS, Seibert AF (2012) The energy Return on Investment for Algal Biocrude: Results for a Research Production Facility. BioEnergy Research 5: 341-362.

Behnke C (2013) Development of value-added products from residual algae biomass. 2013 Project Peer Review: U.S. Department of Energy Biomass Technologies Office. May 20-23, 2013: Alexandria, VA. Accessed 11 September 2013. Available: www2.eere.energy.gov/biomass/peer_review2013/Portal/

Ben-Amotz A (2008) Large scale open algae ponds. The National Institute of Oceanography, Israel. Available: www.nrel.gov/biomass/pdfs/benamotz.pdf Accessed 11 September 2014.

Vigeolas H, Duby F, Kaymak E, Niessen G, Motte P, et al. (2012) Isolation and partial characterization of mutants with elevated lipid content in *Chlorella sorokiniana* and *Scenedesmus obliquus*. J Biotechnol 162: 3-12.

Benemann JR, Oswald WJ (1996) Systems and Economic Analysis of Microalgae Ponds for Conversion of CO_2 to Biomass. Pittsburg, PA: DOE/PC/93204--T5, U.S. Department of Energy.

Chisti Y 2013. Constraints to commercialization of algal fuels. Journal of Biotechnology 167: 201-217.

Energy Information Administration (2010) Average retail price of electricity to ultimate customers by end-use sector, by state. Accessed 22 March 2010 Available: http://www.eia. doe.gov/cneaf/electricity/epm/table5_6_a.html

Blom TJ, Ingratta FJ (1984) The use of polyethylene film as a greenhouse glazing in North America. ISHS Acta Horticulturae 170: 69-80.

Bohutskyi P, Bouwer E (2013) Biogas Production from Algae and Cyanobacteria Through Anaerobic Digestion: A Review, Analysis, and Research Needs. Advanced Biofuels and Bioproducts. pp 873-975.

Both AJ (2014) Section 1: Greenhouse Lighting. In Greenhouse Energy Cost Reduction Strategies. Rutgers University, Bioresource Engineering & Dept. of Plant Biology & Pathology. Accessed 30 August 2014. Available: hrt.msu.edu/Energy/Notebook/pdf/Sec1/AJ_Both_Greenhouse_Glazing.pdf

Brown LM (1996) Uptake of carbon dioxide from flue gas by microalgae. Energy Conversion and Management 37: 1363-1367.

Brown P (2009) Algal Biofuels Research, Development, and Commercialization Priorities: A Commercial Economics Perspective. Energy Overviews. Available: http://epoverviews.com

Chaumont D (1993) Biotechnology of algal biomass production: a review of systems for outdoor mass culture. Journal of Applied Phycology 5: 593-604.

Chinnasamy S, Ramakrishnan B, Bhatnagar A, Das KC (2009) Biomass production potential of a wastewater alga *Chlorella vulgaris* ARC 1 under elevated levels of CO_2 and temperature. Int J Mol Sci 10: 518-532.

Chisti Y (2007) Biodiesel from microalgae. Biotechnology Advances 25: 294-306.

Climate Zone (2010) Climate information for Sioux City, Iowa. Available: http://www.climate-zone.com/climate/united-states/iowa/sioux-city Accessed 22 March 2010.

CoStar Company: Lands of New Mexico (2013) Accessed 5 May 2013. Available: http://www.landsofnewmexico.com/new_mexico/index.cfm

Craggs JR, McAuley PJ, Smith VJ (1997) Wastewater nutrient removal by marine microalgae grown on a corrugated raceway. Water Research 31: 1701-1707.

DARPA (2013) Defense Sciences Office: Biofuels. Accessed 29 August 2014. Available: http://www.darpa.mil/Our_Work/DSO/Programs/Biofuels.aspx

Davis R, Fishman D, Frank ED, Wigmosta MS, et al. (2012) Renewable Diesel from Algal Lipids: An Integrated Baseline for Cost, Emissions, and Resource Potential from a Harmonized Model. Argonne National Laboratory, Technical Report: ANL/ESD/12-4, NREL/TP-5100-55431, PNNL-21437. Available at: www.nrel.gov/docs/fy12osti/55431.pdf

Dhargalkar VK, Verlecar XN (2009) Southern Ocean seaweeds: a resource for exploration in food and drugs. Aquaculture 287: 229-242.

Donohue MD, Betenbaugh MJ, Oyler GA, Rosenberg JN (2012) Method for extraction and purification of oils from microalgal biomass using high- pressure CO_2 as a solute, U.S. Application No. 13/8167/737.

Donohue MD, Williams SH (2013) Methods for extraction of lipids from wet algal biomass. International Application No. PCT/US2013/061535.

Doucha J, Livansky K (1995) Novel outdoor thin-layer high density microalgal culture system: productivity and operational parameters. Algological Studies 76: 129-147.

EERE (2013) Bioenergy Technologies Office At-a-Glance. Accessed 23 May 2013. Available: energy.gov/sites/prod/files/2013/11/f4/bioenergy_ataglance_2014.pdf

EPA (2007) EISA Mandates Renewable Fuel Standard. Accessed 29 August 2014. Available: http://www2.epa.gov/laws-regulations/summary-energy-independence-and-security-act

EPA (2013) CO_2 Emissions Estimates, Accessed 26 April 2013. Available: http://www.epa. gov/greenpower/pubs/calcmeth.htm.

Flynn KJ, Greenwell HC, Lovitt RW, Shields RJ (2010) Selection for fitness at the individual or population levels: Modeling effects of genetic modifications in microalgae on productivity and environmental safety. Journal of Theoretical Biology 263: 269-280.

Flynn KJ, Mitra A, Greenwell HC, Sui J (2013) Monster potential meets potential monster: pros and cons of deploying genetically modified microalgae for biofuels production. J R Soc Interface Focus. 3: 20120037.

Ghernaouta B, Ghernaoutb D, Saibabpages (2010) Algae and cyanotoxins removal by coagulation/flocculation: A review. Desalination and Water Treatment 20: 133-143.

Good M (2008) Railroad Construction Cost Estimates. Accessed 13 December 2012. Available: http://tacnet.missouri.org/history/railroads/rrcosts.html

Gouveia L, Oliveira AC (2009) Microalgae as a raw material for biofuels production. J Ind Microbiol Biotechnol 36: 269-274.

Gressel J, van der Vlugt CJB, Bergmans HEN (2013) Environmental risks of large scale cultivation of microalgae: Mitigation of spills. Algal Research 2: 286-298.

Grobbelaar JU (1999) Physiological and technological considerations for optimising mass algal cultures. Journal of Applied Phycology. Journal of Applied Phycology 12: 201-206.

Guarnieri MT, Nag A, Smolinski SL, Darzins A, Seibert M, et al. (2011) Examination of triacylglycerol biosynthetic pathways via *de novo* transcriptomic and proteomic analyses in an unsequenced microalga. PLoS ONE (6:10): e25851.

Guarnieri MT, Nag A, Yang S, Pienkos PT (2013) Proteomic analysis of *Chlorella vulgaris*: Potential targets for enhanced lipid accumulation. J Proteomics 93: 245-253.

Gutzeit G, Lorch D, Weber A, Engels M, Neis U (2005) Bioflocculent algal-bacterial biomass improves low-cost wastewater treatment. Water Science & Technology 52: 9-18.

Hase R, Oikawa H, Sasao C, Morita M, Watana Y (2000) Photosynthetic production of microalgal biomass in a raceway system under greenhouse conditions in Sendai city. Journal of Bioscience and Bioengineering 89: 157-163.

Hellwig S, Drossard J, Twyman RM, Fischer R (2004) Plant cell cultures for the production of recombinant proteins. Nature Biotechnology 22: 1415-1422.

Henley WJ, Litaker RW, Novoveská L, Duke CS, Quemada HD, Sayre RT (2013) Initial risk assessment of genetically modified (GM) microalgae for commodity-scale biofuel cultivation. Algal Research 2: 66-77.

Ho S-H, Huang S-W, Chen C-Y, Hasunuma T, Kondo A, Chang J-S (2013) Characterization and optimization of carbohydrate production from an indigenous microalga *Chlorella vulgaris* FSP-E. Bioresource Technology 135: 157-165.

Huntley M, Redalje D (2007) CO_2 mitigation and renewable oil from photosynthetic microbes: a new appraisal. Mitigation and Adaptation Strategies for Global Change 12: 573-608.

Illman AM, Scragg AH, Shales SW (2000) Increase in *Chlorella* strains calorific values when grown in low nitrogen medium. Enzyme and Microbial Technology 27: 631-635.

Index Mundi (2012) DAP fertilizer vs Urea. Accessed 13 December 2012. www.indexmundi.com/commodities/?commodity=dap-fertilizer&commodity=urea

Iyovo GD, Du G, Chen J (2010) Sustainable bioenergy bioprocessing: biomethane Production, digestate as biofertilizer and as supplemental feed in slgae cultivation to promote algae biofuel commercialization. Journal of Microbial & Biochemical Technology 2: 100-106.

Kadam KL (1997) Power Plant Flue Gas as a Source of CO2 for Microalgae Cultivation: Economic Impact of Different Process Options. Energy Conversion and Management 38: S505-S510.

Kagan ML, West AL, Zante C, Calder PC (2013) Acute appearance of fatty acids in human plasma – a comparative study between polar-lipid rich oil from the microalgae *Nannochloropsis oculata* and krill oil in healthy young males. Lipids in Health and Disease 12: 102.

Keeling RF (2008) Recording Earth's vital signs. Science 319: 1771e2.

Ketheesan B, Nirmalakhandan N (2012) Feasibility of microalgal cultivation in a pilot-scale airlift-driven raceway reactor. Bioresource Technology 108: 196-202.

Khasanova VM, Gusakova SD, Taubaev TT (1978) Composition of the neutral lipids of *Chlorella vulgaris*. Chemistry of Natural Compounds 14: 37-40.

Lang I, Hodac L, Friedl T, Feussner I (2011) Fatty acid profiles and their distribution patterns in microalgae: a comprehensive analysis of more than 2,000 strains from the SAG culture collection. BMC Plant Biology 11: 124.

Lansford R, Hernandez J, Enis PJ, Truby D, Mapel C (1990) Evaluation of available saline water resources in New Mexico for the production of microalgae. Report, Solar Energy Research Institute, Golden, Colorado, SERI/TP 232-3597

Lee C-G, Palsson B (1994) High-density algal photobioreactors using light-emitting diodes. Biomolecular Bioengineering 44: 1161-1167.

Lee, Y-K (2001) Microalgal mass culture systems and methods: their limitation and potential. Journal of Applied Phycology 13: 307-315.

Lundquist TJ, Hammond D, Green FB, Oswald WJ (2004) Tertiary Pilot Study Report, Recycled Wastewater Facilities Plan, Oswald Engineering Associates, Inc., City of St. Helena, California, pp. 70.

Mann NR, Herbst RS, Hess JR, Kochergin V (2004) Enhanced flux, erosion resistant membranes for biomass separations — Part II Membrane Technology: 5-9.

Maxwell DP, Falk S, Trick CG, Huner NPA (1994) Growth at low temperature mimics high-light acclimation in *Chlorella vulgaris*. Plant Physiol 105: 535-543.

Metzger P, Berkaloff C, Casadevall E, Coute A. (1985) Alkadiene and botryococcene-producing races of wild strains of *Botryococcus braunii.* Phytochemistry 24: 2305-2312.

Mile Models (2012) Generic Cost Per Mile. Accessed 13 December 2012. Available: http://citizensforsouthernillinois.org/?page_id=72

Mulbry WW, Ingram SK, Buyer JS (2008) Treatment of dairy and swine manure effluents using freshwater algae: fatty acid content and composition of algal biomass at different manure loading rates. Journal of Applied Phycology 20: 1079-1085.

Neenan B, Feinberg D, Mcintosh A, Terry K (1986) Fuels from Microalgae: Technology Status, Potential, and Research Requirements. Golden, CO: SERI/SP-231-2550, Solar Energy Research Institute.

Nichols BW, James AT, Breuer J. (1967) Interrelationships between fatty acid biosynthesis and acyl-lipid synthesis in *Chlorella vulgaris*. Biochemical Journal 104: 486-496.

Noue JD, Basseres A (1989) Biotreatment of anaerobically digested swine manure with microalgae. Biological Wastes 29: 17-31.

Oakland URS (2007) Oakland County Water and Wastewater Masterplan. Project No. 13647263 Volume 4: Alternative Analysis. Accessed 13 December 2012. Available: www.oakgov.com/water/Documents/vol_4_alternatives_analysis.pdf

Olivares JA (2011) Challenges and opportunities in algal biodiesel development. Los Alamos National Laboratory (LANL) Report No. LA-UR-11-00834.

Oyler GA, Rosenberg JN, Weeks DP (2012) Single chain antibodies for photosynthetic microorganisms and method of use. U.S. Application No. 13/441,951.

Peters MS, Timmerhaus K, West R (2002) *Plant Design and Economics for Chemical Engineers.* 5th ed., McGraw-Hill. p. 793.

Rafferty K, Culver G (1998) Chapter 11: Heat Exchangers. In: Lienau P, Lunis, BC, editors. Geothermal Direct Use Engineering and Design Guidebook, Kalamath Falls, OR: Oregon Institute of Technology, p. 261-277.

Redfield AC (1934) On the proportions of organic derivatives in seawater and their relation to the composition of plankton. University Press of Liverpool. 177-192.

Renaud SM, Thinh L-V, Lambrinidis G, Parry DL (2002) Effect of temperature on growth, chemical composition and fatty acid composition of tropical Australian microalgae grown in batch cultures. Aquaculture 211: 195-214.

Rogers JN, Rosenberg JN, Guzman BJ, Oh VH, Mimbela LE, et al. (2014) A critical analysis of paddlewheel-driven raceway ponds for algal biofuel production at commercial scales. Algal Res 4: 76-88.

Rosenberg JN, Kobayashi N, Barnes A, Noel EA, Betenbaugh MJ, Oyler GA. (2014) Comparative analyses of three *Chlorella* species in response to light and sugar reveal distinctive lipid accumulation patterns in *C. sorokiniana*. PLoS ONE 9:e92460.

Rosenberg JN, Mathias A, Korth K, Betenbaugh MJ, Oyler GA (2011) Microalgal biomass production and CO_2 sequestration from an integrated ethanol biorefinery in Iowa: a technical appraisal and economic feasibility evaluation. Biomass Bioenerg 35: 3865-3876.

Rosenberg JN, Oyler GA, Wilkinson L, Betenbaugh MJ (2008) A green light for engineered algae: redirecting metabolism to fuel a biotechnology revolution. Current Opinion in Biotechnology 19: 430-436.

Salim S, Bosma R, Vermuë MH, Wijffels RH (2010) Harvesting of microalgae by bio-flocculation. J Appl Phycol 23: 849-855.

Salim S, Vermuë MH, Wijffels RH (2012) Ratio between autoflocculating and target microalgae affects the energy-efficient harvesting by bio-flocculation. Bioresource Technol 118: 49-55.

Sanford S (2005) Greenhouse Energy Efficiency*: Rural Energy Issues*, Biological Systems Engineering, University of Wisconsin – Madison. Available: hrt.msu.edu/energy/pdf/Greenhouse%20Energy%20Efficiency,%20S.%20Sanford, %20Nov%202005.pdf Accessed 30 August 2014.

Schlesinger A, Eisenstadt D, Bar-Gil A, Carmely H, Einbinder S, Gressel J (2012) Inexpensive non-toxic flocculation of microalgae contradicts theories; overcoming a major hurdle to bulk algal production. Biotechnology Advances 30: 1023-1030.

Schlesinger A, Eisenstadt D, Einbinder S, Gressel J (2011) Method and system for efficient harvesting of microalgae and cyanobacteria. U.S. Patent No. 2011/0081706.

Schoepp NG, Stewart RL, Sun V, Quigley AJ, Mendola D, et al. (2014) System and method for research-scale outdoor production of microalgae and cyanobacteria. Bioresource Technology 166: 273-281.

Sheehan J, Dunahay T, Benemann J, Roessler P (1998) A Look Back at the U.S. Department of Energy's Aquatic Species Program: Biodiesel from Microalgae. Report Number: TP-580-24190. Golden, Colorado: National Renewable Energy Lab.

Skjanes K, Lindbald P, Muller J (2007) BioCO_2 – a multidisciplinary, biological approach using solar energy to capture CO_2 while producing H_2 and high value products. Biomol Eng 24: 405e13.

Stoever HJ (1941) Applied Heat Transmission, 1st ed. New York, NY: McGraw-Hill Book Company.

Subhadra B, Edwards M (2010) An integrated renewable energy park approach for algal biofuel production in United States. Energy Policy 38: 4897-4902.

Sun A, Davis R, Starbuck M, Ben-Amotz A, Pate R, Pienkos, PT (2011) Comparative cost analysis of algal oil production for biofuels. Energy 36: 5169-5179.

Thomas P (2010) Lecture 5: Greenhouse Construction and Glazing. Available: faculty.caes.uga.edu/pthomas/hort4050.web/Hort4050web/lectures/03/lec3.html Accessed 22 March 2010.

Tipinis HP, Pratt R (1960) Protein and Lipid Content of *Chlorella vulgaris* in Relation to Light. Nature 188: 1031-1032.

Tsygankov AA, Laurinavichene TV, Gogotov IN (1994) Laboratory scale photobioreactor. Biotechnology Techniques 8: 575-578.

Urbanchuk JM (2014) Contribution Of The Biofuels Industry To the Economy of Iowa. Available: iowarfa.org/documents/2014IowaEconomicImpact.Final.pdf Accessed 11 September 2014.

Valdés FJ, Hernández MR, Gómez A, Marcilla A, Chápuli E. (2008) Study of the efficiency of different flocculants for effective microalgae harvesting. Universidad de Alicante. Departamento de Ingeniería Química; Available: http://rua.ua.es/dspace/handle/10045/8536 Accessed 30 August 2014.

Venteris ER, R Skaggs, AM Coleman, MS Wigmosta (2013) A GIS cost model to assess the availability of freshwater, seawater, and saline groundwater for algal biofuel production in the United States. Environmental Science & Technology 47: 4840-4849.

Vonshank A (1997) *Spirulina platensis* (*Arthrospira*): physiology, cell-biology, and biotechnology. 1st ed. Boca Raton, FL: CRC Press.

Waller P, Ryan R, Kacira M, Li P (2012) The algae raceway integrated design for optimal temperature management. Biomass Bioenergy 46: 702–709.

Wang B, Li Y, Wu N, Lan CQ (2008) CO_2 bio-mitigation using microalgae. Appl Microbiol Biotechnol 79: 707e18.

Wang L, Wang Y, Chen P, Ruan R (2010) Semi-continuous cultivation of *Chlorella vulgaris* for treating undigested and digested dairy manures. Appl Biochem Biotechnol 162: 2324-2332.

Wijanarko A, Dianursanti D, Witarto AB, Soemartojo RW (2004) Effect of photoperiodicity on CO_2 fixation by *Chlorella vulgaris* buitenzorg in bubble column photobioreactor for food supplement production. Makara Teknol 8: 35-43.

Williams BJLB, Laurens LML (2010) Microalgae as biodiesel & biomass feedstocks: Review & analysis of the biochemistry, energetics & economics. Energy & Environmental Science 3: 554-590.

Miao X, Wu Q (2006) Biodiesel production from heterotrophic microalgal oil. Bioresource Technol 97: 841-846.

Wyatt NB, Gloe LM, Brady PV, Hewson JC, Grillet AM, Hankins MG, Pohl PI. (2012) Critical conditions for ferric chloride-induced flocculation of freshwater algae. Biotechnol Bioeng 109: 493-501.

3

COMPARATIVE ANALYSES OF *CHLORELLA* SPECIES REVEAL DISTINCTIVE LIPID ACCUMULATION PATTERNS IN *C. SOROKINIANA* DURING HETEROTROPHY[†]

Based on the technoeconomic choke points forecasted in the previous chapter, attaining consistently high lipid content in harvested biomass remains paramount to both the financial viability and long-term sustainability of algal biofuels. As such, this chapter describes an algal strain selection pipeline based on phylogenetic species identification, physiological growth response to light and/or sugar, and biochemical

[†] This chapter contains excerpts from the paper by ROSENBERG *et al.* 2014 entitled *Comparative analyses of three Chlorella species in response to light and sugar reveal distinctive lipid accumulation patterns in the microalga* C. sorokiniana, which was published in *PLOS ONE* (9:e92460) and is reprinted here with permission to redistribute under a Creative Commons License.

characterization of shifts in fatty acid composition imposed by heterotrophic metabolism. Focusing on the *Chlorella* genus, these species differ significantly in their photoautotrophic and heterotrophic characteristics. Certain species have the potential to achieve high cell densities under heterotrophic conditions and can accumulate energy-dense neutral lipids as triacylglycerol (TAG), which is amenable to extraction and conversion to biofuel. In this chapter, the molecular phylogeny of thirty *Chlorella* strains was determined in order to inform bioprospecting efforts and detailed physiological assessment of three species. The growth kinetics and lipid biochemistry of *C. protothecoides* UTEX 411, *C. vulgaris* UTEX 265, and *C. sorokiniana* UTEX 1230 were quantified during photoautotrophy in Bold's basal medium (BBM) and heterotrophy in BBM supplemented with glucose (10 g L^{-1}). Heterotrophic growth rates of UTEX 411, 265, and 1230 were found to be 1.5-, 3.7-, and 5-fold higher than their respective autotrophic rates. With a rapid nine-hour heterotrophic doubling time, *Chlorella sorokiniana* UTEX 1230 maximally accumulated 39% total lipids by dry weight during heterotrophy compared to 18% autotrophically. Furthermore, the discrete fatty acid composition of each strain was examined in order to elucidate lipid accumulation patterns under the two trophic conditions. In both modes of growth, UTEX 411 and 265 produced 18:1 as the principal fatty acid while UTEX 1230 exhibited a 2.5-fold enrichment in 18:2 relative to 18:1. Although the total lipid content was highest in UTEX 411 during heterotrophy, UTEX 1230 demonstrated a two-fold increase in its heterotrophic TAG fraction at a rate of 28.9 mg L^{-1} d^{-1} to reach 22% of the biomass, corresponding to as much as 90% of its total lipids. Interestingly, UTEX 1230

growth was restricted during mixotrophy and its TAG production rate was suppressed to 18.2 mg L^{-1} d^{-1}. This constraint on carbon flow raises intriguing questions about the impact of sugar and light on the metabolic regulation of microalgal lipid biosynthesis.

3.1 Introduction

While many benefits of microalgae production are inherent to photosynthetic carbon dioxide assimilation, heterotrophic growth can circumvent certain limitations of photoautotrophic cultivation, such as ineffective light transfer in saturated cultures and low photosynthetic efficiencies (Blankenship *et al.* 2011; Zhu *et al.* 2008). During heterotrophy, the presence of a fixed carbon source (*i.e.*, sugar) can promote rapid growth, support high cell densities, and augment lipid accumulation (Bumback *et al.* 2011). As such, this mode of growth has been exploited for the industrial production of polyunsaturated fatty acids and bioactive pigments to serve nutritional markets (Senanayake *et al.* 2010; Patnaik *et al.* 2006). In recent years, however, incentives to grow oleaginous microalgae have shifted toward biofuels as an end product (Davis *et al.* 2012; Schenk *et al.* 2008; Miao & Wu 2006). Triacylglycerol (TAG) is a preferred renewable oil because it possesses a high molar ratio of hydrogen to carbon, can be easily extracted from biomass and directly converted to drop-in biofuels by transesterification, hydrotreating, or pyrolysis (Li *et al.* 2007; Harwood *et al.* 2009). If heterotrophic substrates can be sustainably sourced for relatively low cost (*e.g.*, derived from cellulosic biomass, wastewater, or directly produced by other photoautotrophs) (Niederholtmeyer *et al.* 2010), the

bioconversion of organic compounds to lipids may be a viable model for algal biofuel production (National Research Council 2012; Vasudevan *et al.* 2012).

For the commercial cultivation of microalgae, nitrogen limitation is a well studied environmental stressor known to induce lipid accumulation (Converti *et al.* 2009; Msanne *et al.* 2011; Sheehan *et al.* 1998; Stephenson *et al.* 2010). Detailed analyses of heterotrophic algal oil production have also been reported and recently reviewed (Spoehr *et al.* 1949; Samejima *et al.* 1958; Perez-Garcia *et al.* 2011; Xiong *et al.* 2010; Fan *et al.* 2012a; Zheng *et al.* 2012). Additionally, mixotrophic cultivation with sugar and light can stimulate high oil yields (Lee *et al.* 2006). While we have previously assessed the biomass and lipid productivities of *Nannochloropsis*, *Dunaliella*, and *Chlorella* species grown on a wide variety of sugars (Wan *et al.* 2012a), the present study focuses on the *Chlorella* genus of green algae *(Chlorophyceae)*, most commonly known for its nutritional benefits when consumed in whole cell dietary supplements (Kiron *et al.* 2012; Tredici *et al.* 2009; Gouveia *et al.* 2008). Various aspects of plant physiology and metabolism have also been studied in *Chlorella* for nearly a century (Warburg & Negelein 1920; Kessler 1976). In the early 1950s, when open pond cultivation systems first became prevalent, *Chlorella* species were some of the first microalgae to be produced in mass quantities and an investigation of scale-up "from laboratory to pilot plant" was reported by Burlew (1953).

Despite the long history of the *Chlorella* genus, currently the only species with a fully sequenced, annotated, and publicly available genome is *Chlorella variabilis* NC64A

(Blanc *et al.* 2010). This unique strain is both the host to large DNA chloroviruses and can be an endosymbiont of *Paramecium bursaria*, surviving through mixotrophic nutrient exchange (McAuley 1986; Muscatine *et al.* 1967; Ziesenisz *et al.* 1981). When NC64A is not harbored by *P. bursaria*, it is susceptible to viral infection and requires nutrient supplementation to grow (Dunigan *et al.* 2012; Van Etten 2003; Yamada *et al.* 2006). While its genome remains a valuable resource for understanding the balance of carbon metabolism, symbiosis, and pathogen-host interactions, NC64A is not a likely candidate for biomass production due to its low yields. Instead, other *Chlorella* species have been cultivated under mixo– and heterotrophic conditions for the production of lutein and astaxanthin (antioxidants) and have served as the basis for mathematical models of sugar-based growth (Shi *et al.* 2006; Shi *et al.* 2000; Ip & Chen *et al.* 2005; Sun *et al.* 2008; Feng *et al.* 2012; Matsukawa *et al.* 2000). Recent metabolic flux analyses and transcriptomic studies performed under different trophic conditions also provide compelling information about shifts in *Chlorella* lipid metabolism (Xiong *et al.* 2010; Guarnieri *et al.* 2011; Wan *et al.* 2012b; Fan *et al.* 2012b).

In order to fulfill an ongoing search for production organisms and model algal systems, the present study assesses the biodiversity of *Chlorella* species based on biofuel production qualities of heterotrophic growth and TAG accumulation when supplemented with glucose at 10 g L^{-1}. After phylogenetic sequencing of thirty strains from culture repositories, *C. sorokiniana* UTEX 1230, *C. vulgaris* UTEX 265, and *C. protothecoides* UTEX 411 were selected for comparative analyses based on

growth rates, biomass yield, and lipid productivities in photoautotrophic and heterotrophic culture. The influence of heterotrophy and mixotrophy on lipid biochemistry was also investigated through examination of the abundance, composition, and distribution of total oils as membrane-associated lipids, TAG neutral lipids, or accessory lipophilic molecules. Finally, discrete lipid profiles were determined using gas chromatography–mass spectrometry (GC-MS) to evaluate the dynamics of fatty acid chain length and degree of saturation during the course of cultivation. As a result of this comprehensive *Chlorella* species screening, the occurrence of differential lipid compositions led to further consideration of *C. sorokiniana* as a potential platform for bioenergy and biotechnology.

3.2 Materials and Methods

3.2.1 Microalgal cultivation

Stock samples of microalgal strains were obtained from the Culture Collection of Algae at University of Texas at Austin (http://web.biosci.utexas.edu/utex/) and maintained on sterile agar plates (1.5% w:v) containing Bold's basal medium (BBM) (Nichols & Bold *et al.* 1965). Cells were cultivated in 1.5-L glass Fernbach flasks or 8-L glass Bellco bioreactors (New Jersey, USA) at 27° C (± 1) using BBM. Each axenic batch culture was inoculated with exponentially growing cells at a density of 1 × 10^6 cells ml^{-1}, constantly stirred, and bubbled with sterile air and monitored with a calibrated M240 digital pH meter (Corning, Inc., New York, USA). Photoautotrophic cultures were illuminated with cool-white fluorescent light at an intensity of 100 µE m^{-2} s^{-1}. Heterotrophic and mixotrophic cultures were

supplemented with glucose at a concentration of 10 g L^{-1}. While heterotrophic cultures were grown in complete darkness, mixotrophic cultures were grown with a light intensity of 100 µE m^{-2} s^{-1}. Cell densities were measured by hemocytometer with an Axiovert 100 inverted light microscope (Carl Zeiss, Göttingen, Germany). Measurements were taken in duplicate and experiments were repeated at least three times. Liquid cultures were harvested using a high-speed centrifuge (Sorvall® RC-5B, Delaware, USA) at 6,000 × *g* for 20 minutes.

3.2.2 Species identification by genetic sequencing and phylogeny

Species-specific genetic fingerprints were determined by sequencing the internal transcribed spacer (ITS) regions of ribosomal DNA (An *et al.* 1999; Hoshina *et al.* 2010; Huss *et al.* 1999). Nucleic acids were extracted from clonal algal populations using a 5% Chelex-100 solution as described previously (Wan *et al.* 2011b). After boiling at 100° C for 15 minutes, samples were centrifuged at 16,000 × *g* for 2 minutes and DNA recovery was quantified using a NanoDrop 2000 spectrophotometer (Thermo Fisher Scientific, Delaware, USA). The primers designed for this study (5'-ACTCCGCCGGCACCTTATGAG-3'; 5'-CCGGTTCGCTCGCCGTTACTA-3') were used to amplify the ITS regions with the Top Taq Master Mix Kit (Qiagen, California, USA) according to the manufacturer's protocol employing thermocycler conditions with an initial melting at 95° C for 2 minutes, followed by 35 cycles of [94° C for 30 sec, 60° C for 30 sec, 72° C for 2 min] and a final elongation at 72° C for 10 minutes. Amplified fragments were separated by electrophoresis on an acrylamide (1% w:v) tris-borate-EDTA gel. Molecular weights were determined with a

GeneRuler 1 kb Plus DNA Ladder (Fermentas, Delaware, USA) and ultimately purified using the GenCatch^{TM} PCR Extraction Kit (Epoch). The resulting nucleotide sequences of 18S ITS regions (Eurofins MWG Operon, Ebersberg, Germany) can be found as annotated entries in the GenBank database (http://www.ncbi.nlm.nih.gov/genbank/) and were aligned using version five of the Molecular Evolutionary Genetics Analysis (MEGA) software suite employing the MUSCLE alignment feature and neighbor joining method to produce phylogenetic trees (Tamura *et al.* 2011).

3.2.3 Measurement of algal biomass dry weight and total lipid content

In order to measure dry biomass yield, algal cultures were harvested as described previously, dried overnight in a vacuum oven at 60° C (Precision Scientific Model 5831, NAPCO, Virginia, USA) and weighed in triplicate. For total lipid extraction, washed cell pellets were freeze-dried with a lyophilizer (Model 25 SRC, Virtis, New York, USA) to preserve the integrity of fatty acids and homogenized with a mortar and pestle in liquid nitrogen. For each sample, 100 mg of homogenized biomass was extracted in 6 ml of 1:2 (v:v) chloroform:methanol containing 0.01% butylhydroxyltoluene and 500 µg of tripentadecanoin (15:0 TAG, Nu-Check Prep, Minnesota, USA) was added as an internal standard (Bligh & Dyer *et al.* 1959). To the 6 ml total extraction volume, 1 ml of 0.7 mm diameter zirconia beads (BioSpec Products, Oklahoma, USA) was added and vortexed at room temperature for 30 minutes. After centrifugation at 1,500 × g for 5 minutes, the chloroform phase was collected and the water phase was re-extracted using 5 ml of chloroform; re-

extraction was repeated three times. The pooled chloroform phases were evaporated to dryness under a stream of nitrogen. To confirm the methodological validity of manual oil separation (LAURENS *et al.* 2012), total lipid extractions were performed in parallel using an automated Accelerated Solvent Extraction 150 system, which employs elevated temperature and pressure (120° C, 1,500 psi, 4 reflux cycles) to accomplish rigorous oil separation and is generally recognized as the most effective oil extraction equipment (Dionex, Thermo Fischer, Delaware, USA) (LUTHRIA *et al.* 2004; MULBRY *et al.* 2009). The closely comparable total lipid contents of manual and automated extractions were determined in triplicate by gravimetric methods.

3.2.4 Fatty acid methyl ester (FAME) analysis

Extracted lipids were transmethylated to FAME as previously described (MSANNE *et al.* 2011) and TAG separation was accomplished by thin layer chromatography. FAME was analyzed using an Agilent 6890 Series Gas Chromatography System with an Agilent 5973 Network Mass Selective Detector (Agilent Technologies, Delaware, USA). Chromatography was carried out using a 200 m × 250 µm × 0.25 µm Varian GC capillary column (Varian Inc., California, USA) with the inlet held at 270° C while 1 µl of the sample was injected using helium as the carrier gas. The oven temperature was programmed for 130° C (10 min) to 160° C (7 min); 160° C to 190° C (7 min), from 190° C to 220° C (22 min) and from 220° C to 250° C (17 min) at a rate of 10° C min^{-1} for each step. The total analysis time was 75 minutes using 70 eV electron impact ionization and data was evaluated with total ion count.

3.2.5 Relative lipid content analysis in situ by Nile Red fluorescence

Nile Red (AnaSpec, Inc., California, USA) was dissolved in acetone to yield a 250× stock solution following previous protocols (COOKSEY *et al.* 1987). For each *Chlorella* sample, 10 µl of Nile Red stock was mixed with 2.5 ml of algal culture diluted to 4 × 10^7 cells ml^{-1} in a glass fluorometer cuvette (Starna Cells, Inc., California, USA). A PTI spectrofluorometer (Photon Technology International, Inc., New Jersey, USA) comprised of the SC-500 Shutter Control, MD-5020 Motor Driver, LPS-220B Lamp Power Supply, and 814 Photomultiplier Detection System was used to excite samples at 486 nm and collect fluorescent emission spectra over a 500-660 nm range using the accompanying PTI FeliX32 software.

3.3 Results

3.3.1 Phylogenetic analysis of Chlorella *species and strain pedigree*

For our initial species selection, a "genetic fingerprint" based on the 18S ribosomal RNA's internal transcribed spacer (ITS) regions was established for each isolate from a collection of over thirty *Chlorella* strains and used to construct a phylogenetic tree (Figure 15). The annotated 18S ITS sequences for these organisms have been made available online through the NCBI GenBank database under the PopSet ID: 631798695 (ncbi.nlm.nih.gov/popset). During this survey, we encountered some *Chlorella* strains that had been designated as related species (*e.g.*, UTEX 29, 2714) and some strains that group within a separate genus entirely (UTEX 2248, 252). Sequencing of the ITS regions also revealed close phylogenetic relationships between *Chlorella* species in our collection and other strains with active genome projects or

available transcriptomes, including NC64A, CS-01, UTEX 395, 259, and 25 (Guarnieri *et al.* 2011; Wan *et al.* 2012b).

In order to compare autotrophic *Chlorella* species' propensity to grow on glucose and accumulate lipids under uniform heterotrophic conditions, *C. sorokiniana* UTEX 1230, *C. vulgaris* UTEX 265, and *C. protothecoides* UTEX 411 were selected based on vigorous growth attributes during preliminary examination in minimal nutrient Bold's basal medium (BBM) (unpublished data). These three strains were found to be phylogenetically distinguishable within their species groupings and each possesses unique physiological traits. The first in this group, *Chlorella sorokiniana* UTEX 1230, has been studied extensively for its carbohydrate, lipid, protein, and biopolymer content (Takeda *et al.* 1988; Banskota *et al.* 2013; Kodner *et al.* 2009) as well as hydrogen photoproduction (Brand *et al.* 1989), glucose transport (Komor *et al.* 1988), production of biomolecules by fermentation (Lee *et al.* 1996; Running *et al.* 1996), and bioremediation capabilities (Jeong *et al.* 2003; Kobayashi *et al.* 2013a; Li *et al.* 2011; Polakovičová *et al.* 2012). This organism was isolated by Sorokin and Meyers in the early 1950s and maintained in many culture collections under different strain numbers, originally classified as *C. pyrenoidosa* (Sorokin & Meyers 1953; Fahey *et al.* 1987; Haehnel *et al.* 1982; Rosen *et al.* 1985; Zelibor *et al.* 1988).

Chlorella vulgaris is a closely related algal species often used as a health supplement (Tanaka *et al.* 1990). While some annotated genomic sequences have been made available for this species (Wakasugi *et al.* 1997), the *C. vulgaris* strain UTEX 265

examined in the present study has not been fully characterized in this manner. Nonetheless, the population dynamics of UTEX 265 have been studied using genetic probes (Meyer *et al.* 2006) and this particular strain demonstrates heterotrophic growth in medium containing 0.1-0.6% glucose (Yong-Ha *et al.* 1997). A related *C. vulgaris* strain (UTEX 395) is the subject of intense transcriptomic and proteomic analyses of lipid biosynthetic pathways (Guarnieri *et al.* 2011 & 2013).

Chlorella (Auxenochlorella) protothecoides is a well established heterotrophic alga that can utilize glucose as an organic carbon source (Shi *et al.* 2000). Furthermore, *C. protothecoides* UTEX 411 can grow on sucrose and glycerol (Dillon *et al.* 2009a; Dillon *et al.* 2009b) and has been exploited for lutein production (Shi *et al.* 2000). Other *C. protothecoides* strains have been cultivated heterotrophically for lipid production— achieving over 55% lipids by dry weight (Miao & Wu 2006) and scale-up to 10,000-L bioreactors (Li *et al.* 2007). This demonstration has reinforced the potential of heterotrophic *Chlorella* species to generate substantial quantities of lipids for biofuel production.

Figure 15. *(next page)* Proposed phylogenetic tree of *Chlorella* species of interest. Green arrows point to branch placement of the three candidate strains examined in this study (*C. vulgaris* UTEX 265, *C. sorokiniana* UTEX 1230, and *C. protothecoides* UTEX 411); black arrows indicate strains with active genome projects. Asterisks denote strains found to align more closely with a species other than their original labeled speciation. The scale bar represents a 2% difference between distinct ITS region sequences.

Figure 15. Proposed phylogenetic tree of *Chlorella* species of interest.

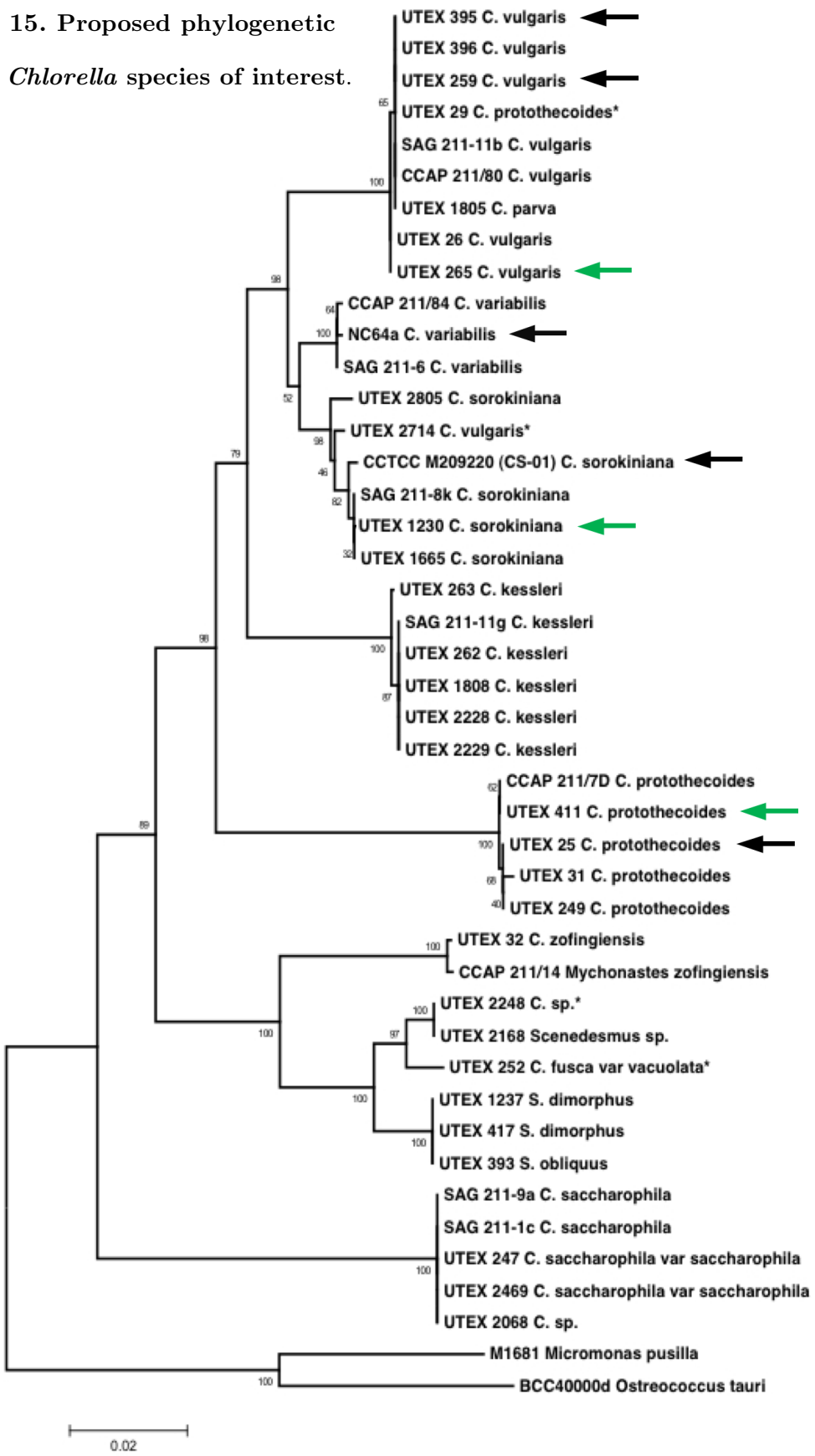

3.3.2 Growth and biomass yields of C. sorokiniana *(UTEX 1230),* C. vulgaris *(UTEX 265), and* C. protothecoides *(UTEX 411)*

The three selected *Chlorella* species were cultivated using previously reported growth methods in separate photoautotrophic and heterotrophic batches for quantitative growth and biomass assessment (Wan *et al.* 2011a). The heterotrophic specific growth rates of UTEX 411, 265, and 1230 (0.48, 0.84, and 1.77 d^{-1}, respectively) were found to be 1.5-, 3.7-, and 5-fold higher than their autotrophic rates (Table 6). A comparison of auto– and heterotrophic growth curves for *C. sorokiniana*, *C. vulgaris*, and *C. protothecoides* cultures inoculated with 1×10^6 cells ml^{-1} is shown in Figure 16A. Although heterotrophic growth has been reported for each algal strain (Li *et al.* 2007; Komor *et al.* 1988; Yong-Ha *et al.* 1997; Dillon *et al.* 2009a; Dillon *et al.* 2009b). *C. sorokiniana* UTEX 1230 demonstrated the most significant heterotrophic advantage in Bold's basal medium with glucose (10 g L^{-1}). Within one week, heterotrophic *C. sorokiniana* UTEX 1230 reached the highest cell density of all strains (113×10^6 cells ml^{-1}), while the final heterotrophic cell densities of *C. vulgaris* and *C. protothecoides* cultures were at least 9-fold lower ($10\text{-}12 \times 10^6$ cells ml^{-1}). Under autotrophic conditions, UTEX 265, 1230, and 411 achieved cell densities of roughly 90, 40, and 10 million cells ml^{-1} at their respective stationary phases with comparable photoautotrophic specific growth rates ($\mu = 0.23\text{-}0.36$ d^{-1}).

At the termination of each culture, the dry biomass weights of *C. sorokiniana*, *C. vulgaris*, and *C. protothecoides* were compared (Figure 16B). Not surprisingly, heterotrophic *C. sorokiniana* UTEX 1230 amassed the greatest final biomass (1.8 g

L^{-1}), while the dry weights of *C. vulgaris* and *C. protothecoides* heterotrophic biomass were both close to 0.5 g L^{-1}. When grown autotrophically, *Chlorella vulgaris* UTEX 265 reached a final biomass density of 1.1 g L^{-1} (94×10^6 cells ml^{-1}) while *C. sorokiniana* UTEX 1230 reached a maximal cell density of 44×10^6 cells ml^{-1} at 0.6 g L^{-1} dry weight, similar to the 0.5 g L^{-1} biomass yield of UTEX 411 from only 10×10^6 cells ml^{-1}. Interestingly, *C. protothecoides* UTEX 411 may possess more massive cells based on dry weight although it was unable to reach cell densities above 10 million cells ml^{-1} during either auto– or heterotrophic modes of cultivation in the present study. Both *C. protothecoides* UTEX 411 and *C. vulgaris* UTEX 265 exhibited an extended lag phase during heterotrophy before expansion of the population, suggesting a lengthy acclimation period for growth on simple sugar. Based on its rapid growth and high biomass yield under heterotrophic conditions, *C. sorokiniana* UTEX 1230 was taken into consideration as a lead candidate for an in depth investigation of oil production from heterotrophically-grown cells.

Chlorella Species	***C. protothecoides***	***C. vulgaris***	***C. sorokiniana***
Strain	UTEX 411	UTEX 265	UTEX 1230
Specific Growth Rate, μ	**0.48 ± 0.01**	**0.84 ± 0.09**	**1.77 ± 0.04**
(d^{-1})	0.32 ± 0.05	0.23 ± 0.01	0.36 ± 0.05
Doubling Time	**35 ± 1**	**20 ± 2**	**9 ± 1**
(hr)	52 ± 4	72 ± 3	46 ± 3

Table 6. Growth characteristics of *C. protothecoides* UTEX 411, *C. vulgaris* UTEX 265, *C. sorokiniana* UTEX 1230. The major heterotrophic and photoautotrophic growth parameters for each *Chlorella* strain were calculated using data points from the exponential phase of batch culture. Bold values correspond to heterotrophic populations; regular typeface represents autotrophic rates. All kinetic quantities are reported as the average of biological replicates ± standard deviations.

Figure 16. *(next page)* Growth curves and volumetric biomass yields of *C. protothecoides*, *C. vulgaris*, and *C. sorokiniana*. (A) Photoautotrophic (□) and heterotrophic (■) cultures were followed over the course of four weeks or until the population reached stationary phase. Data points are representative of biological replicates and error bars denote standard deviations greater than 1×10^6 cells ml^{-1}. **(B)** *C. protothecoides*, *C. vulgaris*, and *C. sorokiniana* final biomass concentrations in 1.5-L culture during auto– (white) and heterotrophy (gray) are compared. Error bars designate standard deviation from the average of three technical replicates.

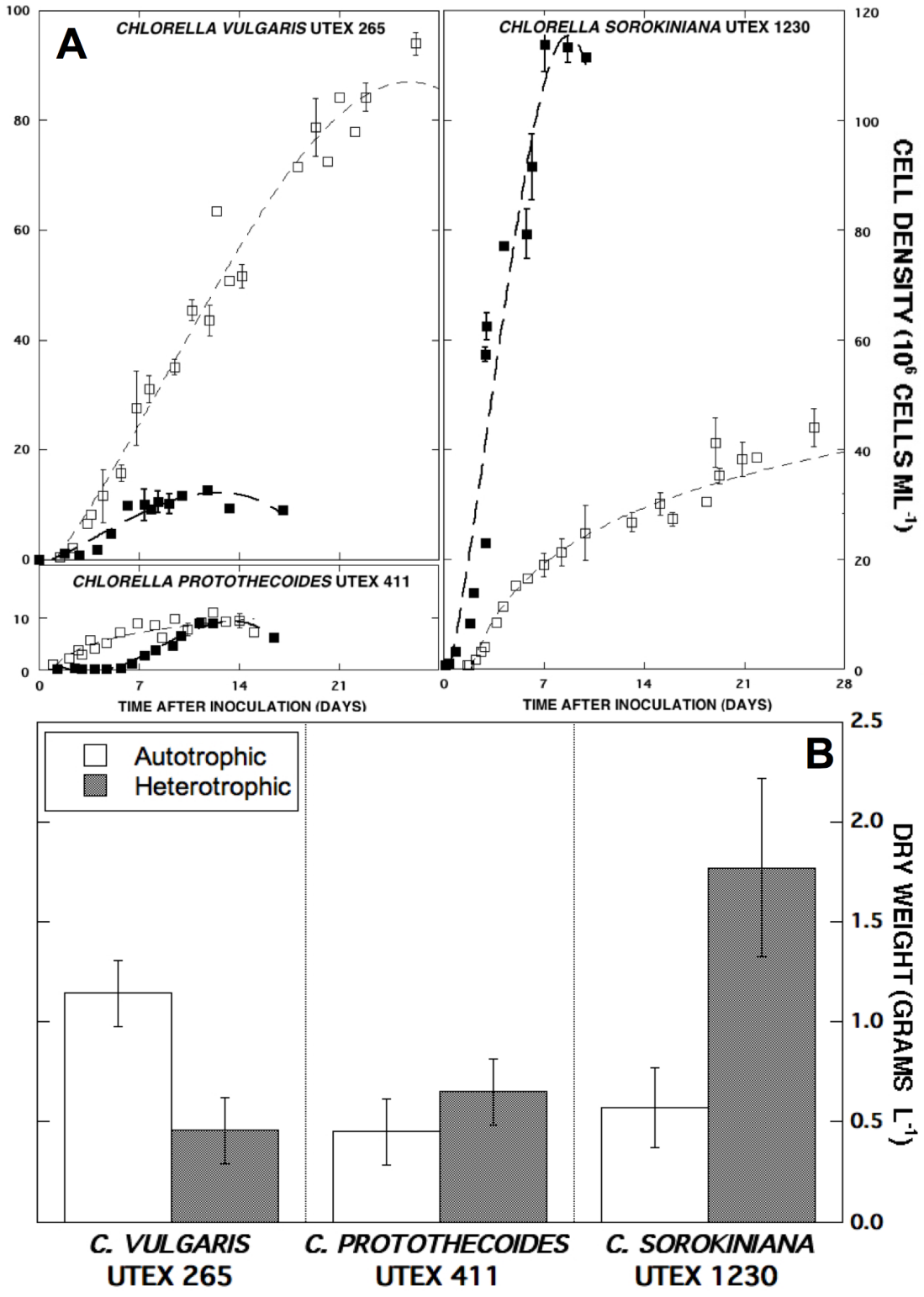

Figure 16. Growth curves and volumetric biomass yields of *C. prototheocoides*, *C. vulgaris*, and *C. sorokiniana*.

3.3.3 Lipid composition of Chlorella *during auto– & heterotrophy*

In order to evaluate oil production during auto– and heterotrophy, total lipids were extracted from the three *Chlorella* strains followed by transesterification to form fatty acid methyl esters (FAME) for GC-MS analysis. While autotrophic UTEX 1230 lipid extracts remained deeply green due to chlorophyll, heterotrophic lipid extracts exhibited a yellow hue (Figure 17A), indicative of inhibited chlorophyll synthesis. The distribution of each strains' lipid extract is categorized in Figure 17B according to its major components: total lipids measured gravimetrically; total fatty acids measured as FAME; and TAG neutral lipids. In this figure, the inferred difference between FAME (gray bars) and TAG lipids (black bars) in each case is assumed to approximate the amount of membrane lipids [+]. In a similar manner, comparing FAME lipids quantified by GC-MS to total lipid extracts (white bars) leads to the recognition of an unaccounted fraction [*], which represents other lipophilic biomolecules that can be extracted by the organic solvent system, but not measured by GC-MS analysis of the FAME component. This residual fraction is likely to be constituted by chlorophylls, lipid-soluble metabolites, and carotenoids such as lutein. Since many of these accessory "lipids" can be molecules associated with photosynthesis, carbon fluxes are likely to be directed toward these biomolecules rather than TAG during photoautotrophy. For example, UTEX 265 and 411 maintained roughly 60% of their total autotrophic lipids as accessory pigments and metabolites compared to only 16% in UTEX 1230. Consequently, UTEX 1230 partitioned more of its total autotrophic biomass as TAG (11% of the biomass; 60% of total lipids) compared to the markedly lower autotrophic TAG levels in UTEX

265 and 411. The photoautotrophic biomass of *C. sorokiniana* UTEX 1230 was comprised of 18% total lipids, 15% fatty acids, and 11% TAG by dry weight, while *C. vulgaris* UTEX 265 accumulated equivalent amounts of total lipids (18%), but considerably lower levels of fatty acids (7.6%) and TAG (6.6%). *Chlorella protothecoides* UTEX 411 biomass contained the lowest lipid contents during autotrophy with 12% total lipids, 4.5% fatty acids, and 2.3% TAG.

As evidenced by the early onset of chlorosis in *C. sorokiniana* UTEX 1230, accessory pigments can be dramatically reduced during heterotrophy (Figure 17A). Accordingly, this unique phenomenon is manifested in the similarity between the total lipid content and total fatty acid content in UTEX 1230 with marginal amounts of accessory metabolites and minimal membrane lipids [×] (Figure 17B). Since the absence of chlorophyll observed during heterotrophic cultivation of UTEX 265 and 411 was not as severe as UTEX 1230, there is not nearly as much parity between their total lipids and total FAME contents. During heterotrophy, UTEX 1230 total lipid, fatty acid, and TAG contents increased to 24%, 23%, and 21%, respectively, amassing the highest TAG level among all strains examined, which was also two-fold higher than the TAG content of UTEX 1230 during autotrophy. The total lipid, FAME, and TAG contents of heterotrophic UTEX 265 exhibited proportional increases to 26%, 16%, and 13%, respectively. Compared to the other strains, UTEX 411 accumulated the highest total lipid content of 31% with 24% fatty acids during heterotrophy. However, a smaller portion of these lipids was stored as TAG (12% of the biomass; 40% of total lipids). Despite the respectable oil

induction in UTEX 265 and 411 with 1.5-2.5 times higher total lipid contents during heterotrophy relative to autotrophy, these two strains possessed slow growth rates and low heterotrophic biomass yields under the current cultivation conditions. Alternatively, UTEX 1230 demonstrated rapid growth during heterotrophy and accrued an overwhelming majority of its total lipid content as TAG.

The quantitative results of neutral lipid induction gathered from UTEX 1230 lipid extracts during heterotrophy were also confirmed with an *in situ* method using Nile Red (NR) to stain whole cells (Cooksey *et al.* 1987). As conveyed by fluorescent emission curves (Appendix B: Figure S1), heterotrophic UTEX 1230 exhibited a clear maximum of 5.8×10^4 fluorescent intensity units (FIU) at its expected emission wavelength of 580 nm compared to 2×10^4 FIU autotrophically. The signatures of these NR profiles indicate that UTEX 1230 accumulated more hydrophobic biomolecules under heterotrophic conditions compared to autotrophy. In addition to different carbon sources, corresponding pH changes in auto– and heterotrophic media during algal growth can also contribute to lipid accumulation and influence fatty acid speciation (Guckert & Cooksey 1990). While autotrophic cultures of *C. sorokiniana* UTEX 1230 became alkaline with pH rising from 7.3 to 10, heterotrophic cultures experienced slight acidification from pH 6 to 4.8 (Appendix B: Figure S2).

Figure 17. ***(next page)*** **Distribution of total lipid extracts as fatty acids and TAG in three *Chlorella* strains. (A)** *C. sorokiniana* UTEX 1230 exhibits more prominent chlorosis during heterotrophy than UTEX 265 and 411, which is readily apparent in the pigmentation of total lipid extracts. **(B)** Total lipids (white) in *C. protothecoides* UTEX 411, *C. vulgaris* UTEX 265, and *C. sorokiniana* UTEX 1230 are classified as FAME (gray) and TAG storage lipids (black). By comparing these values, the relative amounts of supposed accessory metabolites [*] and membrane lipids [+] emerge, while UTEX 1230 appears to be devoid of accessory pigmentation with minimal membrane lipids [×]. Error bars represent one standard deviation from the average of three technical replicates.

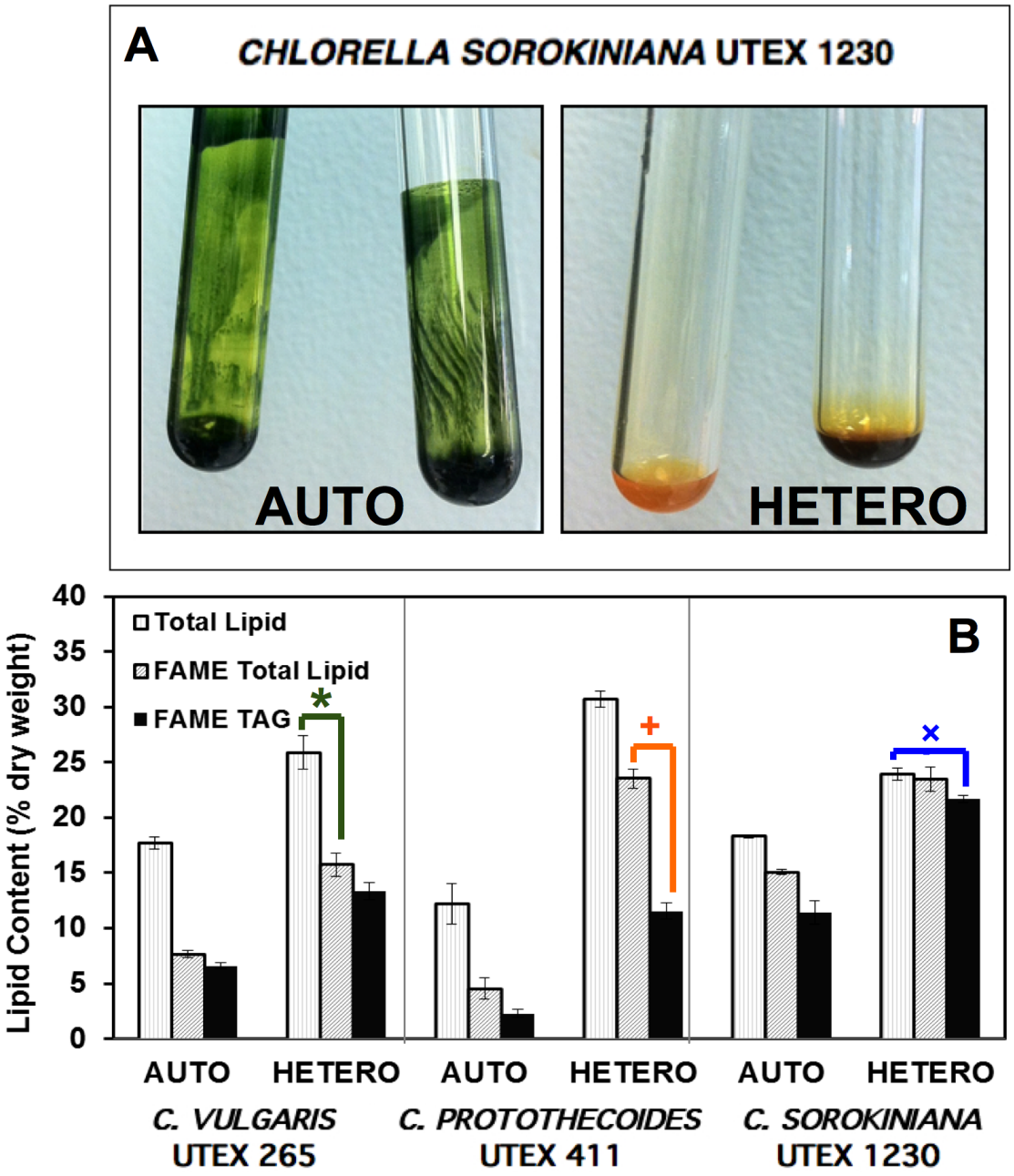

Figure 17. Distribution of total lipid extracts as fatty acids and TAG in three *Chlorella* strains.

3.3.4 Distribution of fatty acid chain length and saturation in Chlorella

In order to further characterize the lipid metabolic profiles of these three *Chlorella* species, detailed fatty acid compositions were elucidated by GC-MS for auto– and heterotrophy (Figure 18). The typical distribution of sixteen- to eighteen-carbon fatty acids with no more than three degrees of unsaturation (16-18 **:** ≤ 3) characteristic of many freshwater green algae was confirmed (Guckert & Cooksey 1990; Hu *et al.* 2008). While all species exhibited increased total lipid and TAG levels during heterotrophy, Figure 18 highlights the species specificity of fatty acid accumulation with respect to lipid chain length. The discernable differences between the three strains are the ratios of fatty acids accumulated as 16:0, 18:1, and 18:2 as well as the amount of TAG, which is consistent with Figure 17B. During both auto– and heterotrophic conditions, UTEX 1230 showed a relatively even distribution of palmitic (16:0) and linoleic (18:2) acids, both between 5-10% by dry weight. In contrast, UTEX 265 and 411 produced oleic acid (18:1) as the principal fatty acid, reaching heterotrophic maxima of 7.5% and 14%, respectively, with secondary storage lipids of 16:0 and 18:2 each at less than 5% of the biomass. Furthermore, UTEX 1230 exhibited greater than 2.5-fold enrichment in 18:2 relative to 18:1, which is in direct opposition with the relative levels of oleic and linoleic acids prevalent in the other strains. This polyunsaturation in UTEX 1230 may indicate higher activity of lipid desaturases during heterotrophy (Nguyen *et al.* 2013; Liu *et al.* 2012).

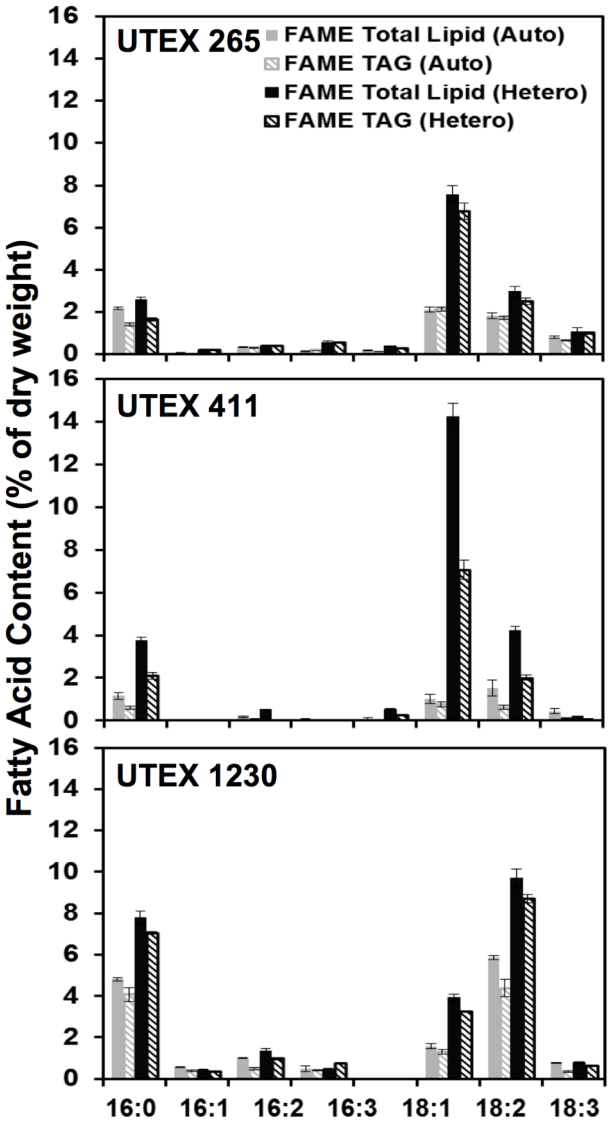

Figure 18. Fatty acid composition of three *Chlorella* strains during auto– and heterotrophy. The distribution of total fatty acids measured as FAME and TAG are plotted as solid and diagonal bars, respectively, for *C. protothecoides* UTEX 411, *C. vulgaris* UTEX 265, and *C. sorokiniana* UTEX 1230. Compared to autotrophy (gray), heterotrophy (black) induces remarkable changes in FAME and TAG lipid profiles. Error bars represent the standard deviation from the average of three biological replicates.

3.3.5 Comparison of lipid production during hetero– and mixotrophy

In order to compare the dynamics of lipid production in *C. sorokiniana* UTEX 1230 during hetero– and mixotrophy, cultures were grown in BBM with glucose (10 g L^{-1}) either in the dark or together with artificial illumination. Separate 8-L bioreactors were sampled over two weeks for cell density, biomass concentration, and total gravimetric lipid measurements followed by GC-MS analysis. Despite the equivalent amounts of initial glucose, mixotrophic cultures displayed significantly reduced biomass and lipid yields compared to heterotrophic cultures (Figure 19). During the first three to five days of cultivation, both populations expanded at similar specific growth rates; however, clear differences arose later in cultivation (Figure 19A). While heterotrophic growth of UTEX 1230 peaked at 130 $\times$ 10^6 cells ml^{-1}, the mixotrophic culture plateaued at only 70 $\times$ 10^6 cells ml^{-1}, which is more similar to the UTEX 1230 growth pattern during photoautotrophy. The respective hetero– and mixotrophic biomass yields of 2 and 1.7 g L^{-1} were more similar than would be expected from the cell densities (Figure 19B), suggesting a possible photoinhibitory or pH-induced effect on cell cycle progression during mixotrophy, which is also reflected in diminished total lipid content (Figure 19C).

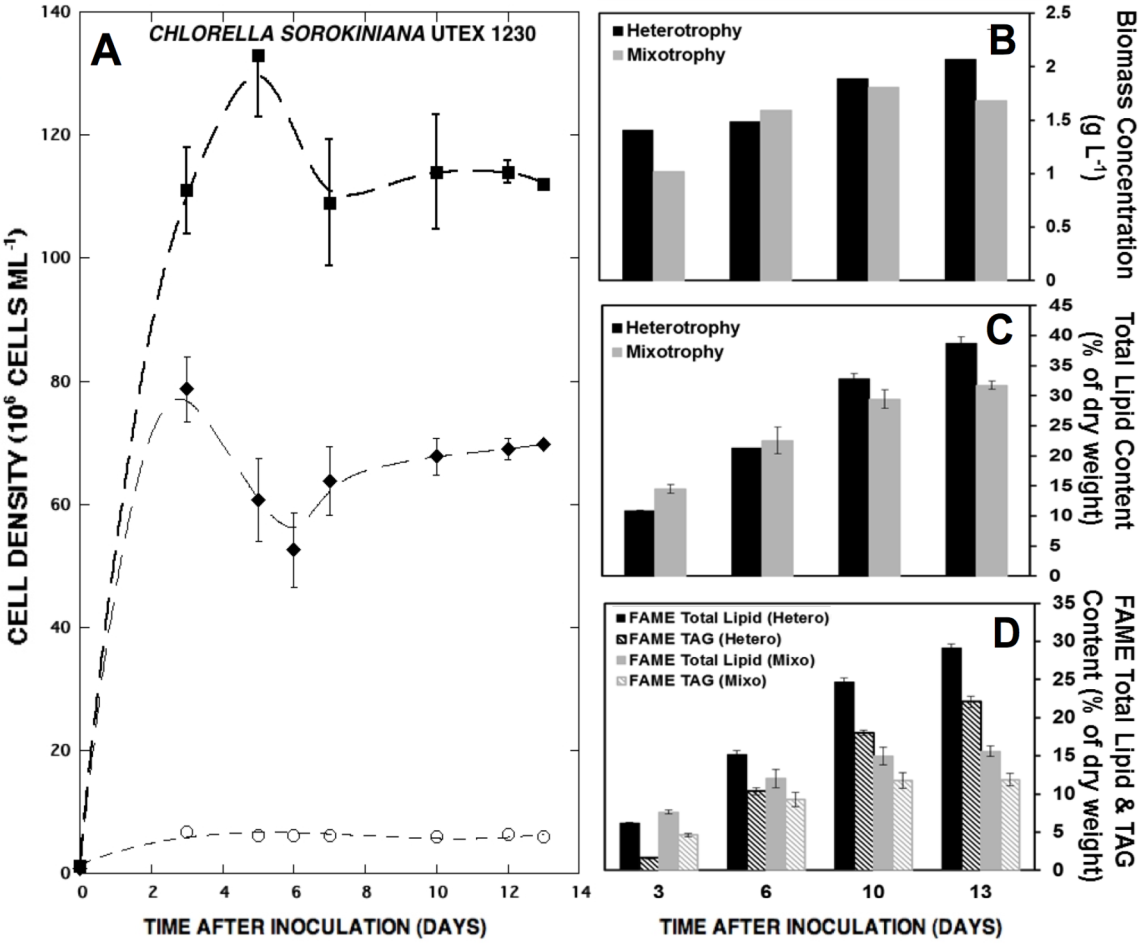

Figure 19. Growth curves, biomass yield, and lipid accumulation of *C. sorokiniana* UTEX 1230 throughout mixo– and heterotrophy in 8-L bioreactors. (A) Heterotrophic (■) and mixotrophic (◆) cell densities are compared to UTEX 1230 grown in BBM without sugar or light (○), which served as a negative control. **(B)** The corresponding dry biomass, **(C)** total lipid content, and **(D)** total FAME and TAG percentages at days 3, 6, 10, and 13 of mixo– (gray) and heterotrophic (black) cultivation are plotted. FAME and TAG contents for each lipid type are plotted as solid and diagonal bars, respectively. Error bars represent the standard deviation from the average of three technical replicates.

3.3.6 Progressive induction of PUFA in UTEX 1230 *during heterotrophy*

Lipid profiles from this time-course evaluation of UTEX 1230 revealed that the kinetics of fatty acid biosynthesis in heterotrophy are accelerated relative to mixotrophy, especially with regard to the 16:0–18:1–18:2 triad (Figure 20). In terms of total lipid content, mixotrophic UTEX 1230 biomass contained 31.8 ± 0.7% total lipids after two weeks compared to 38.7 ± 0.9% in the heterotrophic biomass, but experienced a two-fold reduction in TAG accumulation relative to heterotrophy. While mixotrophy engendered a final TAG content of 11.8 ± 0.8% in UTEX 1230, heterotrophy achieved 22.1 ± 0.7% TAG (Figure 19D), corresponding to volumetric TAG productivities of 18.2 and 28.9 mg L^{-1} d^{-1}, respectively. During heterotriphy, time dependent induction of unsaturation led to the biogenesis of 18:2 (linoleic acid) from precursor 18:1 (oleic acid) and persisted in late-stage heterotrophic cultures (Figure 20A). In this case, both 18:1 and 18:2 showed a steady increase in the first ten days of heterotrophic culture from less than 2% of the biomass (< 0.5% TAG) to nearly 5% and 8%, respectively (5-6% TAG). While 18:1 exhibited an insignificant increase between days ten and thirteen, 18:2 levels reached 10% of the total dry biomass with 7.7% TAG by the end of heterotrophic culture. Conversely, Figure 20B illustrates that 18:1 barely exceeded 2% during mixotrophy and 18:2 reached a peak at approximately 5% dry weight. While total 18:1 content remained unchanged during the final three days of mixotrophic culture, 18:1 TAG levels actually dropped while 18:2 TAG only increased slightly. Interestingly, 16:0, 18:1, and 18:2 TAG fractions had higher initial levels during mixotrophy (closer to 1%), but did not exhibit the high rates of TAG accumulation that occurred during heterotrophy and

subsisted at less than 4% of the total biomass by the end of 2-week cultivation. Furthermore, the increase in unsaturated 18:1 and 18:2 in heterotrophic UTEX 1230 may have been balanced by 16:0 enrichment to lower membrane fluidity as pH became acidic (Poerschmann *et al.* 2004).

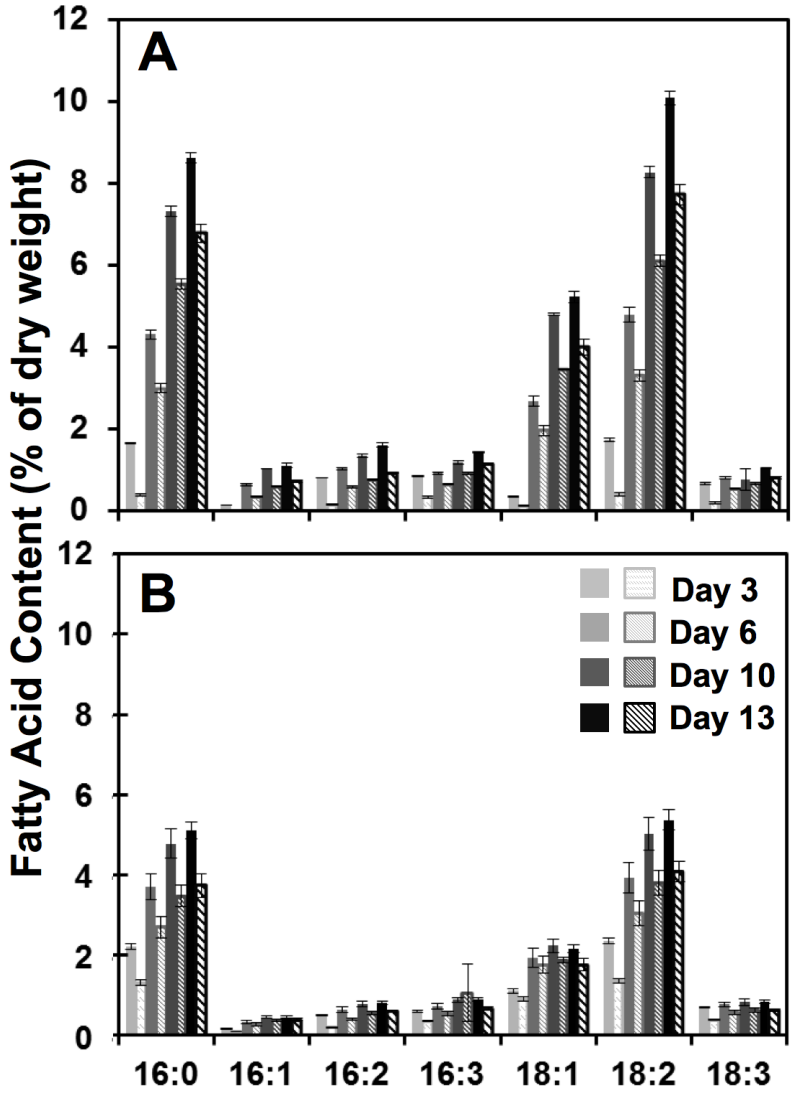

Figure 20. Comparison of total fatty acid and TAG composition of UTEX 1230 during mixo– and heterotrophic cultivation. The discrete lipid profiles of C. sorokiniana UTEX 1230 under **(A)** heterotrophic and **(B)** mixotrophic conditions from samples taken on days 3, 6, 10 and 13 of cultivation show fatty acid accumulation rates and patterns. Total FAME and TAG contents for each lipid type are plotted as solid and diagonal bars, respectively. Error bars represent the standard deviation from the average of three biological replicates.

3.4 Discussion and Conclusions

For the production of microalgal oils, the interdependence of total lipid content, fatty acid composition, and biomass productivity throughout cultivation is critical (Stephens *et al.* 2010; Rogers *et al.* 2014). Novel approaches to maximize carbon storage as neutral lipids can lead to significant benefits for algae biotechnology, biomanufacturing, and bioenergy (Fan *et al.* 2013). The accumulation of different lipids during heterotrophy and autotrophy can be especially important for the interrogation of lipid biosynthetic pathways in commercially relevant *Chlorella* species. Toward this end, the current study has revealed distinctive auto– and heterotrophic capabilities of three phylogenetically classified *Chlorella* strains with respect to the trade-offs between oil content and growth rate.

3.4.1 Molecular phylogeny and genomic resources

While microalgae can be generally classified based on cellular features (Prescott 1954), species of the same genus are nearly morphologically identical and can only be definitively differentiated by genotypic analysis (Bock *et al.* 2011; Luo *et al.* 2006). Therefore, the foundation of our species characterization relied on determining the molecular phylogeny of the conserved 18S sequence and species-specific ITS regions for each *Chlorella* strain (An *et al.* 1999; Hoshina *et al.* 2010; Huss *et al.* 1999) employing a rapid colony PCR method (Wan *et al.* 2011b). Confirming an organism's true phylogeny is important for understanding what adaptive traits have been collected through natural selection and how they may be useful for biotechnology. In the course of mapping the branches of the phylogenetic tree in this

study (Figure 15), the occurrence of mismatched species (*e.g.*, UTEX 29, 252, 2248, 2714) was more prevalent than anticipated. Indeed, another case of species misidentification had previously been identified during genome sequencing of NC64A in tandem with the putative *C. vulgaris* C-169 that is resistant to the *Chlorella* virus (Noutoshi *et al.* 1998). Despite physiological similarities to *C. variabilis*, the C-169 strain was actually determined to be *Coccomyxa subellipsoidea* by comparative genomics (Blanc *et al.* 2012; Joint Genome Institute 2011).

While genetic resources for the *Chlorella* genus are improving with genome sequencing projects underway for many common species (Tirichine & Bowler 2011), the 46-Mb *C. variabilis* NC64A genome is currently the only publicly available *Chlorella* genome (Blanc *et al.* 2010). Although peculiar in its growth habits, this organism holds information about the genetic-basis of sugar transport in green algae during symbiosis, which is of particular relevance to the present study (Ziesenisz *et al.* 1981). Sequencing of *Chlorella* ITS regions fulfills the need to relate macroscopic growth characteristics of potential production organisms to molecular genetic traits (Rosenberg *et al.* 2008). Thus, the ribosomal ITS-based phylogenetic tree constructed during the present investigation can indicate a strain's proximity to *C. variabilis* NC64A or other organisms with available genetic tools. In addition, this map of phylogeny makes it possible to identify *Chlorella* isolates with suitable biomass and lipid productivities that are both close in genetic relation, yet distinct in physiological characteristics.

3.4.2 Physiological and biochemical survey of three Chlorella *species*

While the biomass productivity of *Chlorella* cultures has been extensively studied, there remains little consensus between the research community and commercial endeavors regarding preferred *Chlorella* species or growth methodologies to maximize oil yields. Since *C. vulgaris, C. protothecoides*, and *C. sorokiniana* are the primary organisms used for process development and strain improvement (Campenni *et al.* 2013; He *et al.* 2013), this work focused on representatives of these species.

In measuring the growth characteristics of *C. sorokiniana* UTEX 1230, *C. vulgaris* UTEX 265 and *C. protothecoides* UTEX 411 (Table 6), UTEX 1230 produced the greatest amount of heterotrophic biomass (Figure 16) in general agreement with previous literature supporting the heterotrophic cultivation of *Chlorella* (Heredia-Arroyo *et al.* 2010; Liu *et al.* 2008; Lu *et al.* 2012; Santos *et al.* 2011; Vigeolas *et al.* 2012). However, *C. protothecoides* UTEX 411 growth did not compare well with the other *Chlorellas* during either hetero– or photoautotrophic modes in our experiments. Compositional differences in media or the effect of pH stress on cell cycle may have accounted for this observed growth restriction, cellular enlargement, and reduced lipid productivity (Shen *et al.* 2010). Compared to BBM used in this study, prior heterotrophic *Chlorella* growth media have sometimes replaced sodium nitrate with glycine and vitamin B_1 (Miao & Wu 2006; Wu *et al.* 1992), which implicates a potential vitamin requirement or preferred nitrogen source for UTEX 411. However, we decided to maintain the medium as consistent as possible to limit environmental factors in this comparison. From a technoeconomic perspective, we

recognize that the most cost-effective sources and optimal amounts of fixed carbon, nitrogen, and micronutrients may vary for different *Chlorella* species. Furthermore, microalgal strains that can prosper in relatively low nitrogen and carbon concentrations can be desirable for large-scale biomass production by reducing overall nutrient costs and lowering the impact of these resources on bioprocessing costs.

3.4.3 Lipid allocation between membrane, metabolism, & energy storage

One of the main goals of this study was to quantify and compare the differential apportioning of lipid types in the three *Chlorella* strains during auto– and heterotrophy. The divergence in lipid generation between these algal species was clearly evident from the distribution of total lipids, total fatty acids measured as FAME, and TAG neutral lipids. In Figure 17B, heterotrophic *C. vulgaris* UTEX 265 exhibited roughly 10% accessory pigments and lipid-soluble metabolites by dry weight [*], which can serve as high-value nutritional coproducts (*e.g.*, chlorophylls, carotenoids, phenols, tocopherols, sterols). This may indicate that the cellular metabolism of UTEX 265 remains more active than lipid storage during heterotrophy, as observed previously with *C. sorokiniana* strains UTEX 2714 and CS-01 as well as *Chlamydomonas reinhardtii* (KOBAYASHI *et al.* 2013a; KOBAYASHI *et al.* 2013b). In a complementary case, *C. protothecoides* UTEX 411 produced approximately 10% membrane lipids during heterotrophy [+] (*e.g.*, phospho-, galacto-, and sulpholipids). In addition to these detractions from TAG accumulation due to the competing cellular demand for lipid metabolites and membrane structures,

both UTEX 265 and 411 exhibited less vigorous heterotrophic growth capacities (Figure 16A). Alternatively, *C. sorokiniana* UTEX 1230 benefited from rapid heterotrophic growth and contained 24% total lipids with close to 90% of these total lipids allocated as TAG [×] (Figure 17B). With energy stores accounting for the majority of UTEX 1230 total lipids, this leaves a limited amount of fatty acids available for membranes during heterotrophy, which may arise from a substantial reduction in the number of chloroplast and thylakoid membranes. Combined with the higher cell densities supported during heterotrophy, UTEX 1230 displayed a 3.8-fold increase in lipids per liter at the end of batch culture relative to autotrophy with an abrupt shift from non-fatty acid lipid production to TAG storage. The increase in pH during autotrophy may be primarily responsible for TAG accumulation due to cell cycle arrest (Guckert & Cooksey 1990). Alternatively, during heterotrophic cultivation with minor changes in pH, the ultimate lipid yields of UTEX 1230 increased from 0.14 to 0.53 g L^{-1} perhaps due to the up-regulation of stearoyl-ACP desaturase in the presence of glucose, leading to an abundance of 18:1 precursor fatty acid (Liu *et al.* 2012).

Further mixo– and heterotrophic bioreactor optimization at the 8-L scale enabled UTEX 1230 to accumulate 30-40% of its cell mass as lipids, possibly as a result of increased mixing and enhanced gas exchange. Additionally, nutrient utilization trends in previous *Chlorella* studies using BBM demonstrate that nitrate and nitrite levels were reduced to 5-10% of their initial concentrations, indicating that BBM may not be completely deprived of nitrogen at stationary phase (Kobayashi *et al.*

2013a; KOBAYASHI *et al.* 2013b). This residual nitrogen may, therefore, sustain the presence of chlorophyll and basal metabolic activity. Furthermore, TAG storage in *Chlorella* can exhibit differential responses to reduced nitrogen levels compared to other algae. While *C. reinhardtii* may require complete nitrogen depletion to induce TAG accumulation (WASE *et al.* 2014), *Chlorella* species can store moderate amounts of TAG in nitrogen replete media. This connection between nutrient limitation, cell growth, and lipid biosynthesis offers additional insight into *Chlorella* metabolism.

3.4.4 Bioenergetics of mixo– & heterotrophy affect fatty acid distribution

Considering that the breakdown of sugar by glycolysis may take precedence over carbon dioxide utilization through photosynthesis (WAN *et al.* 2011a), our study of *C. sorokiniana* UTEX 1230 indeed found no apparent metabolic benefit from light input in addition to glucose. Furthermore, this strain appeared to be potentially maladapted for oil accumulation during mixotrophy. Restricted mixotrophic growth suggests that glucose uptake may be inhibited by light or the energy balance of mixotrophic cells is unfavorably altered (Figure 19A). In extreme cases, pH can also negatively affect sugar uptake via the hexose-proton symporter, although the pH drift encountered in the present study fell within the optimal range for glucose uptake by *Chlorella* (Supplementary Figure S2: Appendix B) (KOMOR & TANNER 1974). Interestingly, incongruencies between biomass and cell density in mixo– and heterotrophic comparisons (Figure 19B) also suggest that mixotrophic cells may be larger due to the simultaneous activity of glycolytic lipid accumulation in storage vesicles and photosynthetic carbon fixation, which requires multiple chloroplasts.

While these findings contradict a recent report of high mixotrophic productivities from a different *C. sorokiniana* strain, this discrepancy simply highlights the strain-specific metabolic portraits drawn for different *Chlorella* isolates under investigation (Ngangkhama *et al.* 2013). Previous studies have indeed found evidence for the inhibition of organic carbon uptake by other *Chlorellas* in the presence of light (Haass & Tanner *et al.* 1974; Kamiya & Kowallik *et al.* 1987). In addition, a recent evaluation of *C. sorokiniana* CS-01 (closely related to UTEX 1230) revealed that cytosolic acetyl-coA carboxylase (ACCase) is overexpressed compared to chloroplast ACCase during mixotrophy, suggesting that fatty acid precursors contributing to TAG synthesis are derived from glycolysis of exogenous sugars rather than photosynthetically fixed carbon (wan *et al.* 2011a). This underscores the importance of understanding the bifurcation of carbon utilization during these potentially competing modes of growth.

From the distribution of lipid classes under heterotrophic conditions, it is clear that TAG can constitute a significant portion of lipids in all three of these *Chlorella* strains with 18:1 and 18:2 as the primary fatty acids, which are more suitable for biofuel applications than polyunsaturated lipids. From a bioenergetics standpoint, more cellular energy is expended to generate polyunsaturated fatty acids compared to saturated lipids. Since oxidation also has a negative impact on fuel stability, unsaturated lipids must be catalytically hydrogenated prior to fuel blending, which requires additional capital and operating expenses. While the absence of long-chain polyunsaturated fatty acids is not uncommon in *Chlorella* species (Kim & Hur 2013),

all strains in the present study exhibited surprisingly low levels of 18:3 (linolenic acid). Other studies have demonstrated that UTEX 1230 is capable of 18:3 biosynthesis under autotrophic conditions with nitrogen deprivation (Kobayashi *et al.* 2013b; Reddy *et al.* 2013) and anaerobic digester effluent (Kobayashi *et al.* 2013a). In contrast, UTEX 1230 can accumulate higher levels of 18:1 when supplemented with 3% carbon dioxide (unpublished data).

As a whole, these results support the *Chlorella* genus as a vital source of commercially relevant production organisms with unique lipid metabolic properties, which can vary significantly depending on the presence or absence of sugars and light. While glucose was used in these controlled growth studies, low-cost organic carbon sources are likely to be required for commodity scale biofuel production (Kobayashi *et al.* 2013a; Li *et al.* 2011; Polakovičová *et al.* 2012; Mitra *et al.* 2012). This study's phylogenetic and physiological characterizations of *C. vulgaris* UTEX 265, *C. protothecoides* UTEX 411, and *C. sorokiniana* UTEX 1230 offer insight into the diverse carbon partitioning strategies even within a single genus. In one exemplary case, *C. sorokiniana* UTEX 1230 may serve as a versatile model organism for photosynthetic carbon utilization and heterotrophic lipid biosynthesis with implications for bioenergy and bioprocessing.

3.5 References

An SS, Friedl T, Hegewald E (1999) Phylogenetic relationships of *Scenedesmus* and *Scenedesmus*-like coccoid green algae as inferred from ITS-2 rDNA sequence comparisons. Plant Biol 1: 418-428.

Banskota AH, Stefanova R, Gallant P, Osbornw JA, Melanson R, et al. (2013) Nitric oxide inhibitory activity of monogalactosylmonoacylglycerols from a freshwater microalgae *Chlorella sorokiniana*. Nat Prod Res 27: 1028-1031.

Blanc G, Agarkova I, Grinwood J, Kuo A, Brueggeman A, et al. (2012) The genome of the polar eukaryotic microalga *Coccomyxa subellipsoidea* reveals traits of cold adaptation. Genome Biol 13: R39.

Blanc G, Duncan G, Agarkova I, Borodovsky M, Gurnon J, et al. (2010) The *Chlorella variabilis* NC64A genome reveals adaptation to photosymbiosis, coevolution with viruses, and cryptic sex. Plant Cell 22: 2943-2955.

Blankenship RE, Tiede DM, Barber J, Brudvig GW, Fleming G, et al. (2011) Comparing photosynthetic and photovoltaic efficiencies and recognizing the potential for improvement. Science 332: 805-809.

Bligh EG, Dyer WJ (1959) A rapid method for total lipid extraction and purification. Can J Biochem Phys 37: 911-917.

Bock C, Krienitz L, Pröschold T (2011) Taxonomic reassessment of the genus *Chlorella* (Trebouxiophyceae) using molecular signatures (barcodes), including description of seven new species. Fottea 11: 293-312.

Brand JJ, Wright JN, Lien S (1989) Hydrogen production by eukaryotic algae. Biotechnol Bioeng 33: 1482-1488.

Bumbak F, Cook S, Zachleder V, Hauser S, Kovar K (2011) Best practices in heterotrophic high-cell-density microalgal processes: achievements, potential and possible limitations. Appl Microbiol Biot 91: 31-46.

Burlew JS (1953) Algal Culture from Laboratory to Pilot Plant. Washington DC: Carnegie Institution of Washington.

Campenni L, Nobre BP, Santos CA, Oliveira AC, Aires-Barros MR, et al. (2013) Carotenoid and lipid production by the autotrophic microalga *Chlorella protothecoides* under nutritional, salinity, and luminosity stress conditions. Appl Microbiol Biot 97: 1383-1393.

Converti A, Casazza AA, Ortiz EY, Perego P, Borghi MD (2009) Effect of temperature and nitrogen concentration on the growth and lipid content of

Nannochloropsis oculata and *Chlorella vulgaris* for biodiesel production. Chem Eng Process 48: 1146-1151.

Cooksey KE, Guckert JB, Williams SA, Calli PR (1987) Fluorometric determination of the neutral lipid content of microalgal cells using Nile Red. J Microbiol Meth 6: 333-345.

Davis R, Fishman D, Frank ED, Wigmosta MS, Aden A, et al. (2012) Renewable Diesel from Algal Lipids: An Integrated Baseline for Cost, Emissions, and Resource Potential from a Harmonized Model. Technical Report Numbers: ANL/ESD/12-4; NREL/TP-5100-55431; PNNL-21437. Argonne, IL: Argonne National Laboratory; Golden, CO: National Renewable Energy Laboratory; Richland, WA: Pacific Northwest National Laboratory.

Dillon HF, Day AG, Trimbur DE, Im C-S, Franklin S, et al. (2009a) Sucrose feedstock utilization for oil-based fuel manufacturing. Patent Number: US8476059. Solazyme, Inc.

Dillon HF, Day AG, Trimbur DE, Im C-S, Franklin S, et al. (2009b) Glycerol feedstock utilization for oil-based fuel manufacturing. Patent Application Number: US12/194,389. Solazyme, Inc.

Dunigan DD, Cerny RL, Bauman AT, Roach JC, Lane LC, et al. (2012) *Paramecium bursaria Chlorella* virus 1 proteome reveals novel architectural and regulatory features of a giant virus. J Virol 86: 8821-8834.

Fahey R, Buschbacher R, Newton G (1987) The evolution of glutathione metabolism in phototrophic microorganisms. J Mol Evol 25: 81-88.

Fan J, Huang J, Li Y, Han F, Wang J, et al. (2012a) Sequential heterotrophy-dilution-photoinduction cultivation for efficient microalgal biomass and lipid production. Bioresource Technol 112: 206-211.

Fan J, Cui Y, Huang J, Wang W, Yin W, et al. (2012b) Suppression subtractive hybridization reveals transcript profiling of *Chlorella* under heterotrophy to photoautotrophy transition. PLoS ONE 7: e50414.

Fan J, Yan C, Zhang X, Xu C (2013) Dual role for phospholipid:diacylglycerol acyltransferase: enhancing fatty acid synthesis and diverting fatty acids from membrane lipids to triacylglycerol in *Arabidopsis* leaves. Plant Cell *Online advance.*

Feng P, Deng Z, Fan L, Hu Z (2012) Lipid accumulation and growth characteristics of *Chlorella zofingiensis* under different nitrate and phosphate concentrations. J Biosci Bioeng 114: 405-410.

Gouveia L, Batista AP, Sousa, Raymundo A, Bandarra NM (2008) Microalgae in novel food products. In: N. Konstantinos, P.P. Papadopoulos, editors. Food Chemistry Research Developments. New York, NY: Nova Science Publishers.

Guarnieri MT, Nag A, Smolinski SL, Darzins A, Seibert M, et al. (2011) Examination of triacylglycerol biosynthetic pathways via *de novo* transcriptomic and proteomic analyses in an unsequenced microalga. PLoS ONE (6:10): e25851.

Guarnieri MT, Nag A, Yang S, Pienkos PT (2013) Proteomic analysis of *Chlorella vulgaris*: Potential targets for enhanced lipid accumulation. J Proteomics 93: 245-253.

Guckert JB, Cooksey KE (1990) Triglyceride accumulation and fatty acid profile changes in *Chlorella* (Chlorophyta) during high pH-induced cell cycle inhibition. J Phycol 26: 72-79.

Haass D, Tanner W (1974) Regulation of hexose transport in *Chlorella vulgaris*. Plant Physiol 53: 14-20.

Haehnel W, Nairn JA, Reisberg P, Sauer K (1982) Picosecond fluorescence kinetics and energy transfer in chloroplasts and algae. Biochim Biophys Acta 680: 161-173.

Harwood JL, Guschina IA (2009) The versatility of algae and their lipid metabolism. Biochimie 91: 679-684.

He PJ, Mao B, Shen CM, Shao LM, Lee DJ, et al. (2013) Cultivation of *Chlorella vulgaris* on wastewater that contains high levels of ammonia for biodiesel production. Bioresource Technol 129: 177-181.

Heredia-Arroyo T, Wei W, Hu B (2010) Oil accumulation via heterotrophic/mixotrophic *Chlorella protothecoides*. Appl Biochem Biotechnol 162: 1978-1995.

Hoshina R, Iwataki M, Imamura N (2010) *Chlorella variabilis* and *Micractinium reisseri* sp. nov. (Chlorellaceae, Trebouxiophyceae): Redescription of the endosymbiotic green algae of *Paramecium bursaria* (Peniculia, Oligohymenophorea) in the 120th year. Phycol Res 58: 188-201.

Hu Q, Sommerfeld M, Jarvis E, Ghirardi M, Posewitz M, et al. (2008) Microalgal triacylglycerols as feedstocks for biofuel production: perspectives and advances. Plant J 54: 621-639.

Huss VAR, Frank C, Hartmann EC, Hirmer M, Kloboucek A, et al. (1999) Biochemical taxonomy and molecular phylogeny of the genus *Chlorella* sensu lato (Chlorophyta). J Phycol 35: 587-598.

Ip P-F, Chen F (2005) Production of astaxanthin by the green microalga *Chlorella zofingiensis* in the dark. Process Biochem 40: 733-738.

Jeong ML, Gillis JM, Hwang J-Y (2003) Carbon dioxide mitigation by microalgal photosynthesis. Bull Korean Chem Soc 24: 1763-1766.

Joint Genome Institute (2011) *Coccomyxa subellipsoidea* C-169 v2.0. U.S. Department of Energy. Available: http://genome.jgi.doe.gov/Coc_C169_1. Accessed 28 November 2013.

Kamiya A, Kowallik W (1987) Photoinhibition of glucose uptake in *Chlorella*. Plant Cell Physiol 28: 617-679.

Kessler E (1976) Comparative physiology, biochemistry, and the taxonomy of *Chlorella* (Chlorophyceae). Plant Syst Evol 125: 129-138.

Kim DG, Hur SB (2013) Growth and fatty acid composition of three heterotrophic *Chlorella* species. Algae 28: 101-109.

Kiron V, Phromkunthong W, Huntley M, Archibald I, Scheemaker GD (2012) Marine microalgae from biorefinery as a potential feed protein source for Atlantic salmon, common carp and whiteleg shrimp. Aquacult Nutr 18: 521-531.

Kobayashi N, Noel EA, Barnes A, Watson A, Rosenberg JN, et al. (2013a) Characterization of *Chlorella sorokiniana* strains in anaerobic digested effluent from cattle manure. Bioresource Technol 150: 377-386.

Kobayashi N, Noel EA, Barnes A, Rosenberg J, DiRusso C, et al. (2013b) Rapid detection and quantification of triacylglycerol by HPLC–ELSD in *Chlamydomonas reinhardtii* and *Chlorella* strains. Lipids 48: 1035-1049.

Kodner RB, Summons RE, Knoll AH (2009) Phylogenetic investigation of the aliphatic, nonhydrolyzable biopolymer algaenan, with a focus on green algae. Org Geochem 40: 854-862.

Komor E, Cho B-H, Kraus M (1988) The occurrence of the glucose-inducible transport systems for glucose, proline, and arginine in different species of *Chlorella*. Biotanica Acta 101: 321-326.

Komor E, Tanner W (1974) The hexose-proton cotransport system of *Chlorella*: pH-dependent change in K_m values and translocation constants of the uptake system. J Gen Physiol 64: 568-581.

Laurens LML, Dempster TA, Jones HDT, Wolfrum EJ, Wychen SV, et al. (2012) Algal biomass constituent analysis: method uncertainties and investigation of the underlying measuring chemistries. Anal Chem 84: 1879-1889.

Lee Y-K (2006) Ch. 7 Algal Nutrition: Heterotrophic Carbon Nutrition. In: A. Richmond, editor. Handbook of Microalgal Culture: Biotechnology and Applied Phycology. Oxford, UK: Backwell Science Ltd. pp. 116-124.

Lee YK, Ding SY, Hoe CH, Low CS (1996) Mixotrophic growth of *Chlorella sorokiniana* in outdoor enclosed photobioreactor. J Appl Phycol 8: 163-169.

Li X, Xu H, Wu Q (2007) Large-scale biodiesel production from microalga *Chlorella protothecoides* through heterotrophic cultivation in bioreactors. Biotechnol Bioeng 98: 764-771.

Li Y, Zhou W, Hu B, Min M, Chen P, et al. (2011) Integration of algae cultivation as biodiesel production feedstock with municipal wastewater treatment: Strains screening and significance evaluation of environmental factors. Bioresource Technol 102: 10861-10867.

Liu J, Sun Z, Zhong Y, Huang J, Hu Q, et al. (2012) Stearoyl-acyl carrier protein desaturase gene from the oleaginous microalga *Chlorella zofingiensis*: cloning, characterization and transcriptional analysis. Planta 236: 1665-1676.

Liu ZY, Wang GC, Zhou BC (2008) Effect of iron on growth and lipid accumulation in *Chlorella vulgaris*. Bioresource Technol 99: 4717-4722.

Lu S, Wang J, Niu Y, Yang J, Zhou J, et al. (2012) Metabolic profiling reveals growth related FAME productivity and quality of *Chlorella sorokiniana* with different inoculum sizes. Biotechnol Bioeng 109: 1651-1662.

Luo W, Flugmacher SP, Pröschold N, Walz N, Krienitz L (2006) Genotype versus phenotype variability in *Chlorella* and *Micractinium* (Chlorophyta, Trebouxiophyceae). Protist 157: 315-333.

Luthria D, Vinjamoori D, Noel K, Ezzell J (2004) Chapter 3: Accelerated Solvent Extraction. In: D.L. Luthria, editor. Oil Extraction and Analysis: Critical Issues and Comparative Studies. Champaign, IL: American Oil Chemists' Society Press. pp. 25-38.

Matsukawa R, Hotta M, Masuda Y, Chihara M, Karube I (2000) Antioxidants from carbon dioxide fixing *Chlorella sorokiniana*. J Appl Phycol 12: 263-267.

McAuley PJ (1986) Glucose uptake by symbiotic *Chlorella* in the green-hydra symbiosis. Planta 168: 523-529.

Meyer JR, Ellner SP, Hairston NG, Jones LE, Yoshida T (2006) Prey evolution on the time scale of predator–prey dynamics revealed by allele-specific quantitative PCR. Proc Natl Acad Sci USA 103: 10690-10695.

Mitra D, van Leeuwen J, Lamsal B (2012) Heterotrophic/mixotrophic cultivation of oleaginous *Chlorella vulgaris* on industrial co-products. Algal Res 1: 40-48.

Msanne J, Xu D, Konda AR, Casas-Mollano JA, Awada T, et al. (2011) Metabolic and gene expression changes triggered by nitrogen deprivation in the photoautotrophically grown microalgae *Chlamydomonas reinhardtii* and *Coccomyxa* sp. C-169. Phytochemistry 75: 50-59.

Mulbry W, Kondrad S, Buyer J, Luthria DL (2009) Optimization of an oil extraction process for algae from the treatment of manure effluent. J Am Oil Chem Soc 86: 909-915.

Muscatine L, Karakashian SJ, Karakashian MW (1967) Soluble extracellular products of algae symbiotic with a ciliate, a sponge, and a mutant hydra. Comp Biochem Physiol 20: 1-12.

National Research Council (2012) Sustainable Development of Algal Biofuels in the United States. In: L.G. Coplin, editor. Washington DC: The National Academies Press. Available: http://www.nap.edu/catalog.php?record_id=13437. Accessed 25 October 2012.

Ngangkhama M, Rathaa SK, Prasannaa R, Kumarb R, Babua S, et al. (2013) Substrate amendment mediated enhancement of the valorization potential of microalgal lipids. Biocatal Agric Biotechnol 2: 240-246.

Nguyen HM, Cuiné S, Beyly-Adriano A, Légeret B, Billon E, et al. (2013) The green microalga *Chlamydomonas reinhardtii* has a single ω-3 fatty acid desaturase which localizes to the chloroplast and impacts both plastidic and extraplastidic membrane lipids. Plant Physiol 113: 223941.

Nichols HW, Bold HC (1965) *Trichosarcina polymorpha* Gen. et Sp. Nov. J Phycol 1: 34-38.

Niederholtmeyer H, Wolfstadter BT, Savage DF, Silver PA, Way JC (2010) Engineering cyanobacteria to synthesize and export hydrophilic products. Appl Environ Microb 76: 3462-3466.

Noutoshi Y, Ito Y, Kanetani S, Fujie M, Usami S, et al. (1998) Molecular anatomy of a small chromosome in the green alga *Chlorella vulgaris*. Nucleic Acids Res 26: 3900-3907.

Patnaik S, Samocha TM, Davis DA, Bullis RA, Browdy CL (2006) The use of HUFA-rich algal meals in diets for *Litopenaeus vannamei*. Aquacult Nutr 12: 395-401.

Perez-Garcia O, Escalante FME, de-Bashan LE, Bashan Y (2011) Heterotrophic cultures of microalgae: metabolism and potential products. Water Res 45: 11-36.

Poerschmann J, Spijkerman E, Langer U (2004) Fatty acid patterns in *Chlamydomonas* sp. as a marker for nutritional regimes and temperature under extremely acidic conditions. Microb Ecol 48: 78-89.

Polakovičová G, Kušnír P, Nagyová S, Mikulec J (2012) Process integration of algae production and anaerobic digestion. Chem Eng Trans 29: 1129-1134.

Prescott GW (1954) How to know the fresh-water algae. Dubuque, IA: C. Brown Company.

Reddy HK, Muppaneni T, Rastegary J, Shirazi SA, Ghassemi A, et al. (2013) Hydrothermal extraction and characterization of bio-crude oils from wet *Chlorella sorokiniana* and *Dunaliella tertiolecta*. Environ Prog Sust Energy 32: 910-915.

Rogers JN, Rosenberg JN, Guzman BJ, Oh VH, Mimbela LE, et al. (2014) A critical analysis of paddlewheel-driven raceway ponds for algal biofuel production at commercial scales. Algal Res 4: 76-88.

Rosen BH, Berliner MD, Petro MJ (1985) Protoplast induction in *C. pyrenoidosa*. Plant Sci 41: 23-30.

Rosenberg JN, Oyler GA, Wilkinson L, Betenbaugh MJ (2008) A green light for engineered algae: redirecting metabolism to fuel a biotechnology revolution. Curr Opin Biotech 19: 430-436.

Running JA, Huss RJ, Olson PT (1996) Heterotrophic production of ascorbic acid by microalgae. J Appl Phycol 6: 99-104.

Sakai N, Sakamoto Y, Kishimoto N, Chihara M, Karube I (1995) *Chlorella* strains from hot springs tolerant to high temperature and high CO_2. Energ Convers Manage 36: 693-696.

Samejima H, Meyers J (1958) On the heterotrophic growth of *Chlorella pyrenoidosa*. J Gen Microbiol 18: 107-117.

Santos CA, Ferreira ME, de Silva TL, Gouveia L, Novais JM, et al. (2011) A symbiotic gas exchange between bioreactors enhances microalgal biomass and lipid productivities: taking advantage of complementary nutritional modes. J Ind Microbiol Biotechnol 38: 909-917.

Schenk PM, Thomas-Hall SR, Stephens E, Marx UC, Mussgnug JH, et al. (2008) Second generation biofuels: high-efficiency microalgae for biodiesel production. Bioenerg Res 1: 20-43.

Senanayake SPJN, Ahmed N, Fichtali J (2010) Chapter 37. Nutraceuticals and Bioactives from Marine Algae. In: C. Alasavar, F. Shahidi, K. Miyashita and U. Wanasundara, editors. Handbook of Seafood Quality, Safety and Health Applications. Oxford, UK: Blackwell Publishing Ltd. pp. 455-462.

Sheehan J, Dunahay T, Benemann J, Roessler P (1998) A Look Back at the U.S. Department of Energy's Aquatic Species Program: Biodiesel from Microalgae. Report Number: TP-580-24190. Golden, Colorado: National Renewable Energy Lab.

Shen Y, Yuan W, Pei Z, Mao E (2010) Heterotrophic culture of *Chlorella protothecoides* in various nitrogen sources for lipid production. Appl Biochem Biotechnol 160: 1674-1684.

Shi X, Wu Z, Chen F (2006) Kinetic modeling of lutein production by heterotrophic *Chlorella* at various pH and temperatures. Mol Nutr Food Res 50: 763-768.

Shi X-M, Zhang X-W, Chen F (2000) Heterotrophic production of biomass and lutein by *Chlorella protothecoides* on various nitrogen sources. Enzyme Microb Technol 27: 312-318.

Sorokin C, Meyers J (1953) A high-temperature strain of *Chlorella*. Science 117: 330-331.

Spoehr HA, Milner HW (1949) The chemical composition of *Chlorella*; effect of environmental conditions. Plant Physiol 24: 120-149.

Stephens E, Ross IL, King Z, Mussgnug JH, Kruse O, et al. (2010) An economic and technical evaluation of microalgal biofuels. Nat Biotechnol 28: 126-128.

Stephenson AL, Dennis JS, Howe CJ, Scott SA, Smith AG (2010) Influence of nitrogen-limitation regime on the production by *Chlorella vulgaris* of lipids for biodiesel feedstocks. Biofuels 1: 47-58.

Sun N, Wang Y, Li Y-T, Huang J-C, Chen F (2008) Sugar-based growth, astaxanthin accumulation and carotenogenic transcription of heterotrophic *Chlorella zofingiensis* (Chlorophyta). Process Biochem 43: 1288-1292.

Takeda H (1988) Classification of *Chlorella* strains by cell wall sugar composition. Phytochemistry 27: 3823-3826.

Tamura K, Peterson D, Peterson N, Stecher G, Nei M, et al. (2011) MEGA5: molecular evolutionary genetics analysis using maximum likelihood, evolutionary distance, and maximum parsimony methods. Mol Biol Evol 28: 2731-2739.

Tanaka K, Tomita Y, Tsuruta M, Konishi F, Okuda M, et al. (1990) Oral administration of *Chlorella vulgaris* augments concomitant antitumor immunity. Immunopharmacol Immunotoxicol 12: 277-291.

Tirichine L, Bowler C (2011) Decoding algal genomes: tracing back the history of photosynthetic life on Earth. Plant J 66: 45-67.

Tredici MR, Biondi N, Ponis E, Rodolfi L (2009) Chapter 20: Advances in microalgal culture for aquaculture feed and other uses. In: G. Burnell, G. Allan, editors. New technologies in aquaculture production efficiency, quality and environmental management. Boca Raton, FL: CRC Press. pp. 610-676.

Van Etten JL (2003) Unusual life style of *Chlorella* viruses. Annu Rev Genet 37: 153-195.

Vasudevan V, Stratton RW, Pearlson MN, Jersey GR, Beyene AG, et al. (2012) Environmental performance of algal biofuel technology options. Environ Sci Technol 46: 2451-2459.

Vigeolas H, Duby F, Kaymak E, Niessen G, Motte P, et al. (2012) Isolation and partial characterization of mutants with elevated lipid content in *Chlorella sorokiniana* and *Scenedesmus obliquus*. J Biotechnol 162: 3-12.

Wakasugi T, Nagai T, Kapoor M, Sugita M, Ito M, et al. (1997) Complete nucleotide sequence of the chloroplast genome from the green alga *Chlorella vulgaris*: the existence of genes possibly involved in chloroplast division. Proc Natl Acad Sci USA 94: 5967-5972.

Wan M, Li P, Xia J, Rosenberg JN, Oyler GA, et al. (2011a) The effect of mixotrophy on microalgal growth, lipid content, and expression levels of three pathway genes in *Chlorella sorokiniana*. Appl Microbiol Biot 91: 835-844.

Wan M, Rosenberg JN, Faruq J, Betenbaugh MJ, Xia J (2011b) An improved colony PCR procedure for genetic screening of *Chlorella* and related microalgae. Biotechnol Lett 33: 1615–1619.

Wan M-X, Wang R-M, Xia J-L, Rosenberg JN, Nie Z-Y, et al. (2012a) Physiological evaluation of a new *Chlorella sorokiniana* isolate for its biomass production and lipid accumulation in photoautotrophic and heterotrophic cultures. Biotechnol Bioeng 109: 1958-1964.

Wan M, Faruq J, Rosenberg JN, Xia J, Oyler GA, et al. (2012b) Achieving high throughput sequencing of cDNA library utilizing an alternative protocol for the bench top next-generation sequencing system. J Microbiol Meth 92: 122-126.

Warburg O, Negelein E (1920) Uber die Reduktion der Salpetersaure in griinen Zellen. Biochem Z 110: 66-115.

Wase N, Black PN, Stanley BA, DiRusso CC (2014) Integrated quantitative analysis of nitrogen stress response in *Chlamydomonas reinhardtii* using metabolite and protein profiling. J Proteome Res 13: 1373-1396.

Miao X, Wu Q (2006) Biodiesel production from heterotrophic microalgal oil. Bioresource Technol 97: 841-846.

Wu QY, Yin S, Sheng GY, Fu JM (1992) A comparative study of gases generated from stimulant thermal degradation of autotrophic and heterotrophic *Chlorella*. Prog Nat Sci (in Chinese) 3: 435-440.

Xiong W, Liu L, Wu C, Yang C, Wu Q (2010) ^{13}C-tracer and gas chromatography-mass spectrometry analyses reveal metabolic flux distribution in the oleaginous microalga *Chlorella protothecoides*. Plant Physiol 154: 1001-1011.

Yamada T, Onimatsu H, Van Etten JL (2006) *Chlorella* viruses. Adv Virus Res 66: 293-336.

Yong-Ha P, Seonggi Y, Mi P, Hoon MS (1997) Livestock waste handling and a high degree of functional biological fertilizer. In: O. Huimok, editor: Korean Institute of Science and Technology: Biotechnology Institute. Available: http://attfile.konetic.or.kr/konetic/xml/use/31A1D0205268.pdf. Accessed: 1 March 2014.

Zelibor JL, Romankiw L, Hatcher PG, Colwell RR (1988) Comparative analysis of the chemical composition of mixed and pure cultures of green algae and their decomposed residues by ^{13}C nuclear magnetic resonance spectroscopy. Appl Environ Microb 54: 1051-1060.

Zheng Y, Chi Z, Lucker B, Chen S (2012) Two-stage heterotrophic and phototrophic culture strategy for algal biomass and lipid production. Bioresource Technol 103: 484-488.

Zhu X-G, Long SP, Ort DR (2008) What is the maximum efficiency with which photosynthesis can convert solar energy into biomass? Curr Opin Biotech 19: 153-159.

Ziesenisz E, Reisser W, Wiessner W (1981) Evidence of *de novo* synthesis of maltose excreted by the endosymbiotic *Chlorella* from *Paramecium bursaria*. Planta 153: 481-485.

4

STAGED GROWTH OF *C. SOROKINIANA* IMPROVES NEUTRAL LIPID YIELD DURING THE TRANSITION FROM AUTO– TO HETEROTROPHY

As concluded in Chapter 2, the lipid content and composition of algal biomass grown for biofuel processing is the single most important biological factor to reduce the cost of production. Aside from conventional approaches employing nutrient deprivation alone, the goal to not only increase total lipid content, but also shift its composition toward TAG can be achieved by applying strategic nutrient regimes (*i.e.*, organic supplementation) to augment microalgal oil content. This chapter builds on the findings of the previous chapter by developing a two-stage bioprocess of photosynthetic algal growth followed by heterotrophic oil accumulation to trigger the conversion of organic compounds to TAG in high-density cultures. In Chapter 3, the

green microalga *Chlorella sorokiniana* UTEX 1230 was found to be a suitable candidate for this process due to its robust biomass production under autotrophic conditions and high TAG content during heterotrophic growth. In the present study, the dynamic growth and lipid response of UTEX 1230 was investigated by transferring cells from 150-L scale exponential phase of photoautotrophy to a high-density 36-L heterotrophic culture. Compared to the total lipid productivities achieved during individual batches of autotrophy (8 mg L^{-1} d^{-1}) and heterotrophy (43 mg L^{-1} d^{-1}), sequential auto– and heterotrophic stages accumulated total lipids at a rate of 49 mg L^{-1} d^{-1}. Moreover, this production scheme enabled biomass to reach 7.8 g L^{-1} by dry weight while triacylglycerol (TAG) content increased from 12% to nearly 77% of the total lipid fraction. This redistribution of total lipids to predominantly TAG suggests that the conversion of biomolecules associated with photosynthesis may play a role in neutral lipid biosynthesis during this trophic transition. Based on these results, transcriptomic insights to the metabolic regulation of lipid metabolism and the technoeconomic implications of applying the two-stage methodology to large-scale algal biofuels are discussed.

4.1 Introduction

While microbial fermentation takes advantage of the metabolic conversion of basic carbon substrates into complex biomolecules in controlled bioreactors, plant cells exploit photosynthesis to generate bioproducts ranging from feedstuffs to recombinant proteins literally "in the field" using carbon dioxide (CO_2) and sunlight (Cabanes-Macheteau et al. 1999; Cox et al. 2006; Mayfield & Franklin 2005).

Furthermore, photosynthetic organisms possess intrinsically unique metabolic pathways. As an example, many flowering plants and microalgae are primary producers of nutritional oils and potent antioxidants (Cunningham & Gantt 2011; Hadden et al. 1999; Ip and Chen 2005; Lorenz & Cysewski 2000; Shaish et al. 1992). In biomanufacturing these high-value products, bioprocesses employing conditions of stress after an initial growth phase have been widely used to induce lipid biosynthesis and carotenoid accumulation in algae directly before harvest (Huntley & Redalje 2007). Heterotrophic cultivation with simple sugars can also effectively enrich algal biomass with these desired metabolites (Bumbak *et al.* 2011). Therefore, microalgal strains with metabolic flexibility for carbon substrates are especially attractive biotechnology platforms for pharmaceuticals, nutritional supplements, and biofuel precursors (Rosenberg *et al.* 2008).

Microalgal cultivation under photoautotrophy, mixotrophy, or heterotrophy can heavily influence the balance between lipid content, fatty acid composition, and cellular proliferation. In particular, species of *Chlorella* can readily adapt to conditions of nutrient abundance or starvation in the presence or absence of light (Lee *et al.* 1996; Wan *et al.* 2012; Zheng *et al.* 2012), allowing certain algae to convert exogenous sugars directly to triacylglycerol (TAG), an extractable neutral lipid for biofuel blends (Lown *et al.* 2014). As a result of species bioprospecting, a lead candidate strain of *Chlorella sorokiniana* (UTEX 1230) has demonstrated proficiency in generating substantial amounts of biomass and TAG during mixo– and heterotrophy while also exhibiting robust photoautotrophic growth with relatively

low concentrations of CO_2. Under mixo– or heterotrophic conditions, UTEX 1230 is able to allocate a significant fraction (75-90%) of its total lipid content as TAG (Kobayashi *et al.* 2013b; Rosenberg *et al.* 2014).

While the prospects of heterotrophic algal oil are attractive for biofuel applications, the source and magnitude of fixed carbon required for cultivation poses certain sustainability issues. Historically, heterotrophic algal production has only achieved success in small-volume, high-value dietary lipids for which axenic fed-batch cultures can be carefully maintained (Bailey *et al.* 2003; Gladue & Behrens 2002; Ren *et al.* 2010). For commodity-scale production, however, only a reasonable level of clean handling and contamination control can be expected— not necessarily cGMP or food-grade measures. Consequently, lengthy periods of mixo– and heterotrophic algal cultivation are often encumbered by biological contaminants during scale-up, but may remain necessary to enhance the commercial value of microalgal biomass. As illustrated in Figure 21, TAG storage often coincides with cellular growth under mixo– and heterotrophy, the desire to uncouple the contributions of carbon to biomass production and metabolite accumulation is a worthy target for effective carbon partitioning in biofuel feedstocks (Smith *et al.* 2012).

By balancing the advantages of maximal algal lipid productivity during heterotrophy with its risk of contamination at large scales, the current study examines a two-stage growth regimen with *C. sorokiniana* UTEX 1230, consisting of photoautotrophic growth (150-L) followed by a heterotrophic phase (36-L) rather than a single prolonged stage of either auto–, mixo–, or heterotrophy. This staged bioprocess aims

to capitalize on the favorable aspects of auto– and heterotrophy by generating cells inexpensively with light and CO_2 before using those cells as biocatalysts to convert organic substrates into lipids during the final heterotrophic phase.

In order to understand and optimize the fate of solar and exogenous chemical energy in the ultimate lipid components of algae, the present study focuses on the strategic introduction of glucose as a substrate and its effect on the lipid metabolism of UTEX 1230. Through quantitative evaluation of photoautotrophic biomass production prior to heterotrophic lipid biosynthesis, the total lipid contents, rates of accumulation, and portion of TAG stored were investigated. The results illustrate the applicability of this approach for algal oil production while providing transcriptomic insights into the reorganization and plasticity of microalgal lipid classes and metabolic networks during the transition from auto– to heterotrophy.

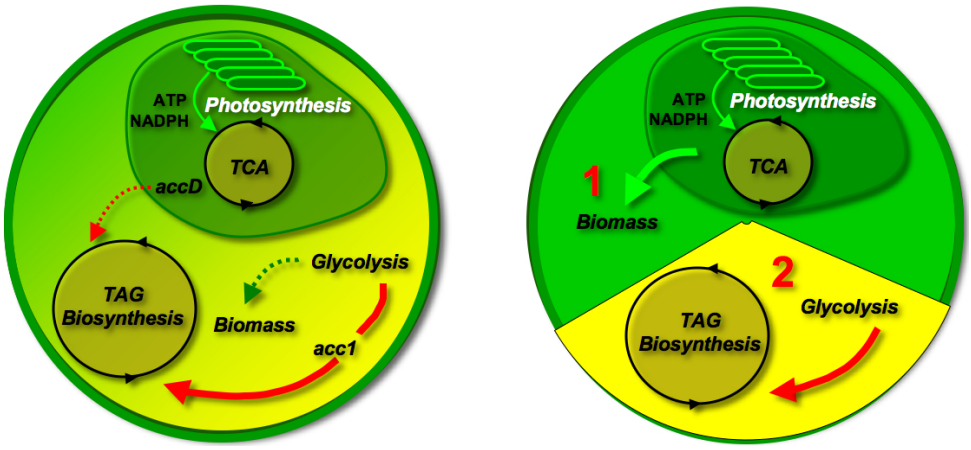

Mixotrophy **Two-Stage**

Figure 21. Cellular depictions of mixotrophy compared to two-stage growth. Algae are useful microbial platforms for biofuel production and can complement existing oil seed crops. However, a balance between algal cell growth and oil biosynthesis often exists. Mixotrophy can lead to sugar utilization primarily for biomass production. Alternatively, two-stage growth processes can uncouple photosynthetic biomass production and lipid accumulation derived from fixed carbon nutrients. This study demonstrates that an initial growth stage with light (photoautotrophy) followed by sugar to induce lipid biosynthesis (heterotrophy) under nitrogen deprivation or other stress can improve neutral lipid yields in *Chlorella sorokiniana* UTEX 1230.

4.1. Materials and Methods

4.1.1 Microalgal cultivation

A stock sample of the alga *C. sorokiniana* UTEX 1230 was obtained from the Culture Collection of Algae at University of Texas at Austin, maintained on sterile agar plates (1.5% w:v), and propagated in axenic liquid culture containing Bold's basal medium (BBM) (NICHOLS & BOLD 1965). Photoautotrophic cultures were illuminated with cool-white fluorescent bulbs at an intensity of 100 µE m^{-2} s^{-1} and maintained at 25 ± 3 °C. Scale-up from plates to production volumes proceeded from 10 ml shake-flasks to 250-ml spinner flasks, 3-, 8- and 15-L bioreactors before inoculating large-scale cultures at 1 × 10^7 cells ml^{-1}. Large-scale autotrophic cultures were aerated with filtered ambient air using an AP-60 PondMaster pump (Danner Manufacturing Inc, New York, USA) and grown in either 150-L glass aquarium tanks (Petco®, 18" × 13" × 48") with an air flow rate of 60 L min^{-1} or 75-L polyethylene hanging bags (6 mil thickness, 14" width; Discount Plastic Bags, Texas, USA) with 45 L air min^{-1}. Heterotrophic cultures were grown in sterile 8-, 15-, or 36-L bioreactors (Bellco Glass, New Jersey, USA), agitated by an impeller at 50 rpm, and supplemented with glucose at a concentration of 10 g L^{-1} in the dark at 25 ± 1 °C. In some cases, 100 µg ml^{-1} tetracycline and 10 µg ml^{-1} ampicillin were added to BBM in order to control bacterial contamination. The cell densities of all algal cultures were monitored with an automated Z1 Coulter Counter (Beckman Coulter, Florida, USA). Periodic biomass samples were harvested using a Sorvall® RC-5B Refrigerated Superspeed Centrifuge (DuPont Instruments, Delaware, USA) at 6,000 × *g* for 20

minutes. Final biomass yields was either concentrated by flocculation using the high molecular weight cationic polymer FLOPAM 4700 SH (SNF Polydyne, Georgia, USA) according to manufacturer's suggested dosing (Haarhoff and Cleasby 1989) or harvested using an Evodos model T-10 continuous spiral plate centrifuge (Raamsdonksveer, The Netherlands). All biomass samples were immediately freeze-dried with a Model 25 SRC lyophilizer (Virtis, New York, USA).

4.1.2 Analysis of lipid content and composition in algal biomass

For total lipid analysis, 30 mg aliquots of each dry biomass sample were ultrasonicated for 1 hour in 1:2 (v:v) chloroform:methanol (Bligh & Dyer 1959). Next, chloroform and a 1% NaCl solution in water were added until the final ratio of the solvent system became 2:2:1 (chloroform:methanol:water). After phase separation produced stratified layers by settling on the benchtop, the extraction tube was centrifuged at 4,000 $\times$ g for 10 minutes. The resulting chloroform layers were collected and subjected to vacuum evaporation leaving only lipid residue for measurement. Replicate total lipid extractions were also performed using an Automated Solvent Extraction 150 system according to the manufacturer's operating manual (Dionex, Thermo Fischer, Delaware, USA) and previously published protocols (Laurens *et al.* 2012; Mulbry *et al.* 2009). All total lipid contents were determined in triplicate by gravimetric methods and compared to dry biomass weight. Subsequent analysis of TAG content was performed following the chromatographic methods described in the prior chapter (Rosenberg *et al.* 2014).

4.1.3. Cultivation of UTEX 395 & generation of transcriptomic data sets

To generate transcriptomic data sets, *Chlorella vulgaris* UTEX 395 was cultivated photoautotrophically in 1-L Roux bottles with 2% CO_2 and heterotrophic samples were grown in shake flasks under ambient CO_2 conditions and 2% glucose in the dark. Transcriptomes were isolated and subjected to RNAseq analysis using previous methods described by Guarnieri *et al.* (2011 & 2013). The photoautotrophic data set analyzed in the present study were harvested at OD = 2 (log phase), while the heterotrophic transcriptome corresponds to a 96 hr time-point (stationary phase with 14.4% FAME). While these transcriptomic data sets originates UTEX 395 rather than UTEX 1230, the two transcriptional time-points correspond well with the two-stage process examined in the present study.

4.2 Results

4.2.1 Biomass and lipid productivities of C. sorokiniana *UTEX 1230*

In order to compare the feasibility of single– and two-stage processes, initial growth studies evaluated the volumetric lipid productivities of distinct auto– and heterotrophic batch cultures of *C. sorokiniana* UTEX 1230 to establish biological reference points before linking auto– and heterotrophic modes of growth. Autotrophic growth was examined at the 75-L scale using the standard minimal medium, Bold's Basal medium (BBM), in which UTEX 1230 cultures grew in the exponential phase for two weeks and were terminated after four weeks at roughly 100×10^6 cells ml^{-1} and 1 g L^{-1} by dry weight (Figure 22a). From biomass samples collected at these two time-points, the total lipid content was found to be 24 ± 2% at the end of stationary phase compared to 8.4 ± 0.4% from exponential phase (Table 7). In terms of autotrophic lipid yields, the one-month batch culture produced 0.24 g L^{-1} oil at an overall rate of 8 mg L^{-1} d^{-1}, which reflects differential oil accumulation rates in stationary and exponential phases (5.5 and 10 mg L^{-1} d^{-1}, respectively).

Heterotrophic cultivation of UTEX 1230 was undertaken in 15-L bioreactors with BBM and 10 g L^{-1} glucose. The population exhibited an extended lag phase before exponential growth (Figure 22b) and the onset of stationary phase, which engendered lipid content increase from 21% to 30%. Combined with the higher final cell concentration, this represents a nearly 2-fold increase in oil productivity from 39 mg L^{-1} d^{-1} during exponential phase to 75 mg L^{-1} d^{-1} during stationary phase, corresponding to an overall heterotrophic lipid production rate of 43 mg L^{-1} d^{-1} and

yield of 0.6 g L^{-1} oil production over the course of two weeks. This more than 5-fold improvement in volumetric lipid productivity relative to photoautotrophy can be attributed not only to the higher lipid content throughout heterotrophy, but also to the 2-fold higher biomass concentration (2 g L^{-1}) supported by glucose feeding. Collectively, these direct comparisons of growth and lipid data during exponential and stationary phases of auto– and heterotrophic growth in Table 7 provide a biological baseline with which to compare the two-stage growth process.

Culture Condition, Time Point (day)	**AUTO 14-d**	**AUTO 30-d**	**HETERO 7-d**[#]	**HETERO 14-d**
Phase of Growth	Exponential	Stationary	Exponential	Stationary
Total Lipid Content (% of dry cell weight)	8.4 ± 0.4%	24 ± 2%	21%	30 ± 2%
Biomass Density ($g\ L^{-1}$)	1.0	1.0	1.5	2.0
Lipid Productivity (volumetric)	5.5 mg L^{-1} d^{-1}	10 mg L^{-1} d^{-1}	39 mg L^{-1} d^{-1}	75 mg L^{-1} d^{-1}
	8 mg L^{-1} d^{-1}		43 mg L^{-1} d^{-1}	

[#] Inferred from previous study (ROSENBERG *et al.* 2014)

Table 7. Biomass and lipid data from autotrophic (75-L) or heterotrophic (15-L) batch cultures. Data describing biomass and lipid performance parameters are reported for both exponential and stationary phases of culture. Additionally, the overall volumetric lipid productivity corresponds to the average lipid accumulation rate over the entire course of cultivation. All values were derived from experiments conducted in this study, unless otherwise designated. Lipid contents are the average of three technical replicates ± one standard deviation.

4.2.2 Scalable two-stage growth of UTEX 1230: high-density heterotrophy

In order to pilot sequential stages of auto– and heterotrophic cultivation, photoautotrophic cultures were first grown in rectangular glass tanks with BBM at the 150-L scale. Despite having half the surface-to-volume ratio of the hanging bags, 150-L aquarium tank cultures followed comparable photoautotrophic growth trends as the hanging bags (Figure 22) and exhibited similar biomass yields (0.75 g L^{-1}), perhaps as a consequence of more effective mixing (data not shown). For the two-stage process, autotrophic UTEX 1230 biomass was harvested from exponential phase, concentrated to wet paste, and resuspended in a 36-L heterotrophic bioreactor at a starting biomass density of 3 g L^{-1} with fresh BBM and 10 g L^{-1} glucose. Over the subsequent two-week period, the heterotrophic culture reached a final biomass concentration of 7.8 g L^{-1} by dry weight as shown in the growth curve depicted in Figure 22 (right axis). The bar graph in this figure quantifies the corresponding linear rate of total lipid accumulation as a percent of total cell mass (left axis) as well as the portion of total lipids stored as neutral TAG. The accelerating rate of neutral lipid biosynthesis during heterotrophy is particularly evident and exhibits the most significant increase of TAG from 31% to 63% of the total lipids after 8-10 days of cultivation. After two weeks, the heterotrophic lipid composition was enriched with 77% of the total lipids as TAG from an initial 12 ± 5% and with an average accumulation rate of 69 mg L^{-1} d^{-1}.

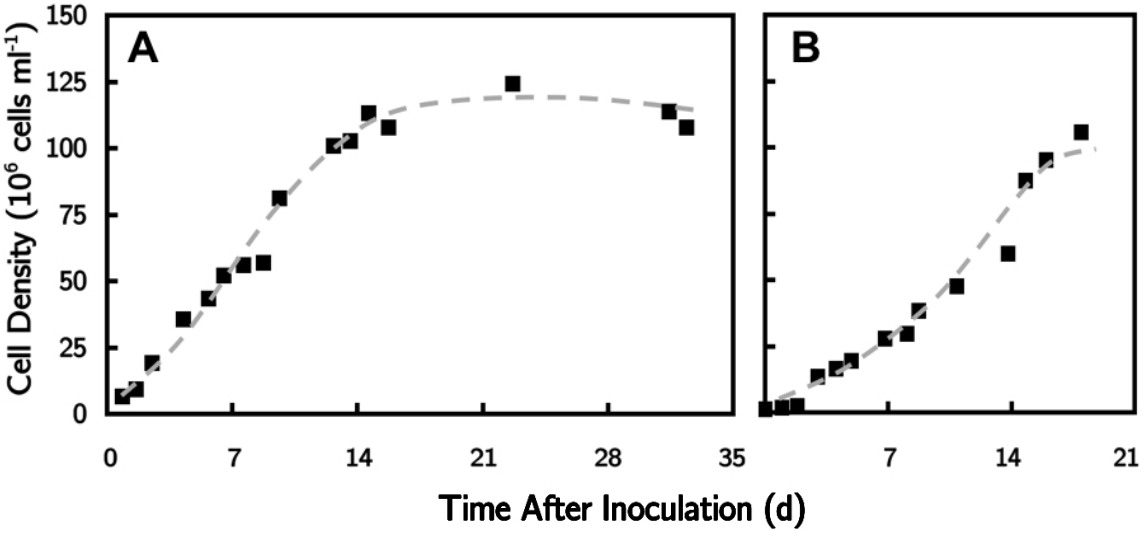

Figure 22. Independent photoautotrophic and heterotrophic growth curves of *C. sorokiniana* UTEX 1230. These representative plots of cell density in **(A)** 75-L hanging bags and **(B)** 15-L fermentors demonstrate the full course of *Chlorella sorokiniana* UTEX 1230 in photoautotrophic and heterotrophic culture, respectively, interpolated from biological replicates. The final cell densities of over 100×10^6 cells ml^{-1} in both stationary phases correspond to biomass densities between 1-2 g L^{-1} by dry weight. The standard deviation for each measured data point (■) is less than 2×10^6 cells ml^{-1} based on three technical replicates.

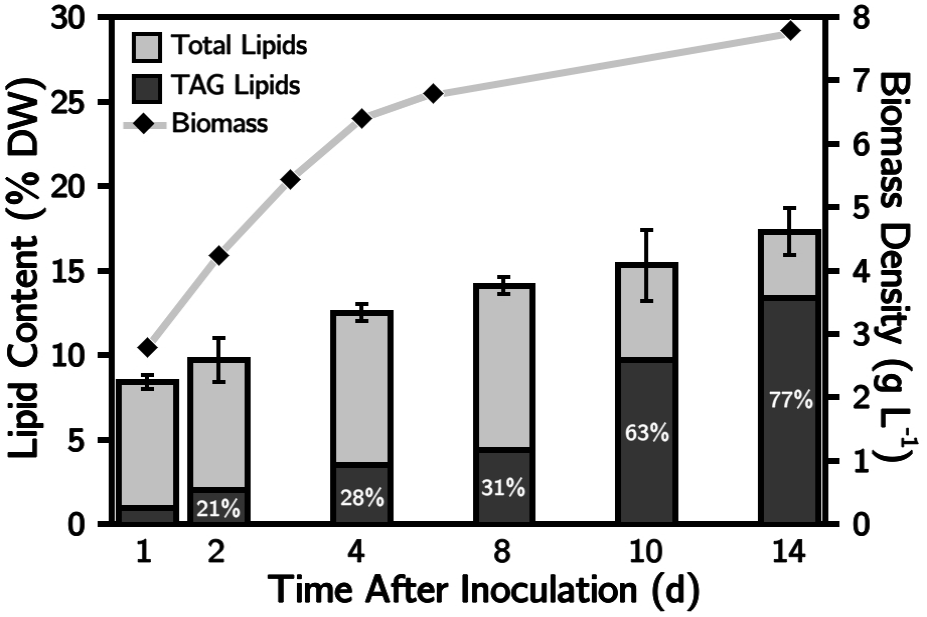

Figure 23. Algal biomass and cumulative lipid accumulation during high-density heterotrophic cultivation at 36-L. The increase in biomass density (◆) during second-stage heterotrophy illustrates the high rate of growth during the first week. As growth slows to reach a final yield of nearly 8 g L^{-1} by dry weight, noticeable neutral lipid accumulation is depicted in the corresponding bar graph. The entire bars (light gray) correspond to the total lipid content while the inset regions (dark gray) represent TAG content, expressed as percent of biomass dry weight (DW) on the left axis. The percentages super-imposed on each bar indicate the fraction of total lipids stored as TAG (percent of total lipids DW). Error bars represent standard deviation associated with three technical replicates.

With the sequential auto-to-heterotrophic transition, the final 36-L fermenter yielded 1.3 g L^{-1} of total lipids, compared to 0.24 and 0.6 g L^{-1} in single-stage auto– and heterotrophic processes, respectively. The TAG biosynthesis during second-stage heterotrophy resulted in a final density of 1 g L^{-1} of TAG in culture, which is substantially higher than TAG production rates for this strain under heterotrophy alone and autotrophy alone (ROSENBERG *et al.* 2014). The second heterotrophic stage elicited total lipid accumulation on the order of 49 mg L^{-1} d^{-1} compared to 43 mg L^{-1} d^{-1} in heterotrophic culture and 8 mg L^{-1} d^{-1} in a single phototrophic batch. Thus, while the two-stage process does not achieve markedly higher *total* lipid accumulation rates, the yield of neutral lipids (TAG) exceeds those of individual auto– or heterotrophic cultures. Figure 3 shows the trajectory of overall lipid accumulation rates to reach the ultimate oil and TAG yields (g L^{-1}) for each of the cultivation modes examined. Since this strain is known to under-perform when grown with light and sugar compared sugar alone (ROSENBERG *et al.* 2014), the mixotrophic case was not examined in the present study. Nonetheless, UTEX 1230 is intuitively appealing for its differential oil production rates with CO_2 or sugar and unique applicability for staged bioprocess design.

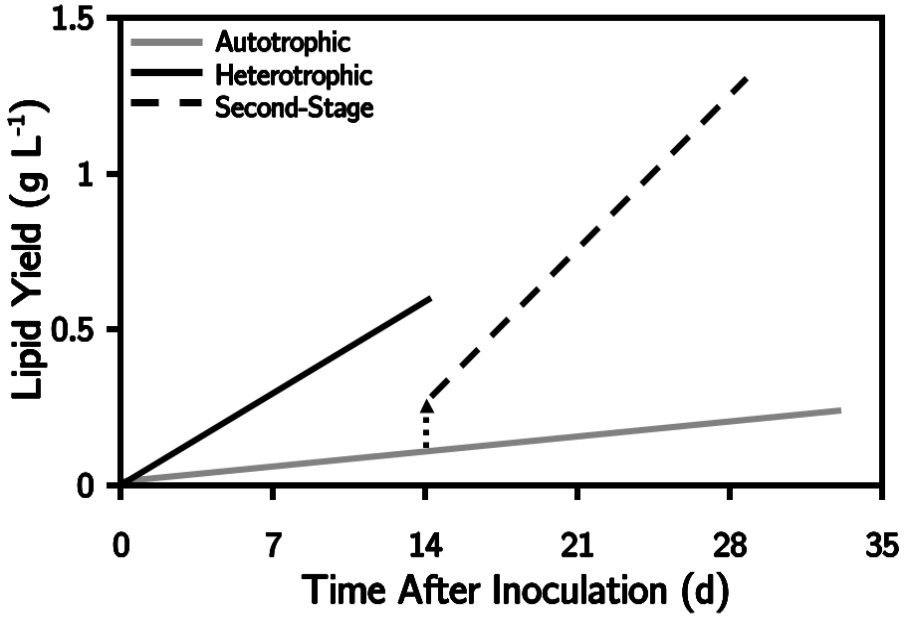

Figure 24. Extrapolated projections of overall volumetric lipid production rates. The average of exponential- and stationary-phase lipid productivities are reflected in the slope of each line. For auto– and heterotrophic modes of culture, these correspond to 8 and 43 mg L^{-1} d^{-1}, respectively. The dotted arrow on day fourteen represents harvesting and concentrating biomass from autotrophy to an initial heterotrophic biomass density of 3 g L^{-1} for the second stage of cultivation (dashed line), which produced lipids at a rate of 49 mg L^{-1} d^{-1}.

4.2.3 Transcriptome analysis of Chlorella *species during trophic shifts*

In order to glean insight into the broad changes in metabolic regulation that occur in *Chlorella* species during the transition from auto- to heterotrophy, corresponding transcriptomic data sets from a related *Chlorella* strain were generated and analyzed by RNAseq. Gene expression profiles from *Chlorella vulgaris* UTEX 395 during autotrophy with CO_2 and heterotrophy with glucose were first narrowed down to transcripts with high statistical relevance ($p < 5 \times 10^{-5}$). From this select list, Table 8 shows genes that were identified to have the highest transcriptional levels during auto- and heterotrophy along with genes that experience the most significant change in expression between auto– and heterotrophic cultivation.

Many anticipated observations in transcript levels correspond well with the respective growth conditions. For example, genes associated with chloroplast biology and the photosynthetic apparatus, such as ATP synthase domains (PFam IDs: PF02874, PF00306, PF00006) and the photosystem II protein (PFam ID: PF00421), were both highly expressed during photoautotrophy and absent from heterotrophic samples. Genes involved in heterotrophic metabolism, such as ABC transporters and translocation domains for citrate and sugar (PFam IDs: PF00664, PF00005, PF01061, PF00083, PF03600) were detected in high abundance, as expected. Concomitant with the observed chlorosis and redistribution of chloroplast biomolecules, phosophlipid menthyltransferase and lipase genes (PFam IDs: PF04191 & PF01764) also showed high transcriptional abundance during heterotrophy, which may support the hypothesis that significant turnover of chloroplast and thylakoid

membrane lipids lead to heterotrophic TAG storage, in addition to *de novo* biosynthesis (Wang *et al.* 2009). Furthermore, down-regulation of dehydrogenases (*e.g.*, PF00389) involved in light-driven biosynthesis implicates a collapse of chloroplasts during heterotrophy, from which biomolecules can be regenerated as TAG (Benstein *et al.* 2013).

Interestingly, the most significantly upregulated genes during autotrophy encode for multi-copper oxidase and heavy metal associated proteins, such as reprolysin, which is completely absent during heterotrophy but present during photoautotrophy (Herbik *et al.* 2002). This finding suggests a major shift in the regulation of iron, copper, and other metal co-factors required for photosynthesis when the cells assume a heterotrophic state. Furthermore, there is a strong relationship between metal starvation and lipid remodeling in algal cells with implications in TAG accumulation, which may occur during heterotrophy (Urzica *et al.* 2013). Additionally, a fascilin domain associated with cellular adhesion is unexpectedly the most highly expressed gene during heterotrophy and remains at very low expression levels in autotrophy (PFam ID: PF02469). Although the turbidity maintained in the fermentor prevented any noticeable biofilm growth, this transcriptional evidence may suggest that *Chlorella* cells prefer sessile modes of growth in the presence of organic carbon and initiate auto-flocculation pathways. Lastly, unique expression levels of two genes with unknown function were identified. While transcript is only present during autotrophy, the other is only present during heterotrophy. BLAST results indicate that these hypothetic proteins are exclusively related to the green algae lineage.

PFam ID	Gene Name	Metabolic Role
Mostly highly expressed during autotrophy		
PF07731	Multicopper oxidase	Photosynthetic co-factors
PF00125	Core histone H2A/H2B/H3/H4	Nuclear gene regulation
PF00403	Heavy-metal-associated domain	Metal co-factor binding
PF00389	D-isomer 2-hydroxyacid dehydrogenase	Photosynthetic biosynthesis
Mostly highly expressed during heterotrophy		
PF02469	Fasciclin domain	Adhesion molecule
PF00125	Core histone H2A/H2B/H3/H4	Nuclear gene regulation
PF00122	E1-E2 ATPase	Energy metabolism
PF00231	ATP synthase	Energy metabolism
Significantly down-regulated during heterotrophy (compared to autotrophy)		
PF07731	Multicopper oxidase	Photosynthetic co-factors
PF02874	ATP synthase, beta-barrel domain	Light-driven energy production
PF00306	ATP synthase, C terminal domain	Light-driven energy production
PF00006	ATP synthase, nucleotide-binding	Light-driven energy production
PF00421	Photosystem II protein	Photosynthetic light harvesting
Significantly upregulated during heterotrophy (compared to autotrophy)		
PF01562	Reprolysin family propeptide	Metal co-factor binding
PF02469	Fasciclin domain	Adhesion molecule
PF03600	Citrate transporter	Carbon metabolism
PF00664	ABC transporter transmembrane region	Homeostatic carbon balance
PF00005	ABC transporter	Homeostatic carbon balance
PF01061	ABC-2 type transporter	Homeostatic carbon balance
PF00083	Sugar (and other) transporter	Carbon metabolism
PF04191	Phospholipid methyltransferase	Lipid metabolism
PF01764	Lipase (class 3)	Lipid metabolism

Table 8. Significant changes in gene regulation in auto- and heterotrophy. This select list of transcripts from *Chlorella vulgaris* UTEX 395 implicates shifts in carbon and lipid metabolism while also suggesting a major change in metal co-factor balance associated with the loss of chloroplasts during heterotrophy. All protein sequences are listed in Appendix B.

4.3. Discussion and Conclusions

Lipid productivity remains one of the most critical bioprocessing parameters for microalgal biofuel production. Technoeconomic analyses performed by Stephens *et al.* set 5 g m^{-2} d^{-1} as a feasibility threshold for areal lipid productivity and more recent appraisals have identified lipid content as the major factor to improve both the economics and sustainability of algal biofuels (Rogers *et al.* 2013; Stephens *et al.* 2010). Most conventional fuels, including diesel and jet fuel, contain aliphatic hydrocarbons that are chemically similar to the fatty acids of TAG (Hsieh *et al.* 2014). As such, novel approaches to maximize oily biomass yields, targeted at either the molecular or bioprocessing scales, are a major bioenergy goal (Fan *et al.* 2013). Furthermore, the cost, sourcing, and distribution of CO_2 are non-trivial components of algal cultivation for biofuels (Chisti 2013; Rogers *et al.* 2014). Therefore, a strain such as UTEX 1230 that can grow in relatively "thin" air (minimal CO_2) during an initial autotrophic stage may alleviate some of the capital and operating costs associated with a final stage of heterotrophy.

In the interest of utilizing algae to produce renewable oils, the major challenge involves partitioning the flow of chemical energy to lipid storage rather than cell proliferation and, furthermore, toward TAG rather than other types of lipids. Compared to the autotrophic lipid production rate of UTEX 1230 determined in the present study (Table 7), the two-stage growth process improves final volumetric oil yields by 12-fold. While this augmented total lipid yield of 1.3 g L^{-1} was only about 2-fold higher than a single heterotrophic batch culture, the TAG productivity of 69

mg L^{-1} d^{-1} compared to 29 mg L^{-1} d^{-1} previously reported for this strain under strict heterotrophy is biochemically significant and can favorably impact downstream extraction and separation of neutral oils compared to polar lipids (Rosenberg *et al.* 2014).

In addition to intensifying biocatalysis by supplying more cells for bioconversion of sugar to oil, the two-stage cultivation strategies benefit from tunable time periods. Interestingly, the reverse order of these growth stages— providing a dense heterotrophic inoculum for final photoautotrophic culture expansion —has been investigated recently with other *Chlorella* species (Fan *et al.* 2012b; Zheng *et al.* 2012). A further permutation of this bioprocess employing sequential auto– and mixotrophic stages has also been examined (Yen & Chang 2013). In all of these cases, extended periods of heterotrophy can be avoided while still benefiting from rapid sugar-based bioproductivity.

4.3.1 Economics of algal lipid productivity in auto– and heterotrophy

From a technoeconomic perspective, the two-stage cultivation strategy allows engineering control to be exerted over the time spent in the heterotrophic stage where the amount of organic substrate can be regulated, which may reduce the cost of algal oil production. While equivalent two-week residence times in auto– and heterotrophic batches were evaluated in the present study based on the differential times required to reach stationary phase, further work is needed to estimate the technoeconomic projections to optimize the time spent in each segment of the two-stage process. This study aimed to maintain nitrogen replete growth during

autotrophy to maximize cell proliferation and then grow the biomass to nitrogen deprivation (late stationary phase) in heterotrophy to maximize TAG storage. Alternative operating scenarios may enable continuous autotrophic growth with periodic harvests to inoculate short heterotrophic batches, but were not examined in the present study. Furthermore, the heterotrophic media can be formulated without nitrogen at all in order to more severely inhibit growth and induce TAG storage in the second stage. Alternative low-cost nutrient sources may also provide TEA benefits by integrating autotrophic cultivation with wastewater effluents, as examined in Chapter 8, or sourcing reduced carbon feedstocks from biomass hydrolysates, glycerol byproducts, or sugars secreted from other microbes in co-culture (NIEDERHOLTMEYER *et al.* 2010). Despite the advantages of using waste nutrient sources, a recent lifecycle analysis suggests that greenhouse gas emissions associated with purely heterotrophic production of algal biofuel remains comparable to petroleum-based diesel (CHANG *et al* 2014). However, a two-stage process employing photoautotrophic growth may beneficially offset the carbon balance of biofuel production. This LCA study modeled a scenario employing waste glycerol as a feedstock and suggests that other sugar byproducts, such as waste molasses from the food industry, serve as both attractive alternatives and technically feasible goals (YAN *et al.* 2011).

In regards to carbon utilization during heterotrophy in this study, the time required for glucose acclimation in UTEX 1230 is apparent in Figure 22B and may be due to substrate inhibition at low cell densities. This latency is overcome by the elevated

biomass loading rate of 3 g L^{-1} in second-stage heterotrophy (Figure 23). The production of nearly 5 g L^{-1} of biomass from 10 g L^{-1} of glucose in this second stage is indicative of more efficient carbon assimilation compared to only 20% conversion of the glucose to biomass in single heterotrophy. This figure is in close accord with a related *Chlorella sorokiniana* strain (CCTCC M209220, formerly CS-01), which also has excellent potential as a feedstock for biofuel production in heterotrophic culture. The highest conversion ratio of glucose achieved with CS-01 was found to be 25% (Wan *et al.* 2012). In using a minimal medium, the two-stage process enables more efficient glucose consumption resulting in high ultimate biomass and oil yields of 7.8 and 1.3 g L^{-1}, respectively. Compared to the 1.2 g L^{-1} lipids achievable from consecutive two-week batches of heterotrophy, an additional 0.1 g L^{-1} of lipids from the two-stage process may also implicate the turnover of polar membrane lipids and hydrocarbon pigments associated with photosynthesis to neutral lipids, as evidenced by the onset of chlorosis (Rosenberg *et al.* 2014). Collectively, these results indicate that sequential auto– and heterotrophic cultivation can significantly improve the conversion efficiency of glucose to biomass due to high-density cultures. It is conjectured that after a sudden transition from auto– to heterotrophy, the complete switch of metabolism from photoautotrophic to heterotrophic growth is not instantaneous and, therefore, restructuring of the cell's lipid constituents occur before any cell proliferation.

4.3.2 Shifts in transcriptomic regulation and lipid composition

Prior to pilot-scale validation of the two-stage process, gene regulation patterns of a related *Chlorella* species was analyzed to determine biochemical and metabolic factors that should be considered in process design. With a focus on fatty acids, there is increasing evidence of lipid biosynthetic pathways participating in different aspects of cellular function by reorganizing the distribution of lipid classes (*e.g.* polar, neutral, glycolipids, phospholipids, TAG, PUFAs, carotenoids, tocopherols) (Doi *et al.* 2014; Sinha *et al.* 2009). In terms of redox potential, membrane fluidity, and energy stores, this flexible carbon network remains important for survival, yet the complex molecular processes regulating these changes are only beginning to be clearly defined in algae (Fan *et al.* 2012a). Preliminary investigation of *C. sorokiniana* in BBM at the bench-scale indicated that nitrogen deprivation, which is known to induce lipid accumulation (Stephenson *et al.* 2010), is coincident with the onset of stationary phase in both auto– and heterotrophic batch cultures. A detailed assessment of UTEX 1230 population dynamics and lipid profiles under these modes of cultivation previously demonstrated that UTEX 1230 can achieve lipid contents as high as 39% and substantially shift its oil profile toward neutral lipids during heterotrophy (22% TAG) compared to autotrophy (11% TAG) (Rosenberg *et al.* 2014). Interestingly, this prior study also found that mixotrophic biomass production and lipid accumulation of UTEX 1230 is hampered relative to heterotrophy and, therefore, mixotrophy was not examined as a component of two-stage growth.

In the present study, the compilation of total lipid contents in both nitrogen-replete

and limited cases (Table 7) supported further characterization of the two-stage process with UTEX 1230 in which the pattern of heterotrophic lipid accumulation was exemplified by a turnover of the majority of total lipids to TAG. Second-stage heterotrophic growth exhibited a nearly 6.5-fold increase in TAG content compared to the exponential phase of autotrophy (Figure 23). However, as a result of the escalated respiratory demand in high-density culture, oxygen limitation may have negatively influenced the accumulation of total lipids (17 ± 1%), which was less than the single heterotrophic stage (30 ± 2%). Nonetheless, an additional benefit to the trophic transition is the likely conversion of residual photosynthetic lipids (*e.g.*, chloroplast membranes and pigments) to TAG rather than additional membrane lipids present at the time of harvest. While there is also an assumed conversion of sugar directly to storage TAG, considerable resculpting of the existing autotrophic lipid landscape may implicate autophagy rather than entirely *de novo* synthesis from sugar (Jiang *et al.* 2012; Singh *et al.* 2009; Wada *et al.* 2009; Wang *et al.* 2009). In order to quantify this hypothesis, ^{13}C-labeling studies are a subject of continued investigation (Xiong *et al.* 2010). Along with the preliminary transcriptomic analysis for *C. vulgaris* summarized in Table 8, further efforts to harmonize genomic, transcriptomic, and proteomic data for *Chlorella* species is underway. For example, the metabolic mechanisms of oil accumulation during auto- and heterotrophy have been recently characterized in *C. protothecoides* strain 0710, which implicate a specific family of hexose uptake proteins (HUP) as the biochemical portals that enable glucose consumption (Gao *et al.* 2014). Although HUP-like genes were not identified in our heterotrophic assessment of the *C. vulgaris* transcriptome, the exact

function of all significant protein sequences was unable to be determined; therefore, the possibility remains that HUP genes could be conserved in other *Chlorella* species. Further comparative genomic analyses also support the use of *Chlorella* species as model organisms to study autophagy, which is consistent with our results regarding membrane degradation and lipid turnover (Jiang *et al.* 2012).

While TAG is a highly energy-dense biomolecule and much research supports its use as a biologically refined lipid for renewable diesel and other drop-in fuels, hydrothermal liquefaction (HTL) of whole biomass also has potential to produce crude bio-oil for fuel applications. A recent investigation of biocrude production from UTEX 1230 grown with geothermal water reported successful HTL of relatively lean autotrophic UTEX 1230 biomass at less than 5% lipids by dry weight (Reddy *et al.* 2013), which further demonstrates the versatility of this strain for other routes of bioconversion for biofuels. Nonetheless, inducing higher TAG content without augmenting the total lipid content in this organism remains somewhat irrelevant for the HTL because all lipids (and residual biomass) will ultimately be converted to a crude oil (Illman *et al.* 2000). Alternatively, for biofuel production processes employing separation technologies to refine lipids from algal biomass, major gains can be achieved by shifting the composition of total lipids to a more easily extractable form (*i.e.*, TAG) and, moreover, converting photosynthetic pigments that are unusable for biodiesel to TAG. By separating oils from protein and carbohydrates, value can be added to the algal biomass by producing co-products other than fuel. For this reason, microalgae represent a point of convergence for the

global focus on the sustainable production of food and fuels. Furthermore, from biochemical and cell physiology perspectives, the impact of environmental conditions on the lipid composition of *C. sorokiniana* UTEX 1230 observed in this study is intriguing. This strain may serve as an industrially relevant model alga with the ability to catabolize a wide range of carbon substrates. For commercialization of microalgae for biofuels and food applications, carbon can be uniquely paired based on the particular end product and locally abundant natural resources sources (*i.e.*, industrial CO_2 or organic wastes).

4.4 References

Bailey RB, Masi DD, Hansen JM, Mirrasoul PJ, Ruecker CM, Veeder GT, Kaneko T, Barclay WR (2003) Enhanced production of lipids containing polyenoic fatty acid by very high density cultures of eukaryotic microbes in fermentors. U.S. Patent No. 6/607/900.

Benstein RM, Ludewig K, Wulfert S, Wittek S, Gigolashvili T, Frerigmann H, Gierth M, et al. (2013) *Arabidopsis* phosphoglycerate dehydrogenase1 of the phosphoserine pathway is essential for development and required for ammonium assimilation and tryptophan biosynthesis. Plant Cell, 25: 5011-5029.

Bligh EG, Dyer WJ (1959) A rapid method for total lipid extraction and purification. Canadian Journal of Biochemistry and Physiology 37: 911-917.

Bohutskyi P, Kula T, Kessler B, Hong Y, Bouwer E, Betenbaugh MJ, Allnutt FCT 2014a. Mixed trophic state production process for microalgal biomass with high lipid content for generating biodiesel and biogas. BioEnergy Research 1-12.

Bohutskyi P, Liu K, Kessler B, Kula T, Hong Y, Bouwer E, Betenbaugh MJ, Allnutt FCT (2014b) Mineral and non-carbon nutrient utilization and recovery during sequential phototrophic-heterotrophic growth of lipid-rich algae. Applied Microbiology and Biotechnology 98: 5261-5273.

Bumbak F, Cook S, Zachleder V, Hauser S, Kovar K (2011) Best practices in heterotrophic high-cell-density microalgal processes: achievements, potential and possible limitations. Applied Microbiology & Biotechnology 91: 31-46.

Cabanes-Macheteau M, Fitchette-Lainé AC, Loutelier-Bourhis C, Lange C, Vine ND, Ma JK, Lerouge P, Faye L (1999) N-glycosylation of a mouse IgG expressed in transgenic tobacco plants. Glycobiology 9: 365-372.

Chang KJL, Rye L, Dunstan GA, Grant T, Koutoulis A, Nichols PD, Blackburn SI (2014) Life cycle assessment: heterotrophic cultivation of thraustochytrids for biodiesel production. J Applied Phycology. *In Press.*

Chisti Y 2013. Constraints to commercialization of algal fuels. Journal of Biotechnology 167: 201-217.

Cox KM, Sterling JD, Regan JT, Gasdaska JR, Frantz KK, Peele CG, Black A, Passmore D, et al. (2006) Glycan optimization of a human monoclonal antibody in the aquatic plant *Lemna minor*. Nature Biotechnology 24: 1591-1597.

Cunningham FX Gantt E (2011) Elucidation of the pathway to astaxanthin in the flowers of *Adonis aestivalis*. Plant Cell 23: 3055-3069.

Doi H, Hoshino Y, Nakase K, Usuda Y (2014) Reduction of hydrogen peroxide stress derived from fatty acid beta-oxidation improves fatty acid utilization in *Escherichia coli*. Appl Microbiol Biotechnol 98: 629-639.

Ducat DC, Avelar-Rivas JA, Way JC, Silver PA (2012) Rerouting carbon flux to enhance photosynthetic productivity. Applied and Environmental Microbiology 78: 2660-2668.

Fan J, Cui Y, Huang J, Wang W, Yin W, Hu Z, Li Y (2012a) Suppression subtractive hybridization reveals transcript profiling of *Chlorella* under heterotrophy to photoautotrophy transition. PLoS ONE 7:e50414.

Fan J, Huang J, Li Y, Han F, Wang J, Li X, Wang W, Li S (2012b) Sequential heterotrophy-dilution-photoinduction cultivation for efficient microalgal biomass and lipid production. Bioresource Technology 112: 206-211.

Fan J, Yan C, Zhang X, Xu C (2013) Dual role for phospholipid:diacylglycerol acyltransferase: enhancing fatty acid synthesis and diverting fatty acids from membrane lipids to triacylglycerol in *Arabidopsis* leaves. The Plant Cell 25: 3506-3516.

Gao C, Wang Y, Shen Y, Yan D, He X, et al. (2014) Oil accumulation mechanisms of the oleaginous microalga Chlorella protothecoides revealed through its genome, transcriptomes, and proteomes**.** BMC Genomics 15: 582.

Gladue RM, Behrens PW (2002) DHA-containing nutritional compositions and methods for their production. U.S. Patent No. 6/372/460.

Guarnieri MT, Nag A, Smolinski SL, Darzins A, Seibert M, et al. (2011) Examination of triacylglycerol biosynthetic pathways via de novo transcriptomic and proteomic analyses in an unsequenced microalga. PLoS ONE (6:10): e25851.

Guarnieri MT, Nag A, Yang S, Pienkos PT (2013) Proteomic analysis of Chlorella vulgaris: Potential targets for enhanced lipid accumulation. J Proteomics 93: 245-253.

Haarhoff J, Cleasby JL (1989) Direct filtration of *Chlorella* with cationic polymer. Journal of Environmental Engineering 115: 248-366.

Hadden WL, Watkins RH, Levy LW, Regalado E, Rivadeneira DM, Breemen RBv, Schwartz SJ (1999) Carotenoid composition of marigold (*Tagetes erecta*) flower extract used as nutritional supplement. J. Agric. Food Chem. 47: 4189-4194.

Herbik A, Bölling C, Buckhout TJ (2002) The involvement of a multicopper oxidase in iron uptake by the green algae *Chlamydomonas reinhardtii*. Plant Physiol 130: 2039-2048.

Hsieh PY, Widegren JA, Fortin TJ, Bruno TJ (2014) Chemical and thermophysical characterization of an algae-based hydrotreated renewable diesel fuel. National Institute of Standards and Technology.

Huntley M, Redalje D (2007) CO_2 mitigation and renewable oil from photosynthetic microbes: a new appraisal. Mitigation and Adaptation Strategies for Global Change 12: 573-608.

Illman AM, Scragg AH, Shales SW (2000) Increase in *Chlorella* strains calorific values when grown in low nitrogen medium. Enzyme and Microbial Technology 27: 631-635.

Ip P-F, Chen F (2005) Production of astaxanthin by the green microalga *Chlorella zofingiensis in* the dark. Process Biochemistry 40: 733-738.

Jiang Q, Zhao L, Dai J, Wu Q (2012) Analysis of autophagy genes in microalgae: *Chlorella* as a potential model to study mechanism of autophagy. PLoS ONE 7: e41826.

Kobayashi N, Barnes A, Jensen T, Noel E, Andlay G, Rosenberg JN, Betenbaugh MJ, Guarnieri MT, Oyler GA (2013a) Comparison of biomass production and lipid contents in Chlorella strains at various photobioreactor scales under low-CO_2 vigorous aeration and high CO_2 conditions. Algal Research *In Preparation*

Kobayashi N, Noel EA, Barnes A, Watson A, Rosenberg JN, Erickson G, Oyler GA (2013b) Characterization of *Chlorella sorokiniana* strains in anaerobic digested effluent from cattle manure. Bioresource Technol 150: 377–386.

Laurens LML, Dempster TA, Jones HDT, Wolfrum EJ, Wychen SV, et al. (2012) Algal biomass constituent analysis: method uncertainties and investigation of the underlying measuring chemistries. Analytical Chemistry 84: 1879-1889.

Lee YK, Ding SY, Hoe CH, Low CS. (1996) Mixotrophic growth of *Chlorella sorokiniana* in outdoor enclosed photobioreactor. Journal of Applied Phycology 8: 163-169.

Lorenz TR, Cysewski GR. (2000) Commercial potential for *Haematococcus* microalgae as a natural source of astaxanthin TIBTECH 18: 160-167.

Lown AL, Peereboom L, Mueller SA, Anderson JE, Miller DJ, Lira CT (2014) Cold flow properties for blends of biofuels with diesel and jet fuels. Fuel 117: 544-551.

Mayfield SP, Franklin SE (2005) Expression of human antibodies in eukaryotic micro-algae. Vaccine 2005: 1828-1832.

McBride RC, Lopez S, Meenach C, M.Burnett, Lee PA, Nohilly F, Behnke C (2014) Contamination management in low cost open algae ponds for biofuels production. Industrial Biotechnology 10: 221-227.

Mulbry W, Kondrad S, Buyer J, Luthria DL (2009) Optimization of an oil extraction process for algae from the treatment of manure effluent. Journal of the American Oil Chemists' Society 86: 909-915.

Nichols HW, Bold HC (1965) *Trichosarcina polymorpha* Gen. et Sp. Nov. J Phycol 1: 34-38.

Niederholtmeyer H, Wolfstadter BT, Savage DF, Silver PA, Way JC (2010) Engineering cyanobacteria to synthesize and export hydrophilic products. Applied and Environmental Microbiology 76: 3462-3466.

Razzak SA, Hossain NM, Lucky RA, Bassi AS, de Lasa H (2013) Integrated CO_2 capture, wastewater treatment and biofuel production by microalgae culturing—A review. Renewable and Sustainable Energy Reviews 27: 622-653.

Reddy HK, Muppaneni T, Rastegary J, Shirazi SA, Ghassemi A, Denga S (2013) Hydrothermal extraction and characterization of bio-crude oils from wet *Chlorella sorokiniana* and *Dunaliella tertiolecta*. Environmental Progress & Sustainable Energy 32: 910-915.

Ren L-J, Ji X-J, Huang H, Qu L, Feng Y, Tong Q-Q, Ouyang PK (2010) Development of a stepwise aeration control strategy for efficient docosahexaenoic acid production by *Schizochytrium* sp. Applied Microbiology and Biotechnology 87: 1649-1656.

Rogers JN, Rosenberg JN, Guzman BJ, Oh VH, Mimbela LE, Ghassemi A, Oyler GA, Betenbaugh MJ, Donohue MD (2013) A critical analysis of paddlewheel-driven raceway ponds for algal biofuel production at commercial scales. Algal Research 4:76-88.

Rosenberg JN, Kobayashi N, Barnes A, Noel EA, Betenbaugh MJ, Oyler GA. (2014) Comparative analyses of three *Chlorella* species in response to light and sugar reveal distinctive lipid accumulation patterns in C. sorokiniana. PLoS ONE, 9:e92460.

Rosenberg JN, Oyler GA, Wilkinson L, Betenbaugh MJ (2008) A green light for engineered algae: redirecting metabolism to fuel a biotechnology revolution. Current Opinion in Biotechnology 19: 430-436.

Scherholz ML, Curtis WR (2013) Achieving pH control in microalgal cultures through fed-batch addition of stoichiometrically-balanced growth media. BMC Biotechnology 13: 39.

Shaish A, Ben-Amotz A, Avron M (1992) Biosynthesis of beta-carotene in *Dunaliella*. Methods Enzymol 213: 439-444.

Singh R, Kaushik S, Wang Y, Xiang Y, Novak I, Komatsu M, et al. (2009) Autophagy regulates lipid metabolism. Nature 458: 1131-1135.

Sinha RA, Khare P, Rai A, Maurya SK, Pathak A, Mohan V, Nagar GK, et al. (2009) Anti-apoptotic role of omega-3-fatty acids in developing brain: perinatal hypothyroid rat cerebellum as apoptotic model. Int. J. Devl Neuroscience 27: 377-383.

Smith SR, Abbriano RM, Hildebrand M (2012) Comparative analysis of diatom genomes reveals substantial differences in the organization of carbon partitioning pathways. Algal Research 1: 2-16.

Stephens E, Ross IL, King Z, Mussgnug JH, Kruse O, Posten C, et al. (2010) An economic and technical evaluation of microalgal biofuels. Nature Biotechnology 28: 126-128.

Stephenson AL, Dennis JS, Howe CJ, Scott SA, Smith AG (2010) Influence of nitrogen-limitation regime on the production by *Chlorella vulgaris* of lipids for biodiesel feedstocks. Biofuels 1: 47-58.

Urzica EI, Vieler A, Hong-Hermesdorf A, Page MD, Casero D, Gallaher SD, Kropat J, Pellegrini M, Benning C, Merchant SS (2013) Remodeling of membrane lipids in iron-starved *Chlamydomonas*. J Biol Chem 288: 30246-30258.

Wada S, Ishida H, Izumi M, Yoshimoto K, Ohsumi Y, Mae T, Makino A (2009) Autophagy plays a role in chloroplast degradation during senescence in individually darkened leaves. Plant Physiology 149: 885-893.

Wan M-X, Wang R-M, Xia J-L, Rosenberg JN, Nie Z-Y, Kobayashi N, et al. (2012) Physiological evaluation of a new *Chlorella sorokiniana* isolate for its biomass production and lipid accumulation in photoautotrophic and heterotrophic cultures Biotechnology and Bioengineering 109: 1958-1964.

Wang ZT, Ullrich N, Joo S, Waffenschmidt S, Goodenough U (2009) Algal lipid bodies: stress induction, purification, and biochemical characterization in wild-type and starch-less *Chlamydomonas reinhardtii*. Eukaryot Cell 8: 1856-1868.

Xiong W, Liu L, Wu C, Yang C, Wu Q (2010) ^{13}C-tracer and gas chromatography-mass spectrometry analyses reveal metabolic flux distribution in the oleaginous microalga *Chlorella protothecoides*. Plant Physiol 154: 1001-1011.

Yan D, Lu Y, Chen Y-F, Wu Q (2011) Waste molasses alone displaces glucose-based medium for microalgal fermentation towards cost-saving biodiesel production. Bioresour Technol 102: 6487-6493

Yen H-W, Chang J-T (2013) A two-stage cultivation process for the growth enhancement of *Chlorella vulgaris*. Bioprocess Biosyst Eng 36: 1797-1801.

Zheng Y, Chi Z, Lucker B, Chen S (2012) Two-stage heterotrophic and phototrophic culture strategy for algal biomass and lipid production. Bioresource Technology 103: 484-488.

5

INTEGRATED ALGAL CULTIVATION WITH SYNTHETIC "LEAF" BIOREACTORS TO FACILITATE NUTRIENT TRANSITIONS

While the prior chapters have examined biochemical shifts in algal biomass during nutrient transitions, the research pursued in the remaining chapters of this dissertation is motivated by the physical challenges facing algae growth systems. Based on the technoeconomic analyses of algal biofuel pursued in Chapter 2, economically feasible large-scale microalgal cultivation is currently encumbered by water handling issues associated with growing and harvesting biomass from relatively dilute solutions. Alternative methods of cultivating and harvesting algal biomass have significant potential to improve some of the fundamental engineering issues related to recirculating ponds and can impact the overall sustainability of algal

biomass production. To this end, the conceptual basis for algal cell immobilization and harvesting using thin film reactors was formed. Just as the leaf is nature's best design for solar collection, retention of microalgae cells onto a membrane may serve as a more evolved format for algae growth. While adhesion-based PBRs are not a new concept, novel membrane-based support systems may have particular advantages for growth and harvesting by maximizing the surface area available for solar collection while reducing water requirements. Additionally, for two-stage bioprocessing, surface-bound algae could be readily switched between nutrient sources without resuspension and harvested without centrifugation.

In addition to leaves, natural photosynthetic biofilms are a source of inspiration for improved algal growth systems for biofuels and bioproducts. Aquatic microbial mats are some of the oldest known evidence of life on Earth— many 3,500 million year old fossils from shallow streambeds are textured with striated cyanobacteria. These pervasive and complex arrangements of microbial consortia are typified by functionally relevant spatial organization (photo- and heterotrophic; aerobic and anaerobic zones) as well as unique niche relationship and metabolite exchange between cyanobacteria, green algae, and bacteria and other heterotrophs. However, natural photosynthetic biofilms once thought to be robust have actually shown surprising fragility; thus, a robust mechanism of attachment may indeed be required to maintain the production longevity of bio-*film*-reactors used for industrial algae production. As an alternative to conventional microalgal cultivation in liquid suspension, desired production species of microalgae may be purposefully "tethered"

to a solid surface by protein-protein interaction. Toward this research objective, the development of a number of molecular and computational tools is described in Chapters 6. As an example, single-chain antibodies with high affinity for the surface of microalgal cells were generated and tested as species-specific binding agents. Furthermore, fluorescent biomarkers can be employed within natural biofilms to monitor synthetic combinations of adherent microbial communities and production strains of unicellular algae on a variety of membrane substrates. With these platforms technologies, detailed imaging and integrative analysis permits more refined studies spatial and temporal relationships within photosynthetic communities of algae and cyanobacteria (Chapters 7 and 8). The current chapter provides an introduction and conceptual basis for engineering such synthetic algal biofilms as well as a summary of the shortcomings of existing algal biofilm designs that motivated the continued study of protein-based adhesion of algal cells to membrane substrates.

5.1 Developing bio-inspired growth systems to reduce water & energy use

Over the past decade, considerable investment in research for advanced biofuels, biomass, and other bioproducts has moved the emerging algal biotechnology industry forward (Spolaore *et al.* 2006; Shenk *et al.* 2008; Specht *et al.* 2010). However, as both pilot- and commercial-scale algal production facilities continue to expand, the predominant cultivation vessel at these sites remains the raceway pond— first used to cultivate *Chlorella* in 1953 (Burlew) and refined by Oswald for wastewater treatment (1995). Since outdoor ponds can only support dilute suspensions of algae

(0.05% solids) and traditional closed photobioreactor designs are capable of only 1% solids (Borowitzka 1999), a departure from these archetypes can benefit from membrane-based growth systems of immobilized microalgae achieving 5-15% solids (Schnurr *et al.* 2013). A biomimetic assembly of photosynthetic cells on or within a flat surface, with likeness to the leaves of terrestrial plants, offers some advantages for solar collection compared to liquid cultures, which are limited by light penetration and necessitate considerable energy input for continuous operation (Rogers *et al.* 2014). Thin film architectures have the potential to reduce harvesting costs at large scales and provide well-controlled microenvironments suitable for basic phycological studies.

5.1.1 Prior approaches to immobilized microalgal cultivation

Advantages of membrane based growth strategies include high cell densities, efficient nutrient and light transfer, as well as the ease and economy of harvesting algae on the large membranes verses single cells. Immobilized microalgae cultivation systems have been previously evaluated for bioenergy applications using perfusion reactors; however, the capital cost of the polymer substrates was deemed to be uneconomical for biofuel production at the time (Ripin 1985). Nonetheless, examples of adherent bioreactor systems are available for the maintenance of extensive algal strain libraries (Nowack *et al.* 2005) and have been used to model mass transfer between the trophic zones of photosynthetic biofilms (Bernstein *et al.* 2014; Murphy & Berberoğlu 2014b). Furthermore, microalgae are routinely propagated on solid media (*e.g.*, 1.5% agar) and while most species thrive in this environment, the cells

would be easily disengaged from this surface by the shear force of flowing growth media (Ozkan & Berberoğlu 2013). Other approaches to algae immobilization range from elegantly engineered mesoporous glass scaffolds and chitosan mats (Jacobi *et al.* 2012; Eroglu *et al.* 2012) to more straightforward preparations of microalgae on cloth or paper surfaces typically seeded with a high cell density liquid inoculum (Johnson & Wen 2010). Alternatively, the natural attachment of benthic macroalgae has been used to assimilate agricultural runoff in open waters (Mulbry *et al.* 2010). Immobilized algal systems are also well suited for hydrogen evolution (Laurinavichene *et al.* 2008) and the secretion of volatile metabolites from microalgae has recently been realized through metabolic engineering (Lindberg *et al.* 2010; Bentley & Melis 2011). This feature of design-for-purpose organisms has been projected to have a positive impact on lifecycle analyses of algal biofuel production paths (Vasudevan *et al.* 2012) and, moreover, encourages the use of immobilized growth systems to prolong the retention of viable cells in order to exploit continuous secretion of molecular products. In addition to favorable exposure to light and routes for secretion, surface immobilization may offer more direct paths for gas exchange and mass transfer of nutrients.

Techniques of cellular immobilization for biofilm reactors have been pioneered with microalgae in biosensors, as bioatalysts in microbial fuels cells, and for the biological remediation of wastewater (Ferro *et al.* 2012). For heterotrophic bioremediation, biofilters comprised of natural bacterial biofilms on the surface of plastic pellets floating in airlift bioreactors are commonly used to effectively treat polluted liquid

permeates. The major difference between immobilized microalgal growth systems and adherent heterotrophic bioreactors stems from the inherent design requirement imposed on photobioreactors to allow sufficient light penetration to support photosynthetic activity. To this end, simple systems involving cloth sheets or filter paper have proved to be effective substrates for algal colonization without the need for any adhesives or other fixatives (Johnson & Wen 2010). The interdependence between light penetration, gas exchange, and water loss in these biofilm systems has also been studied in depth by Murphy *et al.* (2011a, 2011b, 2014a, 2014b). Furthermore, novel tools to directly quantify biomass productivity in both biofilm and suspension cultures has recently been developed, but not yet extensively used (Murphy *et al.* 2014c). At the upper limit of cell packing in photosynthetic biofilms, latex polymer coatings and other non-toxic adhesives have been used as "living paints" and reviewed extensively by Flickinger *et al.* (2007). While higher biological productivities can be achieved with this intensification of photosynthetic activity in surface density coatings containing more than 50% cells by volume (Bernal *et al.* 2014), the binding agents are a permanent method of entrapping cells and are not intended for biomass harvesting. Large-scale algal production for biofuels will require adhesion without substantial chemical additives that would not only contaminate harvested biomass, but also contribute additional cost to algal biofuel facility. Therefore a look toward adapting natural biofilms for biomass production is warranted.

5.2 Symbiosis and the potential fragility of naturally adherent microalgae

While prior examples of immobilized biofilm reactors have focused on monocultures of algae, co-cultures of photosynthetic microorganisms may pose a number of synergistic advantages. Microbial diversity in a photosynthetic biofilm can serve to more efficiently utilize resources such as carbon and nitrogen nutrients, but also the visible light spectrum. For example, complementary chromatic acclimation allows some cyanobacteria to shift their photosynthetically active pigments in response to light availability (Hirose *et al.* 2013). Co-cultures of green algae and cyanobacteria may, therefore, be able to utilize a broader spectrum of incident light for more effective biomass productivity. Many examples of symbiotic multi-organism consortia exist in nature, which perhaps indicates the evolutionary advantage of such systems. Collectively, the multifunctional nature of microbial consortia is apparent in the formation of natural biofilms, in which some organisms provide structural support while other stabilize the metabolic profile through nutrient exchange.

5.2.1 Microbial community organization and mutualism in nature

There are countless examples of organisms from different species, classes, or kingdoms living together to complete tasks that benefit both parties. As a relevant example, microalgae are known to provide energy and nutrients to coral reefs (Muscatine 1990). Similar scenarios are ubiquitous and indispensable for the survival of all organisms involved, which can provide mutual stability and resilience. Any multicellular organism is a system of differentiated cells working together as microscopic cogs in a vastly complex machine. Beyond the different polymorphs of

cells of the same genome, there are many other species working in concert with higher organism often performing essential tasks. As an example, there are more bacterial cells than mammalian cells in the human body. Even within a single cell, such multi-species symbiosis is apparent and essential. The eukaryotic algal cell embodies a microcosm of symbiosis as the product of endosymbiosis between prokaryotic phototrohps and heterotrophs (Tirichine & Bowler 2011). The repeated theme in all of these examples is that the sum of the system is far more powerful than any of its parts.

From a bioprocessing perspective, there are extensive opportunities to exploit these mutualistic relationships between algae, cyanobacteria, and other heterotrophic organisms and it is important to study the cultivation ecology of these systems. The synergistic nature of microbial consortia contributes to their stability by species interdependence (*e.g.*, certain algae rely on bacteria for vitamin B_{12}) (Croft *et al.* 2005). By understanding the growth characteristics and nutrient requirements of microalgae in concert with other organisms, the binary goal of nutrient remediation and biofuel production may be achieved. Conversely, the fragility of monoculture crops has been demonstrated by agriculture (*e.g.*, potato blight) (Gao & Bradeen 2010). Since the next battle of the agricultural revolution may be fought in the water rather than the field, microalgal production calls for a new generation of robust microbial networks and tools to understand their dynamic behavior (Hamilton 2014).

5.2.2 Exploiting natural biofilms for biomass production

By reaching beyond a simple monoculture model for algal production, the bioprocessing potential of biological systems can be dramatically enhanced when it is networked. Biofilms, as they exist in nature, involve incredibly diverse and dynamic species populations. Since cells continually slough off from the surface as they lose viability, the critical thickness of biofilms can range from microns to millimeters. While monocultures can still be introduced to naturally adherent biofilm substrata, this complexity does not always enhance biological resilience or help to achieve an engineering goal (*e.g.*, algal lipid production). In one exemplary study, initial biofilms formed by the natural deposition of microbes and extracellular polymeric substances from wastewater can provide a suitable attachment mechanism for monoculture of green algae or diatoms (SCHNURR *et al.* 2013). However, the resulting algal biofilms were not found to behave in accordance with corresponding suspension monocultures during periods of nutrient shifts. In response to intentional nitrogen deprivation to induce TAG production, the biofilms completely disengaged from the substrate (glass slide). Nutrient starvation may indeed offer a useful mechanism to *harvest* naturally adherent biofilms, the intended goal of lipid accumulation in these attached cultures was not achieved. Larger scale studies of algal biofilms cultivated from wastewater on rotating algae biofilm reactors (RABRs) employing cloth rope as a substrate for natural adhesion of polymicrobial communities of algae have reported similar results. While some reductions in biofilm thickness were observed at the onset of nitrogen deprivation as a result of cells sloughing off, the remaining biomass did not experience any lipid enhancement, perhaps due to the type of natural organisms that

dominated this biofilm population (Bernstein *et al.* 2014). In addition to confirming the unstable nature of natural biofilm adhesion and unsuitable characteristics for lipid production, this RABR study found that oxygen accumulation within photosynthetic biofilms can reduce photosynthetic performance. This result suggests that an optimal biofilm thickness on the order of 100 µm may prevent losses in productivity by allowing sufficient O_2 off-gassing.

While these attempts to exploit biofilms for biofuel production employ natural communities of photosynthetic algae, the lack of control over both stability of adherent cultures as well as their lipid profiles stem from insufficient characterization of their actual microbial composition. Since algal communities grown in open-air systems cannot be kept axenic, it is well understood that biomass composition is strongly affected by intruding organisms. These approaches toward incorporating natural biodiversity of adherent microbes aim to work within the context of the natural environment rather than against it, but may still require intentional mechanisms of binding. As depicted in Figure 25, there are both temporal and physical differences between natural biofilm formation and user-defined communities that must be examined. By studying monoculture biofilms in crop rotation and compared to year-round polycultures, a better understanding of "synthetic ecology" within industrial algal production systems may be achieved (Kazamia *et al.* 2012; Hamilton 2014; Carney *et al.,* 2014). Some conventional approaches to crop protection and biological control have proven effective at large scales (McBride *et al.* 2013), but lipid accumulation phenotypes certainly vary depending on trophic

conditions with interdependence between competing phototrophs and predators (Letcher *et al.* 2013). Future developments in this field may build upon synthetic biology tools for individual organisms by engineering mutualism or symbiosis between two or more organisms with a unique opportunity to engineer an expanded complexity of metabolism within microbial consortia (Zengler & Palsson 2012). Nonetheless, the advantages of unmodified two-dimensional "artificial leaf" growth strategies, including high cell densities, efficient nutrient and light transfer, and ease of harvesting, warrant continued exploration of these concepts with a particular focus on investigating the microbiology and proximity effects in these systems.

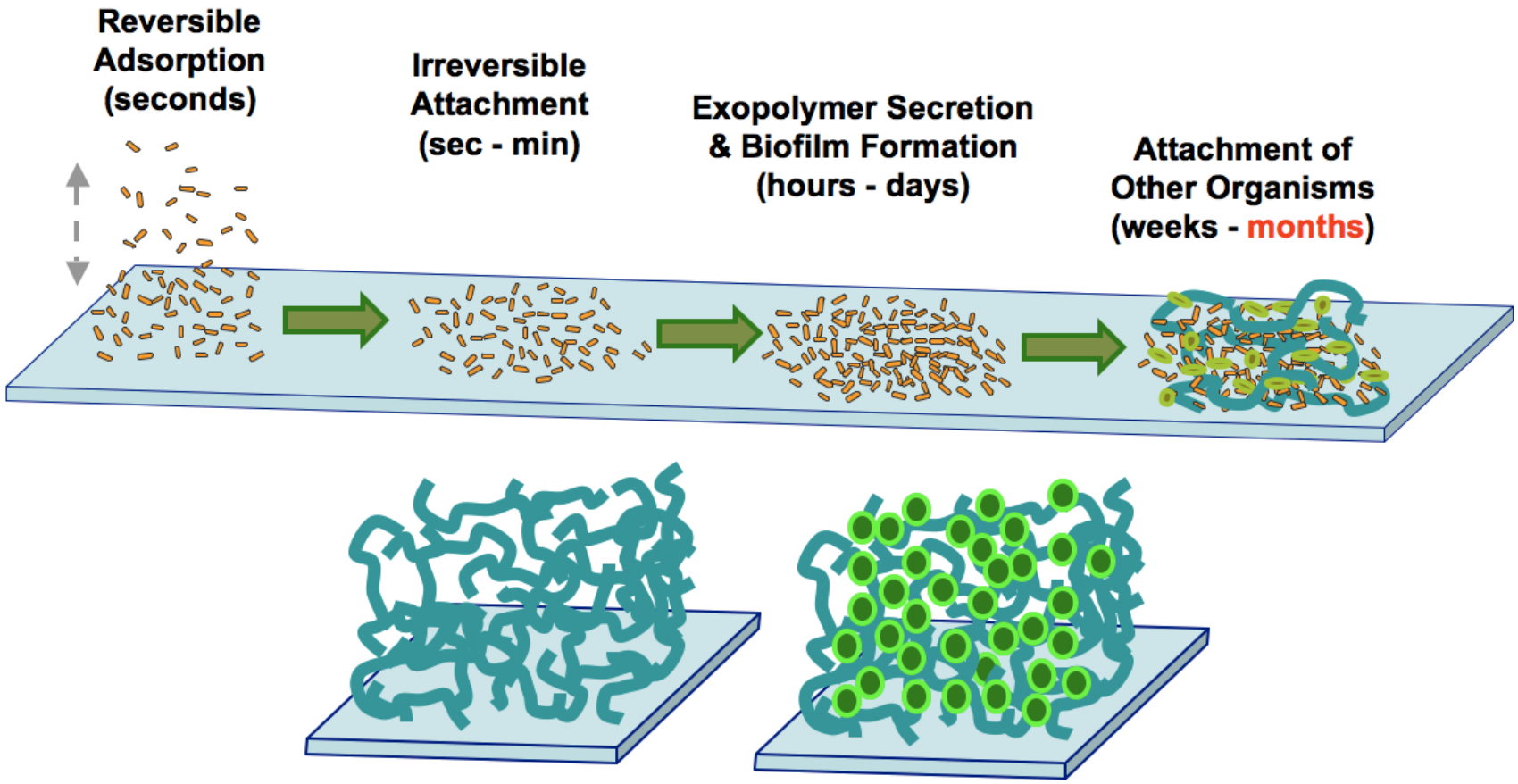

Figure 25. Natural mechanisms of polyculture biofilm formation compared to a scaffold-supported design. While the natural colonization of a flat surface with a polymicrobial biofilms can require extended periods of time to develop a mature community structure **(top)**, filamentous cyanobacteria may be immobilized first, in order to act a suitable matrix structure and promote the retention of unicellular microalgae with desired production qualities (bottom).

5.3 Toward assisted mechanisms of biofilm attachment

Based on the unpredictable nature of natural biofilms, approaches to mediate or stabilize surface interaction between polycultures and solid substrates may be necessary for adherent algal cultures to achieve their full production potential. For example, the natural process of polymicrobial biofilm formation depicted in Figure 25 not only occurs over long time scales, but the longevity of the established community has also been demonstrated to be transient (Schnurr *et al.* 2013). At the sub-micron level, thermodynamic relationships between different algal species and biofilm substrates also reveal significant variation in the inherent attractive (or repulsive) interactions with respect to surface potentials (Ozkan & Berberoğlu 2013). Collectively, prior literature has led to the conceptual development of a hybrid approach to initiating microbial biofilm formation. This approach takes advantage of the structural properties of cyanobacterial biofilms while also dictating stable attachment to a membrane substrate. Furthermore, cyanobacteria and other microbes can effectively form a matrix, in which a monoculture of a production strain can be implanted. The ultimate morphology of this living scaffold has similar properties as an actual leaf, comprised of a hemicellulose matrix to hold an assembly of individual photosynthetic cells (Griffiths & Helliker 2013).

Developing mechanisms of synthetic biofilm formation on a flat surface as opposed to a rough or porous medium may also be more similar to the natural environments that photosynthetic biofilms encounter in nature— commonly coating flat surfaces such as stones in stream beds and the hulls of boats. In this configuration, a flat

morphology can serve as the foundation for monolayers of tightly packed cells to maximize solar utilization for applications in secretion (a non-growing system), but can also allow certain algal species to extend from the surface by producing successive multilayers that remain tethered to the fixed monolayer (a growing system). In either case, the attachment of microalgal cells on a well-defined surface will enable researchers to probe the fate of single cells in biofilm environments and better understand population dynamics in algal co-cultures. While a long-term goal would be to create a scalable architecture for algal cultivation with more effective provisioning of water and energy resources, bench-scale models can allow critical time- and length-scales to be characterized further in these microbial ecosystems.

As described in the next chapters, antibodies with species-specific binding capabilities may offer a unique opportunity for selective retention of microalgal cells, but conventional monoclonal antibodies are most certainly cost prohibitive for industrial algae applications. While single-chain antibodies may offer some advantages with their smaller molecular weight and ease of production in microbial platforms (Jiang *et al.* 2013), other proteins with *non*-specific cell binding capacities may also serve as suitable binding agents. Regardless of the protein mediator, a dedicated mechanism of adhesion without the permanent entrapment may allow natural biofilms to be more successfully transitioned between nutrient regimes and more effectively harvested. These systems can serve as models to engage monocultures of algal biofilms and to explore the symbioses present in polycultures in order to more effectively capture and transform sunlight into bioenergy.

5.4 References

Bar-Zeev E, Berman-Franka I, Girshevitzb O, Bermanc T (2012) Revised paradigm of aquatic biofilm formation facilitated by microgel transparent exopolymer particles. Proc Natl Acad Sci USA. 109: 9119-9124.

Bentley HK, Melis A (2011) Diffusion-based process for carbon dioxide uptake and isoprene emission in gaseous/aqueous two-phase photobioreactors by photosynthetic microorganisms. Biotechnology & Bioengineering 109: 100-109.

Bernal OI, Mooney CB, Flickinger MC (2014) Specific photosynthetic rate enhancement by cyanobacteria coated onto paper enables engineering of highly reactive cellular biocomposite "leaves". Biotechnol Bioeng 111: 1993-2008.

Bernstein HC, Kesaano M, Moll K, Smith T, Gerlach R, Carlson R, et al. (2014) Direct measurement and characterization of active photosynthesis zones inside wastewater remediating and biofuel producing microalgal biofilms. Bioresource Technology 156: 206-215.

Blankenship RE, Tiede DM, Barber J, Brudvig GW, Fleming G, et al. (2011) Comparing photosynthetic and photovoltaic efficiencies and recognizing the potential for improvement. Science. 332: 805-809.

Borowitzka BA (1999) Commercial production of microalgae: ponds, tanks, tubes and fermenters. J Biotechnol 70: 313-321.

Brenner K, Arnold FH (2011) Self-organization, layered structure, and aggregation enhance persistence of a synthetic biofilm consortium. PLoS ONE 6: e16791.

Burlew JS (1953) *Algal Culture from Laboratory to Pilot Plant.* Carnegie Institution of Washington: Washington DC.

Carney LT, Reinsch SS, Lane PD, Solberg OD, Jansen LS, Williams KP, Trent JD, Lane TW (2014) Microbiome analysis of a microalgal mass culture growing in municipal wastewater in a prototype OMEGA photobioreactor. Algal Research. 4, 52-61.

Croft MT, Lawrence AD, Raux-Deery E, Warren MJ, Smith AG (2005) Algae acquire vitamin B_{12} through a symbiotic relationship with bacteria. Nature Letters. 438: 90-93.

Davey ME, O'Toole GA (2000) Microbial biofilms: from ecology to molecular genetics. Microbiology and Molecular Biology Reviews. 64: 847-867.

Eroglu E, Agarwal V, Bradshaw M, Chen X, Smith SM, Raston CL, Iyer KS (2012) Nitrate removal from liquid effluents using microalgae immobilized on chitosan nanofiber mats. Green Chemistry. 14:2682–2685.

Evans JR, Von Caemmerer S (1996) Carbon dioxide diffusion inside leaves. Plant Physiol. 110: 339-346.

Ferro Y, Perullini M, Jobbagy M, Bilmes SA, Durrieu C (2012) Development of a biosensor for environmental monitoring based on microalgae immobilized in silica hydrogels. Sensors 12: 16879-16891.

Flickinger MC, Schottel JL, Bond DR, Aksan A, Scriven LE (2007) Painting and printing living bacteria: engineering nanoporous biocatalytic coatings to preserve microbial viability and intensify reactivity. Biotechnology Progress 23: 2-17.

Gao L, Bradeen JM (2010) Organ-specific disease resistance phenotypes in transgenic potato correlate with R gene dosage and transcription and defense response gene expression dynamics. Presented at the Plant and Animal Genome XVIII Conference, San Diego, CA.

Griffiths H, Helliker BR (2013) Mesophyll conductance: internal insights of leaf carbon exchange. Plant, Cell and Environment 36: 733-735.

Hamilton C (2014) Exploring the utilization of complex algal communities to address algal pond crash and increase annual biomass production for algal biofuels. U.S. Department of Energy. BETO Report DOE/EE-1059.

Hansen SK, Rainey PB, Haagensen JAJ, Molin S (2007) Evolution of species interactions in a biofilm community. Nature. 445: 533-536.

Hertel B, Tayefeh S, Mehmel M, Kast SM, Van Etten J, Moroni A, Thiel G (2006) Elongation of outer transmembrane domain alters function of miniature K+ channel K_{cv}. J Membr Biol. 210: 21-29.

Hirose Y, Rockwell NC, Nishiyama K, Narikawa R, Ukaji Y, Inomata K, et al. (2013) Green/red cyanobacteriochromes regulate complementary chromatic acclimation via a protochromic photocycle. Proc Natl Acad Sci USA 110: 4974-4979.

Jacobi A, Bucharsky EC, Schell KG, Habisreuther P, Oberacker R, Hoffmann MJ, et al. (2012) The application of transparent glass sponges for improvement of light distribution in photobioreactors. J Bioprocess Biotechniq 2:113.

Jiang WZ, Rosenberg JN, Wauchope AD, Tremblay JM, Shoemaker CB, Weeks DP, Oyler GA (2013) Generation of a phage display library of single-domain camelid V_HH antibodies directed against *Chlamydomonas reinhardtii* antigens and characterization of V_HHs binding cell surface antigens. Plant J 76: 709-717.

Johnson MB, Wen Z (2010) Development of an attached microalgal growth system for biofuel production. Appl Microbiol Biotechnol 85: 525-534.

Kazamia E, Aldridge DC, Smith AG (2012) Synthetic ecology – A way forward for sustainable algal biofuel production? Journal of Biotechnology 162, 163–169.

Laurinavichene TV, Kosourov SN, Ghirardi ML, Seibert M, Tsygankov AA (2008) Prolongation of H_2 photoproduction by immobilized, sulfur-limited *Chlamydomonas reinhardtii* cultures. Journal of Biotechnology 134: 275-277.

Letcher PM, Lopez S, Schmieder R, Lee PA, Behnke C, Powell MJ, McBride RC. (2013) Characterization of *Amoeboaphelidium protococcarum*, an algal parasite new to the Cryptomycota isolated from and outdoor algal pond used for the production biofuel. PLoS ONE 8(2), e56232.

Lindberg P, Park S, Melis A. (2010) Engineering a platform for photosynthetic isoprene production in cyanobacteria using *Synechocystis* as the model organism. Metabolic Engineering 12: 70-79.

McBride R, Behnke C, Botsch K, Heaps N, Meenach C (2013) Use of fungicides in liquid systems. PCT/US2012/060120, WO/2013056166.

Mulbry W, Kangas P, Kondrad S (2010) Toward scrubbing the bay: Nutrient removal using small algal turf scrubbers on Chesapeake Bay tributaries Ecological Engineering. 36: 536-541.

Murphy TE, Berberoğlu H (2011a) Effect of algae pigmentation on photobioreactor productivity and scale-up: A light transfer perspective. Journal of Quantitative Spectroscopy and Radiative Transfer 112: 2826-2834.

Murphy TE, Berberoğlu H (2011b) Temperature fluctuation and evaporative loss rate in an algae biofilm photobioreactor J. Sol. Energy Eng. 134: 011002.

Murphy TE, Berberoğlu H (2014b) Flux balancing of light and nutrients in a biofilm photobioreactor for maximizing photosynthetic productivity Issue Biotechnology Progress 30: 348-359.

Murphy TE, Fleming E, Berberoğlu H (2014a) Vascular structure design of an artificial tree for microbial cell cultivation and biofuel production. Transport in Porous Media 104: 25-41.

Murphy TE, Macon K, Berberoğlu H (2014c) Rapid algal culture diagnostics for open ponds using multispectral image analysis. Biotechnol Prog 30: 233-240.

Muscatine, L (1990) The role of symbiotic algae in carbon and energy flux in reef corals. Ecosystems of the World 25: 75-87.

Nowack ECM, Podola B, Melkonian M (2005) The 96-well twin-layer system: a novel approach in the cultivation of microalgae. Protist 156: 239-251.

Oswald WJ (1995) Ponds in the twenty-first century. Wat Sci Tech 31: 1-8.

Ozkan A, Berberoğlu H (2013) Adhesion of algal cells to surfaces, Biofouling: The Journal of Bioadhesion and Biofilm Research, 29: 469-482.

Ozkan A, Kinney K, Katz L, Berberoğlu H (2012) Reduction of water and energy requirement of algae cultivation using an algae biofilm photobioreactor. Bioresource Technology. 114: 542-548.

Plugge, B, Gazzarrini S, Nelson M, Cerana R, Van Etten JL, Derst C, DiFrancesco D, Moroni A, Thiel G (2000) A potassium channel protein encoded by *Chlorella virus* PBCV-1. Science. 287:1641–1644.

Rasala BA, Barrera D, Ng J, Plucinak TM, Rosenberg JN, Weeks DP, Oyler GA, Peterson T, Haerizadeh F, Mayfield SM (2013) Expanding the spectral palette of fluorescent proteins for the green microalga *Chlamydomonas reinhardtii*. The Plant Journal 74: 545-556.

Ripin MJ (1985) Evaluation of immobilized cell systems for the production of fuels from microalgae. In Aquatic Species Program Review: Proceedings of the March 1985 Principal Investigators Meeting. Report No. SERI/CP-231-2700. 336-348.

Rogers JN, Rosenberg JN, Guzman BJ, Oh VH, Mimbela LE, et al. (2014) A critical analysis of paddlewheel-driven raceway ponds for algal biofuel production at commercial scales. Algal Res 4: 76-88.

Schnurr PJ, Espie GS, Allen DG (2013) Algae biofilm growth and the potential to stimulate lipid accumulation through nutrient starvation. Biores Technol, 136: 337-344.

Shenk PM, Thomas-Hall SR, Stephens E, Marx UC, Mussgnug JH, Posten C, Kruse O, Hankamer B (2008) Second generation biofuels: high-efficiency microalgae for biodiesel production. Bioenerg Res, 1:20-43.

Singh G, Thomas PB (2012) Nutrient removal from membrane bioreactor permeate using microalgae and in a microalgae membrane photoreactor. Bioresource Technology. 117: 80-85.

Singh SP, Montgomery BL (2013) Salinity impacts photosynthetic pigmentation and cellular morphology changes by distinct mechanisms in *Fremyella diplosiphon*. Biochem Biophys Res Commun. 433: 84-89.

Specht E, Miyake-Stoner S, Mayfield S (2010) Micro-algae come of age as a platform for recombinant protein production. Biotechnol Lett 32: 1373-83.

Spolaore P, Joannis-Cassan C, Duran E, Isambert A (2006) Commercial applications of microalgae. J Biosci Bioeng 101: 87-96.

Subashchandrabose SR, Ramakrishnana B, Megharaja M, Venkateswarlua K, Naidua R (2011) Consortia of cyanobacteria/microalgae and bacteria: biotechnological potential. Biotechnology Advances 29: 896-907.

The Genome Institute (2011) *Fremyella diplosiphon* genome sequencing project. *Tolypothrix* sp. PCC7601 = UTEX B481. Accessed 17 June 2013. Available: http://www.ncbi.nlm.nih.gov/bioproject/72337

Tirichine L, Bowler C (2011) Decoding algal genomes: tracing back the history of photosynthetic life on Earth. Plant J. 66: 45-57.

Vasudevan V, Stratton RW, Pearlson MN, Jersey GR, Beyene AG, et al. (2012) Environmental performance of algal biofuel technology options. Environ Sci Technol 46: 2451-2459.

Zengler K, and Palsson BO (2012) A road map for the development of community systems (CoSy) biology. 10, 366-372.

Zhu X-G, Long SP, Ort DR (2008) What is the maximum efficiency with which photosynthesis can convert solar energy into biomass? Curr Opin Biotechnol. 19: 153-159.

6

ADVANCES IN MOLECULAR AND COMPUTATIONAL TOOLS TO MONITOR MICROALGAL COMMUNITY DEVELOPMENT[§]

Since microalgae are versatile production platforms for biomanufacturing, many different species have been characterized for specific product applcations (Sheehan *et al.*, 1998; Rodolfi *et al.*, 2009; Griffiths and Harrison, 2009; Li *et al.*, 2011; Liu *et al.*, 2011; Vazhappilly and Chen, 1998). Natural organisms have the potential to contribute substantially to the nutrition, health, and biofuel sectors owing to their photosynthetic capacity and biodiversity. However, some hypothesize that we have reached the limit of naturally occurring traits and further bioprospecting efforts will

[§] This chapter contains figures from papers published by Rasala *et al.* (2013) and Jiang, Rosenberg *et al.* (2013) that both appeared in *The Plant Journal* as well as a publication by Barrera, Rosenberg *et al.* (2014) in the *Plant Biotechnology Journal*. Portions of these works are reprinted here with permission from the publishers (Appendix A).

not yield meaningful results in a timely manner (Gressel 2008), particularly for biofuel production. Others even claim that natural variation and recombination of traits accessible in agriculture by means of cross-breeding will be exhausted by 2050 (Sayre 2014). In direct response to this bottleneck, the ability to manipulate genomes with molecular genetic tools may open the door to previously unattainable traits. However, the accelerating field of algal biotechnology is still faced with a lack of mature technologies to manipulate the microalgal cell with ease. Genetic transformation is currently limited to a small set of algal species and, thus, routine biomolecular engineering has yet to be fully realized with production organisms (Hallman 2007).

Beyond the lab bench, molecular and computational tools can also play a role in manipulating and improving algal cultivation throughout scale-up and production. Applying genetic intervention to strain development can provide opportunities to regulate growth characteristics, maintain culture integrity, increase harvesting efficiency, and probe shifts in cellular metabolism. A major focus of genetic improvement efforts has been to engineer strain dominance. Alternatively, preventative measures against inevitable intrusion of wild contaminant organisms in open algal ponds may employ *extracellular* control using small molecules or regimented culture conditions to change the trajectory of algal cultures. Furthermore, flow cytometric methods can help to diagnose contamination in real-time (Day *et al.* 2012) and may benefit from improved accuracy by coupling sorting

methods with protein recognition tools, such as antibodies, that are specific to production organisms or contaminant microbes.

In order to complement these biological approaches to understanding microalgal population dynamics, computational methods to deconvolute large data sets and interpret meaning from various metrics of culture health will serve as important tools. While common microbiological procedures for approximating cell concentrations in liquid culture are applicable to microalgae, the variety of growth systems pose certain constraints on sample evaluation. For example, biofilm-based reactors require different methods of evaluating biological productivity, as described in the previous chapter. This chapter reviews recent advances in molecular genetic tools for algae and the development of computational approaches to characterize the ecology of microalgal populations in both liquid and biofilm cultures.

6.1 Obstacles to genetic engineering of microalgae

The cell biology of eukaryotic microalgae present a number of challenges that have hampered routine genetic engineering. In addition to the complexity of nuclear transgene regulation, the biodiversity exhibited between potential production organisms makes it difficult to develop genetic tools that are applicable to many species. As an example, *Chlamydomonas reinhardtii* has been long utilized for the study of flagellar motion and photosynthetic function. The development of a variety of selectable genetic markers and basic reporter gene systems has made stable chloroplast and nuclear transformation possible with this alga (Franklin & Mayfield 2004; Lumbreras *et al.* 1998; Sizova *et al.* 2001). Although the

chloroplast genome is generally amenable to homologous genetic recombination and protein overexpression, its ability to affect cellular functions within other organelles is restricted. Alternatively, nuclear genetic engineering can produce useful transformants, but high-level expression and soluble accumulation of recombinant proteins is not always achieved due to random chromosomal integration of vectors and propensity for transgene silencing (Neupert *et al.* 2009).

While *C. reinhardtii* is experimentally tractable thanks to a growing repertoire of molecular and computational tool set (Fuhrmann *et al.* 2002; Grossman *et al.* 2003), a set of robust and reliable molecular genetic tools to engineer and visualize its full biomolecular inventory would greatly enhance the resolution at which intracellular events can be perceived. To the extent that a fully mapped genome can help predict metabolism, the ability to track and redesign biosynthetic pathways is necessary to fully realize the research and commercial potential of this and other algal organisms.

6.2 Toward the robust expression of a suite of fluorescent proteins

In order to improve expression levels of nuclear transgenes in microalgae, a number of approaches have focused on limiting the cells' natural mechanisms of inhibiting foreign DNA expression, thus preventing transgene silencing (Neupert *et al.* 2009; Oyler & Rosenberg 2010). In addition to influencing epigenetic factors that may contribute to poor expression in *C. reinhardtii*, recent approaches to high-level nuclear expression have taken advantage of the well-characterized foot-and-mouth-disease-virus (FMDV) 2A self-cleavage sequence. The 2A peptide is commonly used

in other eukaryotic cell types to generate two separate proteins from a single mRNA transcript. During translation, the 2A sequence causes an error in ribosomal function, resulting in premature cleavage of the protein product. Unlike an internal stop codon, by which the remaining open reading frame may not be fully translated, 2A allows for continued elongation of a separate peptide from the same mRNA. The short 20 amino acid sequence encoded by the FMDV 2A sequence has been investigated extensively and successfully adapted to *C. reinhardtii* (Plucinak 2013).

Furthermore, by linking trangene expression to an antibiotic resistance gene, the use of 2A ensures that high-level expression of the selectable marker (required for survival in the presence of antibiotic) is coupled with expression of the gene of interest (GOI). In particular, antibiotic or herbicide resistance genes that act in stoichiometric equivalent to their substrates rather than enzymatically, such as bleomycin (*ble* gene), require high levels of expression to survive against selective pressure. Consequently, this approach also increases the number of positive transformants that can be reliably recovered by selection since GOI expression and antibiotic resistant are functionally linked. Collectively, these advantageous qualities of 2A were employed to drive the overexpression of an industrially relevant enzyme in nucleus of *C. reinhardtii*. In this example, Rasala *et al.* demonstrated roughly 100-fold increases in functional xylanase (*xyl1*) production with a *ble*-2A-*xyl1* expression construct (Rasala *et al.* 2012). This same strategy was applied to a compendium of fluorescent proteins (XFPs) to enable the first example of robust accumulation and visualization of nuclear expressed fluorescent probes in *C. reinhardtii* (Rasala *et al.*

2013). By codon optimizing the full spectrum of fluorescent colors (blue mTagBFP, cyan mCerulean, green CrGFP, yellow Venus, orange tdTomato, and red mCherry), each product of the *ble*-2A-*XFP* vector was detectable in living cells (Figure 26). When expressed in the cytoplasm, these fluorescent markers illuminate whole cells, which may have useful applications in cell tracking and population dynamics of microalgal communities (Figure 27). Rasala *et al.* further demonstrated that these fluorescent proteins can be fused with endogenous genes, such as tubulin, or organelle targeting sequences to achieve subcellular localization (Rasala *et al.* 2014). While these constructs are codon optimized for expression in *C. reinhardtii*, the same strategy of coupling the expression of a selectable trait (*i.e.*, antibiotic resistance) with a gene of interest could be applied to other organisms.

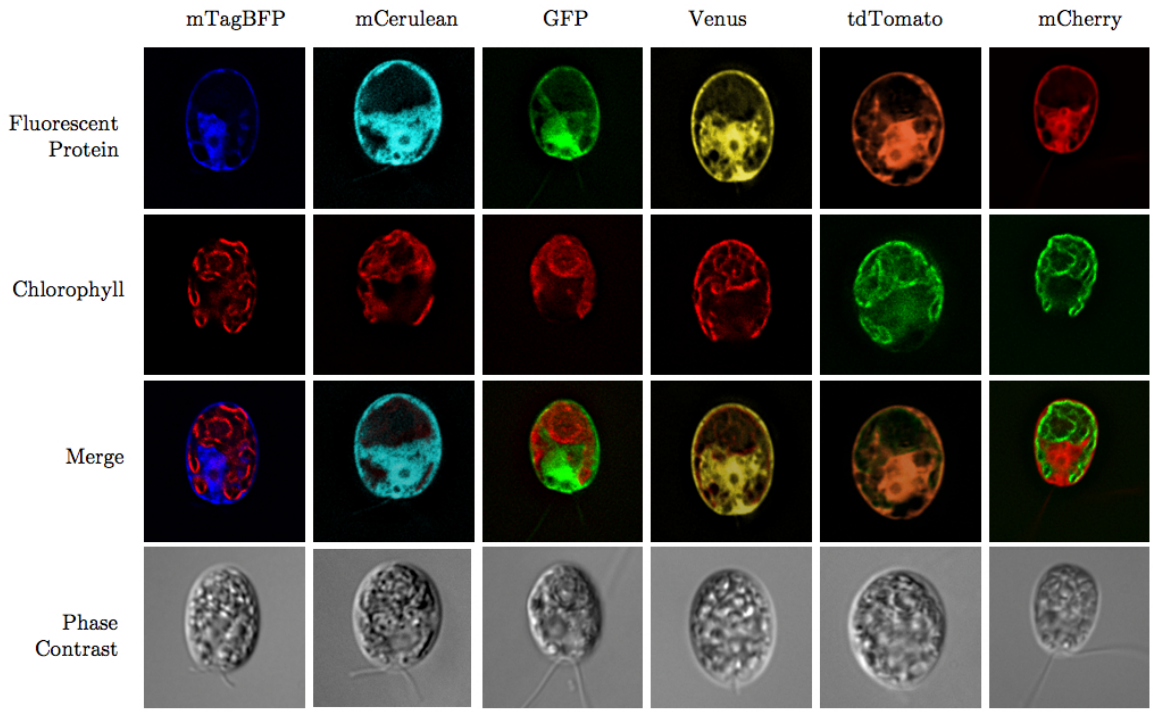

Figure 26. Complete set of fluorescent proteins expressed by *C. reinhardtii*. This panel of live cell images shows the well-expressed, soluble fluorescent proteins localized in the cytoplasm (top row) compared to the chlorophyll autofluorescence, merged channels, and phase contrast micrographs. Confocal images courtesy of Mayfield Lab (UC-San Diego) and reprinted here with permission from *The Plant Journal* (Appendix A).

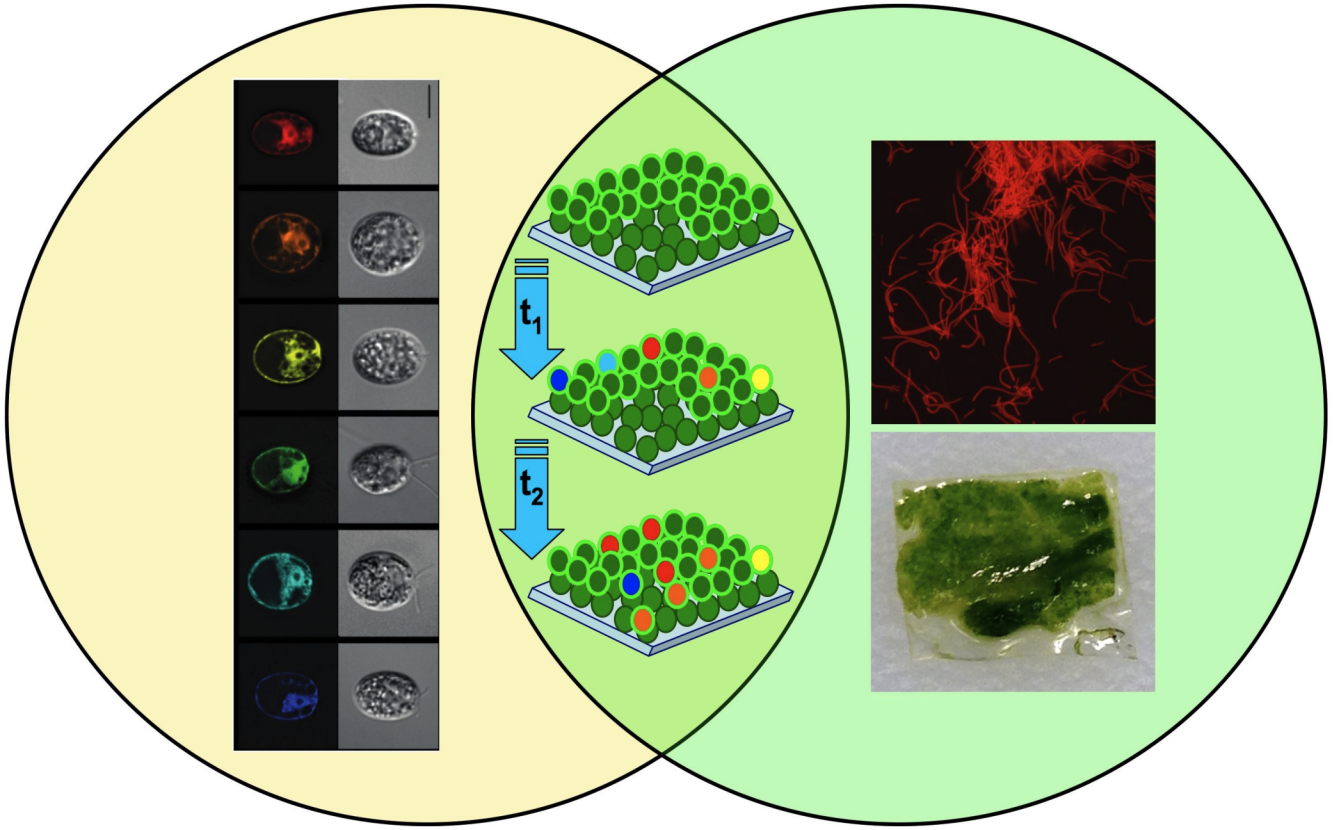

Figure 27. Fertile ground between the cellular and microbial consortium levels. The fate of singe cells within the microbial ecology of photosynthetic biofilm communities may be elucidated by tracking fluorescent cells as biomarkers. Confocal images courtesy of Mayfield Lab (UC-San Diego) and reprinted here with permission from *The Plant Journal* (Appendix A).

6.3 Utility of high-affinity protein binding tools in algal biotechnology

While continual advancements in the understanding of algal genetics has enabled more effective approaches to cellular engineering, the *proteome* of microalgae remains a largely unexploited resource. The potential for antibody fragments to strongly bind algal proteins presents expansive opportunities for basic and applied research tools as well as for commercial applications. As an example, antibodies that recognize specific cell surface antigens associated with particular cancers have been valuable to the medical community as both immunological assays and clinical detection in the body. The same principle could be applied to microalgal cells, not only to determine the presence of invasive species in open culture as a "synthetic immune system," but also to potentially immobilize microalgal cells. These applications will be particularly useful when the desired production algal organism must be grown in the presence of high surrounding contaminant microbes, such as wastewater (Figure 28A). Furthermore, surface-binding antibodies may facilitate rapid algae culture diagnostics and bioprospecting (Figure 28C).

In addition to macroscopic manipulation of algal biomass (*i.e.*, growth, harvesting, species recognition), these antibodies also lend themselves to the interrogation of algal cell biology (Rothbauer *et al.* 2006). Beyond the fluorescent detection reagents for subcellular tracking demonstrated by Rasala *et al.* (2012-2014), antibody-based technologies can serve to knock out specific enzymes as part of an overall synthetic biology approach to microalgae (Figure 28B). In response to environmental cues, proteins and other biomolecules are continually recycled and regenerated within the

cell by degradation and biosynthesis. In this process, cellular proteins are 'flagged' for degradation by the attachment of polyubiquitin chains through the action of ubiquitin ligase enzymes. Recently, it has become possible to hijack this natural process and use it as a means to specifically target cellular proteins for accelerated destruction (Kuo *et al.* 2011; Caussinus *et al.* 2012) by employing a chimeric protein in which one domain binds tightly to the target protein and the second domain promotes polyubiquitination of the bound target protein. Therefore, algae-specific antibodies fused to ubiquitin ligase proteins may effectively degrade target proteins for applications ranging from simple protein knockdowns to advanced metabolic engineering.

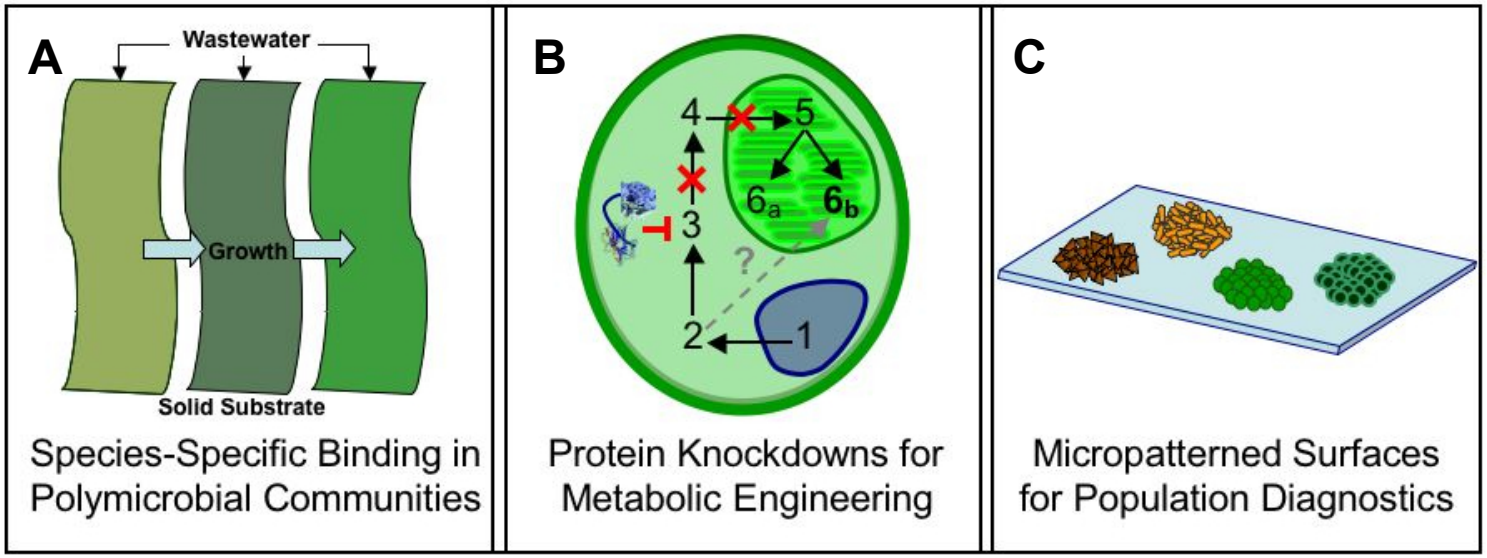

Figure 28. Applications of protein binding domains for algal research and development. Conceivable embodiments of this technology may benefit algal biotechnology by **(A)** mediating the growth of microalgae on membrane surfaces **(B)** intervening in metabolic pathways for cellular engineering and **(C)** enabling species-specific recognition of *external* algal cell surface proteins for culture diagnostics and bioprospecting.

6.3.1 Advantages of single-chain camelid antibodies

In order to meet the low-cost requirements for mass-produced algae applications, conventional antibodies are inappropriate for this approach. As an alternative to typical animal hosts, camelid animals (*e.g.*, camels, llamas, alpacas) as well as cartilaginous fish (*e.g.*, sharks) produce a class of functional antibodies that, unlike conventional antibodies, lack light chains. Therefore, the variable region of these antibodies (antigen binding domain) is comprised of the heavy chain only. These variable heavy chain domains (V_HHs) are able to bind to antigen targets and the encoding genes can readily be cloned and expressed in microbes to yield soluble protein. V_HHs are small (~12 kDa), easy to produce, and generally more stable than conventional antibody fragments. Furthermore, due to their small size, they are often found to have unusual antigen specificities with an improved propensity for binding conformational epitopes on the interstitial surfaces of multimeric proteins and active sites of enzymes. Because of their remarkable properties of subnanomolar affinity and rapid refolding after denaturation, they have become widely used in research and show clear commercial potential (Saerens *et al.* 2008).

Camelid antibodies can be generated with a high degree of specificity for microorganisms and the ability to screen for desired V_HHs by phage display in a high throughput manner is also extremely advantageous. As depicted in Figure 29, animal host-assisted generation of these antibodies by affinity maturation leads to sizable libraries with large complexity, high integrity, and generally good antigenic representation. Specifically, immunization of alpacas with algae protein lysates and

natural affinity maturation of novel V_HHs is followed by DNA amplification from peripheral blood lymphocytes. The V_HH encoding regions are cloned into a phage display platform and can then be panned against target epitopes of interest using the phage library (Maass *et al.* 2007). For a library generated using whole cell lysates, each of the intracellular and extracellular proteins that constitute the cell, there will have a corresponding V_HH; thus, the variety of applications for biotechnology can be fairly expansive and the type of binding agents recovered will be dictated by the panning procedure. As an example, Figure 29 shows panning against whole algal cells to recover surface-binding V_HHs that may act as a tether to promote adhesion of algae to a substrate of interest and/or a bridge between algal cells for collection. Due to the unique surface morphology of each algal species, antibodies specific to algal cell wall proteins may be able to adhere algae on membrane growth systems and function as novel bioflocculation agents (Figure 30).

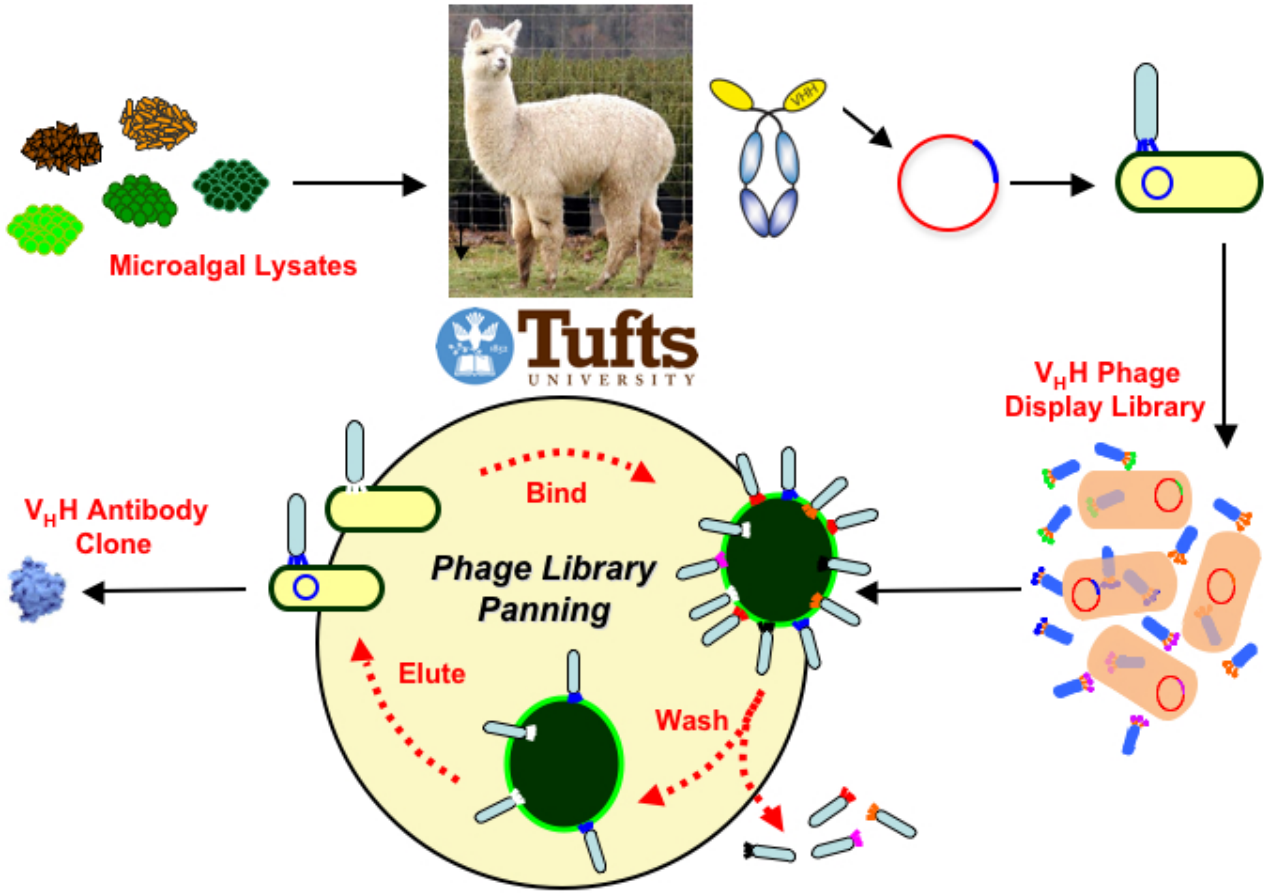

Figure 29. Schematic overview of camelid antibody generation and library panning. After immunizing alpacas with cell lysates, a phage display library can be constructed and panned against target antigens within roughly 4-6 months. Figure adapted from Jiang, Rosenberg *et al.* (2013) and reprinted here with permission from the publisher (Appendix A).

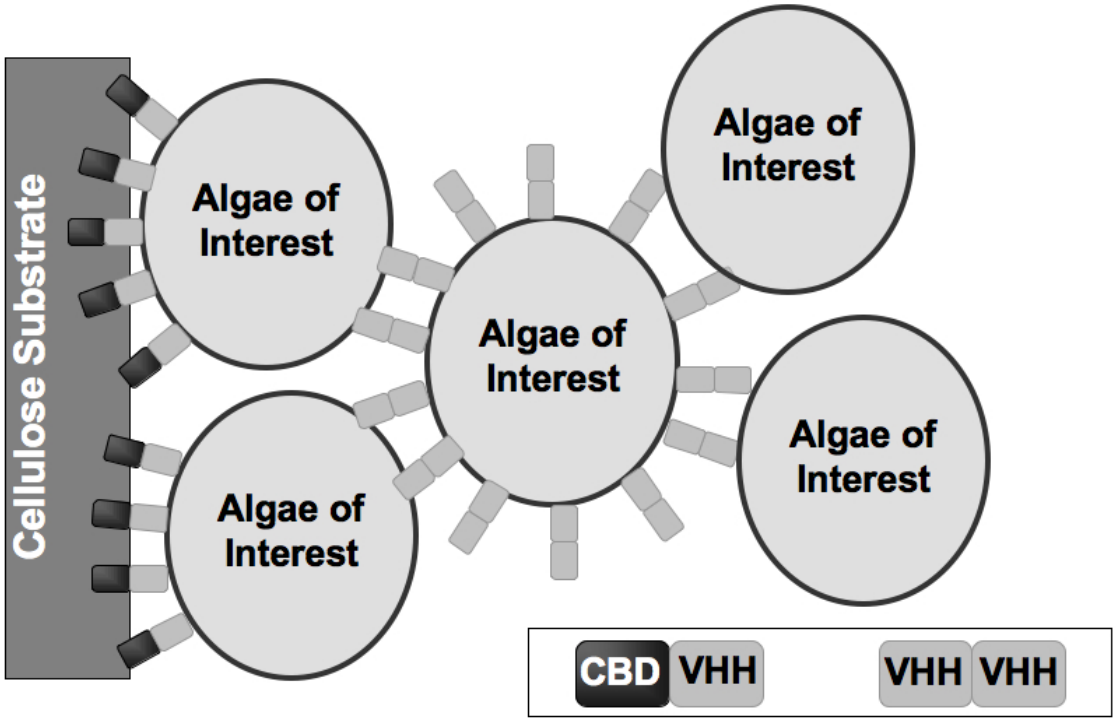

Figure 30. Potential membrane binding applications of V_HHs for algal biotechnology. Possible orientations are shown above employing dimeric protein fusions of an algae-specific V_HH with a cellulose-binding domain (CBD) for membrane substrate binding (Oyler *et al.* 2012).

6.3.2 Recent examples of single-chain antibody applications with algae

Since tools to manipulate microalgae at the protein level remain underdeveloped, a single-chain antibody library was generated against a set of algal organisms. This compendium of V_HHs specific to microalgae will hopefully serve as a useful protein toolkit both to facilitate academic pursuits and impact the feasibility of algae production for food, fuel, and potential high-value coproducts. As a proof of concept of the library's utility, as well as a step toward algal cull immobilization, surface-binding V_HHs were recovered using the previously described panning procedures against intact algal cells. Five commercially relevant and academically important microalgal species were used for this procedure: *Chlamydomonas reinhardtii* UTEX 2244, *Chlorella variabilis* NC64A, *Coccomyxa subellipsoidea* C-169, *Nannochloropsis oceanica* OZ-1, and *Thalassiosira pseudonana* CMMP 1335. The resulting V_HH library created for these algae likely contains numerous unique V_HHs for each of the proteins that constitute the algal cell. This section specifically describes some of the *C. reinhardtii* surface-binding V_HHs that were characterized in depth both by binding affinity and visual distribution on the cell surface.

Species-specific cell wall binding: just scratching the surface

Due to the unique surface morphology of each algal species, the first objective was to characterize V_HHs that are specific to algal cell walls. For example, *Chlamydomonas* species exhibit a hydroxyproteogylcan-rich exterior, while *Chlorella, Coccomyxa* and *Nannochloropsis* spp. are predominantly polysaccharide-based (Harris 2009; Jeanniard *et al.* 2013), and the diatom *T. pseudonana* has a cell wall enriched with

silica. After immunizing alpacas with whole cell lysates from these organisms, the sera immune response exhibited a corresponding specificity to each species with diverse representation of antigenic proteins, as evidenced by ELISA and Western blot analysis. The construction of a high titer phage display library, exceeding 10^{13} phage per ml, further confirmed the complexity of this V_HH library with at least 10^6 individual transformants. Subsequent panning of the phage library using live algal cells resulted in a compendium of V_HH clones with selective recognition of algal cell surface epitopes. Lead candidate clones B11 and H10 bind to *C. reinhardtii* with an $EC_{50} \leq 0.5$ nM and exhibited distinct anisotropic cell surface distributions as demonstrated by confocal microscopy. While these subnanomolar affinity extracellular-binders represent one example of the library's utility, the versatility of this resource holds exciting opportunities for both basic and applied research in algal biotechnology.

Generation of a camelid V_HH library and confirmation of its integrity

The creation of camelid library with high complexity and good representation of V_HHs for algal proteins is described in detail by Jiang, Rosenberg *et al.* 2013. In brief, the peripheral blood lymphocytes from alpacas immunized with algae lysates were used as template DNA to amplify the V_HH coding repertoire by PCR, resulting in over 10^6 independent clones from the purified products of approximately 400 bp. These DNA fragments were used to construct a phage display library using previous methods (Sepulveda & Shoemaker 2008; Tremblay *et al.* 2010; Mukherjee *et al.* 2012).

Before examining the binding abilities of V_HHs, positive immune responses were observed in the two alpaca research animals by ELISA. Western blots using the alpaca sera as a primary antibody also showed good representation of a wide variety of epitopes with molecular weights ranging from 20-200 kDa. Together, these results indicated the high probability of recovering functional V_HHs with specificity for the respective algal organisms. The Western blots developed "post" immunization in Figure 31 demonstrate that the alpaca injected with *C. reinhardtii* only showed a strong immune response to *C. reinhardtii*, but not *N. oceanica*, *C. variabilis*, *C. subellipsoidea*, and *T. pseudonana*, as expected. Conversely, the other alpaca that was injected with *N. oceanica*, *C. variabilis*, *C. subellipsoidea*, and *T. pseudonana* demonstrated a corresponding response to these algae, but not *C. reinhardtii*.

Interestingly, both pre-immunization blots using sera extracted from the research animals prior to any exposure to these five microalgae show that there were some existing V_HHs in the alpacas' immune system that recognize proteins from *C. subellipsoidea*. This may indicate that the alpacas have been exposed to *C. subellipsoidea* in their natural habitat or that this alga shares similar proteins with another plant or alga that the animals had come into contact with previously. Despite this unexpected finding, all other algae show a strong immune response with low background levels of detection in the pre-immunization sera. Therefore, the V_HHs are expected to be a direct result of immunization.

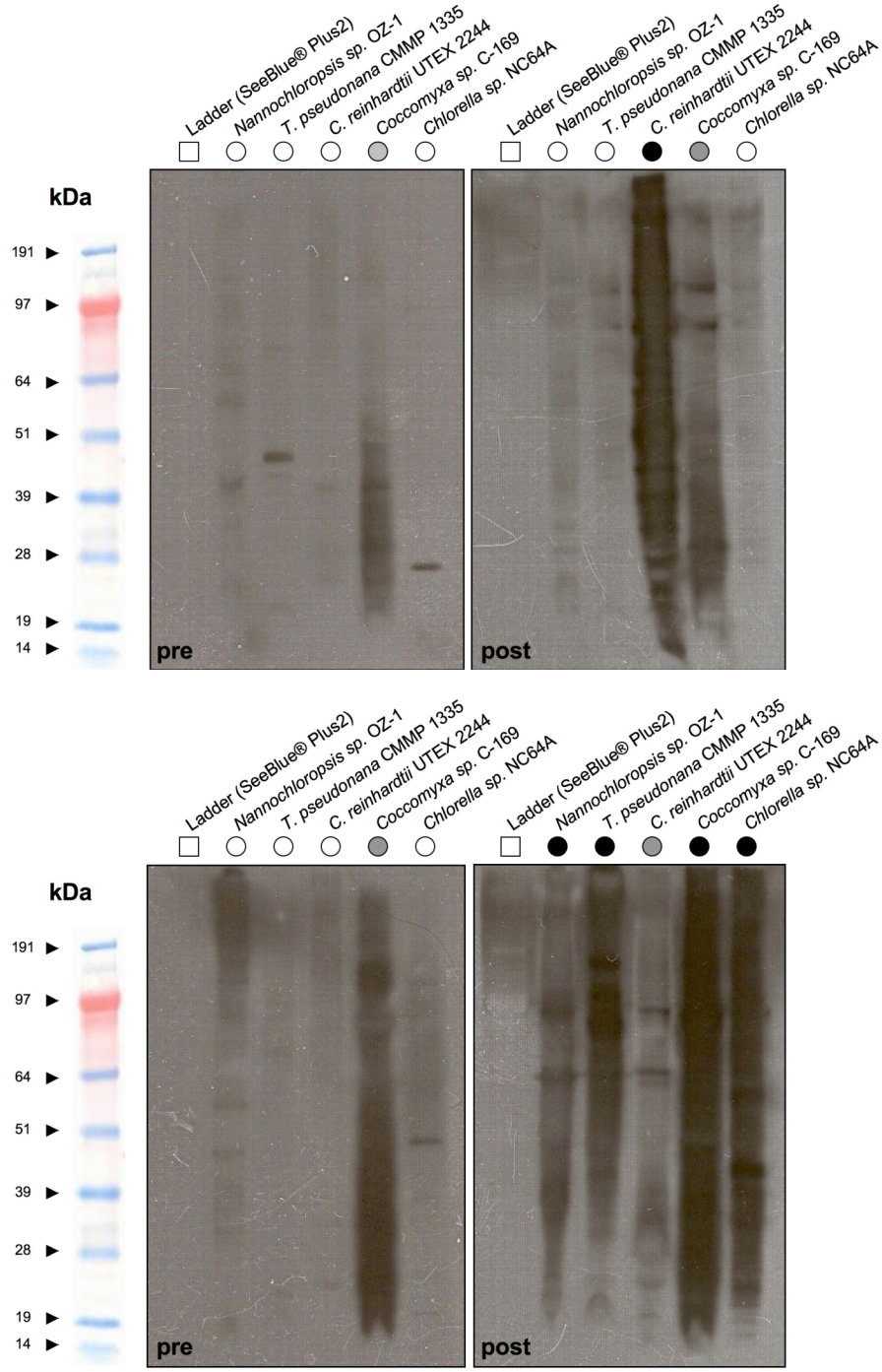

Figure 31. Immunochemistry of alpaca sera pre- and post-immunization with algal lysates. These Western blots demonstrate full representation of species-specific microalgal protein recognition present in the alpaca sera as a result of immunization. While the animal corresponding to the top blots received only *C. reinhardtii* lysates and shows a unique response to that alga, the other animal (bottom blots), received the four other algae of interest and responded accordingly.

Library panning for high affinity V_HH binding to the algal cell surface

After constructing a phage-display library, V_HH clones decorating the surface of phage particles could be panned against live algal cells. Between each round of panning, phage were recovered and evaluated by high-throughput 96-well ELISA, which was employed to quickly determine the relative affinity of surface binding clones in compared to a negative control V_HH that is unspecific to algae. From an initially amplified library with 10^{13} phage per ml, only 10^7 to 10^8 total phage were recovered from the first round of panning, which indicates the selection of potential surface-binding V_HHs and a corresponding loss of the non-binding phage from the original population. Following increasing levels of stringency to narrow this selection procedure and enrich the phage population with only the highest affinity V_HHs**,** the titer of phage recovered after the second round was expectedly 10-100× higher than in the primary panning. Ultimately, following the third round of panning, the majority of phage clones produced ELISA signals exceeding 2-fold that of the negative control, with a subset producing 10-fold higher signals than the background.

For *C. reinhardtii*, lead candidate V_HH clones with the highest ELISA signals were sequenced (Supplementary Table S3: Appendix B) and further characterized by ELISA spanning a full dilution series of each V_HH against algal protein lysates, as show in Figure 32A. From this analysis, clones B11 and H10 demonstrated the highest effective binding concentrations (EC_{50}) of less than 0.5 nM. Furthermore, these clones exhibited high species specificity to *C. reinhardtii* and not any of the other algae species used for immunization in this study (Figure 32B).

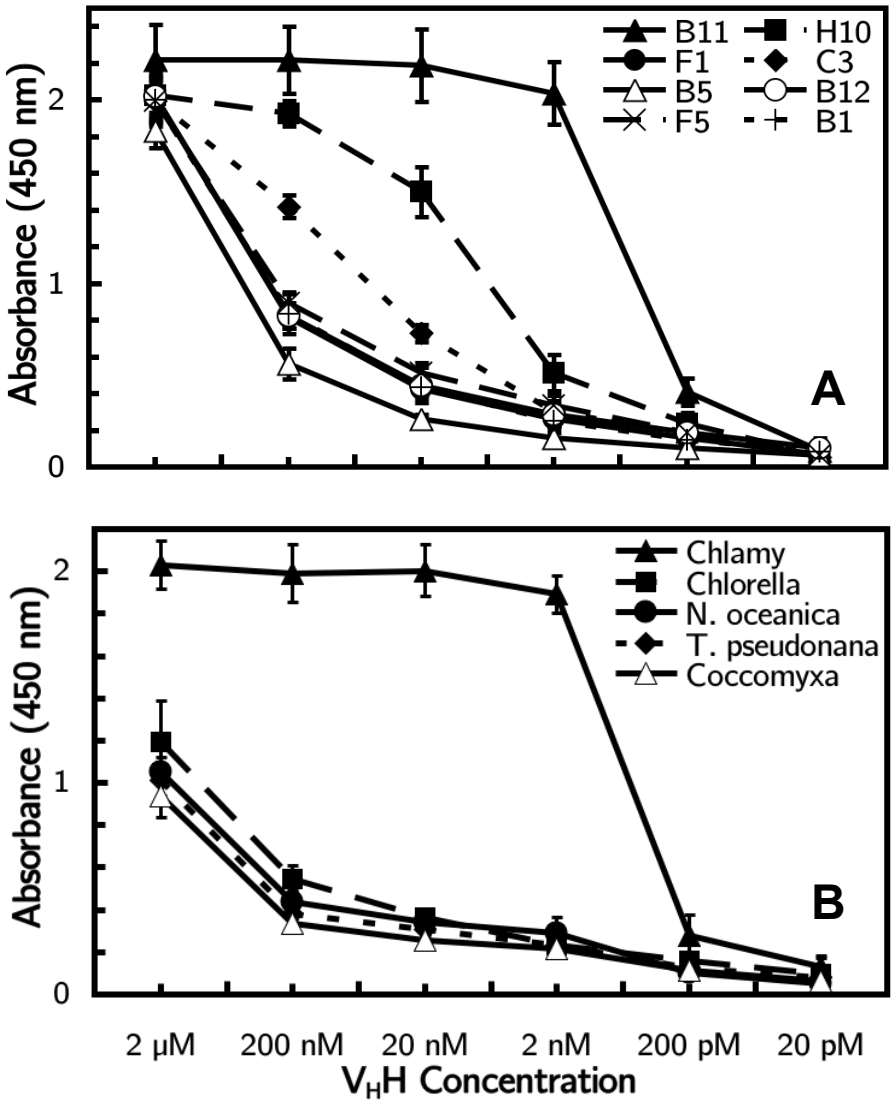

Figure 32. ELISA curves describing the binding affinity of *C. reinhardtii* V_HHs. (A) Lead candidate V_HHs for *C. reinhardtii* cell surface binding demonstrate varying degrees of affinity to *C. reinhardtii* lystate. Clone B5 served as a negative V_HH control that is not specific to algae, while clones B11 and H10 demonstrate the highest affinity to *C. reinhardtii*. **(B)** These two V_HHs also exhibit clear specificity to *C. reinhardtii* lysates without any non-specific binding to the other algae lysates. ELISA curves for clone B11 are shown in this cross-species analysis. This figure is reprinted adapted from Jiang, Rosenberg, *et al.* 2013 with permission from the publisher.

Employing V_HHs for bioprospecting and fluorescent detection of algae

Routine quantification and identification of species within microalgal populations (*e.g.*, production organisms, contaminant algae, protozoa) is necessary for environmental studies as well as algae production. Current methods to evaluate microalgal ecology for environmental studies, bioprospecting, and culture diagnostics involve manual observation by microscopy and phylogenetic sequencing from single colonies, as employed in Chapter 3. However, these approaches may not adequately describe mixed populations since clonal isolates cannot represent the true abundance of subpopulations in cultures. Furthermore, the process of generating single algal colonies by streaking dilute amounts of liquid culture onto solid media can also take weeks to months.

As an alternative methodology, V_HHs may recognize algal organisms in mixed populations based on related surface epitopes. To test this hypothesis, the two lead candidate V_HHs, H10 and B11, were fused to the red fluorescent protein, mCherry, and demonstrated remarkably unique cell surface localization (Figure 33). By coupling these *C. reinhardtii* specific V_HH binding agents with fluorescent probes, the detection of algae and related species has been demonstrated as an effective technique for polyculture identification by Jiang *et al.* (2014). With the ability to rapidly bind species-specific epitopes, this antibody-based approach may provide particular advantages over current techniques for monitoring algae populations in commercial PBRs and ponds as well as natural lakes and oceans.

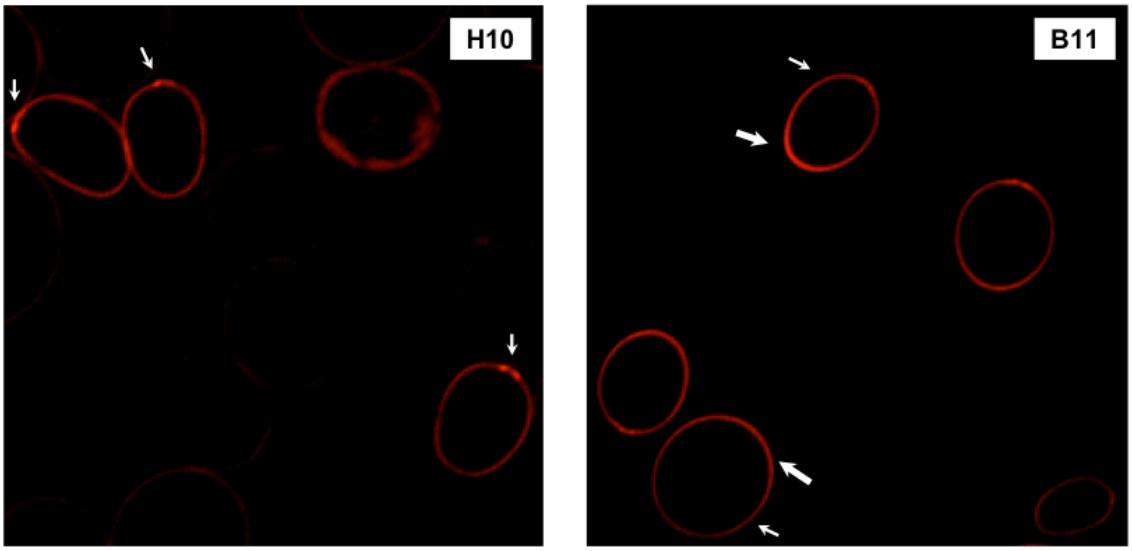

Figure 33. Unique cellular distribution of *C. reinhardtii* surface V_HHs demonstrated by confocal fluorescent microscopy. The V_HH clones H10 and B11 were fused to the red fluorescent protein, mCherry, and imaged using confocal microscopy (Courtesy of Wen Zhi Jiang, University of Nebraska-Lincoln). These micrographs show that H10 exhibits localized binding at the flagellar base and B11 has a more anisotropic distribution, binding to an epitope that may exist in higher abundance opposite to the flagellae.

Algal chloroplast produced V_HHs as protein therapeutics

Microalgae can also be used as a platform to produce single-chain antibodies for high-value pharmaceutical applications. As an example, V_HHs capable of treating of botulism have been successfully expressed in recombinant *C. reinhardtii*. Botulinum poisoning causes an estimated 250 cases of infantile botulism in the U.S. each year (Cox & Hinkle 2002). Currently, the widely accepted treatment for infantile botulism poisoning comes from human-derived antibodies (botulism immune globulin, marketed as BabyBIG®). This antitoxin is not only expensive but must be delivered intravenously (Arnon *et al.* 2006). The development of an inexpensive platform for oral administration of antitoxins would be a tremendous advance for global health. Using similar methods of alpaca immunization as described previously, a library of V_HHs that bind and neutralize botulinum neurotoxin (BoNT) was created and lead candidate clones were selected and extensively characterized (Mukherjee *et al.* 2012). The fusion of two different V_HH clones (H7 and B5) was found to be more effective as a divalent molecule with two distinct binding sites on BoNT than either high affinity antitoxin alone. In a small animal model, H7, B5, and H7-B5 were administered by intraperitoneal injection and shown to afford 100% survival after BoNT exposure at as much as 10,000× the LD_{50} (Mukherjee *et al.* 2012). To reduce the cost of production and potentially expand the availability of such antitoxins, the chloroplast of *Chlamydomonas reinhardtii* has been demonstrated as a suitable platform for robust expression of these V_HHs. Driven by the psbA promoter, each of the BoNT antitoxin V_HHs was successfully transformed into the chloroplast genome of *C. reinhardtii* and shown to have light-inducible

expression. Finally, to demonstrate functional activity of these chloroplast products, Figure 34 shows the similar binding characteristics of algae-produced anti-BoNT V_HHs to the conventional *E. coli* protein expression platform (Barrera, Rosenberg, *et al.* 2014). Materials and methods for this experiment can be found in Appendix B.

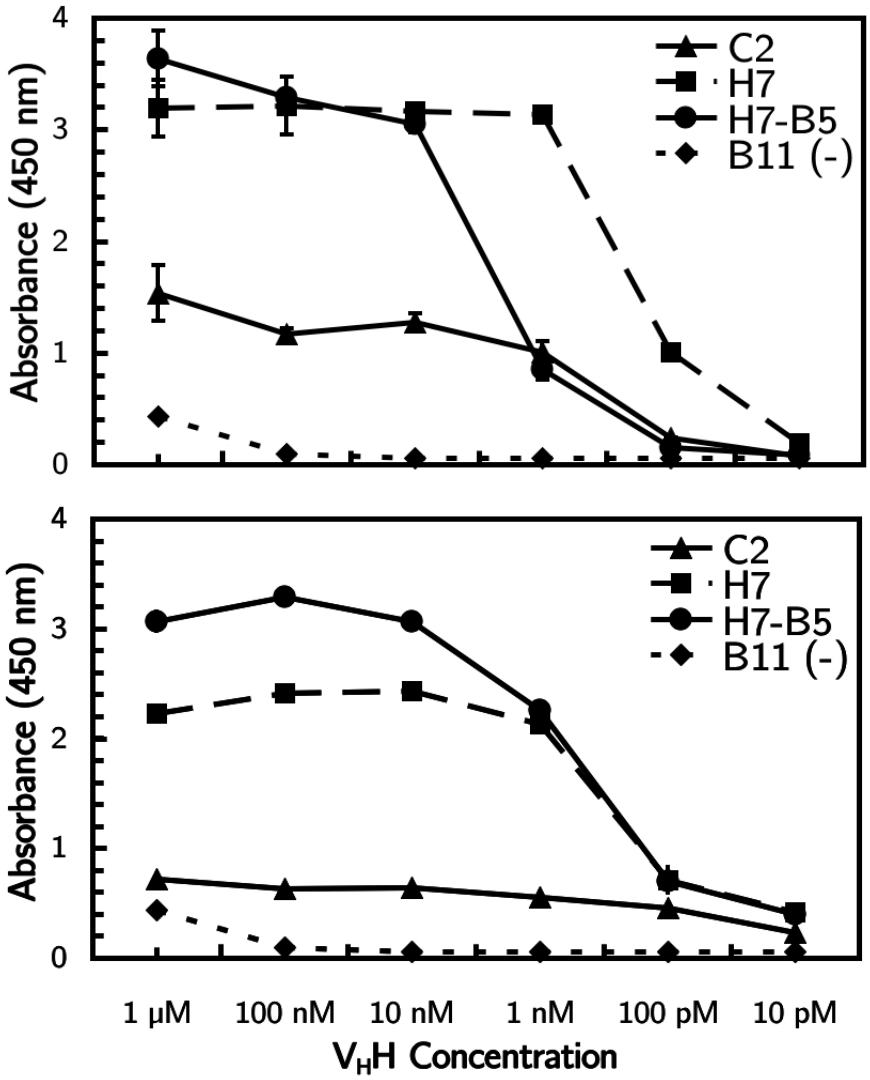

Figure 34. *C. reinhardtii* chloroplast produced V_HH domains bind BoNT. **(A)** Recombinant V_HH domains purified from *E. coli* were subjected to ELISA using anti-E-tag antibodies. All three domains that were also made in algae demonstrated binding to BoNT. The V_HH clone B11, characterized previously as a *C. reinhardtii* surface binder, served as a negative control (–) for BoNT binding. **(B)** All three binding domains produced from algae were capable of binding BoNT with similar affinity to those produced from bacteria. This figure is reprinted adapted from Barrera, Rosenberg, *et al.* 2014 with permission from the publisher.

Using phage display as an enabling technology to isolate highly specific V_HH domains raises the possibility of applying this technology in many fashions and at large scales to provide rapidly adaptive, robust, and uniquely effective crop protection systems. The ability to rapidly generate V_HH libraries and, ultimately, produce these recombinant proteins in algal organisms could have interesting applications ranging from pond culture diagnostics and bioprospecting to high value coproducts. In light of the advances in molecular genetic tools for microalgae that have occurred over the past five years, it is clear that these biological approaches to genome engineering, subcellular visualization, and robust antibody production have improved upon the framework of the traditional microalgal cell. However, computational approaches to accurately quantify algal populations will also be necessary to correlate changes at the microbial level to productivity at larger scales.

6.4 Metrics for determining cell and biomass concentration

6.4.1 Correlation between cell counting and biomass measurements

While growth curves remain a pillar of microbiology, current measurement practices lack uniformity. Microbial populations are typically reported as either optical density at any number of wavelengths or cell density by a variety of counting methods. Counting cells manually with a hemocytometer can allow for the most detailed visual assessment of a culture's health, but also represents the most time consuming method of quantifying cell density. While advances in automated culture monitoring machines can capture digital images for analysis (*e.g.*, Invitrogen Countess™ Automated Cell Counter) or use flow cytometry to count particles (*e.g.*, Coulter Counter), these tools still require timely calibration and can be prohibitively expensive for small research groups (INVITROGEN 2009). Moreover, depending on the method of quantification, cell density data can become convoluted by fully automated mechanisms that lack sufficient user input.

Microalgae, in particular, benefit from visual investigation and counting of cells due to diversity of species, potentially long growth periods, and changes in cellular morphologies throughout growth cycles. As an example, many unicellular species are typified by coenobia (grouped single cells) and can have a high prevalence of predatory microbes due to free organic material. For algae grown in open conditions, axenic cultures are nearly impossible to maintain; therefore, biomass and counting methods must also account for potentially diverse populations. Furthermore, even

axenic cultures can exhibit a complex distribution of cells due to varied cell types with differential rates of division (Tamiya 1966).

In order to gain accurate population information, counting of individual cells using a hemocytometer remains the most basic and direct method of determining cell concentration in liquid culture. The hemocytometer microscope slide is delimited by 1 mm^2 grid and can be viewed under phase contrast at 10× magnification. This visual inspection of algal cells may also serve as the more reliable indicator of microbial demographics because the user is able to differentiate cells, debris, and contaminants; however, this count can also be biased by subjective error (Lund *et al.* 1958). As shown in Figure 35, quantification of algal cultures using automated flow cytometry and spectrophotometry can maintain good correlations with manual counts by hemocytometer. However, all of these methods present inherent limitations because they are only accurate within a limited range of concentrations and, therefore, require sample dilution. In order to combine the user input afforded by hemocytometer counting (*i.e.*, visual distinction of cell types) with the automated nature of particle counting, the following section describes the development of an automated image processing program to analyze hemocytometer micrographs.

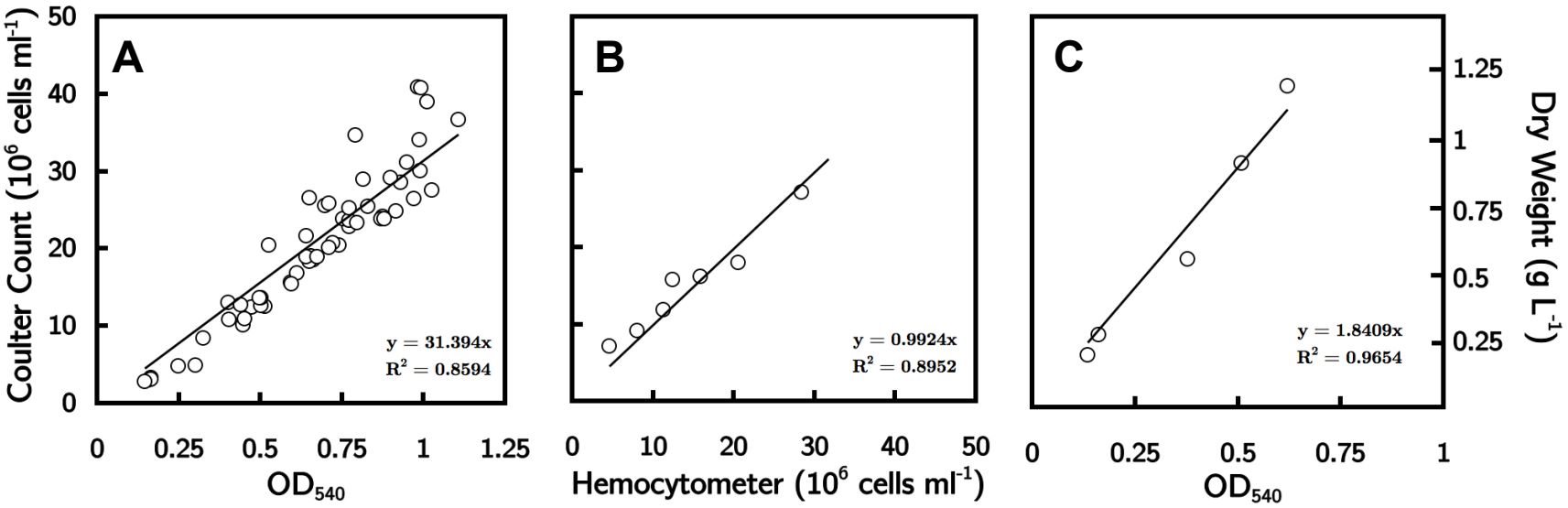

Figure 35. Correlations between metrics of cell and biomass density in culture. The relationships between optical density at 540 nm (OD_{540}), automated Coulter Counter (left axis), manual hemocytometer counts, and dry biomass weight (right axis) are shown with linear trend lines and approximate conversion factors. **(A)** Date from multiple cultures of *Chlorella sorokiniana* are overlaid and demonstrate reasonable correlation with OD_{540} within the linear range ($OD < 1$). Only visual inspection by hemocytometer counting can fully account for nuances of cell shape and potential contamination, but the single growth curve depicted in panel **(B)** shows close accordance between manual and automated counts. Finally, the plot in panel **(C)** conveys a useful conversion of OD_{540} to biomass concentration in culture based on pellet weight.

6.4.2 Automated hemocytometer image processing with CyteSeeker

The development of a simple image analysis program to automatically count cells loaded onto a hemocytometer requires only a basic light microscope with a camera and computer connectivity. This program, called CyteSeeker, aims to eliminate subjective error associated with the hemocytometer by standardizing image capture and counting while also allowing for user-defined, and visually determined, size thresholds. CyteSeeker uses graphical user interface (GUI) to allow accurate determination of cell count and automatic calculation of cell density in liquid culture (million cells per ml). The program is also ideal for calculating surface density values (million cells per cm^2) of immobilized cells on a two-dimensional environment.

The programming of this stand-alone executable file for the 64-bit Windows platform, is relatively straightforward and available as an open source code in the MATLAB environment. There are three simple components of the algorithm. First, the user-defined threshold settings are used to differentiate mean cross-sectional areas of each cell based on particle delineations in the phase contrast image (ideally dark circles on light background). Next, "water shedding" is employed to separate adjacent cells by identifying centers of mass and interpreting any topographic relief. Finally, each particle is registered as a counted event over the regional distribution of the entire image. This method of image processing offers certain advantages over flow cytometry or optical density (*e.g.*, $OD_{540\text{-}720}$) approaches by providing sufficient information on the individual cells that contribute to the final count. While FlowCam® (Fluid Imaging Technologies) has recently developed a small laboratory

unit to both count and photograph single cells in a flow cytometry platform, CyteSeeker provides a simple and inexpensive alternative that is compatible with existing and common microscopy techniques. Moreover, the program handles overpopulated samples well, avoiding the need to dilute before counting. This serves to reduce volumetric errors associated with dilution that would otherwise be propagated and enables more statistically relevant sample sizes to be measured.

The basic method of use requires a standard hemocytometer stage to be loaded with duplicate 10 µl samples of the culture media to be visually appraised by microscopy before proceeding with the count. Employing any simple camera setup paired with the preferred microscope, the user then captures representative micrographs of the different areas of the hemocytometer grid at a reasonable magnification. These images are saved for subsequent analysis with CyteSeeker, which also provides a mechanism of tracking data integrity that is not possible with many other cell counting methods. Therefore, there is a digital (or printed) record of the exact condition of the cells for each sample measurement. Once the program is installed and opened on a PC, the images can be imported one at a time using the GUI. The cell size threshold can be set easily using the sliding bar based on visual assessment of cell coverage and judgment of cell size, shape, and degree of contamination that may be present. Rather than setting global size thresholds that require calibration based on particle size cutoffs, CyteSeeker allows for the threshold to be set for each image and can account for individual cell shape and potential aggregates. A single threshold may also be saved and applied to all images from the same culture, if

desired. Lastly, a dilution factor can be manually input to adjust cell concentration, accordingly, and the cells counted on-screen are directly converted to a volumetric cell density output. A screenshot from CyteSeeker analysis shown in Figure 36 illustrates the differential coloration of counted particles to allow users to meaningfully interact with the program and see which objects are being identified as cells. Depending on the threshold that is set, there is the potential for groups of particles to be counted as a single cell or cells to be omitted from the count, if desired. This type of detailed adjustment is not possible with automated cell sorting or optical density approaches.

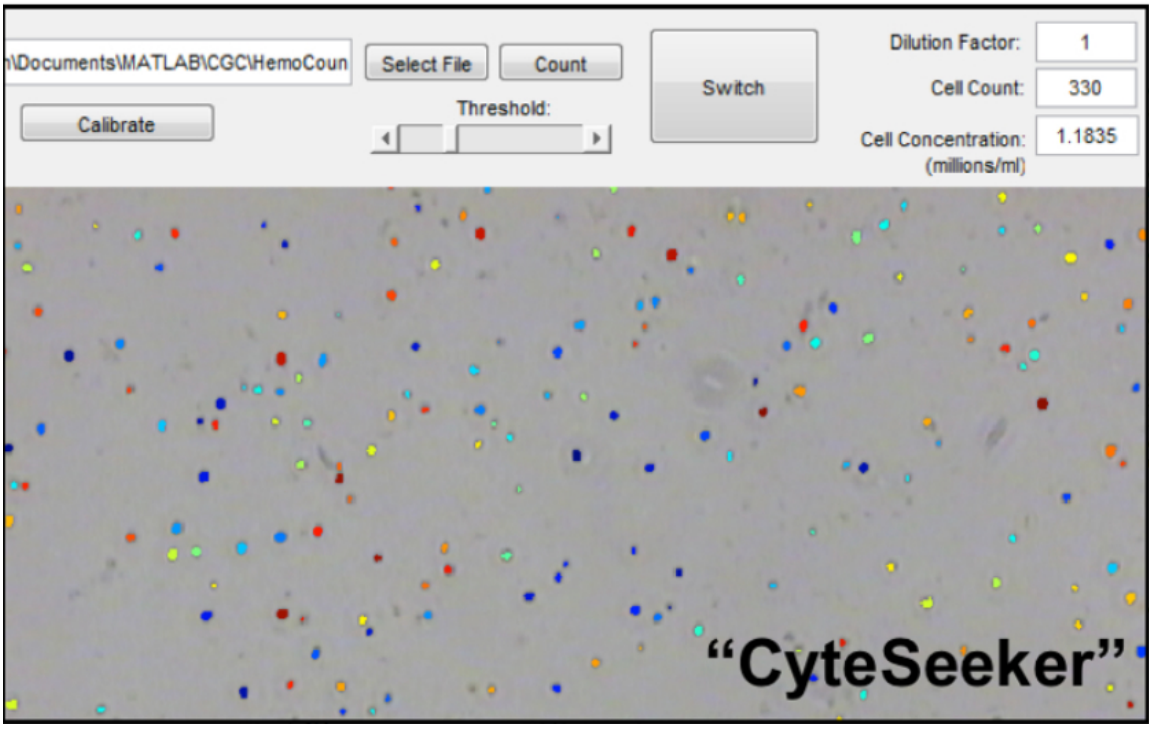

Figure 36. Screenshot of CyteSeeker for automated cell counting. The graphical user interface allows the researcher to import any .jpg or .bmp image file, set the size threshold, and count the particles on the screen. Each counted event is colored randomly to convey the exact cells that were identified and included in the count. The "Switch" button toggles between the color overlay and original image.

In order to examine the ability of this program to recognize cells of varying size, morphology, and relative abundance in the field of view, monocultures of microalgae with diverse cell diameters were chosen for CyteSeeker evaluation. These species included commercially relevant and academically important microalgae: *Haematococcus pluvialis* (~50 µm), *Chlamydomonas reinhardtii* (~10 µm), *Chlorella sorokiniana* (2-5 µm), *Scenedesmus dimorphus* (~8 µm), and *Nannochloropsis oceanica* (1-2 µm). By adjusting the CyteSeeker size threshold accordingly, Figure 37 demonstrates the program's robustness in identifying these diverse algal organisms (*C. reinhardtii* not shown). The overlay of counted output screenshots on top of the raw hemocytometer images show that each cell in the frame is recognized and color-coded for confirmation. Cell debris and possible bacterial contamination that remain out of focus in the *C. sorokiniana* sample were excluded from the count based on the threshold setting.

By displaying a visual confirmation of the counted cells, the user may also decide to manually adjust the total number of cells in order to account for potential false positives or cells that may have been omitted from the count. CyteSeeker will automatically recalculate the volumetric concentration of cells based on any post-processing changes made to the final count.

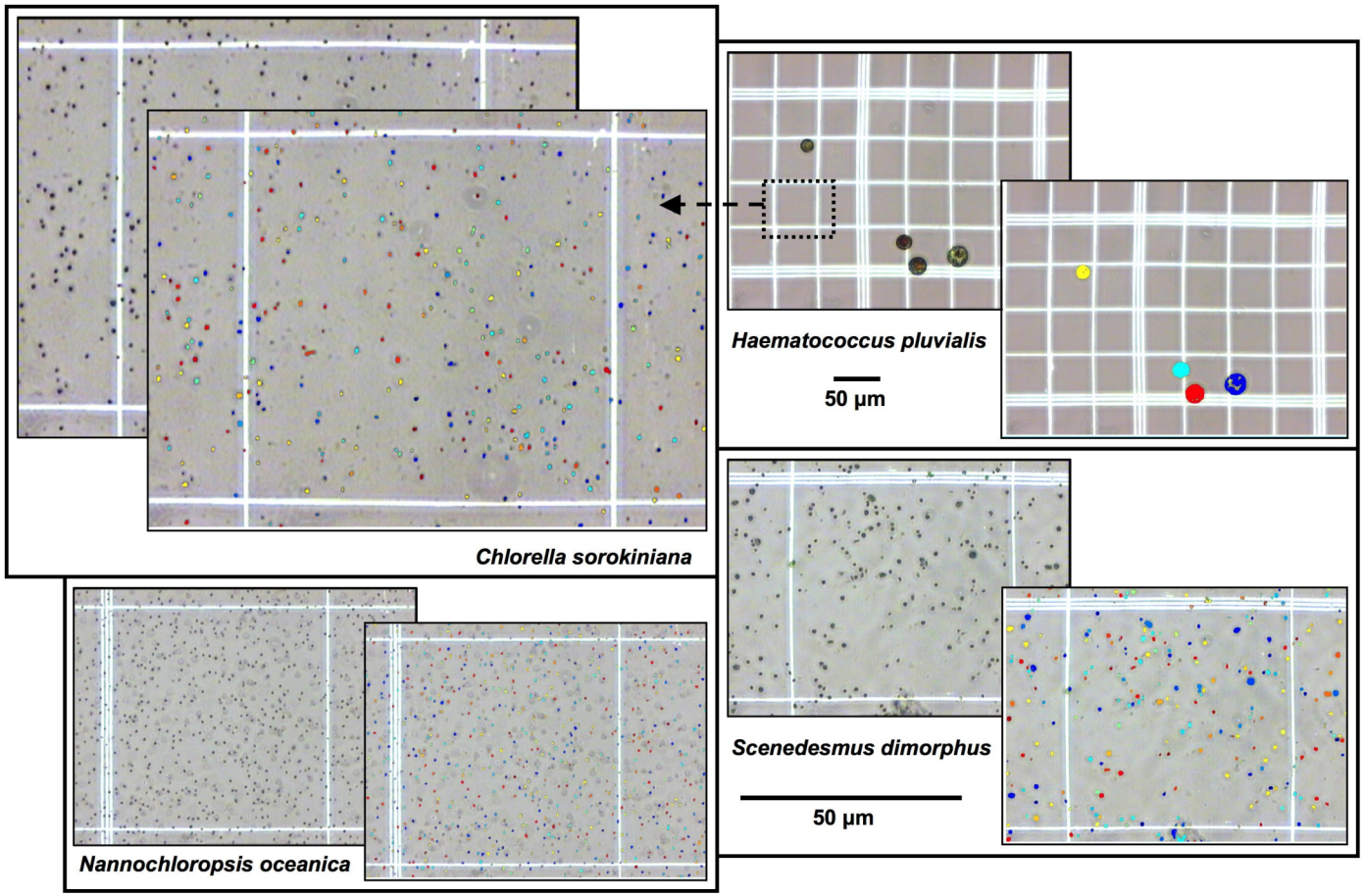

Figure 37. CyteSeeker screenshots validating recognition of different microalgal cell types. Four diverse algal species were counted with different thresholds. The smallest square delineated by white lines represents 50 × 50 µm. All *Chlorella*, *Scenedesmus*, and *Nannochloropsis* species were viewed at 40× magnification, while *H. pluvialis* is shown at 10×.

Results of round-robin cell counting experiment

Three different users familiar with microalgae, but possessing varying degrees of experience (graduate and high school students) were asked to count the same exact images manually and using CyteSeeker. While the time associated with each count actually varied significantly depending on both the user and the cell type, automated counting using CyteSeeker is generally faster relative to manual counting of small cells with higher population density (*e.g.*, *Chlorella* in Table 9), while larger cells can be just as easily observed and enumerated visually. In all cases automated counts compared well with the manual counts (within margin of errors for each) and also approximated the "real count" of each micrograph.

As a result of gathering this information from the users, it is apparent that CyteSeeker remains in close accord with manual counting for most high-density populations of small cells, which is by far the most time consuming to count manually. However, the program does not perform as well as manual counting for medium and large cells due to more complex morphology. The program can be susceptible to over segmentation of the cell, which results in counting organelles and individual ultrastructural components. Based on the diverse algal cell examined, *Chlorella* and *Nannochloropsis* were found to be ideal species to count with CyteSeeker because they appear as single black dots on most micrographs. With further fine-tuning of the threshold and some post-processing adjustment, all three microalgal species can be counted with similar confidence ranges as the manual hemocytometer methods.

Micrograph & Real Count	User	Visual Counts	CyteSeeker
C. reinhardtii: **29** 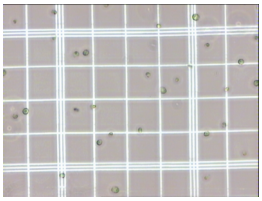	**1**	30 ± 0	31 ± 2
	2	31 ± 1	41 ± 2
	3	32 ± 1	34 ± 2
	AVG:	**31 ± 1**	**35 ± 5**
C. reinhardtii: **19** 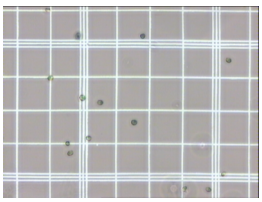	**1**	14 ± 0	13 ± 1
	2	14 ± 1	20 ± 0
	3	20 ± 0	39 ± 2
	AVG:	**16 ± 4**	**24 ± 13**
H. pluvialis: **4** 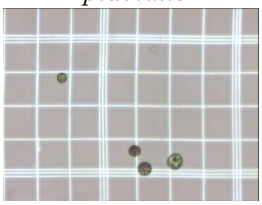	**1**	4 ± 0	4 ± 0
	2	4 ± 0	4 ± 0
	3	4 ± 0	4 ± 0
	AVG:	**4 ± 0**	**4 ± 0**
H. pluvialis: **7** 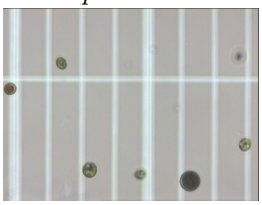	**1**	7 ± 0	5 ± 1
	2	7 ± 0	7 ± 0
	3	7 ± 0	10 ± 0
	AVG:	**7 ± 0**	**7 ± 3**
Chlorella: **348** 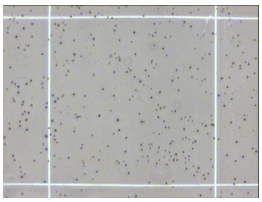	**1**	392 ± 55	384 ± 29
	2	339 ± 13	360 ± 4
	3	385 ± 34	376 ± 3
	AVG:	**372 ± 28**	**373 ± 12**
Chlorella: **328** 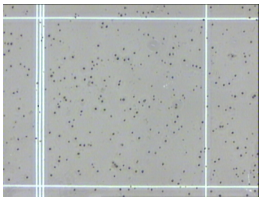	**1**	342 ± 19	384 ± 7
	2	318 ± 1	338 ± 13
	3	362 ± 23	336 ± 1
	AVG:	**341 ± 22**	**353 ± 27**

Table 9. Focus group testing CyteSeeker with different algal species. This table summarizes the results of users' cell counts by manual visualization compared

to CyteSeeker. Micrographs were counted in triplicate at full size, not the thumbnail images depicted above.

Unlike optical density or cell sorting, digital image analysis enables both visual hemocytometer inspection and automated counting. As such, the open source CyteSeeker algorithm reduces sample processing time and aims to eliminate subjective error. A tunable threshold extends particle detection limits for overpopulated cultures. From a statistical standpoint, the more cells that are counted, the less significant the associated error should be. For example, the accuracy of counting 100 cells has confidence limit of roughly ± 20 while counting 40,000 cells can theoretically be ± 400 (1% of total) (LUND *et al.* 1958). Since most accurate cell density measurements come from high counts, CyteSeeker may be a useful program to automate this procedure for both liquid and immobilized cell cultures. Furthermore, this method can eliminate subjective error, while still allowing certain necessary human judgment of discernable cells to be made.

6.5 Characterizing biofilms with a molecular & computational toolkit

Collectively, these tools have applicability for the study of microalgal cell biology as well as applied biofilm research. The following chapters will further demonstrate their utility with immobilized microalgal cell cultures in describing the behavior of algae cells within natural biofilm communities. While V_HHs proved to be unsuccessful as binding intermediates on solid substrates (data not shown), other proteins were successfully used to promote algal cell attachment in monocultures of unicellular *C. reinhardtii* and *Chlorella sorokiniana* UTEX 1230 as quantified using CyteSeeker.

6.6 References

Arnon SS, Schechter R, Maslanka SE, Jewell NP, Hatheway CL (2006) Human botulism immune globulin for the treatment of infant botulism. N Engl J Med 354: 462-471.

Barrera DJ, Rosenberg JN, Chiu JG, Chang Y-N, Debatis M, Ngoi S-M, Chang JT, Shoemaker CB, Oyler GA, Mayfield SP (2014) Algal chloroplast produced camelid V_HH anti-toxins are capable of neutralizing botulinum neurotoxin. Plant Biotech J. *In Press*

Caussinus E, Kanca O, Affolter M (2012) Fluorescent fusion protein knowckdown mediated by anti- GFP nanobody. Nature Structural & Molecular Biology 19: 117-122.

Chen Y-W, Chiang P-J (2001) Automatic cell counting for hemocytometers through image processing. Proceedings of the World Academy of Science, Engineering and Technology. 58, 719-722.

Cox and Hinkle (2002) Infant botulism. Am Fam Physician 65: 1388-1393.

Day JG, Thomas NJ, Achilles-Day UEM, Leakey RJG (2012) Early detection of protozoan grazers in algal biofuel cultures. Bioresource Technology 114: 715-719.

Franklin S E, Mayfield SP (2004) Prospects for molecular farming in the green alga *Chlamydomonas reinhardtii.* Current Opinion in Plant Biology 7: 150-165.

Fuhrmann, M (2002) Expanding the molecular toolkit for *Chlamydomonas reinhardtii* from history to new frontiers. Protist 153: 357-364.

Gressel J. (2008) Genetic glass ceilings: transgenics for crop biodiversity. JHU Press: Baltimore, MD.

Griffiths M, Harrison SL (2009) Lipid productivity as a key characteristic for choosing algal species for biodiesel production. Journal of Applied Phycology 21: 493-507.

Grossman AR, Harris EE, Hauser C, Lefebvre PA, Martinez D, Rokhsar D, Shrager J, Silflow CD, Stern D, Vallon O, Zhang Z (2003) *Chlamydomonas reinhardtii* at the crossroad of genomics. Eukaryotic Cell 2: 1137-1150.

Hallman A (2007) Algal transgenics and biotechnology. Transgenic Plant J 1:81-98.

Harris, EH (2009) *Chlamydomonas* Sourcebook: Introduction to *Chlamydomonas* and its laboratory use. pp 242-248, E. H. Harris (ed.), Elsevier, Oxford

Invitrogen (2009) Comparison of image-based cell counting methods: Countess™ automated cell counter vs. the hemocytometer. Accessed: 12 September 2014 Available: lifetechnologies.com/us/en/home/brands/product-brand/countess-automated-cell-counter.html

Jeanniard UK, Dunigan A, Gurnon DD, Agarkova JR, Kang IV, Vitek M, Duncan J, McClung G, Larsen OW, et al. (2013) Towards defining the chloroviruses: a genomic journey through a genus of large DNA viruses. BMC Genomics 14: 158.

Jiang WZ, Rosenberg JN, Wauchope AD, Tremblay JM, Shoemaker CB, Weeks DP, Oyler GA (2013) Generation of a phage display library of single-domain camelid V_HH antibodies directed against *Chlamydomonas reinhardtii* antigens and characterization of V_HHs binding cell surface antigens. Plant J 76: 709-717.

Jiang WZ, Cossey S, Rosenberg JN, Oyler GA, Olson BJSC, Weeks DP. (2014) A rapid live-cell ELISA for characterizing antibodies against cell surface antigens of *C. reinhardtii* and its use in isolating algae from natural environments with related cell wall components. BMC Plant Biology. *In Press*

Kou C-L, Oyler GA, Shoemaker CB (2011) Accelerated neuronal cell recovery from botulinum neurotoxin intoxication by targeted ubiquitination. PLoS ONE 6: e20352.

Li J, Zhu D, Niu J, Shen S, Wang G (2011) An economic assessment of astaxanthin production by large scale cultivation of *Haematococcus pluvialis*. Biotechnol Adv 29: 568-574.

Liu J, Huang J, Sun Z, Zhong Y, Jiang Y, Chen F (2011) Differential lipid and fatty acid profiles of photoautotrophic and heterotrophic *Chlorella zofingiensis:* Assessment of algal oils for biodiesel production. Bioresource Technology 102: 106-110.

Lumbreras V, Stevens DR, Purton S (1998) Efficient foreign gene expression in *Chlamydomonas reinhardtii* mediated by an endogenous intron. Plant J 14: 441-447.

Lund JWG, Kipling C, Le Cren ED (1958) The inverted microscope method of estimating algal numbers and the statistical basis of estimations by counting. Hydrobiologia 11: 143-170.

Maass DR, Sepulveda J, Pernthaner A, Shoemaker CB (2007) Alpaca (*Lama pacos*) as a convenient source of recombinant camelid heavy chain antibodies (V_HHs). J Immunol Methods 324:13-25.

Manuell AL, Beligni MV, Elder JH, Siefker DT, Tran M, Weber A, McDonald TL, Mayfield SP (2007) Robust expression of a bioactive mammalian protein in *Chlamydomonas* chloroplast. Plant Biotechnol J 5: 402-412.

Mukherjee J, Tremblay JM, Leysath CE, Ofori K, Baldwin K, Feng X, et al. (2012) A novel strategy for development of recombinant antitoxin therapeutics tested in a mouse botulism model. PLoS One, 7(1), e29941.

Neupert J, Karcher D, Bock R (2009) Generation of *Chlamydomonas* strains that efficiently express nuclear transgenes. The Plant Journal 57: 1140-1150.

Nichols, H.W., Bold, H.C. (1965) *Trichosarcina polymorpha* gen. et sp. nov. Journal of Phycology, 1, 34-38.

Oyler GA, Rosenberg JN (2010) Enhanced gene expression in algae, U.S. Application No. 13/925,921; U.S. Patent No. 8,815,568.

Oyler GA, Rosenberg JN, Weeks DP (2012) Single chain antibodies for photosynthetic microorganisms and method of use. U.S. Application No. 13/441,951.

Plucinak TM (2013) Making *Chlamydomonas reinhardtii* a better model organism: tackling the inefficiency of nuclear transgene expression and improving methods for the generation and characterization of insertional mutant libraries. University of Nebraska-Lincoln. Theses and Dissertations in Biochemistry. Paper 15. Available: http://digitalcommons.unl.edu/biochemdiss/15

Rasala BA, Barrera DJ, Ng J, Plucinak TM, Rosenberg JN, Weeks DP, Oyler GA, Peterson TC, Haerizade F, Mayfield SP (2013) Expanding the spectral palette of fluorescent proteins for the green microalgae *Chlamydomonas reinhardtii*. The Plant Journal 74: 545-556.

Rasala BA, Chao SS, Pier M, Barrera DJ, Mayfield SP (2014) Enhanced genetic tools for engineering multigene traits into green algae. PLoS ONE 9(4), e94028.

Rasala BA, Lee PA, Shen Z, Briggs SP, Mendez M, Mayfield SP (2012) Robust expression and secretion of xylanase1 in *Chlamydomonas reinhardtii* by fusion to a selection gene and processing with the FMDV 2A peptide. PLoS ONE. 7(8), e43349.

Rodolfi L, Chini Zittelli G, Bassi N, Padovani G, Biondi N, Bonini G, Tredici MR (2009) Microalgae for oil: strain selection, induction of lipid synthesis and outdoor mass cultivation in a low-cost photobioreactor. Biotechnol Bioeng 102: 100-112.

Rothbauer U, Zolghadr K, Tillib S, Nowak D, Schermelleh L, Gahl A, Backmann N, Conrath K, Muyldermans S, Cardoso MC, Leonhardt H (2006) Targeting and tracing antigens in live cells with fluorescent nanobodies. Nat Methods 3: 887-889.

Saerens D, Ghassabeh GH, Muyldermans S (2008) Single-domain antibodies as building blocks for novel therapeutics. Current Opinion in Pharmacology 8: 600-608.

Sayre R (2014) Genetically Modified Algae: A Risk Benefit Analysis, U.S. Department of Energy Webinar, Accessed: May 22, 2014.

Sepulveda J, Shoemaker CB (2008) Design and testing of PCR primers for the construction of scFv libraries representing the immunoglobulin repertoire of rats. J. Immunol. Methods. 332: 92-102.

Sheehan J, Dunahay T, Benemann J, Roessler P (1998) A Look Back at the U.S. Department of Energy's Aquatic Species Program: Biodiesel from Algae Golden, Colorado: TP-580-24190, National Renewable Energy Laboratory.

Sizova I, Fuhrmann M, Hegemann P (2001) A Streptomyces rimosus aphVIII gene coding for a new type phosphotransferase provides stable antibiotic resistance to *Chlamydomonas reinhardtii*. Gene 277: 221-229.

Tamiya H (1966) Synchronous cultures of algae. Annu Rev Plant Physiol 17: 1-27.

Tremblay JM, Kuo C-L, Abeijon C, Sepulveda J, Oyler G, Hu X, Jin MM, Shoemaker CB (2010) Camelid single domain antibodies (VHHs) as neuronal cell intrabody binding agents and inhibitors of *Clostridium botulinum* neurotoxin (BoNT) proteases. Toxicon, 56: 990–998.

Vazhappilly R, Chen F (1998) Eicosapentaenoic acid and docosahexaenoic acid production potential of microalgae and their heterotrophic growth. Journal of the American Oil Chemists' Society 75: 393-397.

7

PROTEIN-MEDIATED RETENTION AND VISUALIZATION OF ALGAL CELLS IN MONOLAYER BIOFILMS

As described in Chapter 5, many different configurations of algal biofilm reactors have been successfully used for wastewater treatment (WWT) applications. Despite the longstanding efficacy of these phototrophic methods of water remediation, existing technologies may not be directly transferable to biofuel production due to the lack of control over the type and amount of adherent biomass on biofilm substrates, which is largely dependent on climatic and seasonal variation. While high oil content is an important criterion for algal biofuel production, WWT with microalgae relies principally on the bioconversion of N and P where the quality of the biomass grown is irrelevant. Furthermore, naturally occurring biofilms are not necessarily acclimated to abrupt shifts in nutrient availability or other environmental

perturbations. In fact, it has been demonstrated that microalgal biofilms disengage from substrates when transferred to conditions of nutrient starvation, perhaps in an effort to seek "greener pastures" where the biofilm can re-establish itself (SCHNURR *et al.* 2013). Since two-stage growth processes are ubiquitous in microalgal bioprocessing in order to elicit metabolite accumulation (*e.g.*, nitrogen deprivation for lipid induction), algal lipid production using natural biofilms may be a contradictory proposition. In order to make photosynthetic biofilms compatible with staged algal production, cellular binding intermediates may encourage microalgal biofilm formation and provide assisted retention of cells onto a substrate of interest.

In this chapter, transparent biopolymer substrates were evaluated for their capacity to immobilize microalgae while retaining mechanical stability in an aqueous environment. Toward these goals, initial tests determined that the inherent surface properties of polyvinyl alcohol (PVA) hydrogels and thin cellulose films are inadequate for spontaneous algal cell adhesion. Therefore, protein-protein interactions that may enhance the attachment of the green microalgae, *Chlamydomonas reinhardtii* and *Chlorella sorokiniana*, to the membrane surface were investigated. After chemical functionalization with 11-bromoundecanoic acid (BUDA) and carbonyl diimidazole (CDI), covalent amide linkages were formed with a protein topcoat of either purified fibronectin (FN) or bovine serum albumin (BSA). Both FN and BSA were found to promote the immobilization of suspended algal cells from surrounding liquid monoculture with retention rates on the order of 4×10^5 per cm^{-2} d^{-1}, resulting in saturating surface densities of roughly 2×10^6 cells cm^{-2}. Based

on these results, 15% PVA (w:v) and cellulose biomaterials with surface enhancements create a suitable substrate for algae biofilm formation, which can serve as a controlled environment for microbiological research and potentially increase the volumetric efficiency of large-scale microalgal cultures.

7.1 Introduction

While cellular entrapment within simple fibrous and gelatinous materials can be sufficient for solid-state algal cultivation (Johnson & Wen 2010; Aydinoğlu *et al.* 2013), harvesting algal cells from small interstitial spaces can be challenging and light transmission can be limited. To address this, transparent materials with high surface area have been reported to enhance light penetration in adherent algal cultures, but the fabrication of these materials can be cost intensive (Jacobi *et al.* 2012). Based on prior work in this area, this chapter describes the development of protein-mediated attachment of unicellular algae on transparent polymer membranes that can be easily synthesized in the lab or readily sourced from abundant biomaterials.

7.1.1 Polymeric substrates of interest: hydrogels and cellulose

While the mechanisms of natural biofilm formation have been studied extensively (Berk *et al.* 2012), substrates must be optimized to promote maximal biological productivity and robustness of adherent microalgal cells. Suitable materials must have the essential features of structural integrity in an aqueous environment and maintain the viability of microorganisms when placed in direct cellular contact.

Based on these criteria, hydrogels have been widely developed as a polymeric system with high biocompatibility for cell culture applications and reviewed extensively (Webb & Dervakos 1996; Karel & Robertson 1989; De Bont *et al.* 1990; Willert *et al.* 1996; Guisan 2006; Wijffels 2001). While historically used for biomedical applications (*e.g.* tissue culture, stem cell differentiation, and primary neuronal culture), these self-contained bioreactors exploiting flexible, thin film structures may be well suited for bioenergy applications by overcoming obstacles of non-uniform illumination that can negatively affect photosynthetic microbes at high cell densities (Greco Song *et al.* 2014). Rather than composite materials formed by entrapment of microalgae within polymeric matrices (Aydinoğlu *et al.* 2013), the hydrogels in this present study provide an aqueous continuum at the surface to facilitate hydration and mass transfer to the adherent algae biofilms. The lifespan of membrane-based systems depends on both the type of polymer material and possible surface functionalization, which were both investigated in this present study.

In the context of bioethanol production, cellulose is generally thought of as a feedstock for enzymatic or microbial degradation. While this polymer of glucose contains significant chemical energy, its natural biological purpose as a structural biomolecule is often overlooked. As a result of its molecular evolution, crystalline cellulose may also serve as a practical platform for surface retention of microbial biofilms due to its high tensile strength (Serra *et al.* 2013; Karimi *et al.* 2014). While the exposed moieties of cellulose allow for considerable hydrophilic behavior, pure cellulose remains resistant to degradation by water alone. As a common

component in bioplastics, cellulose is a rugged, renewable, and recyclable material. With the concurrent development of depolymerization technologies, the use of cellulose as a structural material in algae bio-*film*-reactors may hold additional potential to be regenerated or potentially converted to bioenergy or other chemical feedstocks along with algae biomass at the end of the bioreactor's life. Furthermore, as a potential additive to livestock feeds, some applications may accept cellulose as a necessary component (*e.g.*, cattle and other herbivores may require cellulose).

7.1.2 Mechanisms of cellular attachment

While many species of microalgae are amenable to spontaneous biofilm formation (*e.g.*, polymicrobial wastewater populations) under certain conditions, not all photosynthetic microbes have this ability. In fact, considerable evidence is building to support the role of quorum sensing molecules as growth inhibitors to modulate sessile algal and bacterial growth (Schatz *et al.* 2013; Teplitski *et al.* 2004). With such diverse sets of microalgae being developed for biofuel applications, immobilized algae growth systems may therefore require a deliberate mechanism of surface binding. While considerable research regarding the flocculation of microalgae from liquid suspensions has identified electrostatic, hydrodynamic, and protein interactions (Salim *et al.* 2010; Danquah *et al.* 2009), an understanding of the cellular and molecular interactions that contribute to algal biofilms is just beginning to be applied to large-scale production (Bernstein *et al.* 2014).

In an effort to establish mechanisms of adherent algal culture for laboratory practices and to reduce water and harvesting investments for potential scalability, this chapter

describes methods devised to adsorb cells to the surface of a hydrophilic substrate rather than physical entrapment within a polymer matrix or natural biofilm scaffold. The attachment capabilities of fibronectin (FN) and bovine serum albumin (BSA) proteins were compared using *Chlamydomonas* and *Chlorella* species. While fibronectin is comprised of distinct cell-binding domains and has been employed for cellular immobilization in the past (Nuttelman *et al.* 2001), BSA is not known to have specific mechanisms of binding and merely acts as a proteinaceous surface to study the mechanisms of biofilm formation without direct protein-protein interactions (Hawser & Islam 1998). Using both a clear polymer thin film (cellulose) and three-dimensional hydrogels coated with each candidate protein, algal cells were found to effectively colonize the solid substrates. Both platforms are mechanically stable in an aqueous environment and can be functionalized with any bio-adhesive protein topcoat for enhanced algal attachment rates. This study demonstrates that microalgal cells can be preferentially captured from suspension onto these surfaces.

7.2 Materials and Methods

7.2.1 Hydrogel synthesis

Synthesis of polyvinyl alcohol (PVA) hydrogels was carried out in an aqueous solution of 15% w:v PVA in deionized water. After completely dissolving the PVA at 80° C, the solution was cooled to room temperature and 25% w:v glutaraldehyde (GA) stock was added as a cross-linking reagent to achieve a final concentration of 1% w:v. The polymerization reaction was initiated with the addition of 300 µl of 2 M hydrochloric acid added drop-wise per 15 ml of PVA/GA mixture (Nuttelman *et al.*

2001). Upon covalent bridging of the soluble PVA polymer via acetalization (Phillip & Hsu 1979), 1.5 ml aliquots were transferred into each well of a 6-well cell culture plate (VWR International) while the emulsion remained viscous enough to pour without unintended entrapment of air bubbles. The 6-well plate was then incubated at 37° C for 10 minutes or until the hydrogels solidified with approximately 0.5 cm thickness. Finally, the set gels were soaked in phosphate buffered saline (PBS) for one hour to allow for full rehydration.

7.2.2 Chemical functionalization of polymer surface

After removing the circular PVA hydrogels from the 6-well plate mold, chemical surface modifications were performed at 37° C in a glass beaker using a two-step functionalization procedure. Gels were first incubated in a solution of 10 mg ml^{-1} 11-bromoundecanoic acid (BUDA) in 3 M sodium hydroxide under gentle agitation (115 RPM) for 2 hours. The gels were then rinsed several times with deionized water to remove unreacted BUDA and dried overnight in a vacuum desiccator. The BUDA spacer molecule was reacted with an excess of carbonyl diimidazole (CDI) in acetone for 2 hours. Hydrogels were then rinsed with acetone, dried and sterilized under an ultraviolet light in the laminar flow biosafety cabinet overnight. Cellulose films were cut into 1 cm squares (*Glass* Transparent Leaves, Luxe) and treated in the same manner with BUDA and CDI before exposure to protein binding intermediates.

7.2.3 Protein coating and detection

In order to bind protein intermediates to the chemically functionalized surface of the membrane substrates, a sterile solution of either fibronectin (FN) or bovine serum albumin (BSA) dissolved in 50 µg ml^{-1} in 0.1 M sodium carbonate buffer was poured over either hydrogels or cellulose squares. The submerged substrates were incubated on an orbital shaker at room temperature for 2 hours and then rinsed with PBS several times to remove unbound protein. To analyze the coverage area for amount and distribution of bound protein, fibronectin was detected by immunochemical methods and colorimetric developing agents. For these immunoassays, a blocking solution of 5% nonfat dry milk and 0.1% tween in PBS (PBST) was applied to the membranes for 2 hours while agitated on the orbital shaker at room temperature. Next, the membranes were rinsed 3 times for ten minutes each in PBST to remove excess milk and coated with primary rabbit antibody (1:500 dilution in 0.1% milk in PBST) for 1 hour at room temperature. After rinsing 3 times for ten minutes each in PBST, membrane substrates were incubated with a secondary antibody solution for 1 hour at room temperature and rinsed 3 times for five minutes each with PBST followed by 2 two-minute rinses with deionized water. Finally, a mixture of 5-bromo-4-chloro-3-indoxyl and nitroblue tetrazolium (BCIP/NBT) substrate for alkaline phosphatase was used to visualize fibronectin attachment by colorimetric verification of a dark purple/gray hue forming on the surface of the substrate.

7.2.4 Microalgal cultivation

Chlamydomonas reinhardtii UTEX 2244 and *Chlorella sorokiniana* UTEX 1230 were grown in batch cultures as previously described in this thesis. Cell concentration in the liquid media was counted using a hemocytometer in concert with an automated cell counting program developed in our laboratory (CyteSeeker, Chapter 6, Section 6.4.2). The surface density of cellular attachment was also quantified by microscopy at 10× magnification (Nikon Eclipse TE2000-U).

7.2.5 Biofilm formation and cell monitoring

After preparing hydrogels and cellulose films using previously describe methods, the protein-coated membranes were allowed to equilibrate in algal culture media for 2 hours. Loading and retention of microalgal cells onto cellulose and hydrogels was carried out in sterile 6-well dishes submerged in 3ml of a dense culture of either *C. reinhardtii* UTEX 2244 or *C. sorokiniana* UTEX 1230. Each day, the membranes were removed from culture and rinsed in the respective culture media 3× before capturing surface images with an inverted light microscope. Cells in solution were also counted daily to create a depletion curve from the liquid seed culture.

7.3 Results

The stabilized substrates developed in this study provide a direct method for microalgal attachment for examination of biofilm growth kinetics and may serve as a potential platform for scale-up. The three-component system relies on a polymer-based membrane (PVA hydrogel or cellulose), a structurally stable chemical bridge

(BUDA/CDI), and a protein topcoat (FN or BSA). These three steps involved in synthesizing the biocompatible membranes are described in the following sections. Using monocultures of either *C. reinhardtii* or *Chlorella sorokiniana*, the cultivation of these organisms when immobilized as photosynthetic biofilms was quantified based on cell retention rates and cell density on the adherent surface.

7.3.1 Hydrogel synthesis and chemical surface modifications

By adapting common emulsion recipes and procedures for hydrogel synthesis (NUTTELMAN *et al.* 2001), polyvinyl alcohol (PVA) gels provided a simple and effective method to create reproducible substrates for laboratory investigation of biofilm formation. After cross-linking with glutyraldehyde, the emulsions of 15% PVA provided the proper balance of elasticity and rigidity, sufficient hydration properties, and optical clarity (Figure 38A). Using the surface area afforded by standard 6-well plates typically used for tissue culture (9.6 cm^2), gels were formed with a high degree of standardization for the proceeding microbiological studies.

In order to both provide attachment sites for the protein of interest and make the gels more suitable for prolonged exposure to algal culture media, surface modification with 11-bromoundecanoic acid (BUDA) and carbonyl diimidazole (CDI) were found to be necessary surface additives. While BUDA serves as a high molecular weight spacer to provide physical distance from the gel surface, CDI permits sites of attachment by amide bonding with proteins of interest. After chemical functionalization with both BUDA and CDI, the color of the hydrogels is visibly altered (Figure 38B).

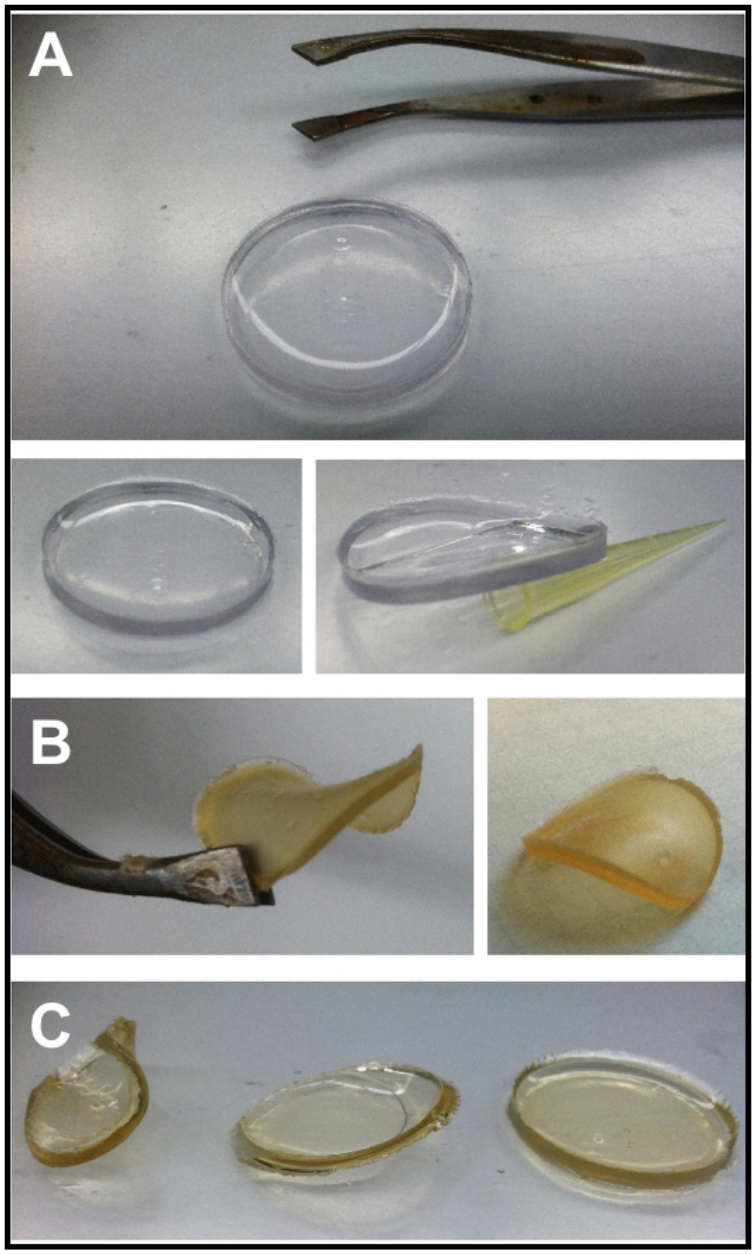

Figure 38. Hydrogel synthesis and chemical functionalization. Photographs of 15% PVA hydrogels demonstrate the physical changes that occur during preparation. **(A)** The PVA hydrogel immediately after solidification with gluteraldehyde cross-linking remains translucent until **(B)** treated with BUDA and CDI and vacuum dried to evaporate residual solvent. **(C)** Finally, the gels are readily rehydrated in PBS.

7.3.2 Verification of covalent protein attachment to hydrogels

After optimizing procedures for hydrogel synthesis and application of protein topcoats, protein binding efficiency and uniformity of surface coverage were assessed. The methods developed for this purpose function, in essence, as a spatial Western blot: a fibronectin-specific antibody is used to probe the hydrogel surface, bind to the immobilized FN, and reveal the distribution of surface-bound FN by a colorimetric reaction. By using different experimental combinations of BUDA/CDI, protein, and antibody treatment with the replicate hydrogels, effective protein coating was confirmed visually. As seen in Figure 39, gels that remained "untreated" by BUDA/CDI have no barrier to prevent the chromogenic reagent from permeating the porous hydrogel, thus turning entirely blue. The BUDA/CDI chemical treatment also improved the ruggedness of these PVA hydrogels, as evidenced by the compromised structural integrity of the untreated hydrogels (blue) in aqueous environments over time with slight agitation. In contrast, the chemically treated gels possess a veneer of BUDA/CDI that prevents internal discoloration and disintegration (translucent gels). Most importantly, the gels that indicate positive attachment of FN show a dark grey coloration over nearly the entire hydrogel surface, as detected by a the fibronectin-specific primary antibody and alkaline phosphatase colorimetric reaction.

Figure 39. ***(next page)*** **Protein topcoat for enhanced bioadhesion.** These photographs convey a comprehensive assessment of hydrogel coverage with **(A)** fibronectin compared to **(B)** BSA using primary (1^{o}) anti-fibronectin antibody at 1:500 dilution paired with an alkaline phosphatase-conjugated secondary antibody. Each horizontal row of gels in panels correspond to treatments with BUDA/CDI or untreated conditions as labeled on the left. Clear differences between these sets are noticeable in both their structural stability as well as their permeability to the chromogenic reagent. While untreated gels turn completely blue, the chemically treated gels are resistant to this discoloration and only exhibit a surface color change to grey in the presence of both **(A)** surface-bound fibronectin and the FN-specific antibody (+ Protein; + Antibody). Therefore, **(B)** BSA-coated gels served as a negative control in this experiment, in which no colorometric reaction was evident in any of the conditions employing the anti-FN probe (+ Antibody) to discount non-specific interaction of the 1^{o} antibody. Panel **(C)** shows a more detailed photograph of hydrogels developed in duplicate, demonstrating the reproducibility of this coating procedure with only slight variations in surface coverage.

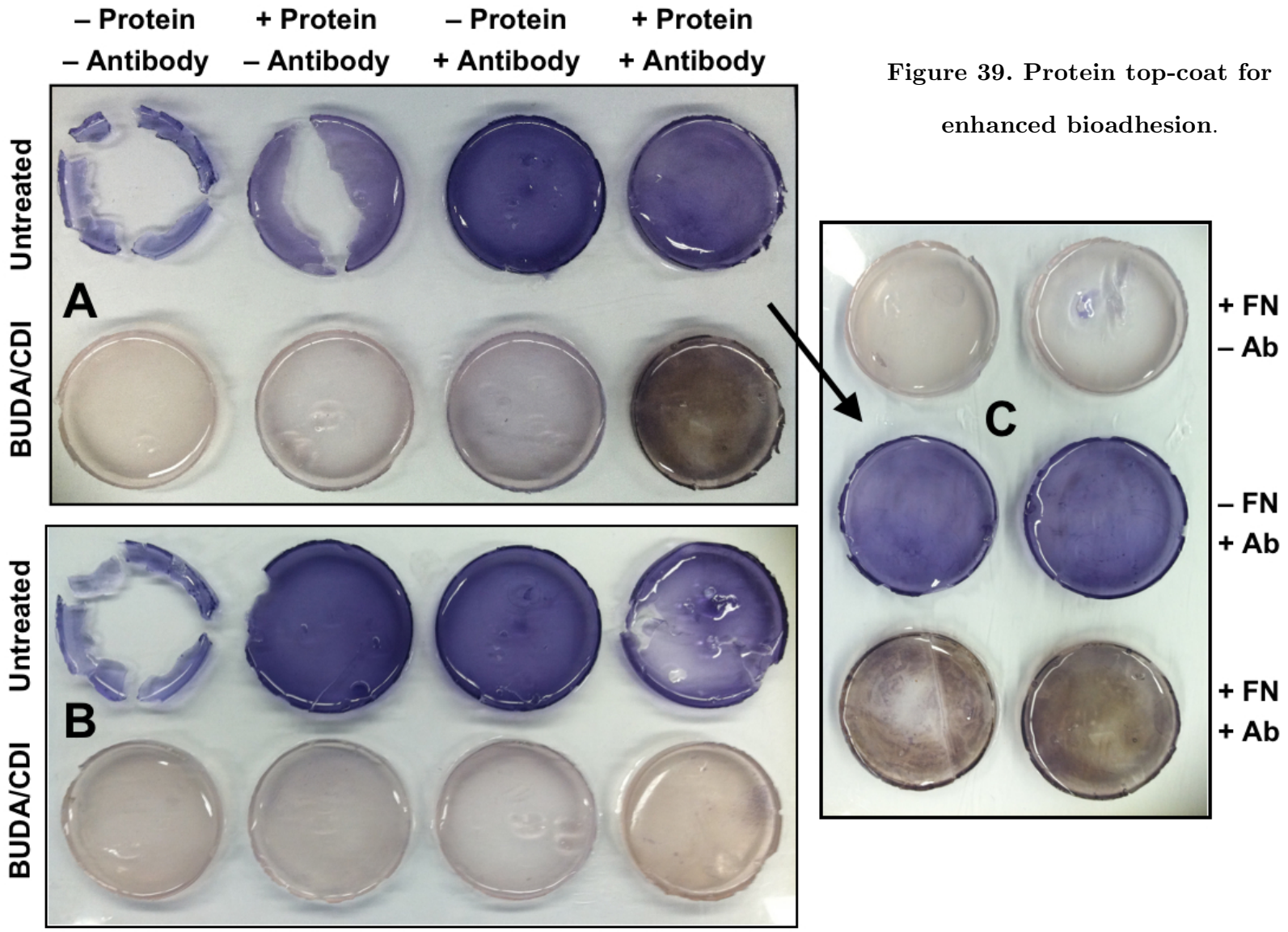

Figure 39. Protein top-coat for enhanced bioadhesion.

7.3.3 Examination of hydrogels as a substrate for microalgal adhesion

Protein-mediated algae biofilm formation was evaluated using hydrogels as a substrate to compare a protein with cell binding domains (fibronectin, FN) to a protein without known biomolecular affinities (bovine serum albumin, BSA) (Pankov & Yamada 2002). The studies were initiated by incubating FN and BSA coated gels in liquid cultures of *C. reinhardtii* to determine the retention periods and immobilized cell densities relative to hydrogels without a protein coating. Within 24 hours, deposition of microalgal cells was observed on the surface of both the FN and BSA coated gels. Although initial cellular adhesion did not proceed in a uniform manner, patches of biofilm grew to cover the entire surface area of each hydrogel over the course of four days. This uneven adhesion of cells was likely due to imperfections in the hydrogel surface, allowing for points of nucleation to instigate small colonies, which ultimately formed islands of monolayer biofilms.

After four days of growth, the rate of cellular adsorption to FN and BSA hydrogel surfaces reached their relative points of saturation. Approximations of cell density on these surfaces were calculated based on candidate regions of the surface (Figure 40, Table 10). Although these micrographs were captured four days after inoculation, the hydrogels remained stable with attachment for up to two weeks in this aqueous environment without any signs of deterioration or loss of bioadhesive function.

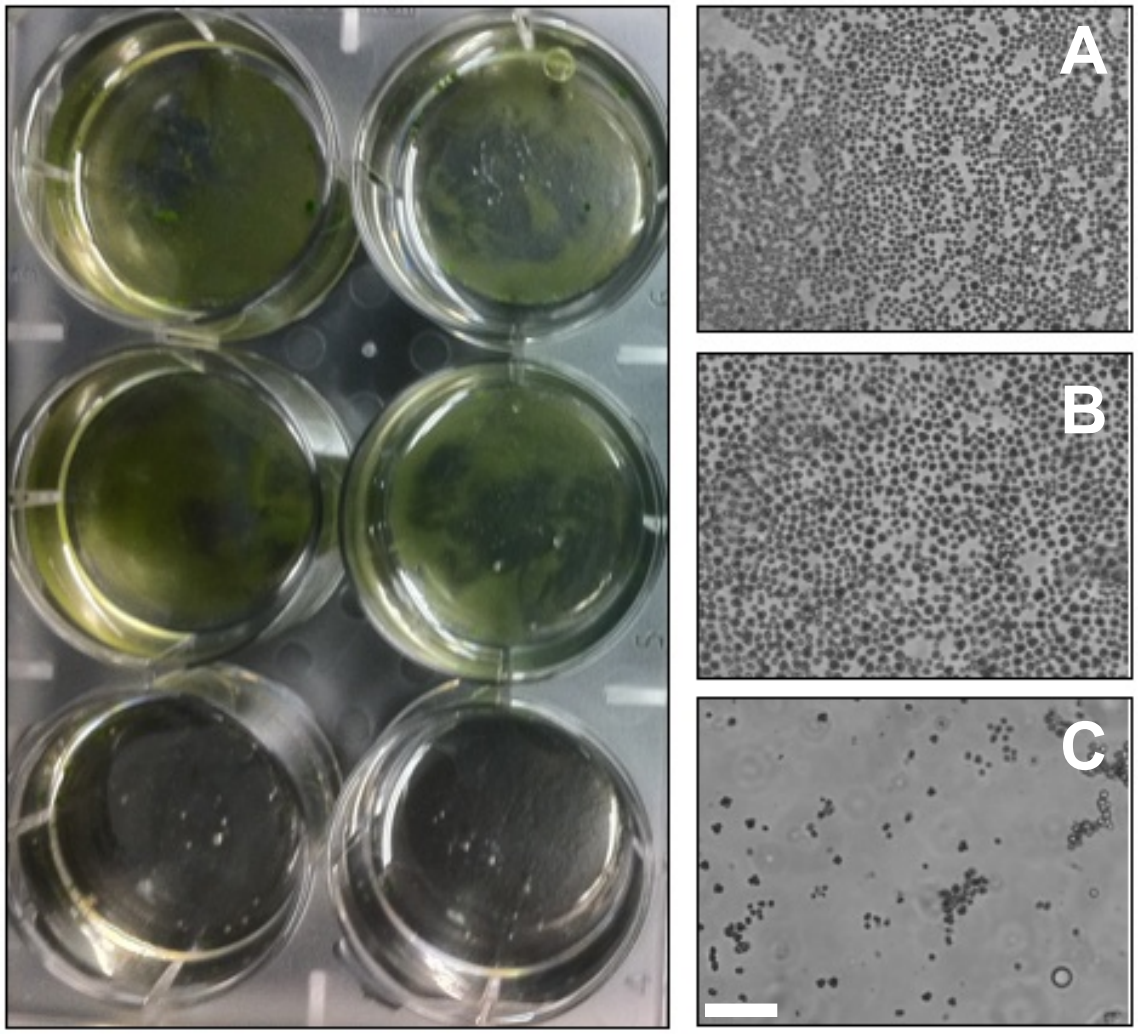

Figure 40. Comparison of protein-mediated cellular adhesion of *Chlamydomonas reinhardtii* to hydrogel surfaces. Binding of *C. reinhardtii* to the hydrogel substrates is enhanced by **(A)** fibronectin and **(B)** bovine serum albumin with approximately 8-fold higher cell coverage compared to **(C)** gels with no protein topcoat. Each micrograph taken at 10× magnification is positioned to the right of its duplicate hydrogels. Scale bar represents 50 µm.

Due to the uneven rate of cellular deposition from the liquid culture, a lack of uniformity in spatial distribution was observed in Figure 40. The retention rate of algal cells was estimated based on (1) measuring a reduction in cell density from the homogeneous liquid suspensions and (2) counting cells on the hydrogel surface. The trends in cellular attachment seen on the hydrogel surface were corroborated by a depletion of cells from liquid media (Figure 41A), in which both FN and BSA coated gels experienced comparable decreases in cell density from an initial concentration of roughly 16×10^6 cells ml^{-1} to a final concentration of 2×10^6 cells ml^{-1}. This removal of algal cells from liquid media implicates both the deposition and retention of cells onto the hydrogel surface, which correlate well with the final saturating surface counts of 2×10^6 cm^{-2} (Table 10). Although some adhesion of cells to the hydrogel without FN or BSA coating is apparent in both the cell deposition curves and the micrograph, this baseline adhesion is 8-fold lower than the cell surface densities achieved with FN- and BSA-mediated binding.

While the formation of a biofilm seed layer is an important objective of this study, the attached cells must also remain viable when immobilized for further proliferation or metabolite secretion in continuous culture. While both protein-coated hydrogels exhibited comparable abilities to adsorb freely suspended cells, *C. reinhardtii* cells were able to undergo cell division more readily on the BSA-coated hydrogel, as evidenced by clusters of numerous cells while the FN-bound organisms appear as mostly single cells or pairs of cells (Supplementary Figure S3: Appendix B). This capacity to adhere and colonize the hydrogel suggests that BSA may be a more

suitable candidate for biomass production with immobilized bio-*film*-reactors. While the higher affinity cellular binding of FN may constrict cellular division, it can sustain viability and may be suitable for applications that require metabolite accumulation or secretion (FLICKINGER *et al.* 2007).

Polymer Substrate	**Chemical Surface**	**Protein Coating**	**Cells per cm^2**
15% PVA	BUDA/CDI	FN	1.9×10^6
15% PVA	BUDA/CDI	BSA	2.0×10^6
15% PVA	BUDA/CDI	None	$\times$
15% PVA	None	None	2.3×10^5

Table 10. Quantitative assessment of biofilm formation from a monoculture. Candidate regions of the hydrogel surface exhibiting full cell coverage were imaged and counted in order to determine the maximal cell density that could be adsorbed per unit area. Interestingly, hydrogels treated with BUDA/CDI actually exhibited a cytotoxic effect ($\times$). Therefore, the complete coverage of the chemically functionalized surface with a protein topcoat is a more important criterion to ensure viability of the immobilized biofilm. The cell density values correspond to the representative micrographs in Figure 40 with error associated with automated counting $< 1\%$.

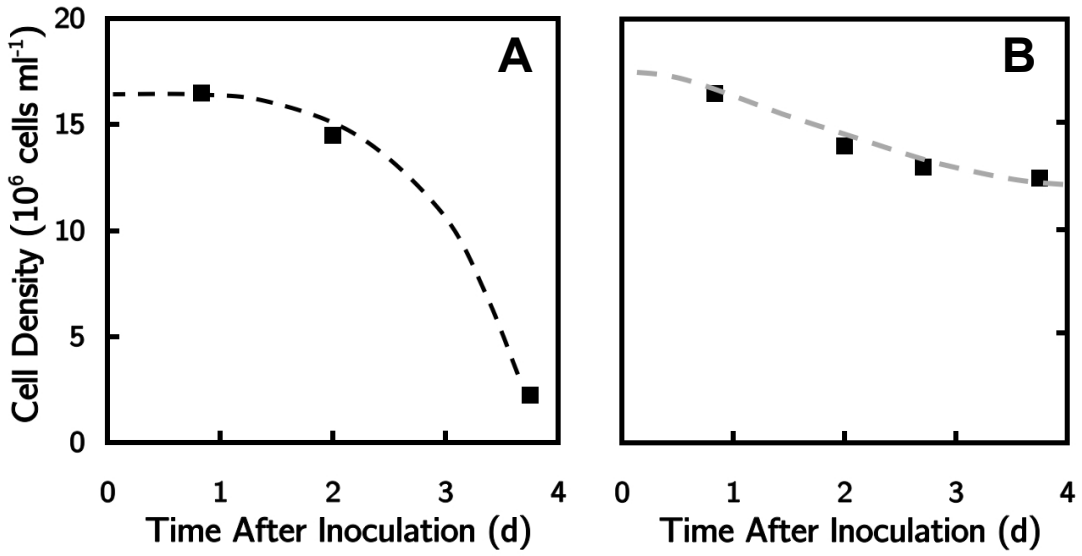

Figure 41. Comparison of microalgal deposition rates onto protein-coated and uncoated hydrogels. Depletion of algal cells from liquid media surrounding the hydrogels demonstrates cellular attachment. While **(A)** shows a relatively rapid reduction in cell density from binding to the FN-coated gel, the cell densities of **(B)** remain greater than 10×10^6 cells ml^{-1} due to marginal amounts of binding to the uncoated hydrogel. BSA-coated gels experienced similar rates of depletion as observed for FN (data not shown). These plots of cell density are representative of biological replicates with standard deviation of each data point less than 1×10^6 cells ml^{-1}.

7.3.4 Initiation of microalgal biofilms on transparent cellulose thin films

In order to transition from laboratory-grade materials and model organisms (*i.e.*, hydrogels and *C. reinhardtii*) to biopolymer feedstocks and microalgal species that may be more suitable for production at larger scales (*i.e.*, cellulose and *Chlorella* spp.), similar coating experiments were performed using pure translucent cellulose as a substrate. Using the same procedures employed for hydrogel biofilm assessment, square cellulose substrates coated with FN were incubated in the presence of a mature *C. sorokiniana* UTEX 1230 and compared to cellulose without any surface modification as well as filter paper, which can easily adsorb microalgae within its interstitial spaces. As shown in Figure 42, qualitative results demonstrate a similar trend as observed with hydrogels with the ability of protein-coated surfaces to promote biofilm formation while cells do not readily adhere to the uncoated cellulose. Unlike the hydrogels examined previously, cellulose remains more tolerant of extended time periods in liquid culture (1-2 months). The micrograph panels in Figure 42 illustrate the detail of cellular aggregation at the edge of the cellulose square. The biofilm on these thin films has more aggregated portions than observed on the hydrogels, but still lack significant multilayers. Due to these irregularities in biofilm thickness, it became difficult to quantify the surface cell density. This issue was addressed in the next chapter by employing more advanced methods of three-dimensional fluorescent microscopy.

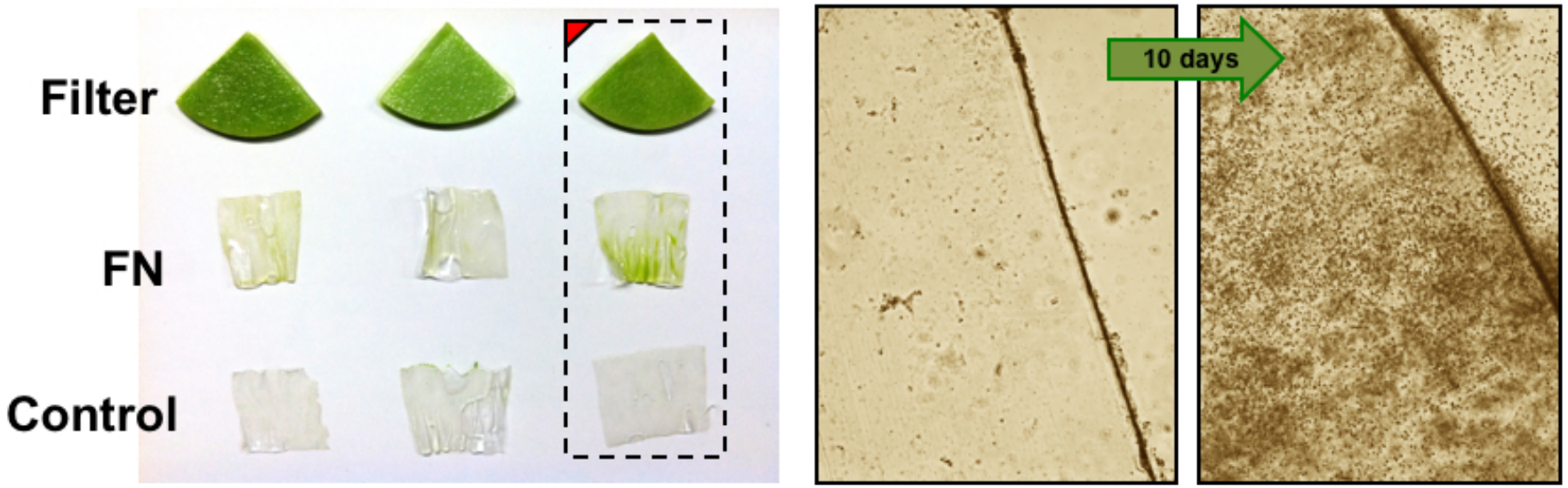

Figure 42. *Chlorella sorokiniana* UTEX 1230 colonizes cellulose with protein coating. While cellular adhesion was noticeable by microscopy within the first days of incubation, this figure shows the development of a mature *Chlorella* biofilm after 10 days in culture. By this qualitative assessment shown as photographs in the left panel and 10× micrographs to the right, fibronectin again serves as a necessary surface coating to initiate biofilm formation compared to the uncoated control in triplicate.

7.4 Discussion and Conclusions

The methods of cellular surface immobilization developed in this study were effectively applied to two different species of unicellular microalgae to accomplish monolayer biofilm formation and generate preliminary results with the adhesion of thicker natural photosynthetic biofilms. Chemical (BUDA/CDI) and protein (FN and BSA) surface functionalization were shown to effectively mediate adhesion to hydrogel and cellulosic substrates (Figures 40 and 42). By changing the micro-topography of these surfaces to nucleate algal attachment, this synthetic biofilm platform offers potential opportunities for metabolite secretion from algal monolayers and biomass production from thicker biofilms.

While the colorimetric methods used to confirm protein coverage on hydrogels showed near-complete surface coverage and maintained cell viability in subsequent cultivation experiments (Figure 39), the gels treated with BUDA and CDI alone were actually found to be toxic to *C. reinhardtii*. Direct contact of this reactive chemistry with the microalgae appears to lyse the cells, as evidenced by only debris remaining on the hydrogel surface. This may be a result of direct covalent binding with the proteinaceous cell wall of *C. reinhardtii*. Alternatively, hydrogel substrates coated with either FN or BSA exhibited an 8-fold reduction in suspended cells relative to uncoated gels (no BUDA, CDI, or protein) within four days of exposure to microalgal suspension. While a marginal level of deposition and retention was observed on the uncoated gels, the protein intermediates clearly have a positive effect on biofilm formation on both hydrogels and cellulose substrates. However, the

deposition curves shown in Figure 41 may show an accentuated rate of cell removal from liquid culture compared to actual amount bound to gel. This is likely attributed to unavoidable cell loss each time the gels were washed to remove non-specific binding of algae to the biofilm surface. In this study, the minimal amount of biomass accumulated as monolayers limited reliable biomass quantification by dry weight and, therefore, growth was quantified by cell density only (Table 10 and Figure 41). The next chapter focuses on methods for generating measurable amounts of algal biomass on cellulose thin films.

In addition to laboratory-scale investigation of microalgal biolfilm growth dynamics, this format may have advantages for large-scale open cultivation. All samples cultivated in the present study were grown in semi-open conditions in which biofilms were removed from the culture media for periodic microscope evaluation. Over the course of these experiments, no samples were compromised due to bacterial, fungal, or other signs of serious contamination. By washing the biofilm substrates before each measurement of cell density, the tangential fluid motion may have served as a sufficient countermeasure against microbial contamination, which could be accomplished in the field by using tricking fed-batch bioreactor systems. The seed layer of microalgae in all cases appears to out-compete any invasive microbes that may have been present.

In terms of cellular attachment rates and the ability for *C. reinhardtii* to proliferate on the biofilm surface, the "molecular ties" between cellular adhesion and surface proteins size appeared to be directly proportional to molecular weight. For example,

the small 12 kDa V_HH proteins described in Chapter 6 were tested in the current configuration for biofilm investigation, but failed to promote any cellular attachment to hydrogel or cellulose surfaces (data not shown), perhaps due to the small nature of the proteins. As such, species-specific interactions were certainly not observed. The potential for the BUDA/CDI chemical linkers to disrupt cell-surface antigen binding and orientation of surface binding is also a complicating factor. Furthermore, V_HHs tend to bind within the pockets of protein antigens, which may also be spatially limited when they are insoluble. Alternatively, the 250 kDa FN resulted in rapid and stable biofilm formation, but also sufficiently limited the ability of algae to divide on the surface, which suggests that the large biomolecule may contribute to tight cellular binding. The total FN monomer is comprised of three distinct domains. These cell-binding modules have specificities to biomolecules ranging from fibulin to heparin and other cell surface markers that could inhibit cell cycle progression (Pankov & Yamada 2002). Lastly, BSA at 66 kDa demonstrated comparable rates of algal adhesion despite the fact that it possesses no dedicated cell binding domains. Moreover, it enabled *C. reinhardtii* cell division to proceed on the biofilm surface. Collectively, these results suggest that specific cell adhesion factors are not necessary to promote biofilm formation in this environment and, instead, the proteinaceous surface may simply mimic a biological surface where natural biofilms readily grow. However, it should be noted that the capacity for FN and other protein domains with specific attachment capabilities may still be necessary to overcome the instability of algal natural biofilm adhesion (Schnurr *et al.* 2013).

While it is unrealistic to use FN for large-scale algal cultivation due to its high cost, residual protein streams from industrial bioprocessing may serve as a useful protein intermediate for attachment. In fact, based on the results achieved with intermediates of different molecular weights, a mixed group of proteins with distributed sizes may serve as an effective approach to create both tight binding and niches for cellular proliferation on the surface (Supplementary Figure S3: Appendix B). In the context of industrial algal production, protein lysates present in downstream processing water after oil extraction maybe serve as a low-cost and locally abundant feedstock for immobilized bioreactors.

While the structural stability of the hydrogels and cellulose films was examined for two weeks and two months, respectively, the integrity of the proteins bound to these surfaces was not investigated in the present study. Degradation over the lifespan of the bioreactor may result in reduced binding over time or cytotoxicity if the cells become directly exposed to BUDA/CDI or unreacted glutyraldehyde. This will likely vary with different protein intermediates used for binding and should be considered as an important performance indicator for potential scale-up. At the bench scale, this study has demonstrated that protein intermediates, such as FN and BSA, can enable monoculture biofilms to form on either a porous hydrated media or a crystalline thin film.

7.5 References

Aydınoğlu D, Şen S, Helvacıoğlu E, Nugay T, Nugay N (2013) Tuning of heavy metal removal efficiency from water via microalgae/hydrogel composites. e-Polymers 13: 163-179.

Berk V, Fong JCN, Dempsey GT, Develioglu ON, Zhuang X, Liphardt J, Yildiz FH, Chu S (2012) Molecular architecture and assembly principles of *Vibrio cholerae* biofilms. Science 337: 236-239.

Bernstein HC, Kesaano M, Moll K, Smith T, Gerlach R, Carlson R, et al. (2014) Direct measurement and characterization of active photosynthesis zones inside wastewater remediating and biofuel producing microalgal biofilms. Bioresource Technology 156: 206-215.

Danquah MK, Gladman B, Moheimani N, Forde GM (2009) Microalgal growth characteristics and subsequent influence on dewatering efficiency. Chemical Engineering Journal 151: 73-78.

De Bont JAM, Visser J, Mattiassen B, Tramper J (1990) Physiology of Immobilized Cells; Elsevier: Amsterdam, The Netherlands.

Eroglu E, Agarwal V, Bradshaw M, Chen X, Smith SM, Raston CL, Iyer KS (2012) Nitrate removal from liquid effluents using microalgae immobilized on chitosan nanofiber mats. Green Chem. 14: 2682-2685.

Flickinger MC, Schottel JL, Bond DR, Aksan A, Scriven LE (2007) Painting and printing living bacteria: engineering nanoporous biocatalytic coatings to preserve microbial viability and intensify reactivity. Biotechnology Progress 23: 2-17.

Greco Song H-H, Park KM, Gerecht S (2014) Hydrogels to model 3D in vitro microenvironment of tumor vascularization Advanced Drug Delivery Reviews. *In Press*

Guisan, JM (2006) Immobilization of Enzymes and Cells. Humana Press: Totowa, NJ.

Hawser SP, Islam K (1998) Binding of *Candida albicans* to immobilized amino acids and bovine serum albumin. Infection and Immunity 66: 140-144.

Jacobi A, Bucharsky EC, Schell KG, Habisreuther P, Oberacker R, Hoffmann MJ, et al. (2012) The application of transparent glass sponges for improvement of light distribution in photobioreactors. J Bioprocess Biotechniq 2: 113.

Johnson MB, Wen Z (2010) Development of an attached microalgal growth system for biofuel production. Appl Microbiol Biotechnol 85: 525-534.

Karel, SF, Robertson CR (1989) Autoradiographic determination of mass-transfer limitations in immobilized cell reactors. Biotechnol Bioeng 34: 320-336.

Karimi S, Tahir PM, Dufresne A, Karimi A, Abdulkhani A (2014) A comparative study on characteristics of nanocellulose reinforced thermoplastic starch biofilms prepared with different techniques. Nordic Pulp & Paper Res J 29: 41-45.

Martens N, Hall EAH (1994) Immobilisation of photosynthetic cells based on film-forming emulsion polymers. Analytica Chimica Acta 292: 49-63.

Nuttelman CR, Mortisen DJ, Henry SM, Anseth KS (2001) Attachment of fibronectin to poly(vinyl alcohol) hydrogels promotes NIH3T3 cell adhesion, proliferation, and migration. J Biomed Mater Res 57: 217-223.

Pankov R, Yamada KM (2002) Fibronectin at a glance. Journal of Cell Science, 115: 3861-3863.

Philipp WH, Hsu L-C (1979) Three methods for *in situ* cross-linking of polyvinyl alcohol films for application as ion-conducting membranes in potassium hydroxide electrolyte. NASA Technical Paper 1407.

Salim S, Bosma R, Vermuë MH, Wijffels RH (2010) Harvesting of microalgae by bio-flocculation. J Appl Phycol 23: 849-855.

Schatz D, Nagar E, Sendersky E, Parnasa R, Zilberman S, Carmeli S, et al. (2013) Self-suppression of biofilm formation in the cyanobacterium *Synechococcus elongatus*. Environ Microbiol. 15: 1786-1794.

Schnurr PJ, Espie GS, Allen DG (2013) Algae biofilm growth and the potential to stimulate lipid accumulation through nutrient starvation. Biores Technol, 136: 337-344.

Serra DO, Richter AM, Hengge R (2013) Cellulose as an architectural element in spatially structured *Escherichia coli* biofilms. Journal of Bacteriology 195: 5540-5554.

Smith MJ, Adam G, Duncan HJ, Cowling MJ (2002) The effects of cationic surfactants on marine biofilm growth on hydrogels. Estuarine, Coastal and Shelf Science 55: 361-367.

Teplitski M, Chen H, Rajamani S, Gao M, Merighi M, Sayre RT, et al. (2004) Chlamydomonas reinhardtii secretes compounds that mimic bacterial

signals and interfere with quorum sensing regulation in bacteria. Plant Physiol 134: 137-146.

Webb C, Dervakos GA (1996) Studies in Viable Cell Immobilization; Academic Press, RG Landes: Austin, TX.

Wijffels, RH (2001) Immobilized Cells. Springer-Verlag: Berlin, Germany.

Willert RG, Baron GV, De Backer L (1996) Immobilized Living Cells, Modeling and Experimental Methods; John Wiley & Sons: Chichester, UK.

8

L.E.A.V.E.S. – LAYERED EXPANSION OF ALGAE BY VIRTUE OF EFFLUENT SALVATION

Based on the lessons learned from the protein-mediated adhesion of algal monolayers on hydrogel and cellulose surfaces, this chapter employs the same transparent cellulose biopolymer to assess microbial combinations that may be well suited for lipid-rich algal biomass growth. The production of such biomass on an immobilized substrate requires biofilm thickness that was not readily achieved in monocultures. In order to engineer a mechanism to promote growth beyond monolayers, the present study employs similar biochemical coatings of fibronectin on cellulose to assist the adhesion of a cyanobacterial scaffold, in which a unicellular algal production organism can be implanted.

Initial bioprospecting of naturally isolated biofilms illustrated the complexities in natural biofilm ecology and morphology. Based on qualitative growth assessments in

chemically formulated media and wastewater effluents, a lead candidate biofilm with filamentous cyanobacteria was selected as a suitable scaffold to be paired with unicellular production organisms. To better understand the spatial and temporal dynamics applicable to algal biomass production in this biofilm configuration, advanced microscopy was used to evaluate the behavior of mixed populations of microalgae and cyanobacteria. Since co-culture populations involving natural microbial communities may not be easily or predictably balanced, the inclusion of *C. reinhardtii* expressing green fluorescent protein (GFP) in naturally isolated biofilms served to determine if a unicellular species of interest could inhabit this environment, thus enriching a biological scaffold of filamentous cyanobacteria with a desired species. These cells over-expressing GFP were also hypothesized to help visualize and track unicellular migration in the polyculture environment. To further dictate the microstructure and biomass composition of the complex algae biofilms relevant to biofuels, the natural cyanobacterial matrix was paired with the previously identified production strain *C. sorokiniana* UTEX 1230, capable of high rates of lipid biosynthesis. Ultimately, multi-layer biofilms with UTEX 1230 achieved a maximal thickness 100-150 µm with an estimated areal productivity of roughly 10 g m^{-2} d^{-1}.

8.1 Introduction

The potential to explore symbiotic relationships between photosynthetic cells and hetero– or mixotrophic microbes within polymicrobial biofilm communities is a design goal in order to both stabilize growth and expand the metabolic profile algal cultures. As seen in nature, polymicrobial biofilms can form readily; however,

monoculture biofilms can be difficult to establish. Having devised methods to adhere monocultures of microalgae in the previous chapter, this platform provides a substrate and architectural opportunity for outgrowth of algal organisms in multiple layers, such as filamentous cyanobacteria. Although similar approaches to algal biomass production with natural biofilms have been pursued, and reviewed in Chapter 5, researchers focusing on cyanobacterial mats have also sought to isolate naturally adherent filamentous cyanobacteria that possess favorable properties for biofuel production (Bruno *et al.* 2012). Cyanobacterial species from the *Trichormus, Anabaena,* and *Phormidium* genera may indeed offer additional biochemical advantages of lipid accumulation, but were not a focus of the present study.

The long-term objective of these biofilm co-cultures is to couple well-controlled adhesion of a biofilm scaffold with the heterotrophic strategy pioneered in Chapter 4 to enhance TAG composition in UTEX 1230. The organic substrates for heterotrophy may eventually be sourced from industrial or municipal effluent. Collectively, these aspects of *layered expansion of algae by virtue of effluent salvation* or *"L.E.A.V.E.S."* aim to address the bioprocessing challenges associated with current algal biofuel production practices by increasing microalgal lipid content and reducing water requirements. From both sustainability and economic standpoints, the incorporation of wastewater in photoautotrophic cultivation is a promising alternative to nitrogen and phosphorus fertilizers. To address nutrient sourcing, primary wastewater and anaerobic digester effluent (ADE) were evaluated by comparative growth curves and shown to support similar growth trends as UTEX

1230 in chemically formulated BBM. Notably, wastewater and ADE-based media was not sterilized before cultivation in order to examine the robustness of UTEX 1230 in an environment that may be encountered during industrial production.

With the component parts described in this chapter, the study lays some of the fundamental groundwork necessary to further develop this bio-*film*-reactor concept, which will be further strengthened by demonstrating its applicability with different nutrient sources and potential for two-stage bioprocessing. With these improvements and the eventual scale-up of L.E.A.V.E.S., this growth system may reduce energy investments in algal biofuel production by enabling transitions between different media and, ultimately, facilitating biomass harvesting. The most significant findings of this study demonstrate that the complex nature of photosynthetic biofilms co-cultured with unicellular algae can be revealed by fluorescent microscopy— rendering a unique glimpse into interactions between algae and cyanobacteria within these biofilm scaffolds. Lastly, this chapter will draw conclusions collectively from this dissertation in order to predict the potential benefits that increased lipid content, reduced water requirements, and alternative nutrient sources may have in improving the cultivation efficiency and ultimate cost of algal biofuel production.

8.2 Materials and Methods

8.2.1 Collection of biofilms from recirculating aquaculture & open waters

Naturally occurring photosynthetic biolfims were isolated from aquaculture tanks located at Clean Green Chesapeake, LLC as well as the Cylburn Aquaponics Farm

(Johns Hopkins School of Public Health). Marine organisms were collected from field excursions in the open waters of the Chesapeake Bay at the Choptank Oyster Farm (Cambridge, MD). When brought back to the laboratory, these samples were adapted to grow on both chemically formulated media (BBM and f/2) as well as wastewater and ADE from the Back River Wastewater Treatment Plant (BRWWTP). The biofilm communities isolated from field excursions were maintained on agar plates and in liquid media in 12-well tissue culture dishes containing cellulose film substrates at the bottom of each well.

8.2.2 Visual determination of biofilm thickness & multicellular structure

In order to study the morphology and fluorescent profile of multicellular algae biofilms using single planar illumination microscopy, biofilm samples were cultured on cellulose membranes or 1% agar for a minimum of one week before visualization with the Zeiss Lightsheet Z.1 microscope. Co-culture samples consisted of unicellular green algae *Chlamydomonas reinhardtii* expressing green fluorescent protein (GFP) or *Chlorella sorokiniana* UTEX 1230 grown as previously described media (TAP and BBM) before being introduced to natural algae biofilms. Z-stacks of these polymicrobial communities were collected using the available GFP (λ_{ex} = 488; λ_{em} = 507) and RFP (λ_{ex} = 587; λ_{em} = 610) filters. The Zeiss Lightsheet Z.1 was setup for automated image capture every 10 minutes for a 12-hr period in addition to short time courses, which were sufficient for visualizing the fast-moving flagellated *C. reinhardtii* cells. Natural biofilm samples co-cultured with *Chlorella sorokiniana* UTEX 1230 were visualized using the same methods with slight modifications to

sample preparation. For 1-2 mm^2 samples of biofilm, heat shrink fluorinated ethylene propylene (FEP) tubes (Zeus, Inc.) were used to take cylindrical sections containing algae biofilm growing on the top surface, similar to a punch biopsy (Kaufmann *et al.* 2012). Micrographs captured with the Zeiss Lightsheet Z.1 and rendered with the accompanying Zen software package.

8.2.3 Monitoring nutrient depletion in liquid algal cultures

Wastewater effluents were collected from the BRWWTP that houses two anaerobic digesters used to treat municipal solid waste in Baltimore, MD. Since secondary effluent from BRWWTP lacks a sufficient balance of nutrients to support microalgal growth, wastewater studies were carried out using a mixture of 10% ADE and 90% secondary effluent. This industrial media was filtered using a 1 mm^2 mesh screen to remove solid particulates, but was not sterilized. Nitrogen levels were measured as ammonia (NH_3/NH_{4+}) and nitrate (NO_{3-}) using the Freshwater Master Test Kit (API, New Jersey, USA). Phosphate (PO_4) was measured using phosphate test strips (Precision Laboratories, Arizona, USA).

8.3 Results

8.3.1 Isolation and characterization of natural photosynthetic biofilms

As a result of bioprospecting photosynthetic biofilms from various aquatic environments, over 70+ separate biofilm communities were isolated and maintained in chemically formulated media. Marine and brackish biofilms present at an oyster farm in a tributary to the Chesapeake Bay (Cambridge, MD) were maintained in f/2

media while all other freshwater organisms collected from tilapia tanks and hydroponics vegetable beds in Baltimore were grown in BBM.

Using cellulose thin films treated with fibronectin, each biofilm sample was first adapted to the respective media in 12-well culture plates for one month before qualitatively examining their growth on alternative nutrient sources. Each biofilm was covered with 3 cm of liquid media— one-tenth of the water requirement for modeled pond production in Chapter 2. Media exchange was performed periodically, although nutrient levels were not quantified at this scale. After one month of cultivation in this environment, the media in duplicate biofilm samples was transitioned to a mixture of primary wastewater and anaerobic digester effluent from the Back River Wastewater Treatment Plant (Baltimore, MD) to examine its potential to sustain these biofilms. Although all photosynthetic communities were found to adhere to cellulose and survive in chemically formulated media, long-term cultivation of these samples (6 months) was not as robust as the same microbial communities' proliferation in a mixture of 90% primary wastewater and 10% ADE (Figure 43). This result may indicate that there are additional unaccounted growth factors in municipal wastewaters. For example, the beneficial effects of bacteria found in the microalgal "microbiome" can provide vitamin B_{12} for green algae that require this micronutrient (Grant *et al.* 2014). While fungal contamination was also observed in some of the isolated biofilms, there were not major differences in the prevalence of fungus, mold, and bacterial contaminants between chemically defined media and the unsterile wastewater.

For selection of a cyanobacterial biofilm with suitable morphologies as a cyanobacterial matrix (*e.g.*, Chapter 5, Figure 25), general assessments were performed using both light and fluorescent microscopy. While many biofilms were encumbered by gelatinous exopolymer (Supplementary Figure S4: Appendix B), some freshwater biofilm isolates from the freshwater tilapia tanks showed impressive growth on solid substrates with minimal exopolymer material. These cyanobacterial mats were thought to be favorable scaffolds for unicellular algae due to their empty interstitial spaces and capability to form striated bands of filamentous cells that protrude from adhesion points. In addition to these unique surface morphologies, the lead candidate biofilms, demonstrated noticeable outgrowth starting from only a bound monolayer. Ultimately, one biofilm with the most rapid and dense growth (determined qualitatively) was selected for further investigation in co-culture with unicellular microalgae.

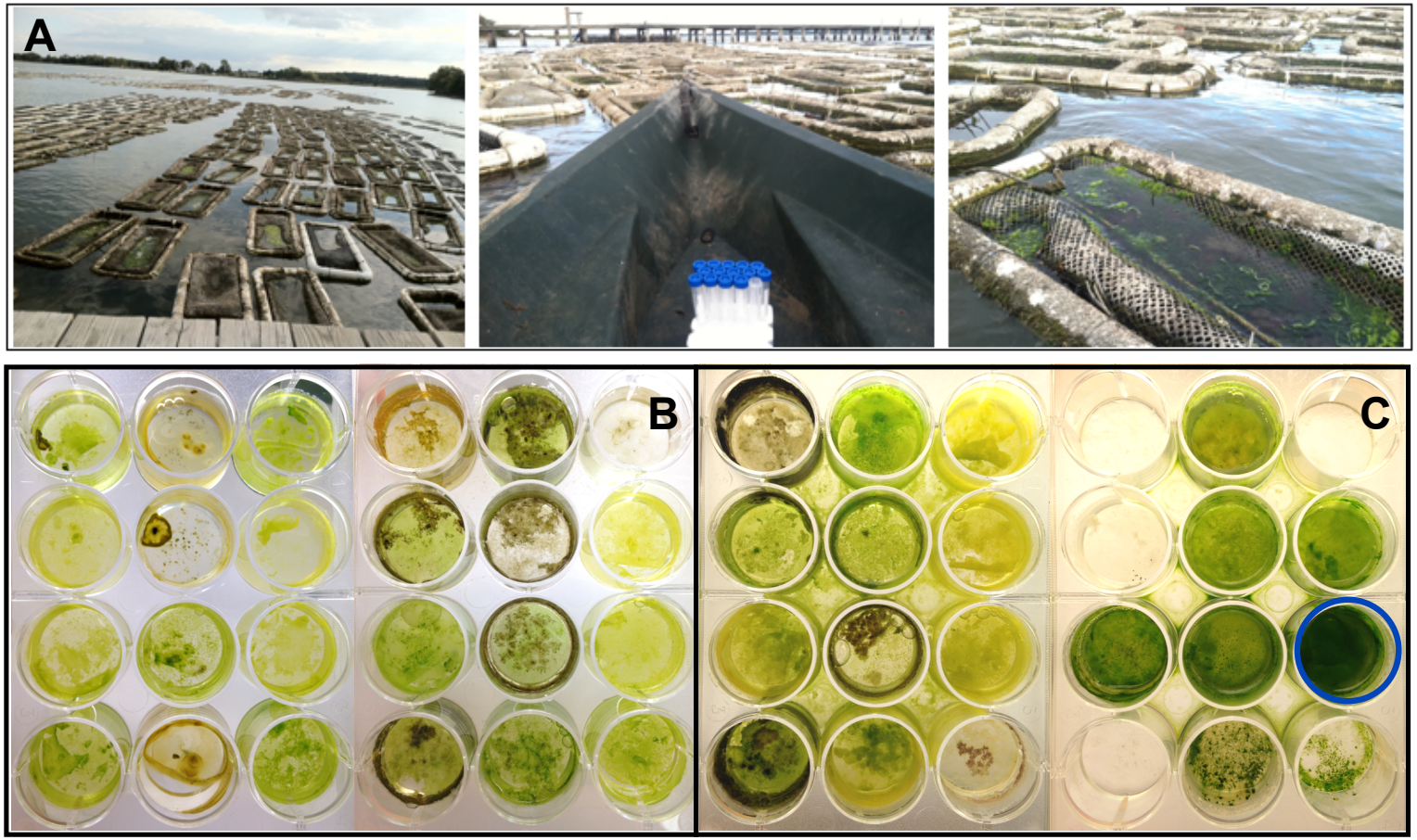

Figure 43. Collection, maintenance, and qualitative selection of natural biofilms on cellulose substrates. (A) An excursion to the Chesapeake Bay recovered biofilms from saline environments. Additionally, cultivation of freshwater isolates was compared between **(B)** BBM and **(C)** wastewater. After six months in culture, more dense growth was observed in the biofilms supplemented with wastewater. One lead candidate biofilm (blue circle) was selected for further characterization.

8.3.2 Preliminary evaluation with conventional fluorescent microscopy

The mixed populations of filamentous cyanobacteria, green algae, diatoms, flagellates, and bacteria found in these natural biofilms are inherently interesting to visualize by microscopy and photosynthetic cells are readily apparent by chlorophyll autofluorescence. For example, epifluorescence of a natural biofilm isolated from freshwater habitats is shown in Figure 44, using an inverted microscope to visualize the biofilm within a 12-well plate. Due to the three-dimensional shape and contours of the biofilm, self-shading becomes an issue when the focal plane is adjusted to visualize the multiple layers. Furthermore, due to the wide range of cell sizes and various intensities of chlorophyll autofluorescence, not all cell types can be adequately represented in the captured images. Due to the extremely bright autofluorescence of some of the larger filamentous cyanobacteria in these samples, the fluorescence of smaller unicellular organisms often becomes obscured. For the monolayer samples previously described in Chapter 7, conventional fluorescent and light microscopy using CyteSeeker to quantify cell abundance worked well. However, as the complexity of biofilm samples increases with polymicrobial multilayers, the spatial features of attachment and biofilm colonization cannot easily be observed in two-dimensional form. Additionally, these samples are susceptible to photobleaching during long exposures to laser illumination. As such, advanced microscopy equipment and sample preparation techniques may provide particular advantages when imaging biofilm samples with more complicated surface morphologies.

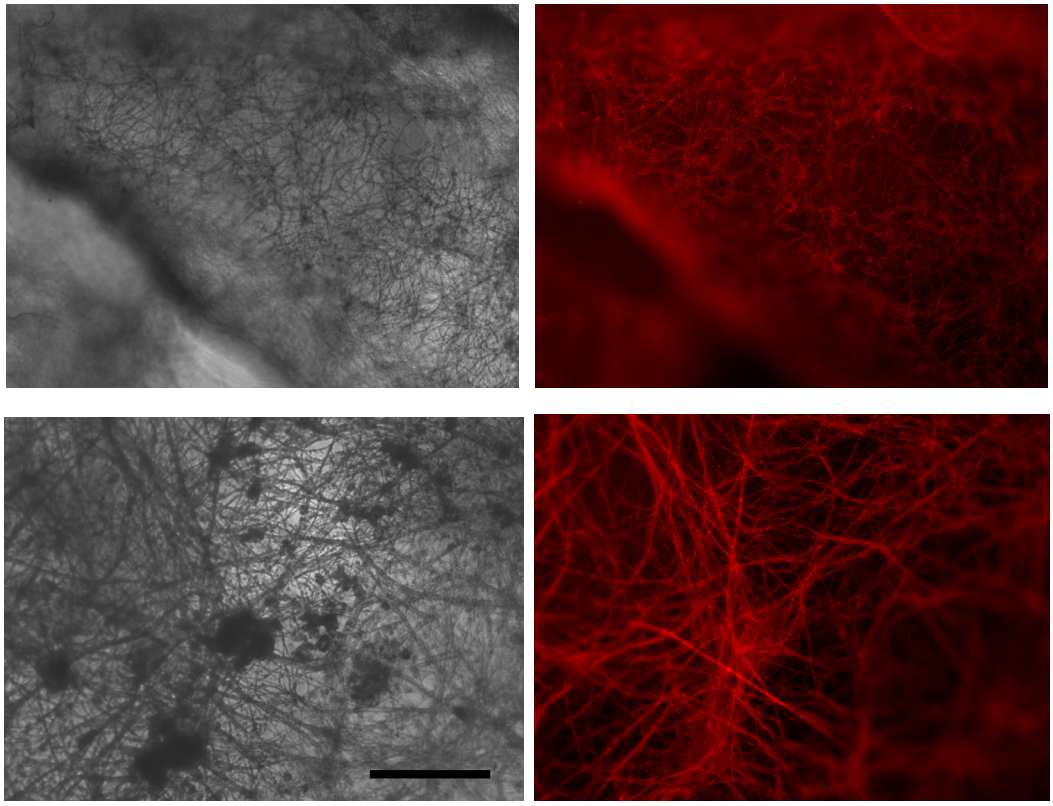

Figure 44. Conventional fluorescent microscopy of biofilm samples. Two separate sections of the same biofilm sample are observed under brightfield microscopy (left panels) compared to chlorophyll autofluorescence (left panels) at 20× magnification. Due to the morphology of the biofilm sample, a single focal plane cannot be easily chosen, which can degrade the integrity of the micrographs. Scale bar represents 10 µm.

Based on the unique traits and moderate sizes (> 1 mm^2) of these multicellular samples of photosynthetic tissue, Lightsheet microscopy proved to be an ideal technique to visualize the microstructure of algae biofilms. Using this technique of "single planar illumination" a thin cross-section of the sample is illuminated by laser light at the desrired excitation wavelength while a lens orthogonal to the excitation beam is used to capture fluorescent emissions. By exposing only a thin slice of the sample to laser light rather than the entire sample, Lightsheet microscopy can avoid photobleaching. Furthermore, the sample arm of the Zeiss Lightsheet Z.1 allows for rapid and facile control over the sample's position in the chamber and does not require fixatives or slide mounting to resolve the fine detail inherent to these intricate biofilm structures. As a result, sample preparation, loading, and image acquisition time are greatly reduced with the Lightsheet compared to confocal microscopy.

8.3.3 Spatial & temporal dynamics of biofilm co-cultures with microalgae

In order to overcome monolayer limitations observed in Chapter 7, a hybrid approach to growing biofilms was examined using the cellulose substrate and naturally occurring biofilm communities isolated from freshwater aquaculture tanks as a scaffold to generate biofilm thickness. Rather than relying on natural mechanisms of primary adhesion as common in prior literature (Bernstein *et al.* 2014; Schnurr *et al.* 2013), the surface of the cellulose film was treated, as before, with BUDA/CDI and FN to promote assisted cellular adhesion. After seeding the biofilm polyculture, consisting of predominantly filamentous cyanobacteria, and

allowing one week of outgrowth (Figure 45A, inset), *Chlamydomonas reinhardtii* cells expressing green fluorescent protein (GFP) were introduced to the liquid culture at t_0 to determine if they would colonize the biofilm scaffold. Using single planar illumination microscopy (*i.e.,* Lightsheet microscopy), these biofilm samples were quickly and easily visualized both in real-time and using automated image acquisition overnight.

The inherent landscape and microenvironment of the biofilm was found to be surprisingly barren, with substantial voids in microbial continuity, which appear as black areas in the micrographs (Figure 45A). Over the course of 12-hours, images captured once every 10 minutes show a merge of fluorescent signals from both GFP (green/yellow) and chlorophyll autofluorescence (red) (Figure 45B). Contrary to the results achieved with hydrogel attachment, *Chlamydomonas* cells failed to colonize the interstitial spaces of the natural filamentous scaffold and, therefore, performed poorly as a biomarker.

However, by capturing the behavior of these cells in real-time with a 20 second video, continuous laser excitation induced rapid phototaxis toward the plane of focus (Figure 45C). Although some *C. reinhardtii* cells remained attached to the filamentous cyanobacteria throughout the period of constant illumination, a flock of other cells quickly converged at the biofilm surface. While this surprising result confounded the intention to view the stationary position of these *C. reinhardtii* cells, it demonstrates that the undisturbed state of the biofilm is not nearly close to reaching is maximal packing density. Thus, the natural algal/cyanobacterial biofilms

exhibit some inefficiencies in volumetric utilization of possible photosynthetic space. Furthermore, it shows that this particular biofilm community does not rely on a thick exopolymer matrix or other secreted biopolymers, thus leaving significant potential for unicellular algae to inhabit the open portions of biofilm and possibly reach the higher packing densities achieved with previously examined formulations of latex binding agents (FLICKINGER *et al.* 2007).

Figure 45. ***(next page)*** **Time-course evaluation of cell migration in natural biofilms**. Using fluorescent microscopy, **(A)** a representative region of the biofilm surface with relatively sparse network of filamentous cyanobacteria and GFP-expressing *C. reinhardtii* cells. In order to visualize the behavior on single cells within the natural biofilm over longer periods of time, **(B)** the panel of overnight (12-hr) image captures demonstrate that *C. reinhardtii* does naturally colonize the cyanobacterial mat. Conversely, snapshots from a real-time video of **(C)** show that *C. reinhardtii* cells respond quickly to illumination by swimming into the frame of view and occupying open spaces in the biofilm. Scale bars in these micrographs represent 50 µm, while the photograph shows a 1 cm^2 section of biofilm growing on cellulose.

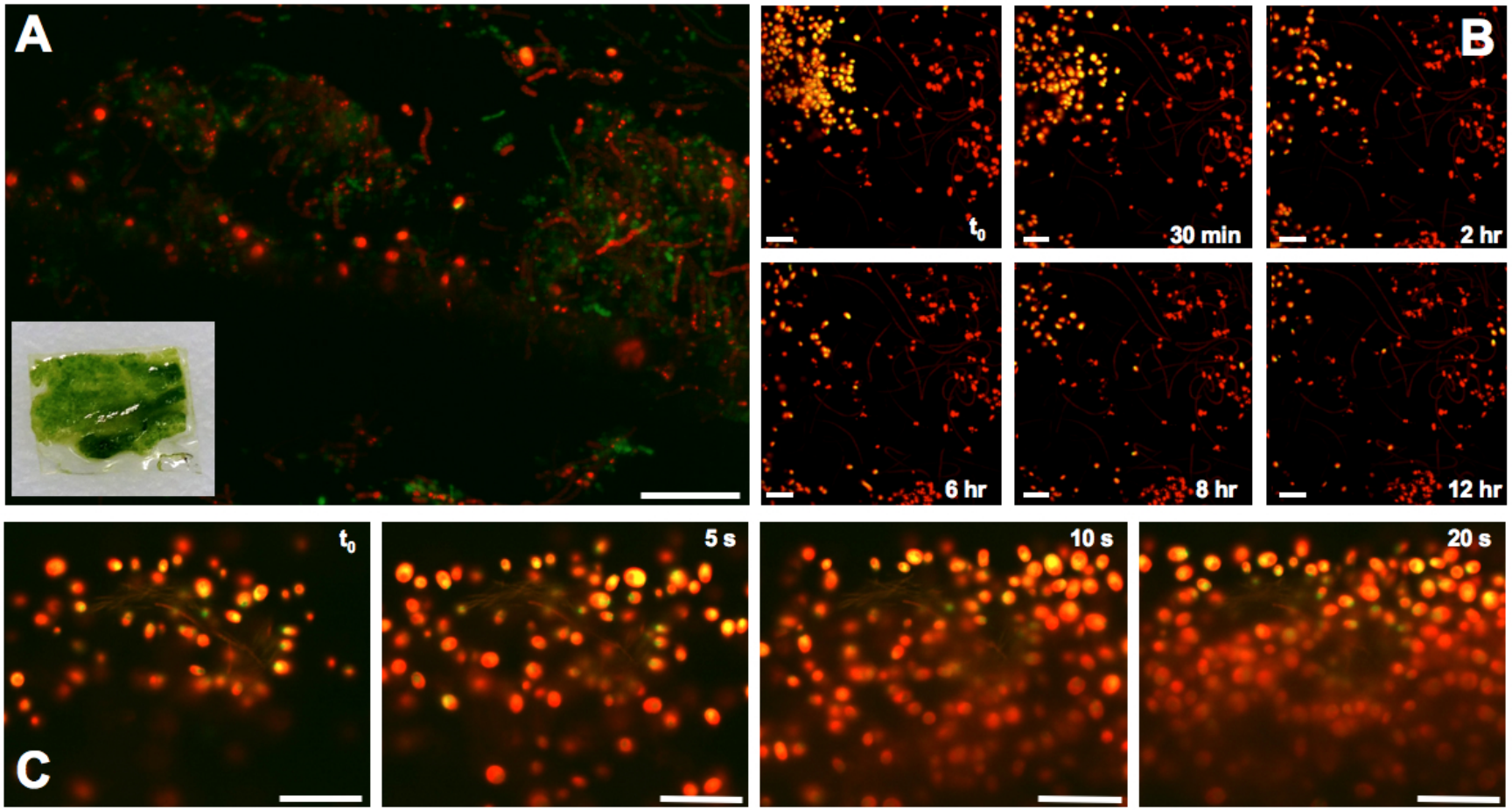

Figure 45. Time-course evaluation of algal cell migration in natural biofilms. **(A)** Surface topography of a filamentous biofilm co-cultured with *C. reinhardtii* (yellow). Panels **(B & C)** show 12-hr and 20-sec behavior, respectively.

8.3.4 Visualizing the proliferation of unicellular UTEX 1230 in biofilms

In order to observe the behavior and morphology of single *C. sorokiniana* cells implanted within a natural biofilm, co-cultures were prepared by growing biofilms on cellulose substrates for up to one week before introducing UTEX 1230 to liquid media. A "punch biopsy" approach was an effective method to maintain a liquid interface at the top of the biofilm while constraining a circular section of the immobilized culture within a transparent plastic tube. Furthermore, the long aspect ratio of the tube permitted stacking of multiple biofilm samples, which greatly reduced the time required to screen these different specimens (Supplementary Figure S5: Appendix B).

The resulting micrographs allowed for further characterization of the biofilm microenvironment and its potential as a scaffold in which to seed the known oil producer *C. sorokiniana* UTEX 1230. It was difficult to visualize all species at the same time due to differential photosynthetic pigmentation. Therefore, images of cyanobacterial mats and unicellular algae were captured using different exposures. As seen in Figure 46, a much richer image can be captured with the Lightsheet by using a rapid z-stack or a maximum intensity projection compared to previous fluorescent micrographs. While these renderings can also be accomplished with confocal fluorescence microscopy, the Lightsheet allows the specimen to be rotated to render exquisitely detailed 3D images of biofilm development. Furthermore, this technique is ideal for biofilm samples, since the specimen should be larger than single cells in suspension, but not greater than 5 mm^2.

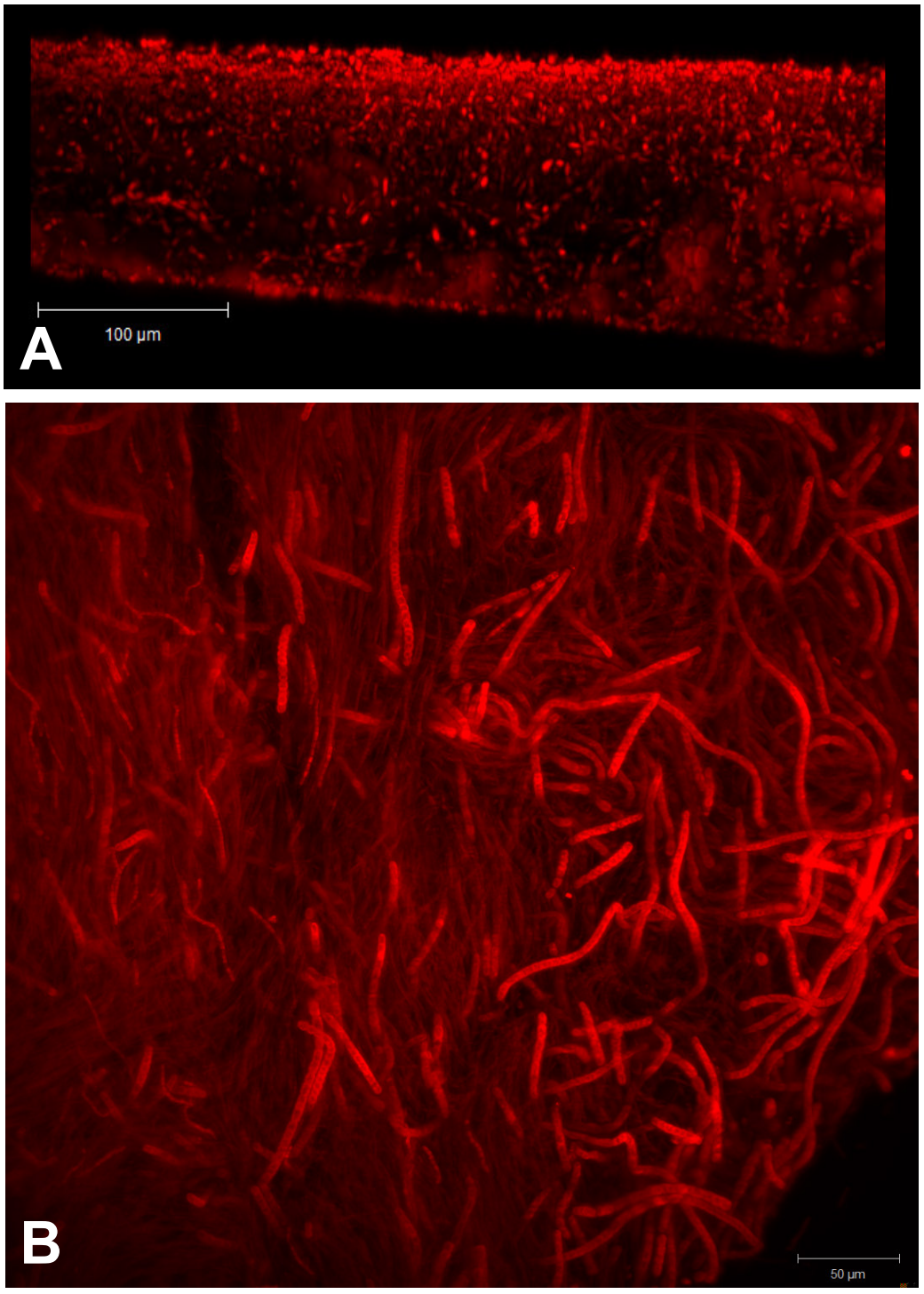

Figure 46. Three-dimensional microscopy of a photosynthetic biofilm co-culture. **(A)** Cross-section of the biofilm acquired using a rapid z-stack and **(B)** a maximum intensity projection of the underside of this biofilm both show autofluorescence from the cultured biofilm of *C. sorokiniana* UTEX 1230 and natural cyanobacteria co-existing in a multi-layer formation.

As seen in Figure 46, the underside of this cyanobacterial mat is a densely populated monolayer (Figure 46B) that give rise to the 100-150 µm thick biofilms. Figure 46A shows the side-view of this scaffold focusing on the single Chlorella cells, which appear dispersed throughout the volume of the biofilm. Moreover, there is a notable prevalence of these unicellular algae proliferating at the top illuminated surface. The biofilms appeared to reach a maximal thickness of roughly 150 µm within two days of cultivation and did not exceed this vertical length with prolonged culture times. Therefore, this critical length of multi-layer biofilm formation may have been dictated by the maximum length of cyanobacterial filaments in this particular polymicrobial community. When cultivated under these laboratory conditions, the average dry weight of various samples was roughly 1 mg cm^{-2} d^{-1}, which corresponds to an estimated areal productivity of 10 g m^{-2} d^{-1}.

8.3.5 Examining alternative nutrient sources for microalgal cultivation

To demonstrate that nitrogen and phosphorus in chemically formulated BBM can be replaced with low-cost alternatives, the growth of *C. sorokiniana* UTEX 1230 was examined using locally sourced municipal wastewater and nutrient-rich effluent from the Back River Wastewater Treatment Plant (BRWWTP). Since these biofilms were already known to grown well in this wastewater media, experiments aimed to quantify growth and nitrogen removal efficiency in liquid cultures of UTEX 1230 for ease of measurement. Since it is not economically feasible to sterilize large volumes of autotrophic media for biofuel production, wastewater samples used to support algal

growth in the current study were not sterilized of biological contaminants.[9] The progression of these non-sterile cultures was monitored from two important perspectives. First, growth curves were measured with respect to a nitrogen budget to assess the types of bioavailable nitrogen and their depletion rates. Secondly, frequent culture diagnostics by microscopy were able to decipher the presence of contaminant algal species. The growth curves and nutrient status of wastewater cultures is shown in Figure 47, which exhibit comparable rates of growth achieved in BBM, exceeding 100×10^6 cells ml^{-1} after two weeks. While BBM contains N in the form of nitrate (NO_{3-}) alone, both ammonia (NH_3/NH_{4+}) and nitrate (NO_{3-}) are present in ADE and wastewater. In both liquid media, N depletion curves reflect biomass generation while phosphate remained in excess of its biological demand.

Despite the occurrence of other algal species from BRWWTP effluent (Figure 48), UTEX 1230 exerted dominance in these liquid cultures. While bacterial contamination can compromise the integrity of algal cultures for nutritional or bioenergy applications, bacterial populations can be kept at manageable levels with the inclusion of low concentrations of common antibiotics and will not compete with photoautotrophic algae without sufficient organic matter. Anaerobic digestion at elevated temperatures may also help to reduce the bioload of aerobic microbes, but non-negligible amounts of predatory amoeba and rotifers may persist. Recent

[9] Sludge from the Back River Wastewater Treatment Plant is categorized as Class B, EPA Solid Waste under the Clean Water Act, Laws and Regulations: 40 CFR Part 503 (personal communication, Mike Gallagher, BRWWTP Manager).

developments in biological control of microbial predators and biocontaminants will likely be able to combat this burden in the future (McBride *et al.* 2014). In terms of the NH_3/NH_{4+} and NO_{3-} composition in ADE/wastewater, the interdependency between nitrogen metabolism and extracellular ion balance may help to stabilize pH and other biochemistries of autotrophic media (Scherholz & Curtis 2013).

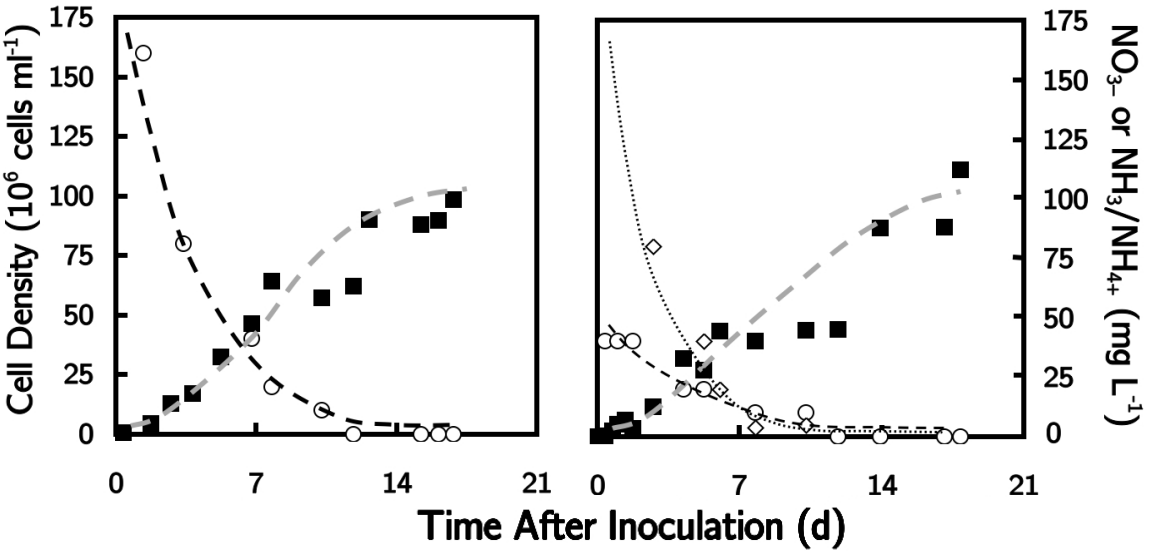

Figure 47. Comparison of UTEX 1230 growth with alternatively sourced autotrophic nutrients. Cell concentration (■) and nitrogen depletion curves in different autotrophic media demonstrate that *Chlorella sorokiniana* UTEX 1230 not only exhibits comparable growth on different chemical sources of nitrogen, but also performs well in low quality water. Separate 3-L batch cultures inoculated with **(A)** fully defined BBM as an axenic experimental control containing ample nitrate (NO_{3-}, ○) and negligible amounts of ammonia (NH_3/NH_{4+}, ◇) were compared to **(B)** a non-sterile mixture of ADE and secondary wastewater effluent containing both NO_{3-} and high levels of NH_{4+}. Phosphate levels in both BBM (100 mg L^{-1}) and the wastewater (25 mg L^{-1}) remained relatively unchanged throughout the course of cultivation. The standard deviation for each measured cell density is less than 5×10^6 cells ml^{-1} based on three technical replicates.

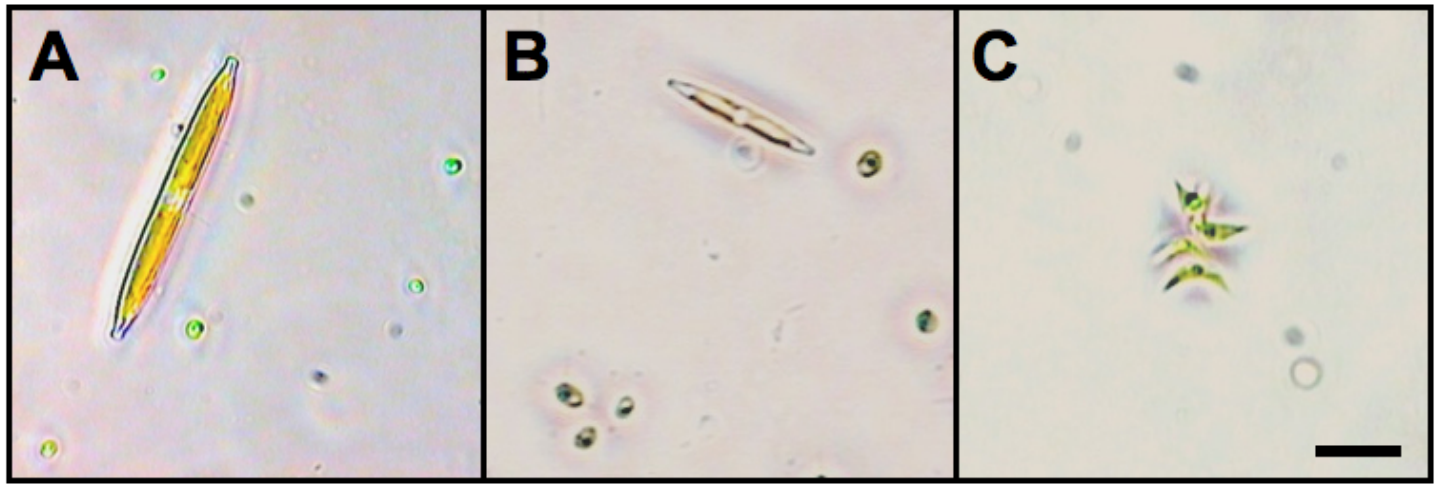

Figure 48. Representative micrographs featuring naturally occurring microalgae in primary effluent from Back River Wastewater Treatment Plant. Various pennate diatoms (**A and B**), presumably *Navicula* species, and coenobia of *Scenedesmus* cells **(C)** were identified by morphology. The spherical green cells surrounding the natural isolates are unicellular *Chlorella* spp. examined in this study. Scale bar = 10 µm. Figure adapted from a manuscript submitted by Bohutskyi *et al.* (2014).

8.4 Discussion and Conclusions

Using a hybrid system combining protein-mediated substratum attachment with the natural extension of a cyanobacterial mat, biofilms co-cultured with unicellular algae were able to reach thicknesses well beyond 10 µm monolayers. The initial experiments in this chapter allowed the topography of these biofilms to be explored using *C. reinhardtii* and a fluorescent biomarker. Interestingly, GFP-expressing *Chlamydomonas* cells were surprisingly motile and fleeting when not directly attached to any substrate (Figure 45B). While previously able to colonize hydrogels with protein linkers, *C. reinhardtii* was not only unable to colonize the interstitial spaces of a cyanobacterial biofilm over the course of 12-hours, but the cells actually migrated away from the previously inhabited locations of the biofilm. Conversely, the laser excitation of fluorescent microscopy caused incredibly rapid phototaxis. This unexpected result of our measurement technique coincidentally provided an artificial stimulus to motivate these motile cells to invade the biofilm and enabled visualization of the maximal cell packing density. This result also suggests that similarly high densities of unicellular algae may be present at the surface of these biofilms when grown under continual illumination. Since, *C. reinhardtii* was grown in mixotrophic TAP media, the localization of these cells at the biofilm surface may not have been as strongly dependent on exposure to light.

By coupling the lead candidate production strain *Chlorella sorokiniana* UTEX 1230 with these same biofilm scaffolds, the technical objective to create a membrane growth system to reduce energy and water inputs with the potential for lipid

enhancement was achieved. Unlike *C. reinhardtii*, UTEX 1230 was grown in photoautotrophic BBM and did, in fact, exhibit preferential growth at the top surface of the biofilm, as shown in Figure 46A. Most importantly, this micrograph demonstrates that the maximal achievable biofilm thickness of 150 µm can be grown in two days, which may correspond to an areal productivity of 75 g m^{-2} d^{-1} (wet biomass) based on volume alone. This matches similar estimates of 75-100 µm thick biofilms correlating to 75-100 g m^{-2} d^{-1} (Oyler *et al.* 2012); however, actual dry weight measurements of the biofilms in this study correspond to approximately 10 g m^{-2} d^{-1} due roughly 15% solids in the hydrated biofilm. Prior estimates may have also assumed a much higher density cell packing. Recently, *Chlorella sorokiniana* biolfilms grown in a well-optimized "Algadisk" reactor have achieved roughly 300 µm thickness and as much as 20 g m^{-2} d^{-1} when supplemented with CO_2 (Blanken *et al.* 2014). Similarly thich biofilms have been grown with *B. braunii*, but reaching much lover areal productivities (~1 g m^{-2} d^{-1} (Ozkan *et al.* 2012). However, both of these transpiration-based systems suffer from high rates of water loss (1-7 L m^{-2} d^{-1}), which were not observed in our closed biofilm cultivation system. Furthermore, as demonstrated by Bernstein *et al.*, a thin biofilm may reduce the negative effects of O_2 build-up within the biofilm substratum (2014). Higher areal productivities conferred by thicker biofilms may not only have detrimental effects on mass and gas transfer, but could require an additional burden of frequent harvesting (Bernstein *et al.* 2014; Murphy & Berberoğlu 2014b). While cellulose substrates and other biopolymers were thought to be useful and harvested together at the end of the bio-

film-reactor's lifespan, nutrient deprivation may also be used as a tactic to harvest biomass (SCHNURR *et al.* 2013).

8.5 Overall Impact and Future Directions

In order to connect increased algal oil yields afforded by organic nutrients and water reductions during growth on biofilms to improved economic projections of algal biofuel, we will revisit the tornado plot (Figure 9) of Chapter 2, which defined the baseline cost sensitivities. First, the TEA framework used in this thesis predicts that the slightly lower areal productivity of 10 g m^{-2} d^{-1} would result in an additional \$7.59 gal^{-1} to the baseline cost of production (COP), making the starting point for biofuel production using this particular biofilm growth system \$23.11 gal^{-1}. Although the biofilms examined in the present study did not achieve significantly higher areal productivities than the raceway ponds modeled in Chapter 2, the cost reductions associated with minimal water usage may hold greater gains to mitigate some burdens associated with raceway pond production.

8.5.1 Potential benefits of water reduction enabled by biofilm growth

Slightly lower areal productivities on biofilm reactors may indeed be balanced by the considerable reductions in water usage, which would otherwise dominate the capital and operating costs of paddlewheel-driven raceway ponds. Areas of an algal biorefinery cost structure that could be reduced by L.E.A.V.E.S. include essentially all aspects of associated raceway ponds and water handling— eliminating the need for a pond liner, flocculant for harvesting, and extensive paddlewheel mixing. The 3

cm of water used to culture biofilms in this study represents a 90% reduction in resident liquid volume compared to raceway ponds, which may fundamentally re-define the sustainability profile of algal biofuels, especially for arid regions were water scarcity is a serious issue.

For hypothetical deployment of biofilm growth systems to replace pond production in the TEA model, diminished energy inputs for paddlewheel operation can reduce COP by \$1.59 gal^{-1}; eliminating flocculant material costs further decreases COP by \$1.74 gal^{-1}; and removing of the pond liner from capital costs would result in a \$1.63 gal^{-1} reduction. However, assuming that the double-lined transparent polyethylene covering and associated support structure could serve as a close approximation of a system used for biofilm growth, this capital still contributes \$2.05 gal^{-1} to the COP. This existing greenhouse-like pond cover has a lower membrane for biofilm attachment and an upper transparent membrane for containment with 3+ cm available in between for a liquid interface and gas exchange. Presumably, the self-contained system would effectively minimized evaporative losses and biofilm growth conditions would remain well controlled. Based on the TEA model for New Mexico, algal biofilm growth at 10 g m^{-2} d^{-1} with aforementioned reductions in water use and pond materials would still only result in a COP of \$18.15 gal^{-1}. Therefore, additional improvements in lipid content and nutrient sourcing must still be coupled with L.E.A.V.E.S. in order to achieve a COP that is more competitive with conventional raceway pond production.

8.5.2 Strategic enhancement of lipid content & quality with heterotrophy

Since increasing lipid content in algal biomass is paramount to the commercial feasibility of algal biofuels, the cultivation of UTEX 1230 cells within natural biofilms also enables potentially high total lipid contents with favorable TAG compositions to be achieved in heterotrophic co-culture. In Chapters 3 and 4, augmented total lipid contents exceeding 35% were shown to be possible with UTEX 1230 under heterotrophic conditions, and could result in COP reduction of at least \$4.33 gal^{-1}. While Chapters 3 and 4 addressed this biological aspect of algal biofuel production by investigating the influence of glucose on the growth kinetics and lipid biosynthetic patterns in UTEX 1230, refined sugar would certainly not serve as a viable feedstock for biofuel production. Other exogenous carbon sources that could be sustainability and inexpensively derived from food processing waste or wastewater effluents have demonstrated similar trends in *Chlorella* lipid induction (Yan *et al.* 2011). Furthermore, if heterotrophic lipid triggers are paired with leaf-like bioreactors in a two-stage process by transitioning from sunlight to organic carbon-rich effluents, the biochemical composition of the algal biomass can be strategically enriched with desired TAG (*i.e.*, lipids as extractable oil). Despite the potential for a 6.5-fold increase in TAG during staged bioprocessing, which may facilitate extraction, the nuanced relationship between fatty acid composition and extraction efficiency were not considered in this TEA model. Interestingly, there may be synergies between biofilm formation and heterotrophic growth. The preliminary transcriptomic analysis performed in Chapter 4 found the expression of fascilin genes with cellular adhesion properties to be co-regulated with heterotrophy, may help to

promote biofilm formation. Assuming that organic carbon can be sourced from waste streams, these changes in structure and composition of conventional algal culture using two-stage growth with L.E.A.V.E.S. would result in a COP of \$13.83 gal^{-1}, which is competitive with the predicted COP for raceway pond production based on a 10-year capital return on investment (\$15.52 gal^{-1}).

8.5.3 Co-localization with wastewater effluent & organic residues

As investigated in the present study (Figure 47), the integration of locally abundant primary wastewater and AD effluent in the cultivation of UTEX 1230 is a suitable replacement for chemically formulated N and P fertilizers. By reducing the nutrient inputs to algal biofuel production, COP can be further reduced by \$2.00 gal^{-1}. Furthermore, UTEX 1230 can be grown minimal CO_2 supplementation, thereby reducing operating costs resulting in a decrease in roughly \$1.00 gal^{-1}. In terms of nutrient recycle, the benefits of co-localization of microalgal production with a wastewater treatment plant are very attractive— not only for an essentially free source of N and P, but also close proximity to existing WWT equipment. Ideally, a side stream from primary effluent and ADE could be re-routed to an algal biorefinery and would eliminate the need for dedicated wastewater treatment processes within the algal farm (\$250M capital investment). As seen in Chapter 2, the availability of sufficient flat land surrounding an industrial or municipal facility can, however, be a limiting factor. For a two-stage process based on waste nutrients, the collective \$3.00 gal^{-1} COP reduction afforded by low CO_2, N, and P sourced from a waste feedstocks may offset any additional costs associated with a heterotrophic lipid induction stage.

Collectively, these assumptions could reduce the modeled cost of algal biocrude production to \$10.83 gal^{-1} for a 10-year capital return on investment. While each aspect of this improved bioprocess has been determined in separate studies, further investigations coupling the proposed advancements should be pursued. For example, while the pairing of *C. sorokiniana* UTEX 1230 in biofilms with wastewater has been demonstrated, heterotrophic studies have not yet been pursued on biofilm substrates. Furthermore, nutrient removal in wastewater was empirically determined in liquid cultures as opposed to biofilms. Nonetheless, the initial findings presented in this chapter encourage growth scenarios in which the *layered expansion of algae by virtue of effluent salvation* can be implemented.

Ultimately, two-stage cultivation of UTEX 1230 with L.E.A.V.E.S. combines the beneficial bioprocessing elements of (1) minimal water requirements for biofilms with the potential for (2) waste nutrient integration and (3) a final stage of lipid induction with UTEX 1230. Together, the impact of organic nutrients on lipid accumulation and potential role of engineered biofilms as a novel growth platform will be strengthened by further demonstrating their applicability at large scales. In particular, increasing the areal productivity of biofilm growth systems should be a focus of future research efforts. While algal biomass is poised to become a widely recognized feedstock, there remains a pressing need to quantify and forecast economic and sustainability improvements. In order to fully understand how algal biofuels may meaningfully contribute to our renewable energy portfolio, the biological productivity of novel cultivation strategies must be compared to the

technological baselines for current best practices. By connecting potential gains from unconventional microalgal cultivation with technoeconomic elucidation of bottlenecks in the algae production process, innovative biochemical and bioprocessing approaches may transform the future of algae as a next-generation biofuel feedstock.

8.6 References

Bernstein HC, Kesaano M, Moll K, Smith T, Gerlach R, Carlson R, et al. (2014) Direct measurement and characterization of active photosynthesis zones inside wastewater remediating and biofuel producing microalgal biofilms. Bioresource Technology 156: 206-215.

Bohutskyi P, Liu K, Nasr LK, Byers N, Rosenberg JN, Oyler GA, Betenbaugh MJ, Bouwer EJ (2014) Microalgal bioprospecting for integrated biofuel feedstock production and phycoremediation of municipal wastewater. Applied Microbiology and Biotechnology. *Submitted*

Blanken W, Janssen M, Cuaresma M, Libor Z, Bhaiji T, Wijffels RH (2014) Biofilm growth of *Chlorella sorokiniana* in a rotating biological contactor based photobioreactor. Biotechnology & Bioengineering. *In Press*

Bruno L1, Di Pippo F, Antonaroli S, Gismondi A, Valentini C, Albertano P (2012) Characterization of biofilm-forming cyanobacteria for biomass and lipid production. J Appl Microbiol 113 :1052-1064.

Flickinger MC, Schottel JL, Bond DR, Aksan A, Scriven LE (2007) Painting and printing living bacteria: engineering nanoporous biocatalytic coatings to preserve microbial viability and intensify reactivity. Biotechnology Progress 23: 2-17.

Grant MAA, Kazamia E, Cicuta P, Smith AG (2014) Direct exchange of vitamin B_{12} is demonstrated by modeling the growth dynamics of algal–bacterial cocultures ISME Journal 4.

Kaufmann A, Mickoleit M, Weber M, Huisken J (2012) Multilayer mounting enables long-term imaging of zebrafish development in a light sheet microscope. Development 139: 3242-3247.

Kazamia E, Czesnick H, Nguyen TTV, Croft MT, Sherwood E, Sasso S, et al. (2012) Mutualistic interactions between vitamin B_{12}-dependent algae and heterotrophic bacteria exhibit regulation, Environmental Microbiology 14 (6), 1466-1476.

McBride RC, Lopez S, Meenach C, M.Burnett, Lee PA, Nohilly F, Behnke C (2014) Contamination management in low cost open algae ponds for biofuels production. Industrial Biotechnology 10: 221-227.

Oyler GA, Rosenberg JN, Weeks DP (2012) Single chain antibodies for photosynthetic microorganisms and method of use. U.S. Application No. 13/441,951.

Ozkan A, Kinney K, Katz L, Berberoğlu H (2012) Reduction of water and energy requirement of algae cultivation using an algae biofilm photobioreactor. Bioresource Technology. 114: 542-548.

Razzak SA, Hossain MM, Lucky RA, Bassi AS, de Lasa H (2013) Integrated CO_2 capture, wastewater treatment and biofuel production by microalgae culturing—A review. Renewable and Sustainable Energy Reviews 27: 622-653.

Scherholz ML, Curtis WR (2013) Achieving pH control in microalgal cultures through fed-batch addition of stoichiometrically-balanced growth media. BMC Biotechnology 13: 39.

Schnurr PJ, Espie GS, Allen DG (2013) Algae biofilm growth and the potential to stimulate lipid accumulation through nutrient starvation. Bioresour Technol 136: 337-344.

Yan D, Lu Y, Chen Y-F, Wu Q (2011) Waste molasses alone displaces glucose-based medium for microalgal fermentation towards cost-saving biodiesel production. Bioresour Technol 102: 6487-6493.

APPENDIX A: PUBLISHER REPRINT PERMISSIONS

Chapters 1 & 2

This is a License Agreement between Julian N Rosenberg ("You") and Elsevier ("Elsevier") provided by Copyright Clearance Center ("CCC"). The license consists of your order details, the terms and conditions provided by Elsevier, and the payment terms and conditions.

Supplier	Elsevier Limited The Boulevard, Langford Lane Kidlington, Oxford, OX5 1GB, UK
Registered Company Number	1982084
Customer name	Julian N Rosenberg
Customer address	3400 North Charles St Baltimore, MD 21218
License number	3446110706734
License date	Aug 11, 2014
Licensed content publisher	Elsevier
Licensed content publication	Biomass and Bioenergy
Licensed content title	Microalgal biomass production and carbon dioxide sequestration from an integrated ethanol biorefinery in Iowa: A technical appraisal and economic feasibility evaluation
Licensed content author	Julian N. Rosenberg, Ashrith Mathias, Karen Korth, Michael J. Betenbaugh, George A. Oyler
Licensed content date	October 2011
Licensed content volume number	35
Licensed content issue number	9
Number of pages	12
Start Page	3865
End Page	3876
Type of Use	reuse in a thesis/dissertation
Portion	full article
Format	both print and electronic
Are you the author of this Elsevier article?	Yes
Will you be translating?	No
Title of your thesis/dissertation	Improving the cultivation efficiency of microalgae for biofuels: spanning biofilm and bioprocessing scales
Expected completion date	Oct 2014
Estimated size (number of pages)	300
Elsevier VAT number	GB 494 6272 12

Chapter 6

This is a License Agreement between Julian N Rosenberg ("You") and John Wiley and Sons ("John Wiley and Sons") provided by Copyright Clearance Center ("CCC"). The license consists of your order details, the terms and conditions provided by John Wiley and Sons, and the payment terms and conditions.

License number	3446240868813
License date	Aug 11, 2014
Licensed content publisher	John Wiley and Sons
Licensed content publication	Plant Journal
Licensed content title	Expanding the spectral palette of fluorescent proteins for the green microalga *Chlamydomonas reinhardtii*
Licensed copyright line	© 2013 The Authors The Plant Journal © 2013 John Wiley & Sons Ltd
Licensed content author	Beth A. Rasala, Daniel J. Barrera, Jenny Ng, Thomas M. Plucinak, Julian N. Rosenberg, Donald P. Weeks, George A. Oyler, Todd C. Peterson, Farzad Haerizadeh, Stephen P. Mayfield
Licensed content date	Apr 8, 2013
Start page	545
End page	556
Type of use	Dissertation/Thesis
Requestor type	Author of this Wiley article
Format	Print and electronic
Portion	Full article
Will you be translating?	No
Title of your thesis / dissertation	Improving the cultivation efficiency of microalgae for biofuels: spanning biofilm and bioprocessing scales
Expected completion date	Oct 2014
Expected size (number of pages)	300

Chapter 6

This is a License Agreement between Julian N Rosenberg ("You") and John Wiley and Sons ("John Wiley and Sons") provided by Copyright Clearance Center ("CCC"). The license consists of your order details, the terms and conditions provided by John Wiley and Sons, and the payment terms and conditions.

License number	3471880468677
License date	Sep 18, 2014
Licensed content publisher	John Wiley and Sons
Licensed content publication	Plant Biotechnology Journal
Licensed content title	Algal chloroplast produced camelid V_HH antitoxins are capable of neutralizing botulinum neurotoxin
Licensed copyright line	© 2014 Society for Experimental Biology, Association of Applied Biologists and John Wiley & Sons Ltd
Licensed content author	Daniel J. Barrera, Julian N. Rosenberg, Joanna G. Chiu, Yung-Nien Chang, Michelle Debatis, Soo-Mun Ngoi, John T. Chang, Charles B. Shoemaker, George A. Oyler, Stephen P. Mayfield
Licensed content date	Sep 17, 2014
Start page	n/a
End page	n/a
Type of use	Dissertation/Thesis
Requestor type	Author of this Wiley article
Format	Print and electronic
Portion	Full article
Will you be translating?	No
Title of your thesis / dissertation	Improving the cultivation efficiency of microalgae for biofuels: spanning biofilm and bioprocessing scales
Expected completion date	Oct 2014
Expected size (number of pages)	300

Chapter 6

This is a License Agreement between Julian N Rosenberg ("You") and John Wiley and Sons ("John Wiley and Sons") provided by Copyright Clearance Center ("CCC"). The license consists of your order details, the terms and conditions provided by John Wiley and Sons, and the payment terms and conditions.

License number	3446071074210
License date	Aug 11, 2014
Licensed content publisher	John Wiley and Sons
Licensed content publication	Plant Journal
Licensed content title	Generation of a phage-display library of single-domain camelid V_HH antibodies directed against *Chlamydomonas reinhardtii* antigens, and characterization of V_HHs binding cell-surface antigens
Licensed copyright line	© 2013 The Authors The Plant Journal © 2013 John Wiley & Sons Ltd
Licensed content author	Wenzhi Jiang, Julian N. Rosenberg, Akelia D. Wauchope, Jacqueline M. Tremblay, Charles B. Shoemaker, Donald P. Weeks, George A. Oyler
Licensed content date	Oct 17, 2013
Start page	709
End page	717
Type of use	Dissertation/Thesis
Requestor type	Author of this Wiley article
Format	Print and electronic
Portion	Full article
Will you be translating?	No
Title of your thesis / dissertation	Improving the cultivation efficiency of microalgae for biofuels: spanning biofilm and bioprocessing scales
Expected completion date	Oct 2014
Expected size (number of pages)	300

THE NATIONAL ACADEMIES PRESS

Marketing Department
Rights & Permissions

August 19, 2014 **Reference #: 08191400**

Julian N. Rosenberg
Department of Chemical & Biomolecular Engineering
Johns Hopkins University
3400 N. Charles St.
Baltimore, MD 21218

Dear Mr. Rosenberg:

You have requested permission to reproduce the following material copyrighted by the National Academy of Sciences in a dissertation:

Figure 6-3, Sustainable Development of Algal Biofuels in the United States, 2012

Your request is granted for the material cited provided that credit is given to the copyright holder. Nonexclusive rights are extended for noncommercial use of this material.

Suggested credit (example):
Reprinted with permission from (title), (year) by the National Academy of Sciences, Courtesy of the National Academies Press, Washington, D.C. (This credit may be edited pursuant to the publisher's house style and format so long as the essential elements are included).

Thank you,

Barbara Murphy
Permissions Coordinator
National Academies Press

THE NATIONAL ACADEMIES
Advisers to the Nation on Science, Engineering, and Medicine

500 Fifth Street, NW
Washington, DC 20001

Phone: 202 334 1960
Fax: 202 334 2451
E-mail: bmurphy@nas.edu
Web: www.nap.edu

APPENDIX B: SUPPLEMENTARY INFORMATION

Chapter 2: Process Flow Diagrams

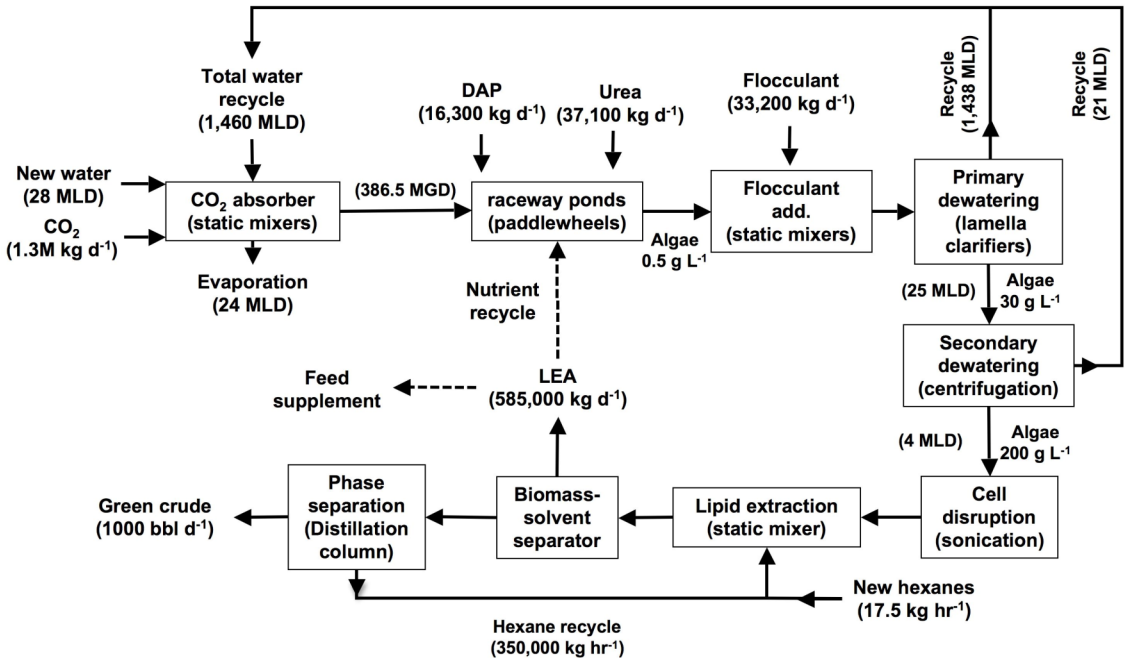

Overall process flow diagram of entire algal biofuel production pathway with associated mass flow rates in SI base units (*e.g.,* MLD = million liters per day). Top row shows upstream algae growth before primary and secondary dewatering lead to downstream processing of algal oil (bottom row). More detailed operating conditions for the separate stages of this process are shown on the following pages as segments the Aspen Plus model.

Upstream ASPEN Model

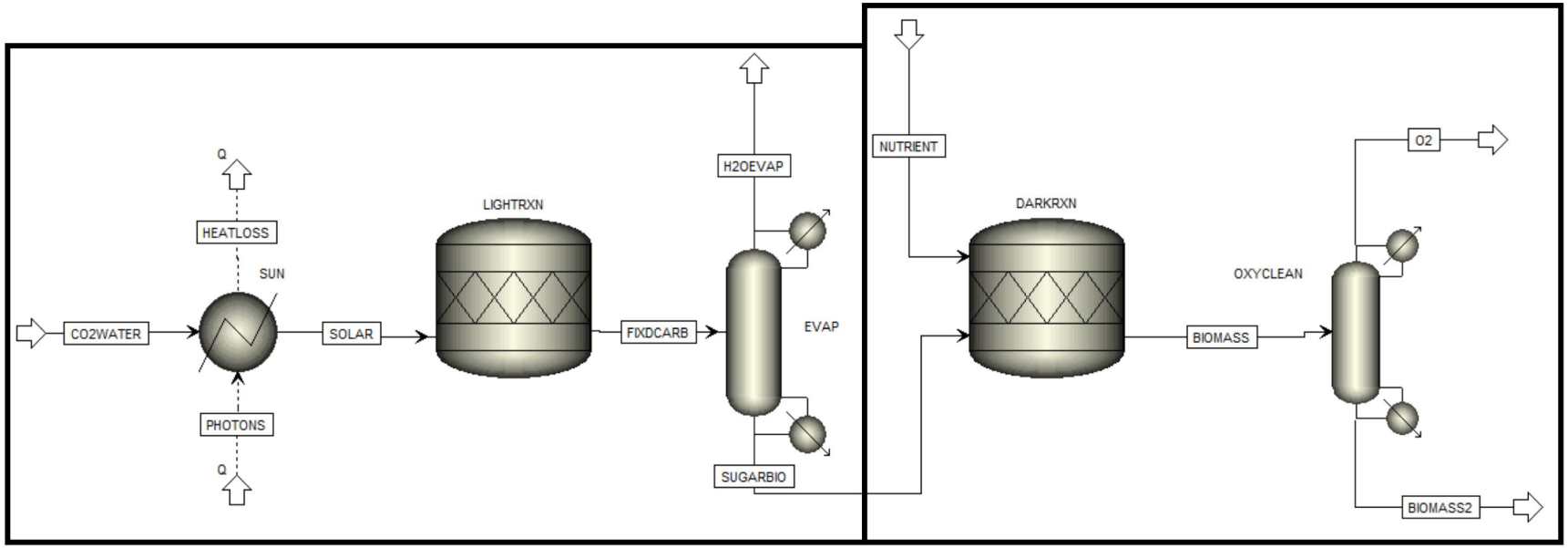

Photosynthesis

$$6CO_2 + 6H_2O \longrightarrow C_6H_{12}O_6 + 6O_2$$

- Solar energy input as heat to system - **SUN (Heater)**
- CO_2 feed based on mass balance for biomass
- Water = pond + evaporation + conversion to algae
- **LIGHTRXN (RStoic); EVAP (Splitter)**

Biosynthesis

$$\mathbf{55.2}C_6H_{12}O_6 + \mathbf{14.7}CO(NH_2)_2 \longrightarrow \mathbf{6}C_{18}H_{30}O_2 + \mathbf{10.2}C_6H_{10}O_5 + \mathbf{29.5}C_6H_{11}NO + \mathbf{57.7}H_2O + \mathbf{98}O_2$$

- **DARKRXN (RStoic); OXYCLEAN (Splitter)**
- Soitchiometry of reaction to yield:
  25% lipid, 25% carbohydrate, 50% protein (by mass)

Downstream ASPEN Model

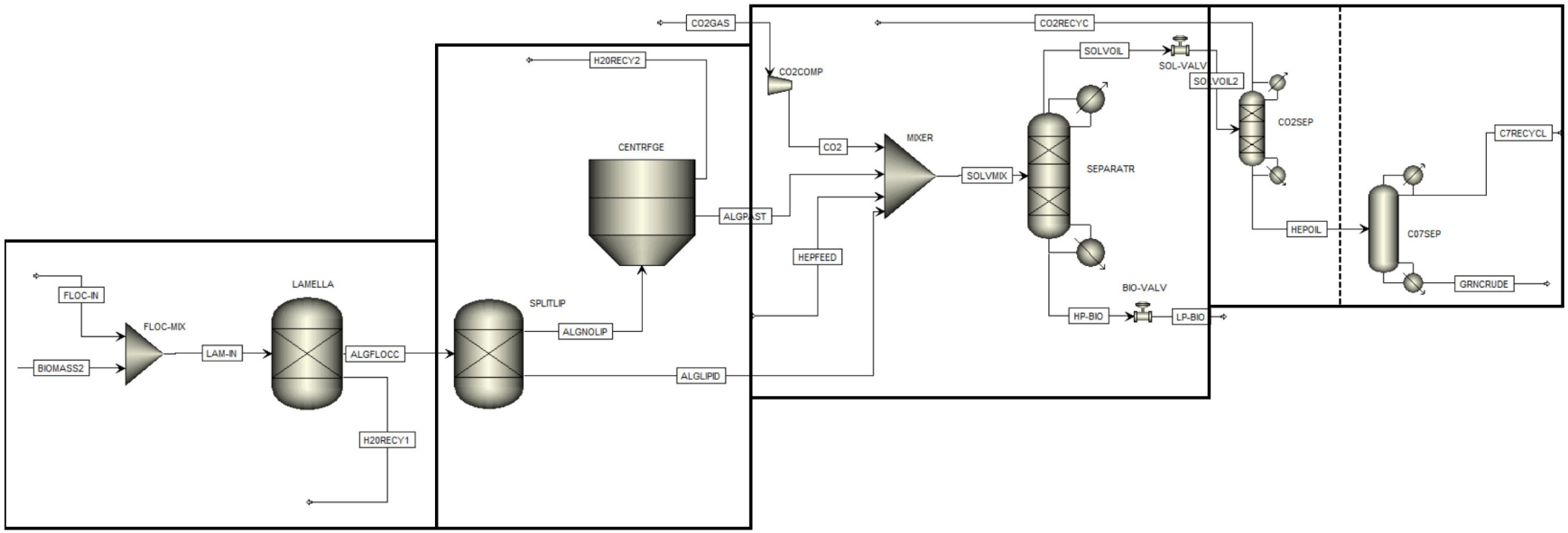

Flocculation:	**Centrifugation**:	**Lipid Extraction:**	**Solvent & Oil Recovery:**
Whole cell concentration *Water recycle* • **FLOC-MIX** 0.02% flocculant added • **LAMELLA** 0.5 --> 30 g L^{-1} (3% solid)	*Solids separation* *Water recycle* • **SPLITLIP** * *Lipid stream* • **CENTRFGE** 30 --> 200 g/L *Carb & Protein*	 • **MIXER** * *Dewatered biomass + oil* *Add CO_2 & C7 solvent* • **SEPARATR** • 80% efficiency • 3% CO_2 in H_2O	• **CO2SEP** 1 atm, T = 25 °C CO_2 in gas phase C7 + C18 in liquid • **C7SEP (Distillation)** 4 stages, T = 99 °C 99.9% pure

Chapter 2: Capital and Operating Costs for Raceway Pond

Table S1. Capital cost for the construction of a quarter-acre covered raceway pond

Materials for ¼ Acre Raceway Pond	Cost
Low Grade Land	$750
Excavation	$500
Pond Lining	$5,000
Double Layer Polyethylene Glazing	$1,500
Paddle Wheel Motor	$2,600
Greenhouse Structure	$5,000
CO_2 Supply System	$5,000
Total	**$20,350**

Table S2. Annual operating costs for a quarter-acre covered raceway pond

Productivity (g m^{-2} d^{-1})	20	30	40	60
Electricity	$370	$660	$1,130	$2,310
Labor	$750	$750	$750	$750
Nutrients	$880	$1,330	$1,770	$2,650
Flocculant	$260	$390	$520	$770
Heating	$14,850	$14,850	$14,850	$14,850
Total Cost	**$17,100**	**$17,970**	**$19,010**	**$21,330**

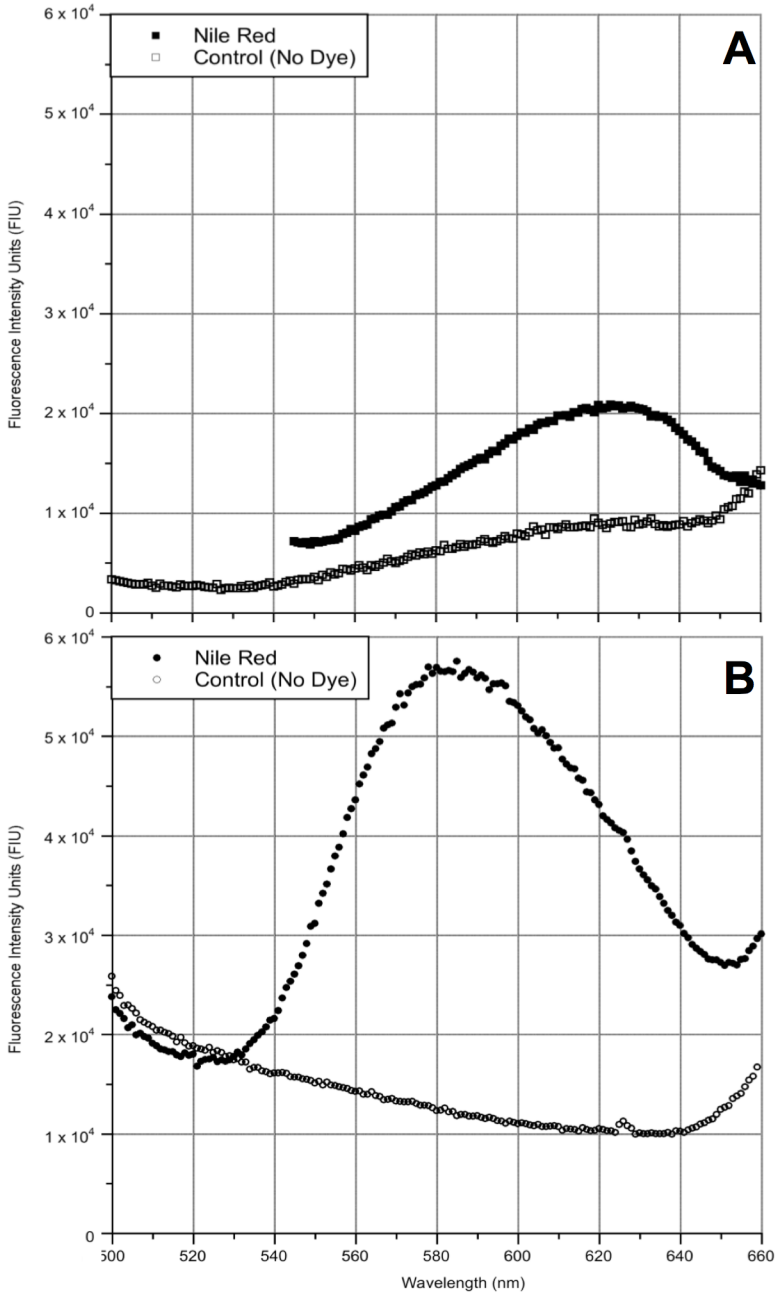

Figure S1. Nile Red fluorescent emission curves of *C. sorokiniana* UTEX 1230. The shifts in emission peaks from UTEX 1230 cultivated under **(A)** autotrophic and **(B)** heterotrophic conditions implicate more significant lipid accumulation during heterotrophy.

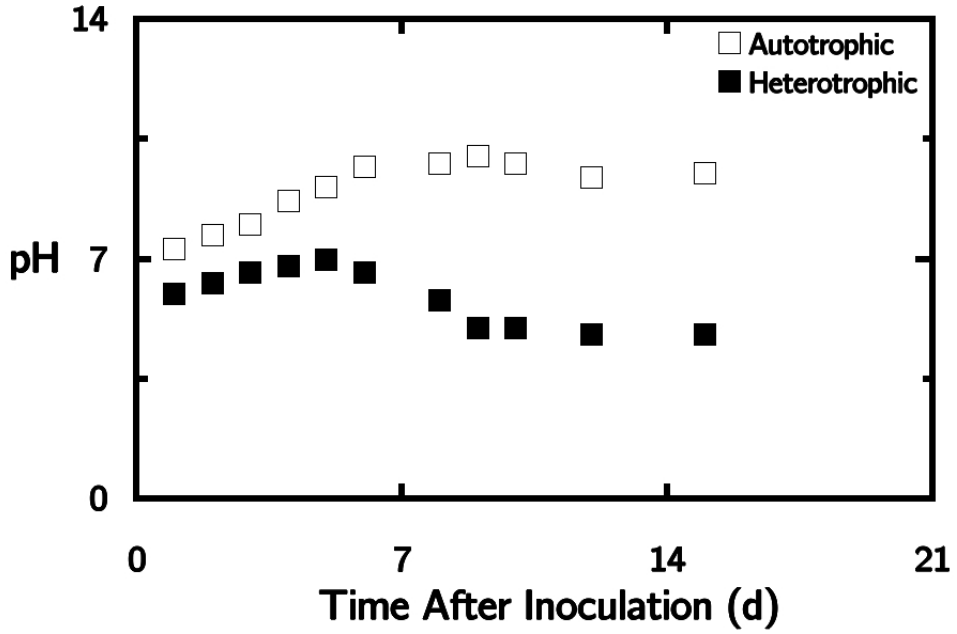

Figure S2. Change in media pH during auto– and heterotrophic growth of *C. sorokiniana*. The pH of auto– (▫) and heterotrophic (■) UTEX 1230 cultures was monitored during exponential growth and remained stable throughout stationary phase. The resulting pH curves demonstrate the interdependence of cell metabolism and the surrounding environment. The standard deviation for each data point is less than 0.5 pH unit (error bars not visible).

Chapter 4: Sequence Listing

Protein sequences and transcriptomic data sets from *C. vulgaris* UTEX 395 are courtesy of Dr. Michael Guarnieri at NREL and were analyzed with help from Dr. Geng Yu.

PF07731:

MNRSMACKAALLLLAAAASVQVAAQGAAADGPTYYIAADVVDWNYAPAGVNLCNGELFTGDP
RLWTQLGMGSVYKKALYQQYTDATFKTLVPKPESEQHTGMLGPIIRAAVGQVVTVVLKNNLS
FPCNLEPSGVQPEKPGADGAAALSPEAAPGATVTYRWLVPKSMGPGPMEPSAKLWLYRSTVD
LMGDGNAGLLGPMLVSNTPEVNTGDVAAGQERDIITVLQVLDENSSPFFDTNLGNRTALSLG
VTDDGLVEGNLKHGINGYLYCNAPGLMMTQGESVRWHMASLGSETDMHNLHIHGNTFLNNGH
RADQLSMIPGTARSVQFSTDNAGQWLLHCHVNDHINAGMKAMYQVARNDSIATELAGVPEEG
LGGTTRTYFIEAEEEEWDYVPLGGDFCSGKKVAWTEEQEVFTTGNAIRPGSKFEKARYVEYT
NDTFTEKKIRGAQDAYLGLLGPIIRAEVGDVIQVVFKNSLRFPATMHPHGVAYLKSSEGSPY
FDGTMGADTDDDMVPPGETYTYTWHVPETAGPGPADASTLLWMYHSHTGECPRLHDSLYEVR
DTYAGLVGAIVIGRKGELKADLTASTVDREVVLFFMVSNEMNSLYADVNAQEWGFNSIQDWE
AVAEEAYNTQAASDQQLALQGEELQQLQAGSGANSTSGTTVQAAGRRLMEEEEEEEGYEEPL
LKHIINGYLFCNMPVLSFNQGDRVRFHVMALGTEVDMHTPNLVGQTMQVDNGQRGAAVAMMP
GAMHSIDVVMANPGTAVVQCRVADHISAGMRALVKVYADGEVAAEQEAAAAKATVKRYYIAA
EPVDWDYTPSGQDACTNSAFGPDAEVFVQRTNATIGSKNVKAQYRQYTDASFTELAPQPASH
GILGPTLVAEVGQTLEIVFFNDLDFEANIMLDGGLELLPAGADGDDASLSAPVAPGGNFTYR
YYVPDSAGPGSEDLSTIAYAYTSSVDLVGHPNAGLIGVLVVGSPGTFKGASEVPEGVDEMLP
LLFTIMDEGASPLLQQSMDAAGLSVAATFQPGWGESNLKHNINGYMYCNLPGFTAARNSTVR
LLLVGMGSEADMHSPIFTGQVLKTKASAYATAELMPTITRVVDVAMEQSGKWPVYCSVHDHY
IAGMRATLVVE

PF00125:

MSGRGKGGKGLGKGGAKRHRKRISGLIYEETRGVLKVFLENVVRDAVTYTEHARRKTVTAFD
VVYALKRQGRTLYGFGA

PF00403:

MQGASGSGPDLFVAGMAEAGAPSTATLLVVYNPQQLTDTAVLLQTLEAAGFGGSLQRVEASV
APPALAHLRVESMTCSSCSSAVESALAALPGVRHASVSLTMQEAKVEYDPGTVAEAQLVQAI
EEAGFSCSPLATGESASLHLAVGGMSCSSCSTAIEAALRGADGVLDASVNLLTNQAEVRYDP
DAVGPRQLLALVSDLGYTVQAMEGAGLVDGSALREREKRFWRRRFLLALAFSAPLFIMSMIL
MYIPGPKQLIELDVGGFELGQIIAFALATPVQFIVGWTFHKGAFKALRRRRANMDVLVSVGT
FAAYIYSIISIVVSRVEAEFESHGLFFETSALLITFICLGKYLEAAAKGRTSSAISELLKLA
PATAILEQEVPASLLQRGDRLKVLPGARLPADGTVVHGRSFVDESMITGESVPVAKRTGDAV
ISGTVNGSGVLMVRAARVGKDTTLSQIVRLVEGAQMSKAPIQAFADRLSAVFVPIIIVAALA
TWLGWFLGGVTGSFPASWVPTGSSPFLFALLFGIAVLVIACPCALGLATPTALMVGTGVAAQ
HGILIKSAEALEKMSGLGTIVFDKTGTLTEGRPSVVDSAVVDERWSLEWVLYLAASAENGSE
HPLARALMRHAALYLEGGSALLEESGSPCSQLAPSEELPASGSFDAAGGVLSGQGTLLHVVH
PEPPPAEQALRSVGWLAPITASEALPGRGLKCWLACPADRAAAILPALLAGRALSVPSPPPS
HSALSAAARVSPVGSSCPSPAGGDGFAPPMPAVAEAGAAAGKGAAPGSLETQEWMRGYEREG
ATCVLLAVEACLVARFAISDPLKLEAPAVIAALRQMGLACHMVTGDNWTTARAIAARLGIID
VSAEVLPAGKAEHVKRLQASSRRAVAMVGDGINDSVALAQADVGIAIGSGTDVAVEAADYVL
MRSDLEDVLVAIDLRWEGPKLLLLLMMCWVFLPPWIAGAAMALSSVTVVCSSLLLRRYKRPQ
PALQHLVEVSCGALSLARM

PF00389:

MHFGFQFTKEALRDDLGVEVVQCERADLQRELANTTVTVPLMSPLDAQVLRSARQLKLIIQF
GVGVEAIDIPTATELGIWVSNIPSGGTGNAISCAEHAIYLMLATLRFHNAMADSIRTRRLGV
PLGQSLFTKTVLIVGFGSIAKELAVRLKPFGVRVTALRRRPWRHSAQVAAAASEQLPQHSKG
ESGAADAGRQQQQQQYLYLQHDAELDVAAEAVLVDRGCWPADSARLAADADIIAVTCHQDAS
NRGMIGSQFLSHCKPGVRIVNVARGGLLDYEAVRVGLDSGRIAGLGLDVQEHEPVDPQHWLA
QHPSVYLTPHIAGVTEMSYRNMAEVVAAAVRRVRQGQAPARLLND

PF02469:

MAQSVLACRTCFHALPQTEFVEVLKYHVVPGQALTLDELTDGQILQTLVEGPAGQLRVIVSP
NAQKPILETSSGEQVPIYQFNLGAGTDTIVHTIRGLLVPGDDTLDAAAPAAV

PF00122:

MQGASGSGPDLFVAGMAEAGAPSTATLLVVYNPQQLTDTAVLLQTLEAAGFGGSLQRVEASV
APPALAHLRVESMTCSSCSSAVESALAALPGVRHASVSLTMQEAKVEYDPGTVAEAQLVQAI
EEAGFSCSPLATGESASLHLAVGGMSCSSCSTAIEAALRGADGVLDASVNLLTNQAEVRYDP
DAVGPRQLLALVSDLGYTVQAMEGAGLVDGSALREREKRFWRRRFLLALAFSAPLFIMSMIL
MYIPGPKQLIELDVGGFELGQIIAFALATPVQFIVGWTFHKGAFKALRRRRANMDVLVSVGT
FAAYIYSIISIVVSRVEAEFESHGLFFETSALLITFICLGKYLEAAAKGRTSSAISELLKLA
PATAILEQEVPASLLQRGDRLKVLPGARLPADGTVVHGRSFVDESMITGESVPVAKRTGDAV
ISGTVNGSGVLMVRAARVGKDTTLSQIVRLVEGAQMSKAPIQAFADRLSAVFVPIIIVAALA
TWLGWFLGGVTGSFPASWVPTGSSPFLFALLFGIAVLVIACPCALGLATPTALMVGTGVAAQ
HGILIKSAEALEKMSGLGTIVFDKTGTLTEGRPSVVDSAVVDERWSLEWVLYLAASAENGSE
HPLARALMRHAALYLEGGSALLEESGSPCSQLAPSEELPASGSFDAAGGVLSGQGTLLHVVH
PEPPPAEQALRSVGWLAPITASEALPGRGLKCWLACPADRAAAILPALLAGRALSVPSPPPS
HSALSAAARVSPVGSSCPSPAGGDGFAPPMPAVAEAGAAAGKGAAPGSLETQEWMRGYEREG
ATCVLLAVEACLVARFAISDPLKLEAPAVIAALRQMGLACHMVTGDNWTTARAIAARLGIID
VSAEVLPAGKAEHVKRLQASSRRAVAMVGDGINDSVALAQADVGIAIGSGTDVAVEAADYVL
MRSDLEDVLVAIDLRWEGPKLLLLLMMCWVFLPPWIAGAAMALSSVTVVCSSLLLRRYKRPQ
PALQHLVEVSCGALSLARM

PF00231:

MQALSCKQALGSVQAFTARPQTSVKRANLQVVAVSIKEVRVRIGSVSNTKKITEAMKLVAAA
KVRRAQEAVVNGRPFAENLVKVLYGVNQRLRVEDVDSPLVAQRPVKSVALVVVTGDRGLCGG
YNNFVIKKTEARAKELEGMGINVRLICVGRKGGVYFRRRPQYNIESTFEVGQQPTIKEAQAI
ADDIFADFVSQEVDKVELIYTKFVSLISGSPVIQTLLPLSPSGEVCDINGNCVDAAEDEVFK
LTTREGQLVVESEQ

PF02874:

MVEFGSGVRGMALNLENDNVGVVLFGSDNAINEGDIVKRTGTIVDVPVGKGTLGRVVDALGN
PIDGKGPLKDVTRRRAEVKAPGIIARQSVHEPMQTGLKAVDSLVPIGRGQRELIIGDRQTGK
TAIAIDAIINQKGVNAGKDESKKLYCVYVAVGQKRSTVAQIVKILSDAGALDYSIIVAATAS
DPAPLQFLAPYSGCAMGEYFRDNGMHALIIYDDLSKQSVAYRQMSLLLRRPPGREAFPGDVF
YLHSRLLERAAKMSNGEGSGSLTALPVIETQAGDVSAYIPTNVISITDGQIFLETELFYKGI
RPAINVGLSVSRVGSAAQVKAMKQVADAATQYLLNRGARLTESYTRQLEAI

PF00306:

MPNIYNALTVGGKNEAGQEISVTCEVQQLLGDHCVRAVAMSATDGLMRGMEVLDSGKPLNVP
VGAATLGRIFNVLGEPVDNLGPVNTKDQLPIHRSAPAFVDLDTKLSIFESGIKVVDLLAPYR
RGGKIGLFGGAGVGKTVLIMELINNIAKAHGGVSVFGGVGERTREGNDLYMEMKESGVINES
NISESKVALVYGQMNEPPGARMRVGLTALTMAEFFRDINKQDVLLFIDNIFRFVQAGSEVSA
LLGRMPSAVGYQPTLATEMGGLQERITSTKDGSITSIQAVYVPADDLTDPAPATTFAHLDAT
TVLSRNLASKGIYPAVDPLDSTSTMLQPWIVGDQHYQCAQNVKQTLQRYKELQDIIAILGLD
ELSEEDRLIVARARKIERFLSQPFFVAEVFTGSPGKYVSLAETIQGFNLILSGELDDLPEQA
FYLVGNLDEAVSKAATLS

PF00006:

MVKIRPDEISSIIKQQIEQYQQEVKAVNVGTVFQVGDGIARIYGLDKVMAGELVEFEDGTVG
IALNLEAKNVGAVLMGEGTRVQEGSSVRATGKIAQIPVGDGYLGRVVNSLARPIDGKGEIAT
KENRLIESPAPGIISRRSVHEPLQTGIVAIDAMIPIGRGQRELIIGDRQTGKTAIAVDTILN
QKGKDVVCVYVAIGQKASSIAQVVNTLQERGAMDYTIIVAATADSPATLQYLSPYTGAALAE
YFMYTGRHTLVIYDDLTKQAQAYREMSLLLRRPPGREAYPGDVFYLHSRLLERAAKLNDKLG
SGSMTALPVVETQEGDVSAYIPTNVISITDGQIFLSADIFNAGIRPAINVGISVSRVGSAAQ
PKAMKQVAGKLKLELAQFAELEAFSQFASDLDQATQNQLARGQRLRELLKQSQSSPLSLEDQ
VASIYAGTNGYLDVLPADRVRAFLVGLRQYLATNKAKYGEILRSTNALTDEAQTLLKEALKE
YTEEFLASAK

PF00421:

MGLPWYRVHTVVLNDPGRLIAVHLMHTSLVSGWAGSMAFYELAVFDPSDPVLNPMWRQGMFV
LPFMTRLGITQSWGGWTISGETAANPGVWSYEGVAAAHIVLSGLLFAASIWHWVYWDLELFR
DPRTSNPALDLPKIFGIHLFLSGVLCFGFGAFHVTGIFGPGIWVSDPYGITGTVQAVAPSWD
ATGFDPYNPGGISAHHIAAGILGVLAGLFHLCVRPPQRLYNGLRMGNIETVLSSSIAAVFWA
AFVVSGTMWYGSAATPIELFGPTRYQWDLGFFQQEIERRVQTNLSEGKSASQAWAEIPEKLA
FYDYIGNNPAKGGLFRAGAMNSGDGIAVGWLGHAVFKEKQGNELFVRRMPTFFETFPVVLVD
KDGVVRADVPFRRSESKYSIEQVGVSVTFYGGELDGVTFNDPATVKKYARRAQLGEIFEFDR
ATLQSDGVFRASPRGWFTFAHLCFALLFFFGHIWHGARTIFRDVFAGIDADLDEQVEFGAFL
KLGDTSTRRQSV

PF01562:

MHADCSRLALAVILDVPVQPPGRQARFTPAAMPANGLLMAATLMLALWASSAAAVPRATVPA
SAAAFAATARAVGKGARLTVTDLQLEGEQEPLSLDLERFEVWSPGAKVVLQGARGAKAREQA
PPATAFFRGSVAGNPGSSVMSRPADMQAKPFECGNDAAGIDPALADTRKLLQFVDDKQYNAH
IALETDAEFLAKFNGDTAAAIDYIGDLMGYADVVYSREINTDILICYLRLWTAGVDSDPWAT
VPDSATALLRFRDYWNANMGGIERTTAHMLSGMSTGGGSSWIGRLCESYGNVLNNFAYGYSG
VLTGTFNWNGDQGSNPEAVVWDVTVVLHELGHNFGSEHSHDYCGIGRNKQPVDRCASSNTCG
AAMGLPSCSSPSPLWNGGAGTLMSYCQRQPGGYSNMVRLRLRL

PF03600:

MARSAFAGLRRWAQQPAVYNTLVISIFIGGVLLMALPAELLSYEAPEKATLNLATTFSDLSS
QGWLSLVFIGLGFFLMVFDIVGADLVMNMVLALCVIFKIVTIKNAVAGFANTGLLTVVVLFM
VAQGLSSTGGADFIITKLLGTPKDTMLAQVRMCLVTAVFSSFVNDTPVFCIMLPIVLTWAAK
ARLPIRQLLIPLSYCCLLGGLNTTIGTSTNLVVTGAFNDRLLDPTRWRAARDEYYQEGLKSI
ELFGIAPYGVPNTFWGIIYIIIASPFLLTGGAGAKAYKRMGRAFSRKTEQGGLVEESGADFF
LGVLVTEGSPVAGLSIQAAGLRNLDGQYVTSVRRGSELVHAVGPEFMLATGDVLYLSGIPDG
TEKLTQLGLVPFTDALEEVGEADLPGLSATFGVKSISVPRVGSFKTASSTGELAHPPPELVE
ATIKKGSEIVGKSIRAAAFRSRFHAAVISIKRNGIPINWSSSQIGDEILRAEDRLLLDVAPQ
FWTEPEVNDAFTDLTKGGQVRSHNEFLLGMRVSKVLAGKSVQKSGLRQLPNAFLVAIDRDSK
TLHAVSPDEVLEVDDILWFAGNAGSVRFIRNTPGLTPLAEKHASKLRSTPKIERRLVQAIVA
PESPLVGSTIRDMRFREQFNAAVVAVARKGERIRSKPGDIELRSGDILLLDTGSAFADQHKD
SKHFTLIIEMPNSNPPRYLHTAIAIASIAIAFTLYAVGIIDILPAATIVVAVMLFTGCMSPE
QARRAIRWDVYLMIAGSFGVSAALEQSGGAAAIANLIVSIGNNAGGGNFTIAAVYVATTLIS
QIIANNSAAALMFPIAATISKNDGVDIYLLSYAIMLGASSVFMSSFGYQTNLMALAAGGHSS
RDFLKFGSPMQIVLAVVSIVSLILHDSWGLVWLVTGLASLVVMGAPQVVELVTLYRATKQKP
VKEFS

PF00664:

MDVQAQHAEACFDELNTAWETAAQEAKKAGQKPKLMKVLWKVYGRQLLLAGIFKLLWSVFVI
LGAYFFTRSILMTIRTLEGKEDSIFDAEWKGWILTAFFFIDAWLLGLMLQRMAYNCLKVGIR
ARAALTTMIARKCYNMAHLTKDTAAEAVGFVASDINKVFEGIQEIHYLWGAPVEAAAILALL
GSLVGVYCIGGVIIVCCVVPLQYIFGYQIIRNKIKNGPNVTERWAVIQEILPAMKLVKYYAW
ERFFEKRVADMRGREKQLMFWNAVVKTINVTMVFGVPPLVLFAVLVPYELWHTDSTSLAPHV
SPTTVFTMLSLFNILRFPLVVLPKAMRCVSEAIRATGNLQHFLAEPAAPRQDLEGKPGAQLS
KAVLRHETDTSGFTLRVPEFSVKPGELVAVVGRVGSGKSSLLQALLGNMQTVEGTAHSGGSI
AYVPQTAWCQNLSLKDNIVFGQPWDEARYKQVLDACALELDLQILAAGDETKAGLRGINLSG
GQRQRLNVARAAYFGGDLVLLDNALSAVDHHTAHHIFDNCVRGMFRDKATVLVTHQVEFLSR
CDKVCIMDEGRSVYFGPWNAAAQQLLSKYLPVSHVLAAGGNAEQPRDVKKAAKKADDKKSEI
AASRARSVHSSSLPLKSALWEYCWDARWTIFVCSLFFFLTAQASRQLADYFVRWWTRDHYGK
YGPGCLESGDDPCGPMYYVTWYGVLGLALFIGLMIPRGAFLYTWAMGASNRQHAKSIHRILY
APLGFFLNTPVGDLLVSFTKDQDVMDDALPDALYYAGIYGLILLATTITVSVTIPLFSAMAG
ALFLVSGIMLTLYLPAATHFKKLRMGTSGDVVTLVAEALDGLTVIQAYNKQQHFTTITSKYV
DDAHRALFGAETLNLWLAFICDFFGACMVLSVACLGIGMWRSLGSSAVGLAFSQSIQMLVFY
TWSIRLVAESIGLFGSVEKIAWLANHTPQEAGVLEPPTLPGGGGGDGKATKKRGTAGKTVPA
LKDDDWNMPPTGGPKLPAGWPRSGTLNFNQVVMKYAPHLPPALRGVSFNIKSGDKVGVVGRT
GSGKSTLLLALYRMFNLESGAVTLDGVDISTLTLEQLRRGLSVIPQDPAIFSGTVRSNLDPF
GEFGHDAVLWEALRDCGLEEQVKACGGLDAELSGTGGNAWSIGQAQLMCLARAALKKVPVLC
LDEATAAMDPHTEAHVLEIIEKLFSDRTTLTIAHRLDNVIRSDLVVVMDAGEVQEMGHPTDL
LANPSSAFSKLVDKTGAASATALRKMAADFQLERERGQQIGFRPRPSLDDMRTSLDQPAP

PF01061:

MLEVSSPANEEALGIDFAQVFSSSSLSRDMDAAIAKHEVPKPGAAPPQYSEMHTSSFGAQLA
ANLRRDFTVYNRAPEYNVVRAVVTILIGFCFGTMFWRQGDNRTTVAGVLNIMGVLYSSTLFL
GISNCLTVQHLVSAQRTVFYRERAAGMYSPFSFALAQQLVEVPYLAGQTVVYAAIVYWMVWF
DRSASKFFWFCLLFYLTLHYFTTLGMAAVNLTASVQLANVLSSFLFGFFNLLADLSGVTMTI
PEFLSSRFQYETYMEGPIVVILIAFVLAFSTLACLSLKMLNFQRR

PF00005:
MFALDKSPSRKGVRIDFSNLDVLACNLFGGGVVSGEVLVNGAPRRASEFAKISSYVLQRDVL
LASSTVRECITVAALLKLPRTLPYNEKIARVDAILRELELEGCQHTLIGDDLLNIKGISGGQ
RRRVSVGIELVKSPKVLFLDEPTSGLDSEMAVSLIDTLVKLAAEGTTICTTIHQPNSMITSN
FDFFMLLHAGSTVYFGPWAECVDYFAGHGCPCPQEHQRRISTTDLEALSLTADDSHMNGGKL
TAAEQEAEDQAVLQPAPKVAWWYQVYVLMGRMARMLWRNPVMFMSETAQYVFMGLFIGLIYL
QLNDSLATGVSDRAASMWFAMAVLSFTPSYTAAVVWDRDRLLLRRESQQGMYSVTAWFAART
ATILPMEVMETALFCVLMYFMVGYYLNVVNFLVFLAAFCMFQLISESIGLMCAIVTPSSTYA
ILILTFILLFLLSFSGFIVADVPVYFRWISKISYLTYAYAAVVQNEFNSVTFYTAGGEAVPG
SQVLSGGVAGVSLSQVNNGLNVGENLAVLLGIAVGARSLAFAMLTSMAKLKRL

PF00083:
MAGGAPILTRASALNISDYESKLTWYVIIVALIASAGGLLFGYDIGVTGGVESFEEFQYKFF
PAVWEAKHGPNAAANNDPYWQITMVVGACWFLAGAGLNAGAQYLWMLVIGRVFLGFGVGMAN
QVVPLYLSEMAPFKYRGGLNMLFQLAVTIGILVAQLINYGVQDWAHGWRLSLGLAAVPAFVL
LMGGIMLPESPNSLIERGHLDKGRAVLEKLRGTTNVHAEYGDIKDASEVAGNIRLRDSWKAM
FTRPYSPMLAVTCMIAMLQQWTGYVPVIFNSLGSGKSASLLNTVIIGAVNVVATFVSILSVD
KFGRRFLFIEGGIQMAVAQTITGVVLAVEFPKYNNVLPSDVAIGVLIVICVFVAGFAWSWGP
LGWLVPSEIQTLETRAAGMSAAVTINFLFSFVVGQAFFTMLCSMRWGVFIFFAGWVVLMTVF
IYFFLPETKNVPVERIQVKFAKHWFWRKWMGPVAQDIINRDETRTASRKAANLEGAAPYPSP
APGDEVPPKIVTAAVA

PF04191:
MHYAVNVVYWSLLLVSVLTGNELISRLVHFEVYSTLMFAASALFTLYHSVRFATDLRRHMKA
LAPPPDLTAGFVLWYAVPPASGVPDYTGAPGVVMCLFGAVLAAGATLQAGMFSFMGAPHVPG
RLHTGGVYALLRHPQALGNMLFLIGFSVAGGALWACAAFCAAFALYVATVVPQEERMLREAF
GEKYERYM

PF01764:
MGTKQLRDVLADANLGTALLWAEAEAVAEAMSATGAQPSQEEPSGPQAASAAVTAGTAAAGA
TAAAAAVAPAQTAAPGVHRGFLGRAQAVQVEPLWTHARQQGLRLVLCGHSLGGAVAQLCTLR
LLHLLRAAPLPADALRCIVFGCPAIGNTALAEHVRQQAWDAHFLSISLPGGRKWGGRDGRDQ
SC

Unknown Protein 1:
MLNWDWLRNQAAEGTDEEMMAKEQGWWYNVRQIIRVPLLDNTLEGPELTAWIDKHTMRVHHG
ILDKLDKLRMDEETQELVLDDPYWQELKVLGVWTPVPTPVPPPLHPMSEGVYPEPRPAPKPA
ADSSGGVEAAA

Unknown Protein 1:
MRDPLALSADKLRVQVRLKRMTAAVKPRLNHLNCVQAIVACSVCLLAASALPVVAYVYVLRF
STTALGPFAWTHWAIVGATCLLGIAAHSLNRRVLLALHVAMCCMLGAALGGFDTAFWYQLTT
RCLTYQAVFKGCQQCPCANTNTCTAANLANDVLCQSCTAYPTEVCKPALQTAQNHVIAFTGL
AAVLFLAVPAFYSLLVLCRMEASTAVAAARRQMVSFAVDQQATMVESNEKPNVTPAMLSAWV
SFLFSTHDPDCVAIGERVSRV

Chapter 6: Additional Materials and Methods

Design and cloning of V_HH transgenes for chloroplast expression[10]

Genes encoding V_HH monomers (C2, B5, H7) and the H7-B5 heterodimer generated by Mukherjee *et al.* (2012) were adapted to the chloroplast codon usage of *C. reinhardtii* (KDRI species number 3055) according to the table in Kazusa DNA Research Institute's Database (http://www.kazusa.or.jp/codon). Further gene optimization and restriction site mapping were performed *in silico* using the Gene Designer bioinformatics software suite prior to synthesis (DNA2.0, Menola Park, CA). Additional protein domains fused to the V_HHs included the mVenus yellow fluorescent protein for subcellular visualization and immunochemistry as well as N-terminal streptavidin binding protein (SBP) and C-terminal 6×His tags to enable purification from either terminus. Alternate versions of these gene constructs were designed without the multiple fusion partners and only a single N-terminal Flag tag. Each cassette was flanked by *NdeI* and *XbaI* restriction sites upstream and downstream, respectively, for ligation in-frame with the chloroplast transformation vector driven by the psbA promoter (Manuell *et al.* 2007). Schematic diagrams of the *C. reinhardtii* chloroplast V_HH expression cassettes related to the present study can be found below. All bacterial proteins were expressed from pET32b plasmid described by Mukherjee *et al.* (2012) with an N-terminal thioredoxin (Trx), internal 6×His, and C-terminal E-tag.

***C. reinhardtii* chloroplast expression cassette:** NdeI-[1×Flag]-[V_HH]-XbaI

***E. coli* expression cassette:** XbaI-[Trx]-[6×His]-[V_HH]-[E-tag]-XhoI (pET32b)

[10] Procedures from Barrera DJ, Rosenberg JN, Chiu JG, Chang Y-N, Debatis M, Ngoi S-M, Chang JT, Shoemaker CB, Oyler GA, Mayfield SP (2014) Algal chloroplast produced camelid V_HH anti-toxins are capable of neutralizing botulinum neurotoxin. *Plant Biotech J. In Press*

***Quantification of V_HH binding affinity to BoNT and algae by ELISA*[10]**

Binding assays comparing the affinity of *E. coli* and *C. reinhardtii* expressed V_HH proteins were performed in 96-well plates pre-coated with BoNT and blocked of non-specific binding sites (Metabiologics, Inc., Madison, WI). *E. coli* expressed V_HH B11 that binds to the cell wall of *C. reinhardtii* and served as a negative control since it does not bind to BoNT. The ELISA procedure used V_HH dilution series ranging from 1-10 pM in phosphate buffered saline (PBS) containing 0.1% tween-20 and 4% non-fat dry milk. Each dilution was administered in 100 µl volumes to duplicate wells and incubated at room temperature for 1 hr in rotary shaker at 40 RPM. All wells were washed three times with 200 µl of phosphate buffered solution with 0.1% tween (PBST) followed by three washes with PBS. Binding was determined by probing with a rabbit anti-E-tag antibody (Bethyl Labs, 1:5,000 in PBST) for the bacterially produced V_HHs and a mouse anti-Flag-tag antibody (Sigma, 1:5,000 in PBST) for the V_HHs derived from algae. For colorimetric detection, both antibodies are conjugated with horseradish peroxidase. After incubation with the respective antibodies for 1 hr at room temperature, each well was washed 3× with 200 µl of PBST and 3× with 200 µl of PBS. The ELISA was developed with 100 µl of 3,3′,5,5′-tetramethylbenzidine (TMB) liquid substrate per well (Sigma) and incubated at room temperature for 2-5 minutes until suitable colorimetric change occurred. The reaction was ceased by adding 100 µl of 1 N HCl and absorbance readings were measured at 450 nm using automated plate reader (Molecular Devices, MicroStation). The same protocol was used to determine the binding affinity of *C. reinhardtii*-specific V_HHs by coating wells of the ELISA plate (Immulon^{TM}) with whole protein lysates from each microalgal species.

										10									20									30									40			
B1	T	G	G	G	L	A	Q	P	G	G	S	L	S	L	S	C	E	L	S	G	G	T	F	S	R	G	T	M	G	W	Y	R	Q	A	P	G	K	Q	R	E	L	V	A	S
F1	T	G	G	G	L	V	Q	P	G	G	S	L	R	L	S	C	A	A	S	G	F	T	F	S	T	Y	W	M	Y	W	V	R	Q	A	P	G	K	G	L	E	W	V	S	A
C3	S	G	G	G	L	V	Q	A	G	G	S	L	R	L	S	C	V	A	S	G	S	A	F	S	K	D	V	W	A	W	Y	R	Q	A	P	G	K	Q	R	T	W	V	A	V
H10	**T**	**G**	**G**	**G**	**L**	**V**	**Q**	**A**	**G**	**G**	**S**	**L**	**R**	**L**	**S**	**C**	**A**	**A**	**S**	**G**	**N**	**I**	**F**	**R**	**V**	**R**	**A**	**M**	**A**	**W**	**Y**	**R**	**Q**	**A**	**P**	**G**	**K**	**Q**	**R**	**E**	**W**	**V**	**A**	**V**
F5	T	G	G	G	L	V	Q	A	G	E	S	L	R	L	S	C	V	A	S	G	F	T	F	S	R	H	P	M	A	W	Y	R	Q	A	P	G	K	A	R	E	L	V	A	S
B12	S	G	G	G	L	V	Q	A	G	G	S	L	R	L	S	C	A	A	S	G	F	D	F	S	R	R	P	M	G	W	Y	R	Q	A	P	G	K	Q	R	E	L	V	A	T
B11	**T**	**G**	**G**	**G**	**L**	**V**	**Q**	**A**	**G**	**G**	**S**	**L**	**R**	**L**	**S**	**C**	**V**	**V**	**S**	**G**	**R**	**N**	**N**	**S**	**G**	**I**	**G**	**M**	**G**	**W**	**F**	**R**	**Q**	**A**	**P**	**G**	**K**	**E**	**R**	**E**	**F**	**V**	**A**	**A**

						50								60									70								80						
B1	M	I	S	-	G	D	Y	I	N	I	V	D	S	V	K	G	R	F	T	I	S	R	D	N	A	K	N	T	V	Y	L	Q	M	N	S	L	K	P	E	D	T	A	V	Y
F1	I	G	T	L	-	G	N	T	H	Y	A	D	S	V	K	G	R	F	T	I	S	R	D	N	A	K	N	T	L	Y	L	Q	M	N	S	L	K	P	E	D	T	A	L	Y
C3	I	G	S	A	-	G	G	T	N	Y	A	E	S	V	K	G	R	F	T	I	S	R	E	N	A	K	N	T	V	Y	L	Q	M	N	S	L	K	P	E	D	T	A	K	Y
H10	**L**	**G**	**S**	**R**	**-**	**G**	**G**	**T**	**N**	**Y**	**A**	**D**	**S**	**V**	**K**	**G**	**R**	**F**	**T**	**I**	**S**	**R**	**D**	**N**	**A**	**A**	**N**	**T**	**I**	**F**	**L**	**Q**	**M**	**N**	**S**	**L**	**K**	**P**	**E**	**D**	**T**	**A**	**V**	**Y**
F5	I	A	S	S	S	G	V	T	D	Y	H	A	S	V	R	G	R	F	T	I	S	R	D	N	A	K	N	T	V	Y	L	Q	I	N	I	L	K	P	E	D	T	A	A	Y
B12	I	A	S	A	S	A	T	T	H	Y	T	D	S	V	K	G	R	F	T	V	S	R	D	N	A	K	N	T	L	Y	L	Q	M	N	S	L	K	S	E	D	T	A	V	Y
B11	**I**	**G**	**W**	**G**	**G**	**S**	**S**	**T**	**I**	**Y**	**A**	**D**	**S**	**V**	**K**	**G**	**R**	**F**	**T**	**V**	**S**	**R**	**D**	**N**	**A**	**K**	**N**	**T**	**V**	**Y**	**L**	**Q**	**M**	**V**	**S**	**L**	**K**	**P**	**D**	**D**	**T**	**A**	**V**	**Y**

		90										100									110								120	
B1	F	C	K	Y	N	-	-	-	-	-	F	E	G	L	A	-	-	-	-	-	Y	W	G	Q	G	T	Q	V	T	V	S	S
F1	Y	C	A	R	D	L	D	G	S	S	W	Y	L	K	P	P	A	V	L	D	S	R	G	Q	G	T	Q	V	T	V	S	S
C3	Y	C	N	-	-	-	-	-	-	-	-	-	K	F	P	D	V	R	G	R	N	W	G	Q	G	T	Q	V	T	V	S	S
H10	**Y**	**C**	**N**	**-**	**-**	**-**	**-**	**-**	**-**	**-**	**-**	**-**	**H**	**Y**	**P**	**P**	**E**	**K**	**R**	**D**	**Y**	**W**	**G**	**Q**	**G**	**T**	**Q**	**V**	**T**	**V**	**S**	**S**
F5	Y	C	N	-	-	-	-	-	-	-	-	-	A	L	P	N	L	P	R	N	Y	W	G	Q	G	T	Q	V	T	V	S	S
B12	Y	C	N	-	-	-	-	-	-	-	-	-	S	L	P	-	V	W	K	N	Y	W	G	Q	G	T	Q	V	T	V	S	S
B11	**V**	**C**	**A**	**A**	**R**	**R**	**R**	**A**	**L**	**T**	**P**	**I**	**S**	**L**	**A**	**A**	**G**	**F**	**-**	**E**	**Y**	**W**	**G**	**Q**	**G**	**T**	**Q**	**V**	**I**	**V**	**S**	**A**

Table S3. Protein alignments of lead candidate V_HHs generated against *C. reinhardtii* cell surface antigens. Protein sequencing and alignment courtesy of the Shoemaker Lab, Tufts Cummings School of Veterinary Medicine.

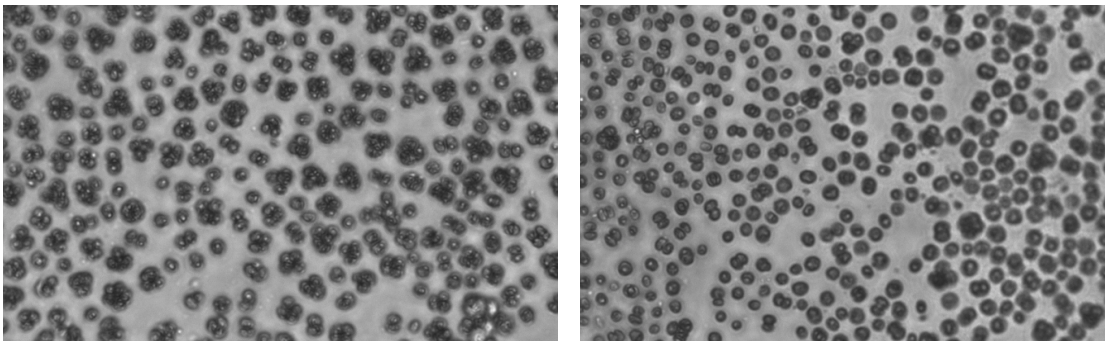

Figure S3. *C. reinhardtii* cells immobilized on hydrogel surface. These enlarged views of the micrographs shown in Figure 40 demonstrate cellular associations more clearly. While the left micrograph shows clusters of cells bound via BSA, the right image has mostly single cells immobilized by FN.

Chapter 8: Photographs of Biofilm Preparation

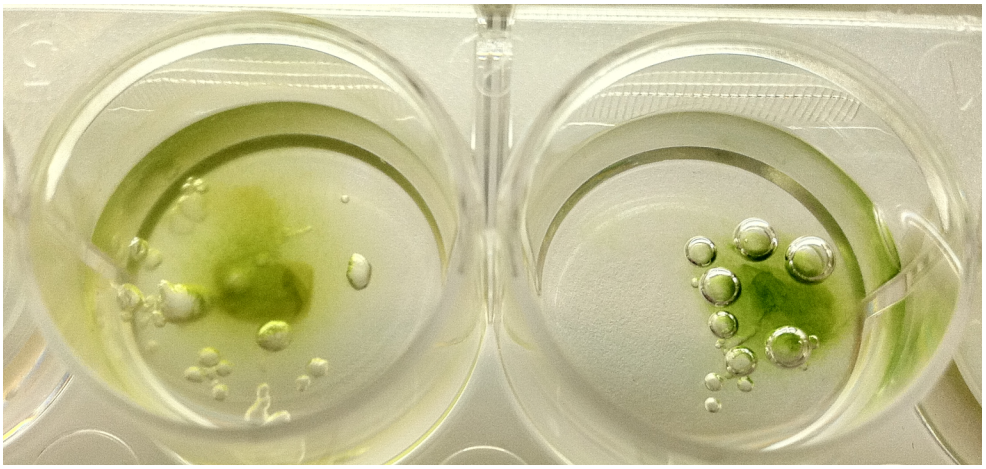

Figure S4. Gas entrapment in exopolymer material produced by biofilms. These two examples of naturally isolated biofilms illustrate differential degrees of gelatinous material forming over the samples. In both cases, gas is not allowed to freely diffuse from the biofilm, resulting in the formation of large bubbles.

Figure S5. Sample preparation of biofilms for Lightsheet microscopy. This photograph shows the preparation of 6 different sections of biofilm for imaging using the Zeiss Lightsheet Z.1.

Vita

Julian Rosenberg was born to Drs. Mark Rosenberg and Andrea Needleman in New Haven, Connecticut. After graduating from high school at Chase Collegiate School (formerly St. Margaret's-McTernan School), he moved to Baltimore to begin his study of engineering at Johns Hopkins University. Following his interests in molecular biology and photosynthetic organisms, Julian worked as a research assistant to Drs. Eric Johnson and Richard McCarty in the JHU Department of Biology, where he contributed to projects involving genetic engineering of photosynthetic proteins in the model green alga *Chlamydomonas reinhardtii*. He received his Bachelor of Science degree in Chemical & Biomolecular Engineering in 2008 and continued to apply chemical engineering principles and molecular biology skills to microalgae for his Masters degree, which was completed in 2009. Julian then worked with local start-up companies led by close collaborator, Dr. George Oyler, where he gained exposure to R&D— bridging gaps between fundamental science and commercial applications including algae-based vaccines, metabolic engineering, and integrated algal cultivation. In 2010, Julian returned to the Betenbaugh laboratory for his PhD to examine methodologies to improve the efficiency and environmental impact of microalgal cultivation by examining less resource-intensive production systems. His current academic interests lie at the interface of cellular engineering and large-scale bioprocessing— ranging from molecular genetics to the practical aspects bioenergy production.

Publications

Peer-Reviewed Papers

1. Wan M, Jin X, Xia J, **Rosenberg JN**, Yu G, Nie A, Oyler GA, Betenbaugh MJ (2014) The effect of iron on growth, lipid accumulation, and gene expression profile of the freshwater microalga *Chlorella sorokiniana*. *Appl Microbiol Biotechnol*. *In Press*

2. Jiang W, Cossey S, **Rosenberg JN**, Oyler GA, Olson BJSC, Weeks DP (2014) A rapid live-cell ELISA for characterizing antibodies against cell surface antigens of *Chlamydomonas reinhardtii* and its use in isolating algae from natural environments with related cell wall components. *BMC Plant Biology*. *In Press*

3. Barrera DJ, **Rosenberg JN**, Chiu JG, Chang Y-N, Debatis M, Ngoi S-M, Chang JT, Shoemaker CB, Oyler GA, Mayfield SP (2014) Algal chloroplast produced camelid V_HH anti-toxins are capable of neutralizing botulinum neurotoxin. *Plant Biotech J*. *In Press*

4. **Rosenberg JN**, Kobayashi N, Barnes A, Noel EA, Betenbaugh MJ, Oyler GA (2014) Comparative analyses of three *Chlorella* species in response to light and sugar reveal distinctive lipid accumulation patterns in the microalga *C. sorokiniana*. *PLoS ONE*, 9:e92460. (Open Access)

5. Rogers JN, **Rosenberg JN**, Guzman BJ, Oh VH, Mimbela LE, Ghassemi A, Betenbaugh MJ, Oyler GA, Donohue MD (2014) A critical analysis of paddlewheel-driven raceway ponds for algal biofuel production at commercial scales. *Algal Research*, 4:76–88. (Open Access)

6. Kobayashi N, Noel EA, Barnes A, Watson A, **Rosenberg JN**, Erickson G, Oyler GA (2013) Characterization of *Chlorella sorokiniana* strains in anaerobic digested effluent from cattle manure. *Bioresource Technol*, 150:377–386.

7. Jiang WZ, **Rosenberg JN**, Wauchope AD, Tremblay JM, Shoemaker CB, Weeks DP, Oyler GA (2013) Generation of a phage display library of single-domain camelid V_HH antibodies directed against *Chlamydomonas reinhardtii* antigens and characterization of V_HHs binding cell surface antigens. *Plant J*, 76:709–717.

8. Kobayashi N, Noel EA, Barnes A, **Rosenberg J**, DiRusso C, Black P, Oyler GA (2013) Rapid detection and quantification of triacylglycerol by HPLC-ELSD in *Chlamydomonas reinhardtii* and *Chlorella* strains. *Lipids*, 48:1035–1049.

9. Rasala BA, Barrera DJ, Ng J, Plucinak TM, **Rosenberg JN**, Weeks DP, Oyler GA, Peterson TC, Haerizadeh F, Mayfield SP (2013) Expanding the spectral palette of fluorescent proteins for the green microalga *Chlamydomonas reinhardtii*. *Plant J*, 74:545–556. (Open Access)

10. Wan M, Faruq J, **Rosenberg JN**, Xia J, Oyler GA, Betenbaugh MJ (2012) Achieving high throughput sequencing of cDNA library utilizing an alternative protocol for the bench top next-generation sequencing system. *J Microbiol Methods*, 92:122–126.

11. Wan M, Wang R, Xia J, **Rosenberg JN**, Nie Z, Kobayashi N, Oyler GA, Betenbaugh MJ (2012) Physiological and genetic evaluation of a new *Chlorella sorokiniana* isolate for its biomass production and lipid accumulation in photoautotrophic and heterotrophic cultures. *Biotechnol Bioeng*, 109:1958–1964.

Peer-Reviewed Papers (cont.)

12. **Rosenberg JN**, Mathias A, Korth K, Betenbaugh MJ, Oyler GA (2011) Microalgal biomass production and CO_2 sequestration from an integrated ethanol biorefinery in Iowa: technical appraisal and economic feasibility evaluation. *Biomass Bioenerg*, 35:3865–3876.

13. Wan M, Liu P, Wang R, Li L, **Rosenberg JN**, Oyler GA, Betenbaugh MJ, Huang B, Xia J (2011) The effect of mixotrophy on microalgal growth, lipid content, and expression levels of three pathway genes in *Chlorella sorokiniana*. *Appl Microbiol Biotechnol*, 91:835–844.

14. Wan M, **Rosenberg JN**, Faruq J, Betenbaugh MJ, Xia J (2011) An improved colony PCR procedure for genetic screening of *Chlorella* and related microalgae. *Biotechnol Lett*, 33:1615–1619.

15. Jones MB, **Rosenberg JN**, Betenbaugh MJ, Krag SS (2009) Structure and synthesis of poly-isoprenoids used in N-glycosylation across the three domains of life. *Biochim Biophys Acta*, 1790:485–494.

16. **Rosenberg JN**, Oyler GA, Wilkinson L, Betenbaugh MJ (2008) A green light for engineered algae: redirecting metabolism to fuel a biotechnology revolution. *Curr Opin Biotechnol*, 19:430–436.

17. Johnson EA, **Rosenberg J**, McCarty RE (2007) Expression by *Chlamydomonas reinhardtii* of a chloroplast ATP synthase with polyhistidine-tagged beta subunits. *Biochim Biophys Acta*, 1767:374–380.

Book Chapters

1. **Rosenberg JN**, Oh VH, Yu G, Guzman BJ, Oyler GA, Betenbaugh MJ (2014) Chapter 25: Exploiting the molecular genetics of microalgae: from strain development pipelines to the uncharted waters of mass production. S-K Kim (Ed.), In: *Handbook of Microalgae: Biotechnology Advances*, Elsevier.

2. **Rosenberg JN**, Betenbaugh MJ, Oyler GA (2011) Chapter 12: Paving the road to algal biofuels with the development of a genetic infrastructure. In: *Biofuel's Engineering Process Technology*, MA dos Santos Bernardes (Ed.), ISBN: 978-953-307-480-1. Rijeka, Croatia: InTech. 267–291. (Open Access)

Intellectual Property

1. Oyler GA, **Rosenberg JN**, Weeks DP. Single chain antibodies for photosynthetic microorganisms and method of use; U.S. Application No. 13/441,951.

2. Corbeil LB, Hildebrand M, Shrestha R, Davis A, Oyler GA, **Rosenberg JN**. Diatom-based vaccines, U.S. Application No. 14/353,721.

3. Donohue MD, Betenbaugh MJ, Oyler GA, **Rosenberg JN**. Method for extraction and purification of oils from microalgal biomass using high- pressure CO_2 as a solute, U.S. Application No. 13/8167,737.

4. Oyler GA, **Rosenberg JN**. Enhanced gene expression in algae, U.S. Application No. 13/925,921; U.S. Patent No. 8,815,568

5. Betenbaugh MJ, Oyler GA, **Rosenberg JN**. Method and composition for creating programmed cell death resistant algal cell lines, U.S. Application No. 13/505,783.